Characterizing and Evaluating the Response of Various Portal Monitors When Used to Screen People for Internal Contamination
Final Report submitted to ORAU/ORISE thrugh March 31, 2010
Under DOE Prime Contract DE-AC05-06OR23100

Nolan E. Hertel, Principal Investigator
Georgia Institute of Technology
September 30, 2011

Presentations and Publications

Presentations were made at the Midyear Health Physics Society (HPS) Meeting in Charleston in February. Dr. Hertel made a presentation on the "Use of Portable Survey Meters and Portal Monitoring for Radiological Triage at the March 19, 2011 training session for the Florida Radiation Response Volunteer Corps sponsored by the Florida Chapter of the HPS. Since those items were provided previously in quarterly reports, they are not appended to this report. Dr. Hertel co-taught a Professional Enrichment Course with Dr. Wesley Bolch of the University of Florida at the 2011 Summer HPS Meeting entitled "Use of Portable Survey meters and Portal Monitors for Radiation Triage." That presentation is attached. A journal article on the use of the TPM-903B Portal Monitor for use in radiation triaging has been submitted and has been submitted to the Radiation Protection Dosimetry Journal. The final draft of that article is attached as is the rough draft of an article on using portal monitors to measure internal contamination of fission products.

Determining Trigger Levels for Various Portal Monitors

Although previously submitted in the second quarter report, the information on determining trigger levels for various portal monitors follows. It has been included in this report to emphasize that the material is in final form.

Background measurements were taken with four different detectors (TPM-903B, MiniSentry, pressurized ion chamber, and micro analyst). Measurements were taken with a 4.4 μCi ^{137}Cs source. For the TPM-903B and MiniSentry portal monitor the source was taped to a string and hung in the center of the portal monitor and the counts per second were recorded. The pressurized ion chamber and micro analyst were held at a distance of 5 cm from the source, again suspended in the air by a string to reduce the effects of backscatter. The data taken during these measurements are shown below in Tables 1-3.

Using the readings measured with the TPM-903B and pressurized ion chamber a ratio of the two detectors will be determined. Each portal monitor user can take the same measurements with their own portal monitor, pressurized ion chamber and 137Cs source and calculate a ratio between their own portal monitor and pressurized ion chamber. Since the pressurized ion chambers are calibrated by a standards lab, scaling both the TPM-903B and the unknown portal

monitors to the pressurized ion chamber characterizes the differences in responses of the two portal monitors, in addition to eliminating the issue of different source activities between measurements taken in this report and measurements taken by the user.

The trigger levels for the unknown portal monitor can be calculated by dividing the ratio of the unknown portal monitor to the user's ion chamber by the ratio of the TPM-903B to the ion chamber and multiplying that ratio by the trigger levels listed for the TPM-903B, as described the equations below. This method will be used to determine trigger levels for the MiniSentry during the next quarter.

$$\frac{\frac{Unknown\ Portal\ Monitor\ Reading}{Ion\ Chamber\ Reading}}{\frac{TPM\ Reading}{Ion\ Chamber\ Reading}} \times Corresponding\ Trigger\ Levels$$

Table 1. Background measurements with various detectors

Thermo Scientiffic TPM-903B		**Pressurized Ion Chamber**	
Background Measurements	CPS	Background Measurements	μR/h
Background 1	4191	Background 1	13
Background 2	4294	Background 2	15
Background 3	4335	Background 3	14
Average	4273	Average	14
Canberra MiniSentry		**Micro Analyst**	
Background Measurements	CPS	Background Measurements	μR/h
Background 1	2572	Background 1	21
Background 2	2589	Background 2	20
Background 3	2600	Background 3	20
Average	2587	Average	20.3

Table 2. Measurements for 4.4 μCi ^{137}Cs source with Portal Monitors

Thermo Scientiffic TPM-903B	
CPS	CPS -Bkg Avg
5851	1578
Canberra MiniSentry	
CPS	CPS -Bkg Avg
4061	1474

Table 3. Measurements for 4.4 μCi ^{137}Cs source with Pressurized Ion Chamber and Micro Analyst

Pressurized Ion Chamber					
Distance from Source (cm)	Reading 1 (μR/h)	Reading 2 (μR/h)	Reading 3 (μR/h)	Average	Average -Bkg Avg
5	140	142	138	140	140
Micro Analyst					
Distance from Source (cm)	Reading 1 (μR/h)	Reading 2 (μR/h)	Reading 3 (μR/h)	Average	Average -Bkg Avg
5	270	260	265	265	265

Updating of the Capintec Thyroid Counter Report

As mentioned previously, the Capintec Captus 3000 report issued 3 years ago had several discrepancies in it that were recently uncovered. One of those discrepancies was the incorrect normalization of the MCNP simulated count rates and another of them involved the inadvertent inclusion of a gamma ray in the Ir-192 spectrum that did not exist. The second item did not require any code reruns; rather it required a renormalization of the simulated photopeak count rates. The updated version of that report is attached to this final report.

PEP T-6
Use of Portable Survey Meters and Portal Monitors for Radiological Triage Part I

Nolan Hertel

GEORGIA INSTITUTE OF TECHNOLOGY

NUCLEAR AND RADIOLOGICAL ENGINEERING/ MEDICAL PHYSICS PROGRAMS

G. W. WOODRUFF SCHOOL OF MECHANICAL ENGINEERING

WORK FUNDED THROUGH TKCIS BY THE RADIATION STUDIES BRANCH OF THE CDC

Includes work of Emily Freibert, Randahl Palmer, Sarah Scarboro, Ryan Manger, Shaheen Dewji, Eric Burgett, Michael Bellamy, Michael Shannon

Motivation

- Goal
  - To initially identify individuals who may have received a committed effective dose (CED) ≥ 250 mSv from internal contamination via ingestion or inhalation after a radiological dispersal device or fission product release
    - Further testing and potential treatment would occur after this 1st cut screening
- Purpose
  - To determine the validity of using portable detectors to achieve the aforementioned goal
- End Goal
  - Procedure sheets for the usage of portable detectors

Assumptions

- External contamination removed (i.e. changing clothing and showering)
- Only to be used as 1st stage of triage of internal contamination
- Count rates listed in procedure sheets correspond to a committed effective dose of 250 mSv
- People with count rates equal to or higher than those listed in the procedure sheet need further evaluation
  - Treatment should be based upon further evaluation

Contamination Scenarios

- Two possible exposure scenarios were investigated
  - **Radiological Dispersal Device**
    - Inhalation
    - Ingestion
  - **Fission Product release from a nuclear reactor**
    - Inhalation

Radiological Dispersal Device

Only one isotope is used in the RDD and the isotope has been identified prior to triage

Triage Decision Making

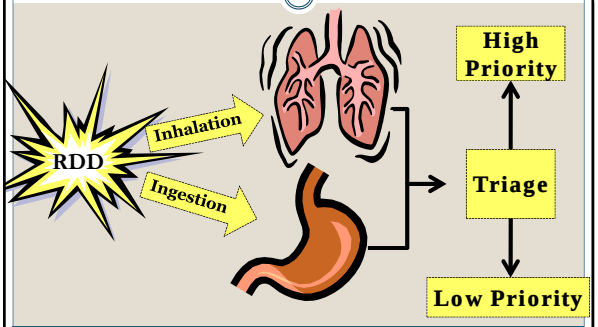

Detectors

- Exploranium GR-130
- Canberra UltraRadiac
- Canberra Inspector 1000
- Ludlum Pancake Probe
- NaI (1", 2" and 3")
- Syrena Plastic Scintillator
- Thermo-Bicron Microanlyst
- Thermo-Bicron Identifinder
- Capintec, Inc Captus 3000 Thyroid Uptake System
- Thermo Scientific TPM-903B Transportable Portal Monitor

Method Overview

- Create a computational model of the detector
- Perform measurements using a PMMA slab and point sources to validate the detector model
  - Calculate Scaling Factor = (MCNP Counts)/(Experimental Counts)
- Simulate the detector response to distributed sources in anthropomorphic phantoms
  - Count rate or other detector output for unit sources in organs of the body
- Determine radionuclide distribution in the body as a function of time
- Generate the count rate corresponding to a Committed Effective Dose of 250 mSv

Simulations of RDD Victims

- MIRD V Phantoms developed at ORNL
- MCNP Model of MIRD V Phantoms created at PNNL in the early 1990's
- Esophagus and Colon Walls added to Reference Male and Female at Georgia Tech by Simpkins and Hertel
- Adipose Male, Adipose Female and Postmenopausal Adipose Female developed at Georgia Tech by Simpkins and Hertel
- Skin added to all phantoms at Georgia Tech

Source Distribution

- **Dose and Risk Calculation Software (DCAL)**
  - **Biokinetic and Dosimetric Calculations of acute intake of radionuclide by inhalation and ingestion**
- **ACTCAL –Activity as a function of time**
- **Input:**
  - **Radionuclide**
  - **Method of Uptake (Inhalation)**
  - **Inhalation Class (S, M, F)**
  - **Environmental or Occupational (Env.)**
  - **AMAD (default - 1μm)**
- **Output – Compartmental activity as a function of time**

Detector Characterization Method

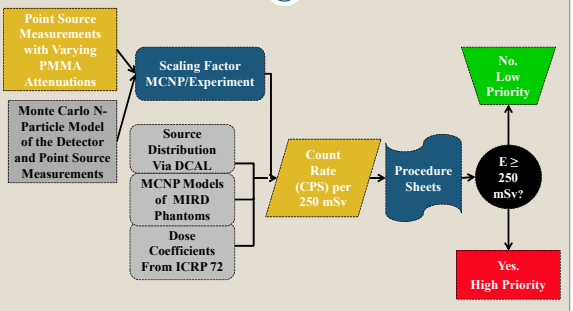

Isotopes of Concern and Phantom Characteristics

- Identified by the DOE/NRC Working Group on Radiological Dispersal Devices as being of "greatest concern"
  ^{241}Am, ^{60}Co, ^{137}Cs, ^{192}Ir
- Investigated at the Request of the CDC
  ^{131}I

Anthropomorphic Phantoms	Height (cm)	Mass (kg)	BMI	Adipose Mass (kg)
Reference Male	179	73.1	23	11
Reference Female	168	56.5	20	15
Adipose Male	179	93.7	30	22
Adipose Female	168	73.9	26	15
Post-Menopausal Adipose Female	168	85.9	30	27
10-year Androgynous Child	140	32.7	n/a	n/a

Adipose Phantom Overview

- **Adipose Male**
  - 22 kg additional body mass added as homogenous tissue to the breast, torso, abdomen
- **Adipose Post Menopausal Female**
  - 27 kg additional body mass added as homogeneous tissue to the breast, torso, abdomen, legs
- **Adipose Female**
  - 15 kg additional body mass added as homogeneous tissue to the breast, torso, abdomen, legs

Slab Phantom and Isotopes in Benchmark Measurements

- Simulate chest wall thickness
  - Varying thickness of PMMA
  - 100 mm backscatter material – virtual water
  - Source holder placed behind PMMA, holds small cylindrical source

Isotope	Photon Energy (MeV)
Am-241	0.059
Ba-133	0.031, 0.356
Cs-137	0.662
Co-60	1.173, 1.332
Mn-54	0.8348
Na-22	0.511, 1.275

Cover broad range of energies

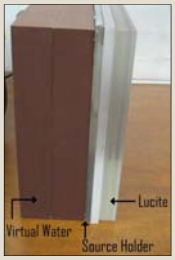

Determining Count Rate per 250 mSv CED

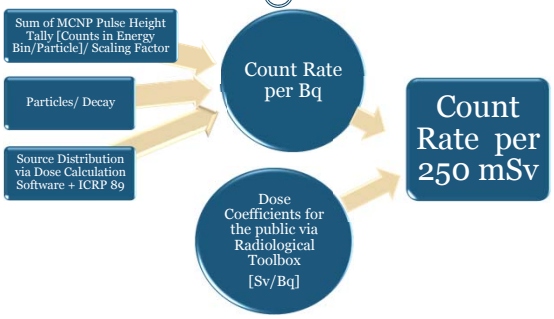

CAPTUS 3000 Thyroid Uptake System

- Thyroid Uptake Collimator
- 2"x2"Ø NaI detector
- 1024-channel Multi-Channel Analyzer (MCA)
- Auto-Calibration with Cs-137 and Eu-152 sources
- Nuclide ROI Identification Software
- Manual ROI identification

Slab Phantom – Data Collection

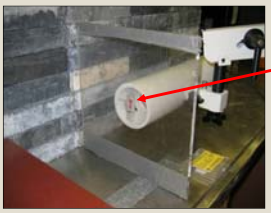

Source placement relative to collimator

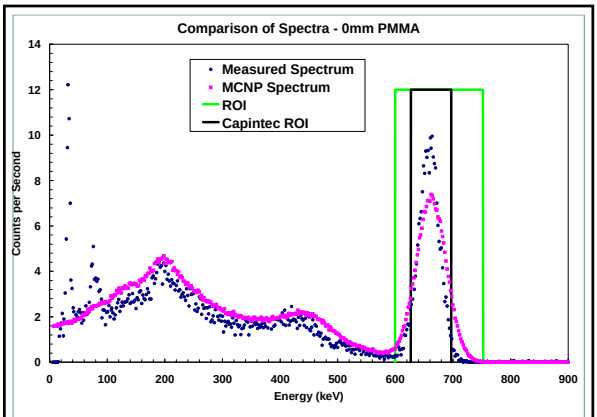

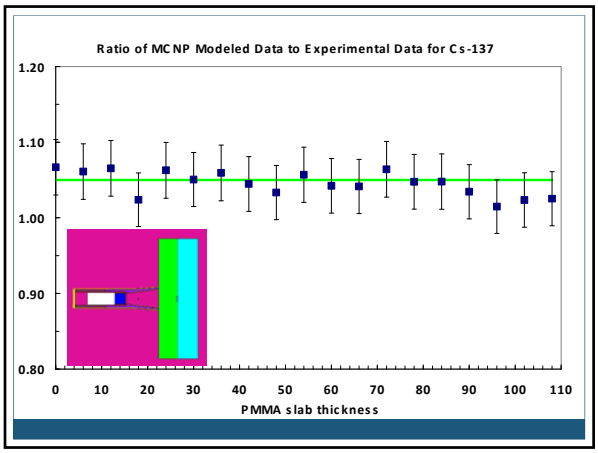

Anthropomorphic Phantoms Handheld Detector Placement

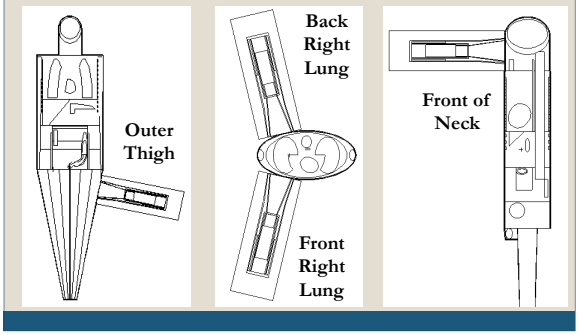

R10

Capintec 3000

Adipose Male- Cs-137			
	Back Right Lung cpm per 250 mSv	Neck cpm per 250 mSv	Thigh cpm per 250 mSv
0	4.92E+04	4.14E+03	2.58E+02
1	1.58E+04	1.29E+04	1.46E+04
2	1.45E+04	1.26E+04	1.44E+04
3	1.42E+04	1.23E+04	1.41E+04
4	1.39E+04	1.21E+04	1.38E+04
5	1.37E+04	1.19E+04	1.36E+04
6	1.35E+04	1.17E+04	1.35E+04
7	1.33E+04	1.16E+04	1.33E+04
8	1.32E+04	1.15E+04	1.32E+04
9	1.31E+04	1.14E+04	1.31E+04
10	1.30E+04	1.13E+04	1.29E+04
20	1.21E+04	1.05E+04	1.21E+04
30	1.14E+04	9.89E+03	1.13E+04

Capintec Absorbed Dose Alert System

22

Canberra Syrena/ E Gamma Detection Beacon

- BC409 Plastic Scintillator
  - 8 cm x 12.5 cm x 4 cm
- 40 keV threshold

Cs-137 Scaling Factor

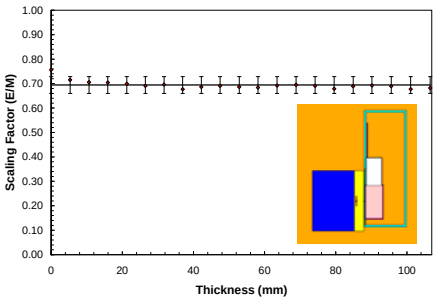

Slide 21

R10 CHECK numbers
Randi, 6/1/2011

DCAL Activity - Co-60 Moderate

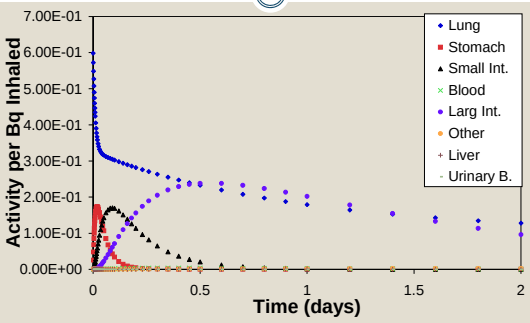

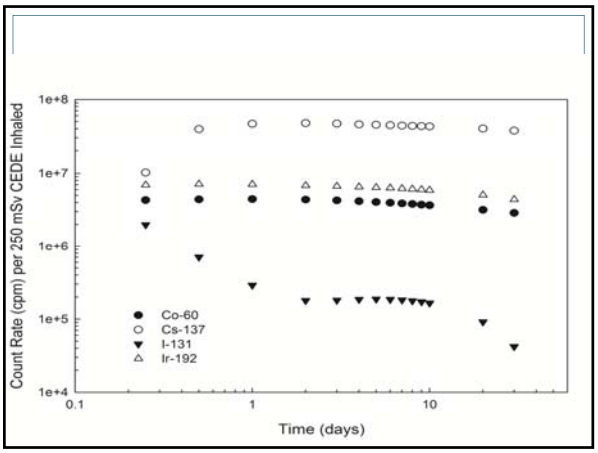

R1

Simulation and Testing of Various Radiation Survey Meters as Monitors of Internal Contamination Levels

Canberra Syrena/E Gamma Detection Beacon FINAL REPORT

June 2008 Page B-3

Canberra Syrena/E Gamma Detection Beacon (Male)

Basic Operation

- Attach detector to computer via provided cable.
- Depress ON/OFF button to turn ON detector.
- Open the Syrena program using provided software.
- Click "Card" and then select "Best Adjustment."
- Follow on-screen commands to calibrate detector.
- Select "Card" and then "Parameter Modification."
- Change the value "increment duration" to 60s and click "validate."
- Change the value "number of increments" to 1 and click "validate."
- Change the value of "alarm fct" to "1" and click "validate" then click "OK."

- Disconnect detector from cable.
- Press button corresponding to "Manual Mode" and allow detector to acquire background.
- Upon completion, detector is ready to acquire data.
- Ensure time switch on side of detector is set to "x1."
- Depress "Start" button to acquire data.
- If the alarm notification appears, acknowledge the alarm and continue collecting counts.
- After 60 seconds, compare the number following "Net = +" to the proper trigger level.

Trigger Levels

Time (days)	Co-60 (cpm)	Cs-137 (cpm)	I-131 (cpm)	Ir-192 (cpm)
0.00	5.7E5	5.9E5	3.1E5	7.9E5
0.25	3.9E5	8.7E5	1.9E5	5.2E5
0.50	3.2E5	2.2E6	8.9E4	4.2E5
1.00	2.8E5	2.5E6	4.6E4	3.6E5
2.00	2.3E5	2.4E6	1.9E4	2.9E5
3.00	2.1E5	2.4E6	1.2E4	2.7E5
4.00	2.0E5	2.3E6	1.0E4	2.5E5
5.00	1.9E5	2.3E6	9.3E3	2.5E5
6.00	1.9E5	2.2E6	9.0E3	2.4E5
7.00	1.8E5	2.2E6	8.7E3	2.4E5
10.00	1.8E5	2.1E6	7.9E3	2.3E5

R2

Micro Rem meter

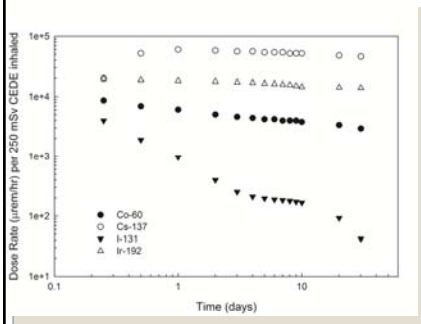

Transportable Portal Monitor

- Whole body counters
- Easy to assemble and operate
- Readily available
- Relatively large throughput compared to smaller detectors

TPM -903B Transportable Portal Monitor

- Transportable portal monitor
- 2 x BC408 plastic scintillators
  - Volume 10.6 liters
  - Detector thickness 3.8 mm
- 1.6 mm of lead shielding around 3 sides
- Energy Range: 60 keV to 2 MeV

Slide 27

R1 CHECK these numbers
Randi, 6/1/2011

Slide 28

R2 Check these number
Randi, 6/1/2011

MCNP Models of the Detectors

TPM - 903B with slab phantom
(with minimum and maximum attenuation)

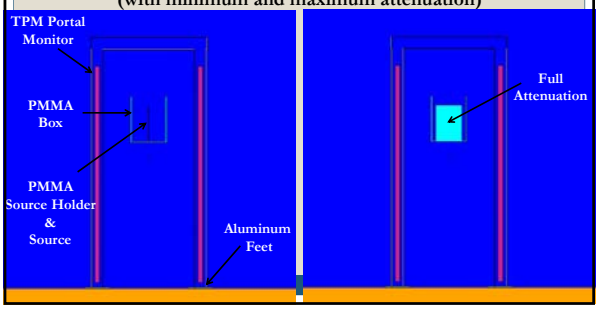

Experimental Data

- Experimental Measurement
  - 5 positions
  - 13 PMMA thicknesses
    - ~6 mm - ~12 cm
  - 4 sources

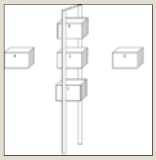

Isotope	Photon Energy (MeV)	Photon Emission Intensity
Ba-133	0.384, 0.356, 0.303, 0.276, 0.081, 0.035, 0.031, 0.030	0.089, 0.622, 0.184, 0.071, 0.338, 0.122, 0.631, 0.341
Co-60	1.332, 1.1730	0.999, 0.999
Cs-137	0.662	0.853
Na-22	1.275, 0.511	0.999, 1.798

Experimental Data

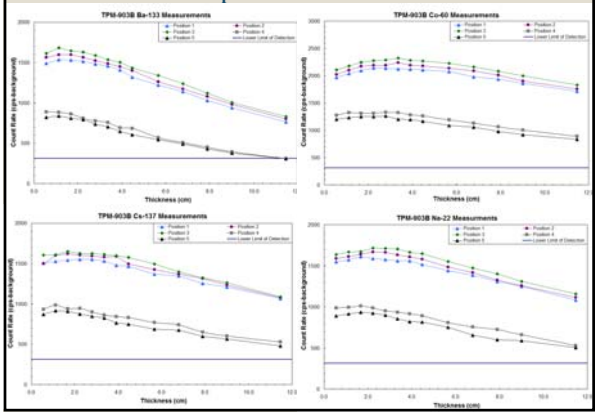

TPM 903B Count Rate Dependence on Position

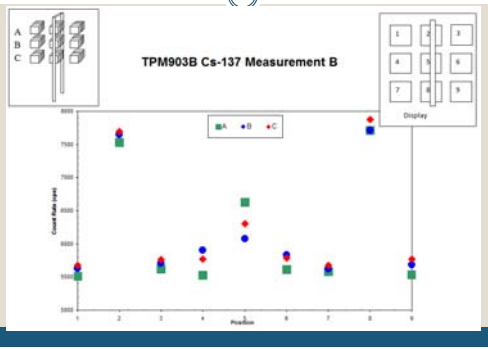

Lower Limit of Detection and Energy Cutoff of TPM 903B

TPM Portal Monitor Lower Limit of Detection	
Background Level at Which Data Was Taken	
Background	4477 CPS
Standard Deviation	67 CPS
Lower Limit of Detection (above background)	314 CPS
Lower Limit of Detection	4791 CPS
Double Background Level	
Background	8954 CPS
Standard Deviation	95 CPS
Lower Limit of Detection (above background)	443 CPS
Lower Limit of Detection	9397 CPS

TPM 903B Energy Cutoff:
60 keV

Table values calculated according to: Knoll, Glenn F. Radiation Detection and Measurements. 3rd Edition. Pgs94-96, 116.

Example of TPM 903 B MCNP Output with Energy Cutoff of 60 keV for Cs-137

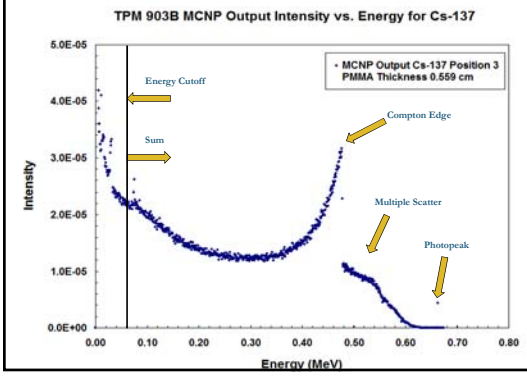

Determining the Cutoff Energy

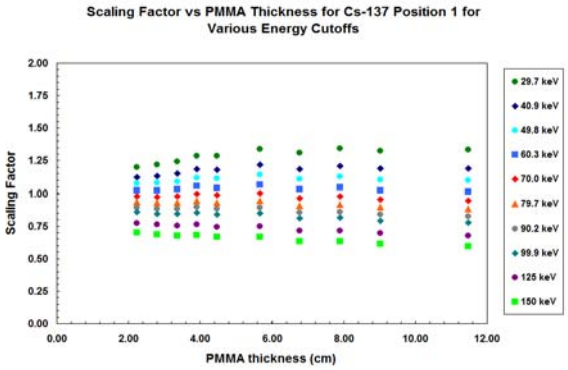

TPM 903B MCNP vs. Experiment

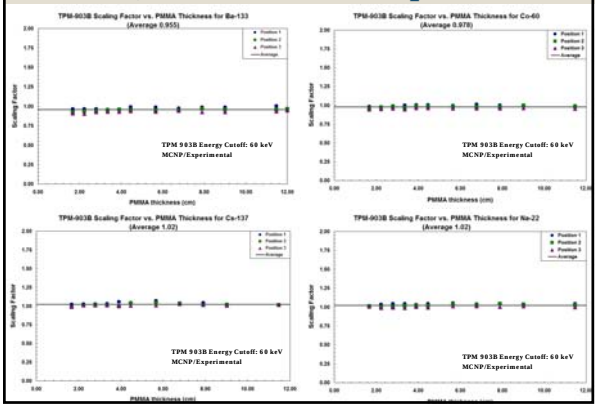

ICRP 72 Dose Coefficients and Calculation of Count Rates Corresponding to 250 mSv

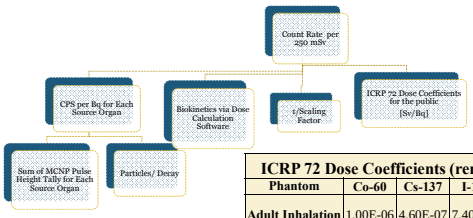

ICRP 72 Dose Coefficients (rem per Bq)				
Phantom	Co-60	Cs-137	I-131	Ir-192
Adult Inhalation	1.00E-06	4.60E-07	7.40E-07	5.20E-07
Child Inhalation	1.50E-06	3.70E-07	1.90E-06	7.60E-07
Adult Ingestion	3.40E-07	1.30E-06	2.20E-06	1.40E-07
Child Ingestion	1.10E-06	1.00E-06	5.20E-06	2.80E-07

Cs-137 Source Distribution Over Time For Inhalation

40

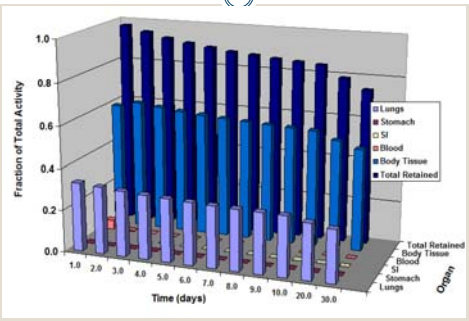

Cs-137 Source Distribution Over Time For Ingestion

41

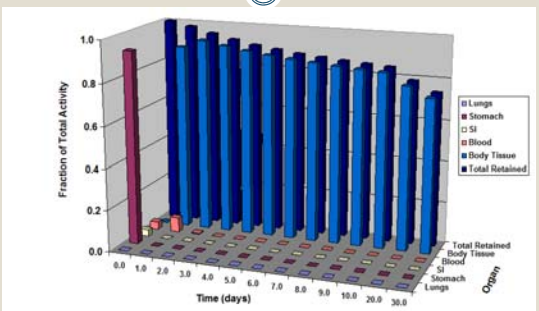

I-131 Source Distribution Over Time For Inhalation

42

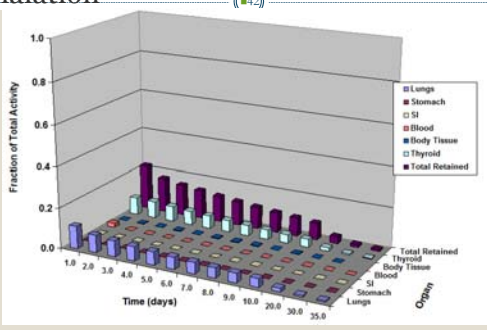

I-131 Source Distribution Over Time For Ingestion

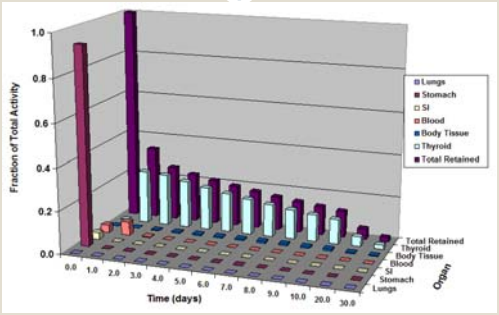

Detector Limitations and Sensitivity

- Count rates calculated for a committed effective dose of 250 mSv
  - Thermo Scientific estimates that the upper count rate for which no pileup/deadtime effects become important is ~30,000 CPS (this is being investigated now)
  - The count rates corresponding to 250 mSv are too high and quantitatively unreliable
- Therefore, a significantly lower committed effective dose threshold can be used for prioritization and initial screening

Comparison of MIRD Phantom Results

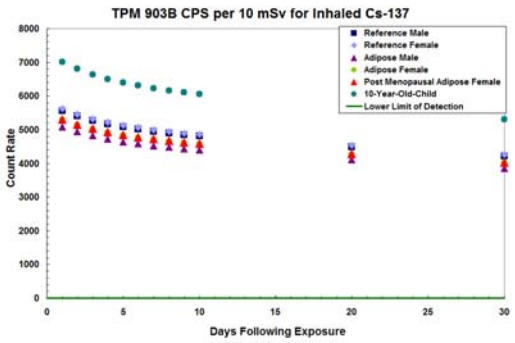

Comparison of MIRD Phantom Results

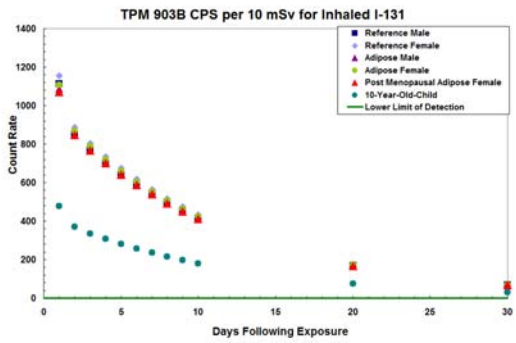

Comparison of MIRD Phantom Results

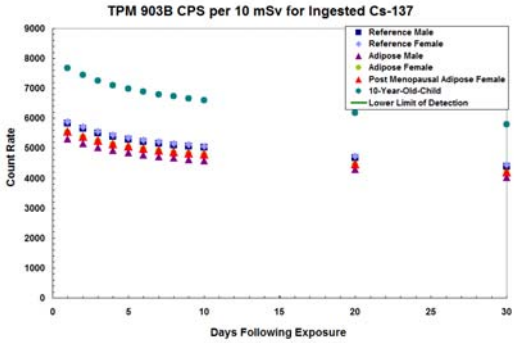

Comparison of MIRD Phantom Results

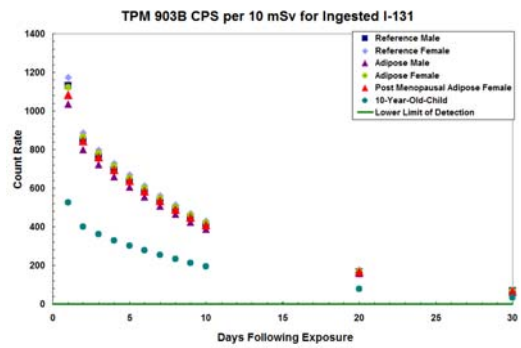

TPM-903B (Adult with Inhaled Radioactivity) Basic Operation

- Attach aluminum feet to bottom of the PVC pipes.
- String cables through top PVC pipe and place on top of the two sides.
- Connect the portal monitor to AC power or D-cell batteries and turn on.
- Acquire the background count by pressing the "Start" button and record value.
- Once background has been acquired data can be taken. Have the person stand sideways inside the center of the portal monitor facing the display unit.
- Depress "Start" button to acquire data.
- If the alarm goes off, ignore and continue collecting counts.
- After a count rate has been obtained, subtract the background count from the number on the display and compare the result to the proper trigger level.

CPS per 10 mSv

Inhalation and Ingestion for Adult Body Type

Adult	Trigger Levels if Inhaled				Trigger Levels if Ingested			
Time (days)	Co-60 (cps per 10 mSv)	Cs-137 (cps per 10 mSv)	I-131 (cps per 10 mSv)	Ir-192 (cps per 10 mSv)	Co-60 (cps per 10 mSv)	Cs-137 (cps per 10 mSv)	I-131 (cps per 10 mSv)	Ir-192 (cps per 10 mSv)
0.25	5633	5157	2320	8003	46618	5409	2264	73423
0.50	5404	5142	1650	7757	43612	5393	1603	69610
1.00	4699	5079	1086	6901	33649	5321	1036	54253
2.00	3476	4940	852	5274	16449	5164	801	25229
3.00	2838	4821	772	4390	7842	5034	723	10485
4.00	2547	4724	706	3976	4232	4930	661	4416
5.00	2408	4646	647	3770	2769	4848	605	2081
6.00	2331	4582	592	3647	2152	4780	554	1201
7.00	2278	4529	543	3557	1866	4724	507	867
8.00	2235	4482	497	3480	1704	4675	464	735
9.00	2198	4441	455	3410	1597	4633	425	677
10.00	2163	4404	416	3343	1513	4594	389	648
20.00	1885	4113	169	2772	1072	4290	158	528
30.00	1683	3859	68	2330	904	4025	64	451

CPS per 10 mSv

Inhalation and Ingestion for Child Body Type

Child	Trigger Levels if Inhaled				Trigger Levels if Ingested			
Time (days)	Co-60 (cps per 10 mSv)	Cs-137 (cps per 10 mSv)	I-131 (cps per 10 mSv)	Ir-192 (cps per 10 mSv)	Co-60 (cps per 10 mSv)	Cs-137 (cps per 10 mSv)	I-131 (cps per 10 mSv)	Ir-192 (cps per 10 mSv)
0.25	4324	7190	1049	7754	17112	7907	1181	24967
0.50	4136	7124	739	7471	15923	7828	829	23691
1.00	3574	7004	476	6534	12202	7683	525	27519
2.00	2613	6802	369	4833	5901	7442	401	16831
3.00	2115	6637	334	3932	2770	7251	361	7508
4.00	1889	6503	306	3518	1462	7100	330	3196
5.00	1782	6394	280	3317	935	6979	302	1469
6.00	1723	6305	257	3202	715	6881	276	808
7.00	1684	6230	235	3120	614	6798	253	557
8.00	1652	6165	215	3051	559	6728	232	459
9.00	1625	6109	197	2989	523	6666	212	418
10.00	1599	6058	180	2929	495	6610	194	397
20.00	1394	5656	73	2425	350	6172	79	323
30.00	1244	5306	30	2034	295	5790	32	276

Fission Product Release

Investigation into internal contamination from a mixed fission product inhalation

Purpose

- To determine the validity of using the TPM 903B Portal Monitor in **triage** of the public after a nuclear reactor accident resulting in a fission product release
- The purpose is **NOT** to determine the level of patient dose but to prioritize individuals for further testing and possible treatment

Methodology

- Determine fission products of concern
- Establish detector response to gamma-emitting fission products for adipose male and child phantoms
  - MCNP Model
  - Biokinetic Data
- Determine dose contribution from non-gamma-emitting fission products
- Determine total body counts registered by the detector equivalent to a committed effective dose of 250mSv

Reactor Model

- ORIGEN Reactor Model Characteristics:
  - Type: PWR Westinghouse 17 x 17
  - Fuel: 27271 kg Uranium, 3.3% enrichment
  - Burn-up: 33,000 MWd
  - Operating Power: 1000MW_e , average: 95.5 MW/MTU
- Reactor accident resulting in a severe core melt at the end of the fuel cycle, allowing a release of fission products into the atmosphere
- Release is characterized as an ex-vessel release

Method: Fission Product Selection

- Use ORIGEN to determine fission products produced
- Determine release fractions for fission products based on accident scenario
- Use toxicity index to focus list of fission products
- Separate fission products into 2 groups: gamma-emitting and non-gamma emitting fission products

Release Fractions

Nuclide	Ex-Vessel release
I, Br	0.25
Cs, Rb	0.35
Te, Sb, Se	0.25
Ba, Sr	0.1
Ru, Rh, Pd, Mo, Tc, Co	0.0025
La, Zr, Nd, Eu, Nb, Pm, Pr, Sm, Y, Cm, Am	0.005
Ce, Pu, Np	0.005

Releases are Fractions of Core Inventory. Source: NUREG-1465

Released fission products

- Ba-131
- Ba-133
- Ba-135m
- Ba-137m
- Ba-139
- Ba-140
- Ba-141
- Ba-142
- Be-80
- Be-80m
- Be-82
- Be-83
- Be-84
- Ce-137
- Ce-139
- Ce-139m
- Ce-141
- Ce-143
- Ce-144
- Cs-131
- Cs-132
- Cs-134
- Cs-134m
- Cs-135
- Cs-135m
- Cs-136
- Cs-137
- Cs-138
- Eu-149
- Eu-152
- Eu-152m
- Eu-154
- Eu-155
- Eu-156
- Eu-157
- Eu-158
- I-125
- I-126
- I-128
- I-129
- I-130
- I-131
- I-132
- I-133
- I-134
- I-135
- La-137
- La-138
- La-140
- La-141
- La-142
- La-143
- Mo-101
- Mo-93
- Mo-93m
- Mo-99
- Nb-93m
- Nb-94
- Nb-95
- Nb-95m
- Nb-96
- Nb-97
- Nb-97m
- Nb-98
- Nb-98m
- Nd-141
- Nd-149
- Nd-151
- Pd-103
- Pd-107
- Pd-109
- Pm-145
- Pm-146
- Pm-147
- Pm-148
- Pm-148m
- Pm-149
- Pm-150
- Pm-151
- Pr-139
- Pr-140
- Pr-142
- Pr-142m
- Pr-143
- Pr-144
- Pr-144m
- Pr-145
- Pr-146
- Pr-147
- Rb-86
- Rb-86m
- Rb-87
- Rb-88
- Rb-89
- Rh-102
- Rh-103m
- Rh-105
- Rh-106
- Rh-106m
- Rh-107
- Ru-103
- Ru-105
- Ru-106
- Ru-97
- Sb-122
- Sb-124
- Sb-124m
- Sb-125
- Sb-126
- Sb-126m
- Sb-127
- Sb-128
- Sb-129
- Sb-130
- Sb-131
- Se-75
- Se-77m
- Se-79
- Se-81
- Se-81m
- Se-83
- Sm-145
- Sm-146
- Sm-147
- Sm-151
- Sm-153
- Sm-155
- Sm-156
- Sr-85
- Sr-85m
- Sr-87m
- Sr-89
- Sr-90
- Sr-91
- Sr-92
- Tc-101
- Tc-104
- Tc-97
- Tc-97m
- Tc-98
- Tc-99
- Tc-99m
- Te-121
- Te-121m
- Te-123
- Te-123m
- Te-125m
- Te-127
- Te-127m
- Te-129
- Te-129m
- Te-131
- Te-131m
- Te-132
- Te-133
- Te-133m
- Te-134
- Y-90
- Y-90m
- Y-91
- Y-91m
- Y-92
- Y-93
- Y-94
- Y-95
- Zr-89
- Zr-93
- Zr-95
- Zr-97

Toxicity Index

$$T.I. = RF \times A \times DC$$

The release fractions, *RF*, were normalized to the percentage of total release for each specific isotope

The activity, *A*, of each fission product was normalized to the fraction of core activity

DC represents the dose coefficient

Cut off was determined to be $\mathbf{10^{-17}}$

Final list of fission products

- Ba-139
- Ba-140
- Br-82
- Br-83
- Br-84
- Ce-141
- Ce-143
- Ce-144
- Cs-134
- Cs-134m
- Cs-135m
- Cs-136
- Cs-137/Ba-137m
- Cs-138
- Eu-154
- Eu-156
- I-130
- I-131
- I-132
- I-133
- I-134
- I-135
- La-140
- La-141
- La-142
- Mo-99
- Nb-95
- Nb-97
- Nd-149
- Pd-109
- Pm-147
- Pm-148
- Pm-148m
- Pm-149
- Pm-151
- Pr-142
- Pr-143
- Pr-145
- Rb-86
- Rh-105
- Ru-103
- Ru-105
- Ru-106/Rh-106
- Sb-122
- Sb-124
- Sb-125
- Sb-126
- Sb-127
- Sb-129
- Sb-130
- Sb-131
- Se-83
- Sm-153
- Sr-89
- Sr-90
- Sr-91
- Sr-92
- Te-125m
- Te-127
- Te-127m
- Te-129
- Te-129m
- Te-131
- Te-131m
- Te-132
- Te-133
- Te-133m
- Te-134
- Y-90
- Y-91
- Y-92
- Y-93
- Zr-95
- Zr-97/Nb-97m

Parent/Daughter Relationships

- All decay products were investigated to determine whether they should be included in the analysis
- Criteria for inclusion:
  - Emission of gamma rays
    - > 40 keV and > 0.5% intensity
  - Non-gamma emitting progeny were eliminated along with those not meeting energy and intensity cutoffs

Group 1: Gamma-emitting Fission Products

- Ba-139
- Ba-140
- Br-82
- Br-83
- Br-84
- Ce-141
- Ce-143
- Ce-144
- Cs-134
- Cs-134m
- Cs-135m
- Cs-136
- Cs-137/Ba-137m
- Cs-138
- Eu-154
- Eu-156
- I-130
- I-131
- I-132
- I-133
- I-134
- I-135
- La-140
- La-141
- La-142
- Mo-99
- Nb-95
- Nb-97
- Nd-149
- Pd-109
- Pm-148
- Pm-148m
- Pm-149
- Pm-151
- Pr-142
- Rb-86
- Rh-105
- Ru-103
- Ru-105
- Ru-106/Rh-106
- Sb-122
- Sb-124
- Sb-125
- Sb-126
- Sb-127
- Sb-129
- Sb-130
- Sb-131
- Se-83
- Sm-153
- Sr-91
- Sr-92
- Te-127
- Te-127m
- Te-129
- Te-129m
- Te-131
- Te-131m
- Te-132
- Te-133
- Te-133m
- Te-134
- Y-92
- Y-93
- Zr-95
- Zr-97/Nb-97m

Group 2: Non-Gamma-emitting Fission Products

- Pm-147
- Pr-143
- Pr-145
- Sr-89
- Sr-90
- Te-125m
- Y-90
- Y-91

MCNP Input Files

- Previously validated Model of TPM-903B portal monitor
- MIRD anthropomorphic Phantom
  - Adipose Male
  - Child
- Group 1 fission products run individually with source definition populated by gamma energies and intensities
  - Energy cut off: 40keV
  - Intensity cut off: 0.5%
- Unit volume source placed in each organ of interest
- F8 Pulse-height tally for each organ of interest

MCNP Output

- Response of detector model for each source organ, separated into energy bins
- Sum over energy bins (above 60keV) to get tally for each organ
- Counts per second per source particle for each organ of interest
- CPS/Bq

Biokinetic Data

- Dose and Risk Calculation Software (DCAL)
- Inputs:
  - Inhalation Class: F, M, S
  - Absorbed Dose
  - Age: 25 years
  - Environmental Exposure
  - AMAD 1μm
- Determine fission product activity distribution in body organs as a function of time

Inhalation Classes

Fission Products	Inhalation Class
Ba-137m, Ba-140, Cs-134, Cs-136, Cs-137, I-131, Sr-89, Sr-90	Fast
Eu-152, Eu-154, Eu-155, Eu-156, La-140, Sb-124, Sb-125, Sb-126m, Sb-126, Se-79, Sm-151, Tc-99, Te-123m, Te-125m, Te-127m, Te-127, Te-129m, Te-129, Zr-93, Zr-95	Moderate
Ce-141, Ce-144, Nb-93m, Nb-95m, Nb-95, Nd-147, Pm-147, Pm-148m, Pm-148, Pr-143, Pr-144, Rh-103m, Rh-106, Ru-103, Ru-106, Y-90, Y-91	Slow

Source: Oak Ridge National Lab

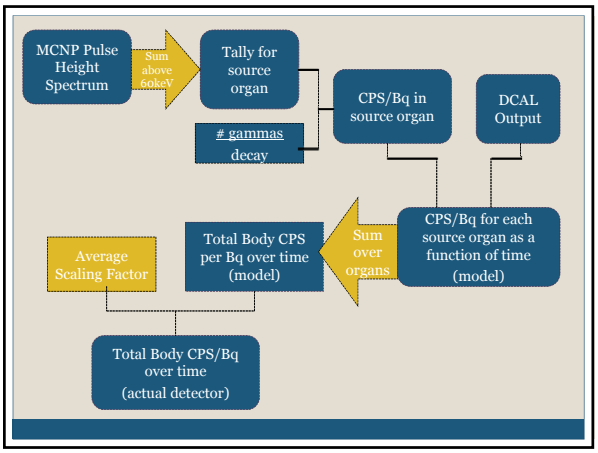

Count Rate for Mixture of Fission Products

$$C_{Mix} = \frac{\sum_F A_F \times RF_F \times C_F}{\sum_F A_F \times RF_F}$$

$$DC_{eff} = \frac{\sum_F A_F \times RF_F \times DC_F}{\sum_F A_F \times RF_F}$$

$$\frac{C_{Mix}}{mSv} = C_{mix} / DC_{eff} = \frac{\left[\frac{\sum_F A_F \times RF_F \times C_F}{\sum_F A_F \times RF_F}\right]}{\left[\frac{\sum_F A_F \times RF_F \times DC_F}{\sum_F A_F \times RF_F}\right]} = \frac{\sum_F A_F \times RF_F \times C_F}{\sum_F A_F \times RF_F \times DC_F}$$

$$\frac{C_{Mix}}{250mSv} = \frac{\sum_F A_F \times RF_F \times C_F}{\sum_F A_F \times RF_F \times DC_F} \times 250$$

Group 1 Count Rates

Days following exposure	Total Body Count cps per 250 mSv
0.25	3.69E+05
0.5	3.27E+05
1	2.94E+05
2	2.52E+05
3	2.19E+05
4	1.90E+05
5	1.66E+05
6	1.47E+05
7	1.31E+05
8	1.18E+05
9	1.07E+05
10	9.78E+04
20	5.03E+04
30	2.99E+04

Group 2 Fission Products

- Dose coefficients take into account all forms of radiation emitted
  - Contribution from Group 1 fission products—including non-gamma particles—has already been accounted for
- Group 2 fission products are all strictly beta emitters
- Ratio of weighted dose coefficients from Group 1 to the weighted dose coefficients from both Groups 1 and 2

Gamma/Beta Ratio

$$Ratio = \frac{\sum DC_F^1 \times R_F^1 \times A_F^1}{\sum DC_F^1 \times R_F^1 \times A_F^1 + \sum DC_F^2 \times R_F^2 \times A_F^2}$$

DC → dose coefficient
R → normalized release fraction
A → normalized activity
1 → Group 1 fission products
2 → Group 2 fission products

Adipose Male : 0.953

Trigger Levels

Days following exposure	Total Body Count cps per 250 mSv
0.25	3.52E+05
0.5	3.12E+05
1	2.80E+05
2	2.40E+05
3	2.08E+05
4	1.81E+05
5	1.58E+05
6	1.40E+05
7	1.25E+05
8	1.12E+05
9	1.02E+05
10	9.32E+04
20	4.79E+04
30	2.85E+04

Detector Sensitivity

- Detector dead time and pulse-pile up become significant at count rates approaching 60,000 CPS
- Instrument sensitivity allows for screening levels lower than 250 mSv

Overall Conclusions

- A variety of available instruments can be used for 1st level screening
- Not surprisingly, Am-241 is difficult to screen for
- Portal monitors are very sensitive

Dose to Healthcare Givers

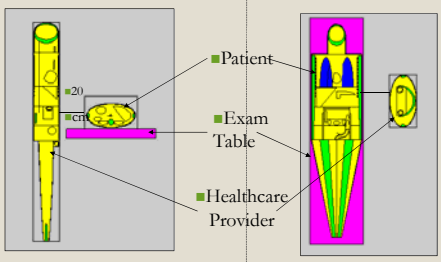

Externally Contaminated Victims

- Sandia explosives testing – maximum external contamination level of 37 GBq/m² for a victim surviving the explosion
- 2-mm thick uniform volume source
- Other contamination levels are multiples of results

Healthcare Provider Effective Dose Due to 37 GBq/m² of External Contamination of ^{137}Cs on the Victim

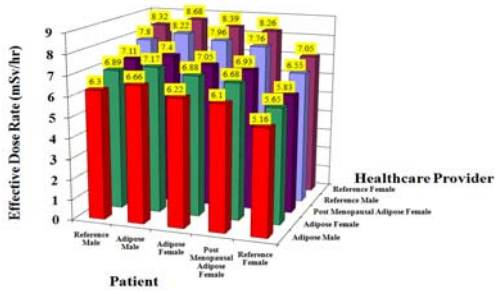

Internally Contaminated Victims

- 1 ALI Internal Contamination
- DCAL used to determine the distribution of the radioactive material over time
- Inhalation classes
  - Determined according to the rate of clearance of the material from the pulmonary region of the lungs
  - Slow, moderate and fast

Effective Dose Rate to Healthcare Provider Due to Patient Internally Contaminated with ^{60}Co

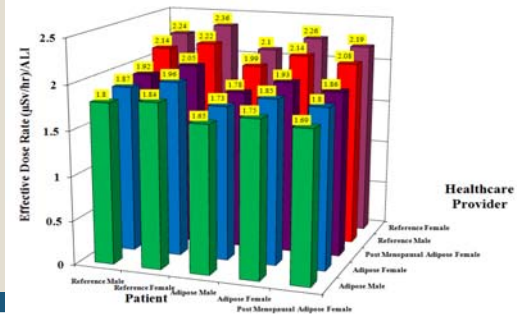

Effective Dose Rate to Healthcare Provider Due to Patient Internally Contaminated with ^{241}Am

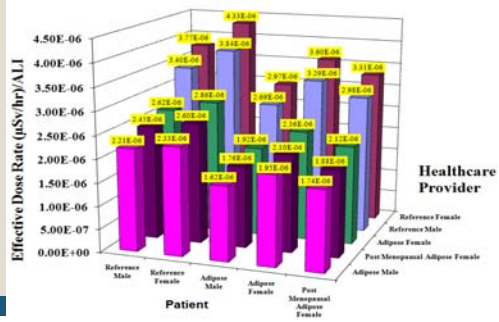

Effective Dose Rate to Healthcare Provider Due to Patient Internally Contaminated with ^{131}I

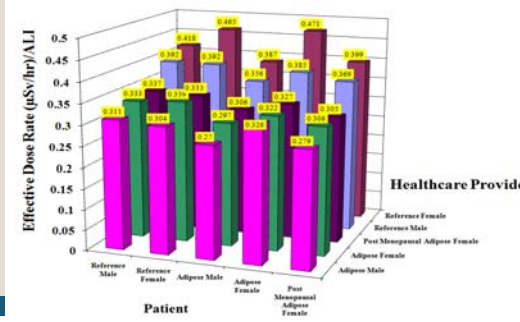

What I Learned as a Talking Head

- Difference between Radioactivity and Radiation is not understood
- Does the General Public understand logarithmic scales for reporting accidents and earthquakes, for that matter
- Are all nuclear accidents slowly evolving compared to other "disaster"
  - BTW, what is a catastrophic disaster
- How meaningful is just a count rate?
- DHHS Radiation Emergency Medical Management webpage is a good resource
  - http://www.remm.nlm.gov/index.html
- The wrong people talk; the "best" qualified people are not allowed to talk!

Hertel on the Weather Channel

- http://pri-nat1.mediavsn.net/MVSavedClips/548d604b-507a-46b5-8cc4-b1915508e0b1.wmv

Simulation and Testing of Radiation Detection Instruments as Monitors of Internal Contamination Levels

Capintec Captus 3000 Thyroid Uptake System Final Report

Team Hertel Research Group

Principal Investigator - Nolan E. Hertel, Ph.D., P.E.

Nuclear and Radiological Engineering Program
George W. Woodruff School of Mechanical Engineering
Georgia Institute of Technology
Atlanta, GA

Technical Report GT_TH-11-01, Rev. 0.
(Merged Technical Reports GT-TH-08-03& GT-TH-09-01, Rev. 1.0)
Issued: September, 2011

Work funded by the
Radiation Studies Branch
Centers for Disease Control and Prevention
through TKCIS

Simulation and Testing of Radiation Detection Instruments as Monitors of Internal Contamination Levels: Capintec Captus 3000 Thyroid Uptake System

Team Hertel Research Group
Principal Investigator: Nolan E. Hertel, Ph.D., P.E.
Nuclear and Radiological Engineering Program
George W. Woodruff School of Mechanical Engineering
Georgia Institute of Technology
Atlanta, GA

Work funded by the
Radiation Studies Branch
Centers for Disease Control and Prevention
through TKCIS

Project Background

The terrorist threat presents numerous challenges for public health professionals. One such challenge is the rapid and effective triage of potentially contaminated victims of a Radiological Dispersal Device (RDD) event. In such an event, victims would potentially be both internally and externally contaminated. Methods for assessing external contamination are more well-defined than those for internal contamination. The preferred method to assess internal contamination is the use of traditional whole body counters; however, that level of sensitivity is not required for triaging and such counters are limited in availability. The present work was undertaken to assess whether thyroid uptake collimators can be used to assess internal contamination following the inhalation or ingestion of radionuclides emitted from an RDD.

Principal Authors
Sarah Scarboro
Randahl Palmer
Nolan Hertel

Supporting Research Performed by
Emily Freibert
Ryan Manger
Eric Burgett
Rebecca Howell
Jason Stewart

TABLE OF CONTENTS

LIST OF TABLES

LIST OF FIGURES

NOMENCLATURE

Americium 241	(^{241}Am)
Activity Median Aerodynamic Diameter	(AMAD)
Barium 133	(^{133}Ba)
Barium 137m	(^{137m}Ba)
Becquerel	(Bq)
Cesium 137	(^{137}Cs)
Centers for Disease Control and Prevention	(CDC)
Cobalt 60	(^{60}Co)
Committed Effective Dose	(CED)
Counts per Second	(CPS)
Department of Energy	(DOE)
Dose and Risk Calculation Software	(DCAL)
International Commission on Radiological Protection	(ICRP)
Iodine 131	(^{131}I)
Iridium 192	(^{192}Ir)
Manganese 54	(^{54}Mn)
Medical Internal Radiation Dose	(MIRD)
miliSievert	(mSv)
Monte Carlo N-Particle Transport Code	(MCNP)
National Council on Radiation Protection and Measurements	(NCRP)
Nuclear Regulatory Commission	(NRC)
Oak Ridge National Laboratory	(ORNL)
Polymethyl Methacrylate	(PMMA)
Radiological Dispersal Device	(RDD)
Radiological Toolbox	(Rad Toolbox)
Region of Interest	(ROI)
Sodium 22	(^{22}Na)

1. Synopsis of Results

This work investigated the use of a common medical device, a thyroid uptake system or thyroid probe, in assessing internal contamination received by an individual following a Radiological Dispersal Device (RDD) event. The Captus 3000 model Thyroid Uptake System, manufactured by Capintec, Inc. was chosen for this work due to the widespread use of this model throughout hospitals and medical offices in the United States. The standard thyroid uptake collimator includes a 2 x 2 Ø NaI detector and was modeled using the Los Alamos N-Particle Transport Code MCNP 5 [(1)]. This model was validated through comparisons to benchmark measurements made using a polymethyl methacrylate (PMMA) slab phantom and gamma-ray point sources. The validated MCNP model was then used in conjunction with MCNP models of the MIRD male and female anthropomorphic phantoms to simulate the count rate of the detector system to inhaled or ingested radionuclides. The MIRD phantoms are stylized phantoms based on the reference man and were originally developed at Oak Ridge National Laboratory [(2)].

The MCNP5 models used in this work are modified versions of MCNP input files for the male and female phantoms created at Pacific Northwest National Laboratory [(3)]. Three additional anthropomorphic phantoms have been generated at Georgia Tech for use in dose conversion coefficient studies by adding adipose tissue on the male and female phantoms [(4,5)]. Finally, a 10-yr old androgynous child phantom was used to simulate of the count rates from the internal contamination of a child. The child phantom was generated using the Bodybuilder code [(6)]. In total, six phantom models were used to calculate the count rate response of the Captus 3000 Thyroid Uptake System assuming a committed effective dose, CED, of 250 mSv. A CED of 250 mSv was chosen for this study because it corresponds to the recommended treatment threshold set forth by National Council on Radiation Protection and Measurements (NCRP) Publication 161 [(7)]. The isotopes under consideration were ^{241}Am, ^{60}Co, ^{137}Cs, and ^{192}Ir and were selected because they have been identified as "isotopes of greatest concern" by the Nuclear Regulatory Commission and Department of Energy Working Group (NRC/DOE) on RDDs[(8)]. The "isotopes of greatest concern" were determined by radiological toxicity, quantity and accessibility, half-life, and dispersibility[(8)]. In addition, the response to internal contamination of ^{131}I was modeled at the request of the Centers for Disease Control and Prevention (CDC). This work determined that the Captus 3000 Thyroid Uptake System can detect a CED of 250 mSv of ^{137}Cs, ^{60}Co, ^{131}I and ^{192}Ir with counting times of one minute or less. The device was not able to detect a CED of 250 mSv of Am-241 within a reasonable counting time (less than 10 minutes detector live time). Despite this, the count rate tables and graphs for Am-241 were created and are included in Appendices A and B.

The count rate threshold values resulting from internal contamination of a CED of 250 mSv for each isotope and phantom combination have been compiled in a series of tables. For inhalation the count rates were evaluated for all six phantom types and all of these tables and corresponding graph are included in Appendix A. Count rates per CED of 250 mSv after ingestion were calculated for the Reference Male, Adipose Male and Child phantoms, since these phantoms provided the most conservative screening criteria for triage. Ingestion graphs and tables are presented in Appendix B.

For use in the Capintec Emergency Screening Protocol software, three representative phantom types were chosen for inhalation and ingestion: Adult (Reference Male), Adipose Adult (Adipose Male) and Pediatric (Child). These tables are of particular interest for this project, and are presented in Results. Each table shows the count rate data for multiple detection locations, with the maximum count rate position highlighted in yellow.

2. Purpose

The release of radioactive materials can pose a potential health threat to society. One type of radioactive release of concern is an RDD, which is any method of dispersing radioactive material; this can be done through active or passive means. An active method would be through an explosive, referred to as a dirty bomb; while examples of passive methods include an aerial release of a radionuclide or contamination of a water supply. When radioactivity is released in an RDD, human beings may be subject to internal dose via inhalation or ingestion if they are in the vicinity of the RDD. In highly populated areas, the use of an RDD could result in thousands of potentially contaminated individuals. The ability to determine which victims of an RDD are at risk due to inhalation or ingestion of a significant amount of radioactivity is important in terms of emergency preparedness and response. Certain medical devices may be used in such a situation to assay internal contamination. The purpose of this work is to identify and further investigate the use of common handheld radiation detectors and medical radiation detectors for their feasibility and applicability in the assay of radioactive materials in humans. Thyroid uptake systems are readily available in most hospitals, and were investigated for their ability to effectively detect levels of internal contamination that would require medical follow-up for the victim. The final products of this work are count rate thresholds indicating a CED of 250 mSv of inhalation or ingestion for use in Capintec's Emergency Screening Protocol module. This software will provide a built-in procedure for technicians to rapidly and efficiently prioritize potential victims for further screening and possible medical treatments.

3. Method of Analysis

To determine the response of the Captus 3000 Thyroid Uptake System to various isotopes and human phantom types, a series of measurements and models were used. Benchmark measurements were made with a polymethyl methacrylate (PMMA) slab phantom and a variety of gamma-ray emitting isotopes using the standard thyroid uptake collimator. PMMA was chosen due to the similarities of its properties to body tissue in radiation dosimetry studies. Using the Captus 3000 Multi-Channel Analyzer (MCA) interface, pulse-height spectral measurements were performed for PMMA slab thickness ranging from 0mm to 108mm in 6mm increments for six different isotopes. Three of the sources chosen for the benchmark measurements (Cs-137, Am-241, and Co-60) were selected based on those noted as being "isotopes of greatest concern" for RDDs [8]. These isotopes are also used in the calculation of detector response using the anthropomorphic phantom models. In addition, three other isotopes were selected based on availability to encompass a broad range of gamma-ray energies in the slab tests.

Following the laboratory measurements using the thyroid uptake system, an MCNP model of the PMMA slab phantom with each source was constructed. In addition, a detailed model of the thyroid uptake collimator and associated NaI detector was constructed in MCNP format. A pulse-height tally (the energy distribution of pulses) was performed over the NaI crystal to directly imitate the MCA interface of the device itself. The energy spectrum was divided into 1024 channels, with one channel equal to 2keV. The count rate in the Region of Interest (ROI) surrounding the photopeak from MCNP was compared to the experimental measurements for each respective isotope to validate the detector model. The ratio of the measured response to the calculated response was computed and analyzed at all PMMA thicknesses to ensure that the detector model was valid regardless of attenuator thickness. In an ideal simulation, this ratio should be unity regardless of attenuator thickness. However, effects not included in the modeling as well as variation in material compositions/densities and unknown variations in detector dimensions can lead to ratios that are not unity. Additionally, mismatches in the detector resolution in the simulation and for the actual detector can contribute to any such differences. In this case, the mean value of the ratio for a given isotope over all thicknesses, called the scaling factor, can be used to adjust the simulated response for other more complicated geometries.

In order to simulate the use of the thyroid uptake system with an actual human, six anthropomorphic human phantom MCNP models were used. The validated detector MCNP model was placed at four location for inhalation (neck, right back chest, right back chest, and left leg) on the reference male phantom and three locations for inhalation (neck, right back chest, and left leg) on the remaining five phantoms. For ingestion four locations (neck, right back chest, left leg, and umbilicus) were used for the adipose male and the child phantoms. A unit source of each of the gamma emitting isotopes cited as potential RDD radioisotopes was distributed in the organs of interest for each phantom. The organs of interest were determined using Dose Calculation Software (DCAL) biokinetic modeling to determine where each isotope would concentrate over a period of 30 days after inhalation or ingestion [9]. The time-dependent activities in each of these organs were then determined using DCAL [9]. Simultaneous pulse-height tallies were performed over the crystal volume at each detector position. For each phantoms type, the MCNP computed data for a unit source in each organ was folded with time-dependent source activity data to determine the count rate corresponding to a committed effective dose of 250 mSv of inhaled or ingested radioactivity. The scaling factors were then applied to the computed count rates to project the count rates that would be observed in practice.

4. Model Specifications and Assumptions

4.1. Model Specifications

The Captus 3000 consists of a 2” x 2” Ø NaI detector surrounded in one of two collimators, each composed of a lead and antimony composite material. The more standard of the two collimator types is the thyroid uptake collimator, which extends approximately 16cm from the detector face.

The second collimator is a shorter bioassay collimator, which extends approximately 6cm from the detector face. Each collimator is mounted on an articulating spring arm, which can be positioned as needed. The standard thyroid uptake collimator was selected for this work. Dimensions were measured on the physical device, and then verified using drawings provided by the manufacturer.

The following materials were used in the computations:

- The PMMA material for the slab phantoms had a density of 1.19 g/cm^3 and consisted of 33.3% carbon, 13.3% oxygen, and 53.3% hydrogen [10].
- The backscatter portion of the PMMA slab phantom was Virtual Water™ supplied by the CNMC Company, 865 Easthagan Dr., Nashville, TN, USA. The density used for Virtual Water was 1.03 g/cm^3 and the composition, by weight percent, used was:
  - 8.02% hydrogen
  - 67.03% carbon
  - 2.14% nitrogen
  - 19.91% oxygen
  - 0.14% chlorine
  - 2.31% calcium
- The NaI crystal was manufactured by Saint Gobain, and was surrounded by 0.508mm of pure aluminum with a density of 2.7 g/cm^3.
- The photomultiplier tube is mounted directly against the back of the crystal, and was modeled as an enclosed cylindrical vacuum in the model.
- A detector side shield (3.175mm thick lead) wraps around the detector and connects to the collimator. The density of the lead was 11.4g/cm^3.
- The collimator is primarily composed of an antimony and lead material (4% antimony). The density of this material is 11.4 g/cm^3.
- AISI 1000 type steel was used for the steel layer surrounding the collimator. The composition of the steel by atom fraction is as follows [10]:
  - 0.002786 carbon
  - 8.687E-5 oxygen
  - 7.1946E-5 phosphorus
  - 0.003549 manganese
  - 0.9935 iron

In addition, the isotopes and the corresponding gamma ray energies used in the point source measurements and in the anthropomorphic phantom models, based on the recommendations from the NRC/DOE report on RDDs, are listed below in Table 1[8]. Emission data were taken from RadToolbox[11].

Table 1. Isotopes Used in Point Source Measurements and MCNP Phantom Models

Isotope	Photon Energy (MeV)	Photon Emission Intensity
^{241}Am	0.059, 0.026, 0.021, 0.0179, 0.0177, 0.017, 0.0168, 0.0139, 0.0137	0.357, 0.024, 0.045, 0.019, 0.188, 0.022, 0.058, 0.219, 0.024
^{133}Ba	0.384, 0.356, 0.303, 0.276, 0.081, 0.035, 0.031, 0.030	0.089, 0.622, 0.184, 0.071, 0.338, 0.122, 0.631, 0.341
^{60}Co	1.332, 1.1730	0.999, 0.999
^{137}Cs	0.662, 0.0322, 0.0318	0.898, 0.0392, 0.0213
^{131}I	364, 637, 284, 80.2, 29.8, 723, 29.0	0.812, 0.0727, 0.0606, 0.0262, 0.0259, 0.0180, 0.0140
^{192}Ir	317, 468, 308, 296, 604, 612, 66.8, 589, 206, 485, 65.1, 63, 9.44, 11.1, 61.5, 75.2	0.828, 0.478, 0.297, 0.29, 0.0818, 0.0533, 0.0458, 0.0452, 0.0329, 0.0316, 0.0267, 0.0218, 0.0151, 0.0132, 0.0127, 0.0103
^{54}Mn	0.8348	0.999
^{22}Na	1.275, 0.511	0.999, 1.798

The assay data for the isotopes used in the point source measurements are shown below in Table 2.The cross section libraries used in the MCNP simulations were MCPLIB04 which was officially released in 2002 and derived from the ENDF/B-VI.8 data library, which are derived from EPDL97 [(1)].

Table 2. Assay Data of Isotopes Used in the Slab Measurements

Isotope	Assay Date	Initial Activity (µCi)	Half Life (y)	Experiment Date	Experiment Activity (µCi)
^{241}Am	12/09/05	7.50	432	08/02/07	7.48
^{133}Ba	12/13/05	5.2	10.7	08/03/07	4.67
^{60}Co	12/09/05	5.1	5.27	08/03/07	4.11
^{137}Cs/^{137m}Ba	12/09/05	4.9	30.0	08/06/07	4.72
^{54}Mn	12/09/05	5.00	0.86	07/09/07	1.45
^{22}Na	12/09/05	5.0	2.60	07/09/07	3.33

4.2. Assumptions

In order to characterize the detectors for use in the event of an RDD, several assumptions were made. The first assumption made was that all external contamination will be removed by showering and changing clothing before the victim enters the portal monitors. In addition, the

results of this research will only be used for first stage triage of internal contamination. The count rates presented correspond to a committed effective dose of 250mSv and further evaluation is needed for people with count rates equal to or higher than the listed count rates. It is also assumed that only one isotope is used in the RDD, and that the isotope has been identified prior to triage. Finally, it was assumed that the first cut screening of the victim will occur between six hours and 30 days after the time of contamination of the victim and that the initial time of inhalation or ingestion by the victim is known.

5. Analysis

5.1. Slab Benchmark Measurements

Benchmark measurements were performed using a slab phantom as part of the methodology to validate the MCNP model of the thyroid uptake collimator. The slab phantom was composed of 100 mm of Virtual Water™ and PMMA slabs of different thicknesses. The virtual water served to simulate backscatter that would occur from tissue behind a source in the body. The various thicknesses of PMMA served to represent the attenuation effect of tissue between the source and the detector on the surface of the body. PMMA and virtual water were chosen as the attenuating material in the phantom due to their tissue equivalent properties with regard to photons. A source holder consisting of a 6 mm slab of PMMA with a small cylindrical source at its center was positioned in front of the virtual water. Then varying thicknesses of PMMA were positioned between the source and the detector face. Measurements were taken at PMMA thicknesses between 0 mm and 108 mm of PMMA at 6 mm increments for each of the following isotopes: ^{241}Am,^{133}Ba, ^{137}Cs, ^{60}Co, ^{54}Mn, and ^{22}Na. A maximum statistical counting error of 1% was allowed in the Region of Interest (ROI) surrounding the photopeak. The collimator opening of the thyroid probe was positioned flush against the PMMA slab. A typical measurement setup with the slab phantom and thyroid uptake collimator is shown in Figure 1.

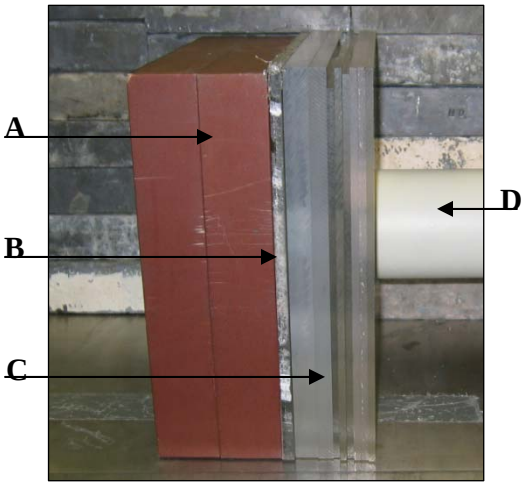

Figure1. PMMA Slab Phantom. (A) Virtual Water (B) Source Holder (C) PMMA Slabs (D) Thyroid Uptake Collimator

5.2. MCNP5 Model of Detector and Slab Benchmark

The slab phantom and thyroid uptake collimator were modeled in MCNP5 to simulate the benchmark measurements. The actual thyroid uptake collimator is shown in Figure 2A, and the MCNP model of the device is shown in Figure 2B. An MCNP input was created for each PMMA thickness corresponding to the various laboratory measurements. The sources and source holder were also defined in the model. The detector response was simulated using a pulse-height tally (F8 tally) over the detector crystal. The pulse height spectra were compared to those collected in the laboratory by means of the count rate in the defined ROI surrounding the photopeak. The ROIs for each isotope were defined using the Capintec Nuclide Identification software. By examining the ratio of the measured count rate in the ROI to the calculated count rate in the ROI for each attenuation thickness, the MCNP model was verified and a count rate scaling factor was determined for each isotope for use with the MCNP model. A constant ratio between these values over varied attenuator thickness deemed the MCNP model valid for use with the anthropomorphic phantoms. Scaling factors for each radioisotope used in the measurements are presented in Results. An example input file for the slab phantom and thyroid uptake collimator is provided in Appendix C.

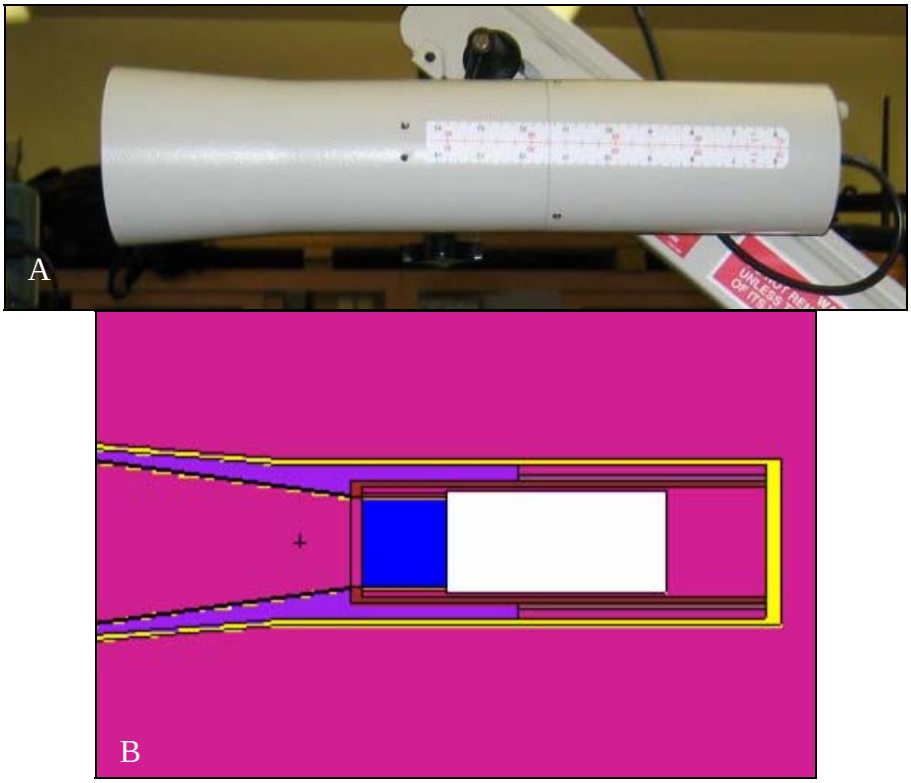

Figure 1. Collimator Images.(A) Captus 3000 thyroid uptake collimator. (B) MCNP model of thyroid uptake collimator as displayed in VisEd[12].

5.3. MCNP5 Model of MIRD and Bodybuilder Phantoms

Upon verification of the detector model, the following anthropomorphic phantoms were used in MCNP simulations: Reference Male, Reference Female, Adipose Male, Adipose Female, Post-Menopausal Adipose Female, and Child. The Reference Male and Reference Female phantoms are based on the Medical Internal Radiation Dose (MIRD) model and the 10 year old child was based on the Bodybuilder Phantom [6].The reference phantoms were originally developed at Oak Ridge National Laboratory and the MCNP inputs for the adipose male and female phantoms are extensions of the reference male and female phantom MCNP inputs created by Pacific Northwest National Laboratory [2,3]. Further work performed by Simpkins and Hertel at Georgia Institute of Technology included the addition of adipose tissue to create the three adipose phantoms as well as the addition of the esophagus and intestine wall among other things [4,5]. The anthropomorphic phantom models can be characterized by their height, total mass and mass of adipose tissue. The Body Mass Index (BMI) is a useful tool for measuring body type for adults age 17 and over. The BMI is calculated by taking the ratio of the mass (kg) to the square of the height (m). Detailed information on each of the anthropomorphic phantoms used in this study is shown in Table 3.

Table3. Characteristics of the Anthropomorphic Phantoms

Phantom Type	Height (cm)	Mass (kg)	BMI
Reference Male	179	70	22
Reference Female	168	58	21
Adipose Male	179	92	29
Adipose Female	168	73	26
Post-Menopausal Adipose Female	168	85	30
10-year Androgynous Child	140	32.7	n/a

The isotopes investigated concentrate in different organs when inhaled and ingested. The organs that would be affected were first determined for each isotope and phantom type. For a particular isotope-phantom pairing, a unit source was placed in each of the affected organs and a pulse-height tally was performed to determine the counts per unit source in the organ. For inhalation the detector was placed in four locations on the reference man, the front of the neck, the right side of the chest, the right side of the back, and the outside of the left leg. For the remaining phantoms, the detector was placed in the front of the neck, the right side of the back, and the outside of the left leg. For ingestion the detector was also placed on the umbilicus for all phantoms. An example MCNP input file for the Reference Male phantom is presented in Appendix C. The resulting data obtained from the MCNP5 phantom simulations were the count

rates at a specific detector location due to a unit source in each organ. However, to replicate the actual count rate of the detector, the MCNP results were multiplied by the scaling factor determined using the benchmark measurements. Each phantom had a matrix of source organ-detector count rate pairings for each detector location and source organ.

5.4. DCAL Source Distribution and Count Rate per 250 mSv

The isotopes under consideration were ^{241}Am, ^{60}Co, ^{137}Cs, and ^{192}Ir and were selected based on NRC/DOE recommendations and ^{131}I was studied at the request of the CDC [8]. The Oak Ridge National Laboratory Dose and Risk Calculation software (DCAL) was used to determine the radioactive source distribution in the body as a function of post-ingestion time [9]. The adult DCAL was used in determining the count rate for the child. This was chosen because it resulted in a lower count rate for a committed effective dose 250 mSv than the use of child DCAL, leading to more conservative selection criteria. The fraction of activity in the blood was distributed within the organs of the body according to ICRP Publication 89[13]. The parameters which can be varied in DCAL include: radionuclide, mode of uptake, method of uptake, particle size, and inhalation classes. The mode of uptake was set to inhalation or ingestion and the method of uptake was set to environmental with an acute intake assumed. The aerosol particle size was set to the default size of 1µmactivity median aerodynamic diameter (AMAD).The inhalation classes were chosen based on recommendations from ICRP Publication 72 and the inhalation classes were used in the selection of dose coefficients [14, 15].The inhalation class was set to moderate for ^{241}Am, ^{60}Co, and ^{192}Ir and fast for ^{137}Cs and ^{131}I. The dose coefficients for each isotope were obtained from RadToolbox, which used ICRP 72 data [15].Dose coefficients were given in Bq/rem. The dose coefficients were converted to Bq/(250 mSv) by multiplying by 25 rem. Finally, the count rate (CPM) per 250 mSv as a function of time was calculated using the source distribution over time from DCAL, the ICRP 72 dose coefficients, and the count rates per unit source in each organ computed previously with MCNP5.

6. Results

The first step in determining internal contamination levels using the Captus 3000 Thyroid Uptake Collimator, was the acquisition of benchmark measurements used to validate an MCNP model of the Captus 3000. The validation of the MCNP model led to scaling factors that relate the model to the measured values. Once the detector model was validated the MNCP model was combined with MIRD Phantoms to determine the count rate corresponding to a committed effective dose of 250 mSv. The results of these steps are presented in this section.

6.1 Model Validation

For ^{133}Ba, ^{60}Co, ^{137}Cs,^{54}Mn and ^{22}Na, the count rates from the MCNP simulations were compared to the benchmark measurement in order to validate the detector model. The ratios of the simulated count rates to the measured readings were computed and analyzed for all PMMA thicknesses. In an ideal simulation the MCNP output would be exactly the same as the measured count rates resulting in a ratio of one regardless of the thicknesses of attenuation. The scaling factor, which is the mean value of the ratio for a given isotope over all thicknesses, can be used to adjust the simulated response to the response that would be observed by the detector when the anthropomorphic phantom models are used. The calculated scaling factors are shown below in Table 4.

Table 4. Scaling Factors

Isotope	Scaling Factor
^{241}Am	1.31
^{133}Ba	0.93
^{60}Co	1.11
^{137}Cs	0.93
^{54}Mn	1.06
^{22}Na	0.97

The ratios of the simulated count rates to the measured readings for all six isotopes were relatively constant over all thicknesses, with the majority of the error bars overlapping with the scaling factor for each isotope. The ratios with error bars and the average scaling factor for each isotope can be seen in Figures 3-8.

Benchmark measurements were not taken with ^{131}I and ^{192}Ir; therefore their scaling factors were determined by interpolation of a graph of scaling factor versus average energy. Based on the interpolation, the scaling factors for both ^{131}I and ^{192}Ir were approximated to a value of 1.

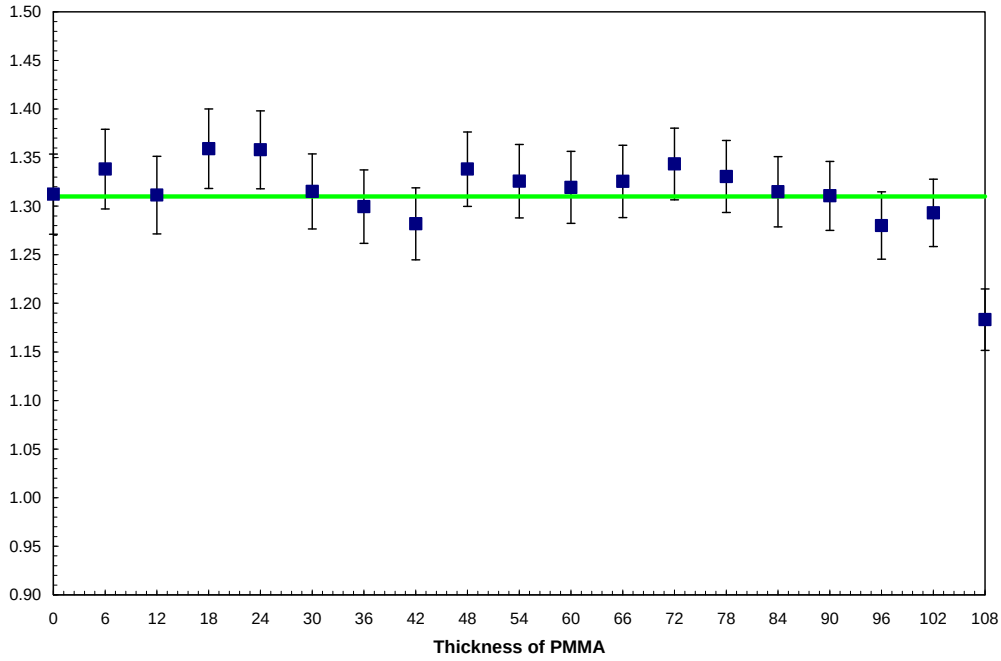

Figure 3. ^{241}Am Scaling Factor (1.31)

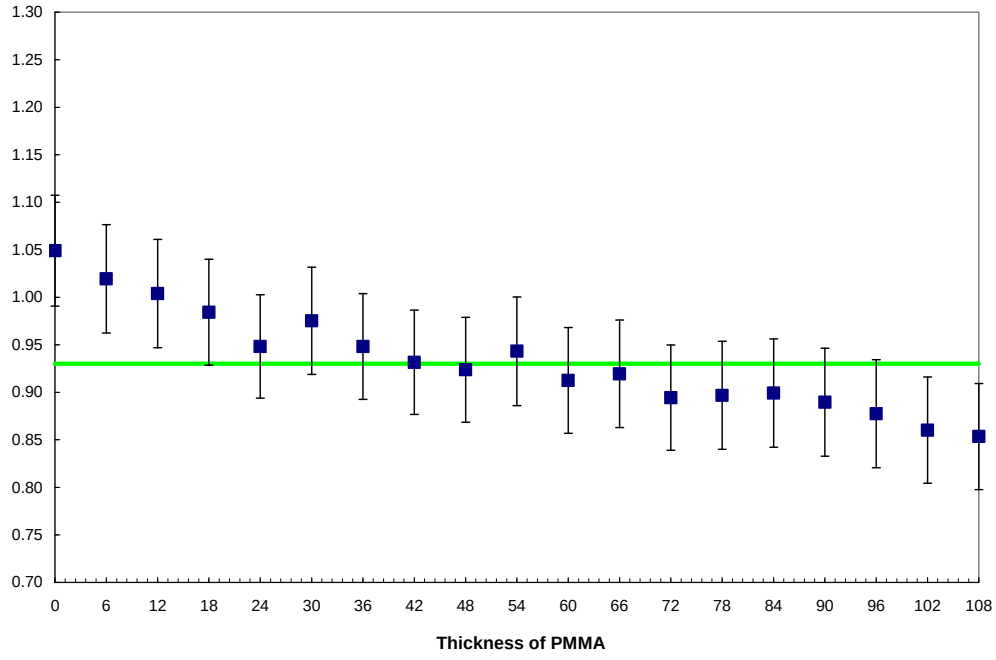

Figure 4. ^{133}Ba Scaling Factor (0.93)

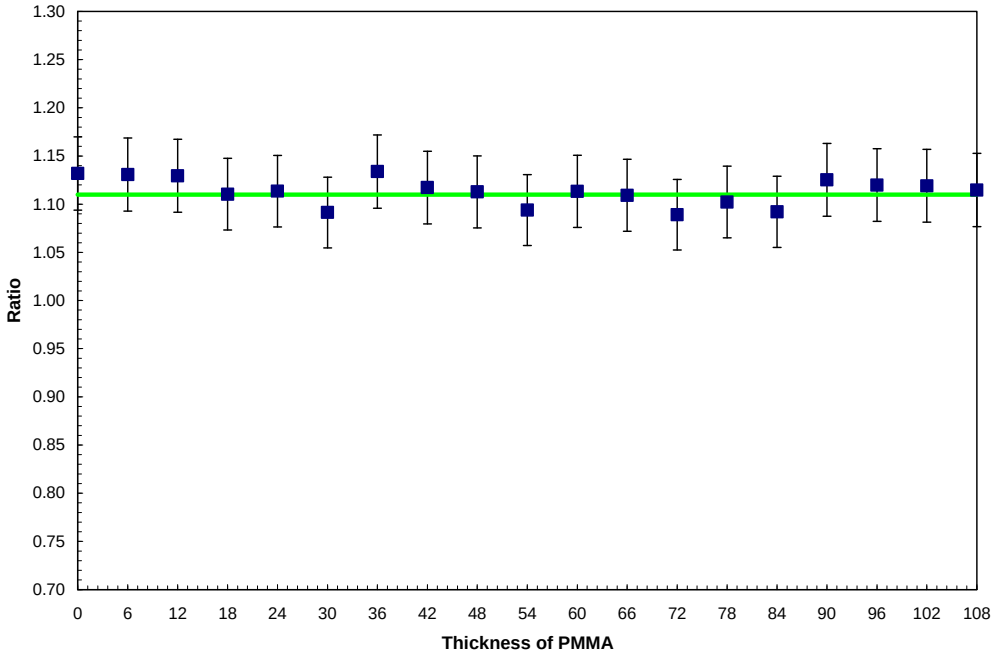

Figure 5. ^{60}Co Scaling Factor (1.11)

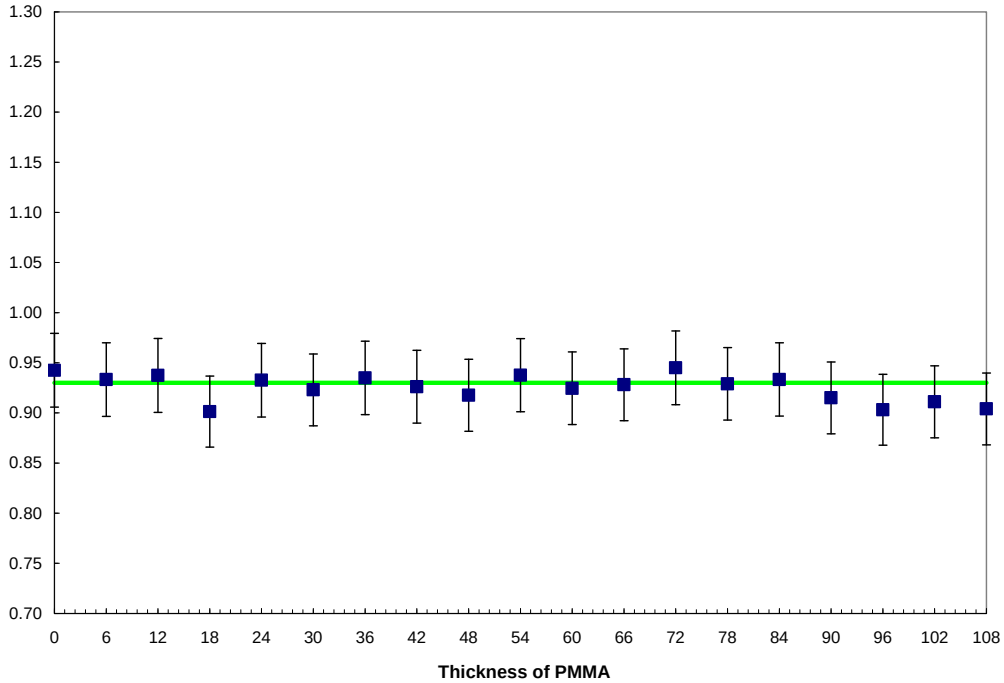

Figure 6. ^{137}Cs Scaling Factor (0.93)

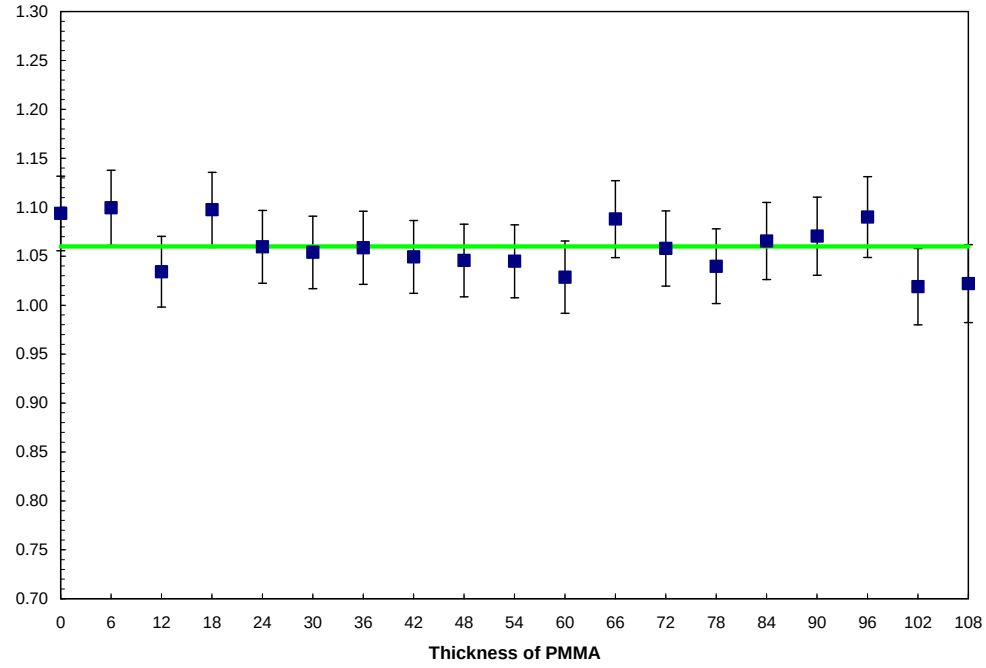

Figure 7. ^{54}Mn Scaling Factor (1.06)

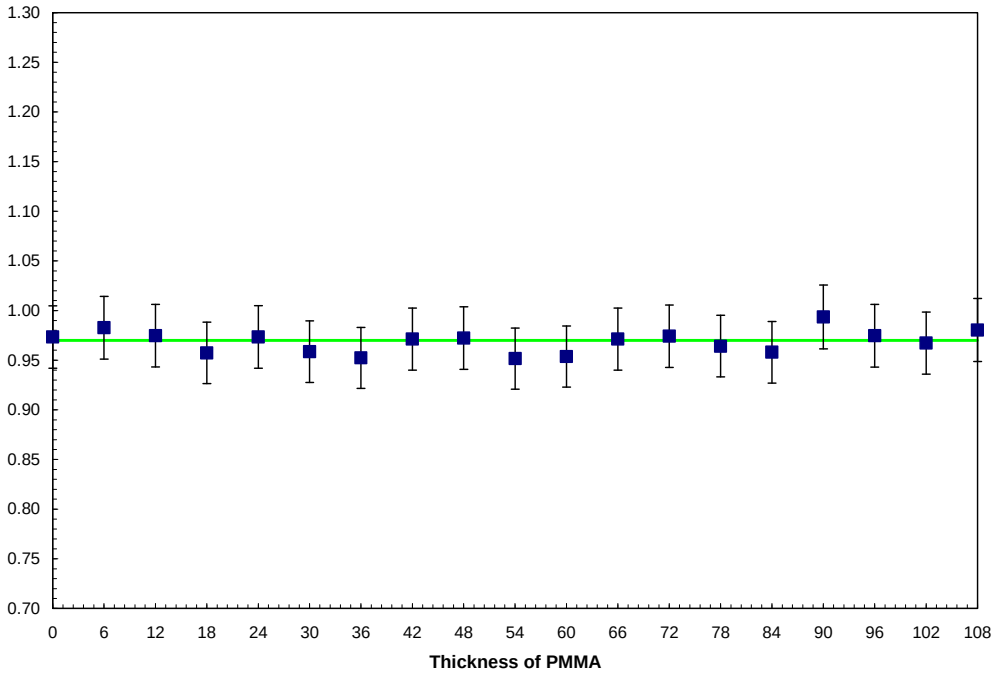

Figure 8. ^{22}Na Scaling Factor (0.97)

6.2 MIRD Phantom Results

With the validation of the MCNP model of the Captus 3000 complete, the Captus 3000's count rates corresponding to a committed effective dose of 250 mSv were determined. Count rates were determined for both the inhalation and ingestion of ^{241}Am, ^{60}Co, ^{137}Cs, ^{131}I and ^{192}Ir. For inhalation, the isotopes were used in conjunction with six anthropomorphic stylized phantoms: Reference Male, Reference Female, Adipose Male, Adipose Female, Post-Menopausal Adipose Female, and 10-Year Old Child. For ingestion the three conservative human phantom types were used: Reference Male, Adipose Male, and 10-Year Old Child. The male phantoms were considered more conservative due to the generally lower count rate than the female counterparts, providing more conservative selection criteria. Also, the size and weight of the Male phantoms provides a closer approximation to the average American (male or female) than do the female phantoms. For these reasons the generalized phantom types that will be used in the Capintec Emergency Protocol Software for assaying internal contamination in the event of an RDD (Adult, Adipose Adult and Pediatric) are based on the male phantom types and the 10-Year Old child. The Captus 3000's count rates corresponding to a committed effective dose of 250 mSv for the three conservative human phantom types are shown below in Tables 5-34.

Table 5. Adult Inhaled ^{241}Am

^{241}Am		Back Right Lung	Front Right Lung	Neck	Thigh
		CPM per 250 mSv	CPM per 250 mSv	CPM per 250 mSv	CPM per 250 mSv
Days following exposure	0	6.28E+00	5.99E+00	4.16E-02	0.00E+00
	1	5.21E+00	4.96E+00	4.84E-02	7.09E-02
	2	5.10E+00	4.85E+00	4.30E-02	4.67E-02
	3	5.03E+00	4.79E+00	4.07E-02	2.74E-02
	4	4.96E+00	4.73E+00	3.97E-02	1.84E-02
	5	4.90E+00	4.67E+00	3.91E-02	1.48E-02
	6	4.84E+00	4.61E+00	3.86E-02	1.35E-02
	7	4.79E+00	4.55E+00	3.82E-02	1.31E-02
	8	4.73E+00	4.50E+00	3.79E-02	1.30E-02
	9	4.67E+00	4.45E+00	3.76E-02	1.30E-02
	10	4.62E+00	4.39E+00	3.73E-02	1.31E-02
	20	4.14E+00	3.93E+00	3.44E-02	1.39E-02
	30	3.75E+00	3.56E+00	3.21E-02	1.46E-02

Table 6. Adult Inhaled ^{60}Co

^{60}Co		Back Right Lung	Front Right Lung	Neck	Thigh
		CPM per 250 mSv	CPM per 250 mSv	CPM per 250 mSv	CPM per 250 mSv
Days following exposure	0	4.39E+04	4.21E+04	1.02E+04	1.04E+03
	1	4.18E+04	4.25E+04	1.22E+04	5.45E+03
	2	3.81E+04	3.75E+04	1.03E+04	4.00E+03
	3	3.60E+04	3.50E+04	9.33E+03	2.79E+03
	4	3.49E+04	3.38E+04	8.83E+03	2.20E+03
	5	3.42E+04	3.30E+04	8.56E+03	1.93E+03
	6	3.36E+04	3.24E+04	8.37E+03	1.79E+03
	7	3.30E+04	3.18E+04	8.21E+03	1.72E+03
	8	3.26E+04	3.14E+04	8.08E+03	1.66E+03
	9	3.21E+04	3.09E+04	7.95E+03	1.62E+03
	10	3.16E+04	3.05E+04	7.83E+03	1.58E+03
	20	2.77E+04	2.67E+04	6.84E+03	1.36E+03
	30	2.46E+04	2.37E+04	6.10E+03	1.24E+03

Table 7. Adult Inhaled ^{137}Cs

^{137}Cs		Back Right Lung	Front Right Lung	Neck	Thigh
		CPM per 250 mSv	CPM per 250 mSv	CPM per 250 mSv	CPM per 250 mSv
Days following exposure	0	6.48E+04	6.21E+04	5.28E+03	4.58E+02
	1	1.73E+04	1.77E+04	1.48E+04	2.01E+04
	2	1.57E+04	1.64E+04	1.44E+04	1.98E+04
	3	1.52E+04	1.59E+04	1.41E+04	1.94E+04
	4	1.49E+04	1.56E+04	1.38E+04	1.90E+04
	5	1.47E+04	1.53E+04	1.36E+04	1.87E+04
	6	1.45E+04	1.51E+04	1.34E+04	1.85E+04
	7	1.43E+04	1.50E+04	1.33E+04	1.83E+04
	8	1.42E+04	1.48E+04	1.31E+04	1.81E+04
	9	1.41E+04	1.47E+04	1.30E+04	1.79E+04
	10	1.40E+04	1.46E+04	1.29E+04	1.78E+04
	20	1.30E+04	1.36E+04	1.21E+04	1.66E+04
	30	1.22E+04	1.28E+04	1.13E+04	1.56E+04

Table 8. Adult Inhaled ^{131}I

^{131}I		Back Right Lung	Front Right Lung	Neck	Thigh
		CPM per 250 mSv	CPM per 250 mSv	CPM per 250 mSv	CPM per 250 mSv
Days following exposure	0	6.57E+04	6.31E+04	5.55E+02	4.35E+01
	1	1.93E+03	2.34E+03	6.30E+04	8.09E+02
	2	2.23E+02	8.45E+02	6.07E+04	1.10E+02
	3	1.32E+02	7.13E+02	5.55E+04	9.23E+01
	4	1.30E+02	6.60E+02	5.05E+04	1.08E+02
	5	1.32E+02	6.15E+02	4.59E+04	1.21E+02
	6	1.32E+02	5.72E+02	4.18E+04	1.30E+02
	7	1.30E+02	5.31E+02	3.81E+04	1.36E+02
	8	1.27E+02	4.92E+02	3.47E+04	1.39E+02
	9	1.23E+02	4.56E+02	3.15E+04	1.39E+02
	10	1.19E+02	4.22E+02	2.87E+04	1.38E+02
	20	6.63E+01	1.86E+02	1.13E+04	8.77E+01
	30	3.07E+01	7.80E+01	4.45E+03	4.24E+01

Table 9. Adult Inhaled ^{192}Ir

^{192}Ir		Back Right Lung	Front Right Lung	Neck	Thigh
		CPM per 250 mSv	CPM per 250 mSv	CPM per 250 mSv	CPM per 250 mSv
Days following exposure	0	1.88E+05	1.80E+05	1.67E+03	9.41E+01
	1	1.53E+05	1.47E+05	3.00E+03	5.55E+03
	2	1.48E+05	1.42E+05	2.74E+03	4.30E+03
	3	1.44E+05	1.38E+05	2.60E+03	3.12E+03
	4	1.41E+05	1.35E+05	2.52E+03	2.56E+03
	5	1.37E+05	1.32E+05	2.47E+03	2.33E+03
	6	1.34E+05	1.29E+05	2.43E+03	2.23E+03
	7	1.31E+05	1.26E+05	2.40E+03	2.19E+03
	8	1.28E+05	1.23E+05	2.36E+03	2.17E+03
	9	1.26E+05	1.20E+05	2.33E+03	2.15E+03
	10	1.23E+05	1.18E+05	2.31E+03	2.14E+03
	20	9.91E+04	9.49E+04	2.06E+03	2.06E+03
	30	8.08E+04	7.74E+04	1.86E+03	1.99E+03

Table 10. Adipose Adult Inhaled ^{241}Am

^{241}Am		Back Right Lung	Neck	Thigh
		CPM per 250 mSv	CPM per 250 mSv	CPM per 250 mSv
Days following exposure	0	3.86E+00	4.21E-02	0.00E+00
	1	3.15E+00	4.46E-02	5.92E-02
	2	3.07E+00	4.04E-02	3.87E-02
	3	3.02E+00	3.87E-02	2.18E-02
	4	2.98E+00	3.78E-02	1.39E-02
	5	2.94E+00	3.72E-02	1.07E-02
	6	2.90E+00	3.67E-02	9.50E-03
	7	2.87E+00	3.64E-02	9.10E-03
	8	2.83E+00	3.60E-02	8.99E-03
	9	2.79E+00	3.56E-02	8.99E-03
	10	2.76E+00	3.53E-02	9.03E-03
	20	2.45E+00	3.23E-02	9.56E-03
	30	2.20E+00	2.98E-02	9.96E-03

Table 11. Adipose Adult Inhaled ^{60}Co

^{60}Co		Back Right Lung	Neck	Thigh
		CPM per 250 mSv	CPM per 250 mSv	CPM per 250 mSv
Days following exposure	0	3.48E+04	8.60E+03	7.24E+02
	1	3.25E+04	1.02E+04	4.64E+03
	2	2.98E+04	8.70E+03	3.34E+03
	3	2.84E+04	7.94E+03	2.25E+03
	4	2.76E+04	7.55E+03	1.71E+03
	5	2.70E+04	7.33E+03	1.47E+03
	6	2.66E+04	7.17E+03	1.35E+03
	7	2.62E+04	7.04E+03	1.29E+03
	8	2.58E+04	6.92E+03	1.25E+03
	9	2.54E+04	6.81E+03	1.21E+03
	10	2.50E+04	6.71E+03	1.18E+03
	20	2.20E+04	5.86E+03	1.01E+03
	30	1.95E+04	5.23E+03	9.25E+02

Table 12. Adipose Adult Inhaled ^{137}Cs

^{137}Cs		Back Right Lung	Neck	Thigh
		CPM per 250 mSv	CPM per 250 mSv	CPM per 250 mSv
Days following exposure	0	4.92E+04	4.14E+03	2.58E+02
	1	1.58E+04	1.29E+04	1.46E+04
	2	1.45E+04	1.26E+04	1.44E+04
	3	1.42E+04	1.23E+04	1.41E+04
	4	1.39E+04	1.21E+04	1.38E+04
	5	1.37E+04	1.19E+04	1.36E+04
	6	1.35E+04	1.17E+04	1.35E+04
	7	1.33E+04	1.16E+04	1.33E+04
	8	1.32E+04	1.15E+04	1.32E+04
	9	1.31E+04	1.14E+04	1.31E+04
	10	1.30E+04	1.13E+04	1.29E+04
	20	1.21E+04	1.05E+04	1.21E+04
	30	1.14E+04	9.89E+03	1.13E+04

Table 13. Adipose Adult Inhaled ^{131}I

^{131}I		Back Right Lung	Neck	Thigh
		CPM per 250 mSv	CPM per 250 mSv	CPM per 250 mSv
Days following exposure	0	4.80E+04	4.65E+02	2.81E+01
	1	1.61E+03	6.28E+04	5.64E+02
	2	2.68E+02	6.07E+04	7.57E+01
	3	1.93E+02	5.54E+04	6.29E+01
	4	1.88E+02	5.04E+04	7.38E+01
	5	1.85E+02	4.59E+04	8.29E+01
	6	1.81E+02	4.18E+04	8.93E+01
	7	1.75E+02	3.80E+04	9.32E+01
	8	1.69E+02	3.46E+04	9.52E+01
	9	1.61E+02	3.15E+04	9.57E+01
	10	1.54E+02	2.87E+04	9.48E+01
	20	8.10E+01	1.13E+04	6.04E+01
	30	3.68E+01	4.44E+03	2.92E+01

Table 14. Adipose Adult Inhaled ^{192}Ir

^{192}Ir		Back Right Lung	Neck	Thigh
		CPM per 250 mSv	CPM per 250 mSv	CPM per 250 mSv
Days following exposure	0	1.37E+05	1.48E+03	4.47E+01
	1	1.10E+05	2.38E+03	4.71E+03
	2	1.06E+05	2.19E+03	3.57E+03
	3	1.04E+05	2.09E+03	2.41E+03
	4	1.01E+05	2.03E+03	1.86E+03
	5	9.89E+04	1.99E+03	1.63E+03
	6	9.67E+04	1.96E+03	1.54E+03
	7	9.45E+04	1.93E+03	1.50E+03
	8	9.24E+04	1.90E+03	1.48E+03
	9	9.03E+04	1.88E+03	1.47E+03
	10	8.83E+04	1.85E+03	1.46E+03
	20	7.11E+04	1.64E+03	1.41E+03
	30	5.79E+04	1.47E+03	1.36E+03

Table 15. Pediatric Inhaled ^{241}Am

^{241}Am		Back Right Lung	Neck	Thigh
		CPM per 250 mSv	CPM per 250 mSv	CPM per 250 mSv
Days following exposure	0	8.70E+00	1.47E-01	0.00E+00
	1	7.12E+00	2.15E-01	2.53E-01
	2	6.95E+00	2.08E-01	1.79E-01
	3	6.84E+00	2.05E-01	1.21E-01
	4	6.75E+00	2.04E-01	9.52E-02
	5	6.66E+00	2.04E-01	8.55E-02
	6	6.57E+00	2.05E-01	8.27E-02
	7	6.49E+00	2.05E-01	8.24E-02
	8	6.41E+00	2.05E-01	8.32E-02
	9	6.33E+00	2.06E-01	8.43E-02
	10	6.25E+00	2.06E-01	8.55E-02
	20	5.56E+00	2.11E-01	9.76E-02
	30	4.99E+00	2.15E-01	1.08E-01

Table 16. Pediatric Inhaled ^{60}Co

^{60}Co		Back Right Lung	Neck	Thigh
		CPM per 250 mSv	CPM per 250 mSv	CPM per 250 mSv
Days following exposure	0	3.73E+04	7.40E+03	2.13E+03
	1	3.56E+04	1.12E+04	6.56E+03
	2	3.22E+04	8.66E+03	4.81E+03
	3	3.06E+04	7.52E+03	3.65E+03
	4	2.97E+04	6.99E+03	3.09E+03
	5	2.90E+04	6.72E+03	2.83E+03
	6	2.86E+04	6.54E+03	2.69E+03
	7	2.81E+04	6.41E+03	2.60E+03
	8	2.77E+04	6.29E+03	2.53E+03
	9	2.73E+04	6.19E+03	2.48E+03
	10	2.69E+04	6.09E+03	2.43E+03
	20	2.36E+04	5.31E+03	2.09E+03
	30	2.10E+04	4.75E+03	1.90E+03

Table 17. Pediatric Inhaled ^{137}Cs

^{137}Cs		Back Right Lung	Neck	Thigh
		CPM per 250 mSv	CPM per 250 mSv	CPM per 250 mSv
Days following exposure	0	1.04E+05	8.67E+03	0.00E+00
	1	4.28E+04	3.15E+04	5.92E+04
	2	3.96E+04	3.08E+04	5.85E+04
	3	3.85E+04	3.00E+04	5.72E+04
	4	3.78E+04	2.95E+04	5.61E+04
	5	3.72E+04	2.90E+04	5.52E+04
	6	3.67E+04	2.86E+04	5.45E+04
	7	3.63E+04	2.83E+04	5.39E+04
	8	3.59E+04	2.80E+04	5.34E+04
	9	3.56E+04	2.78E+04	5.29E+04
	10	3.53E+04	2.75E+04	5.25E+04
	20	3.30E+04	2.57E+04	4.90E+04
	30	3.10E+04	2.41E+04	4.60E+04

Table 18. Pediatric Inhaled ^{131}I

^{131}I		Back Right Lung	Neck	Thigh
		CPM per 250 mSv	CPM per 250 mSv	CPM per 250 mSv
Days following exposure	0	3.42E+04	2.08E+02	7.52E+01
	1	1.51E+03	1.59E+04	6.00E+02
	2	3.21E+02	1.50E+04	9.64E+01
	3	2.48E+02	1.37E+04	8.25E+01
	4	2.36E+02	1.25E+04	9.27E+01
	5	2.27E+02	1.14E+04	1.01E+02
	6	2.18E+02	1.04E+04	1.06E+02
	7	2.07E+02	9.43E+03	1.09E+02
	8	1.97E+02	8.59E+03	1.10E+02
	9	1.86E+02	7.83E+03	1.10E+02
	10	1.76E+02	7.13E+03	1.08E+02
	20	8.70E+01	2.82E+03	6.66E+01
	30	3.85E+01	1.11E+03	3.19E+01

Table 19. Pediatric Inhaled ^{192}Ir

^{192}Ir		Back Right Lung	Neck	Thigh
		CPM per 250 mSv	CPM per 250 mSv	CPM per 250 mSv
Days following exposure	0	1.71E+05	1.67E+03	2.24E+02
	1	1.39E+05	3.85E+03	5.19E+03
	2	1.34E+05	3.59E+03	4.34E+03
	3	1.30E+05	3.42E+03	3.49E+03
	4	1.27E+05	3.32E+03	3.07E+03
	5	1.24E+05	3.26E+03	2.90E+03
	6	1.21E+05	3.22E+03	2.82E+03
	7	1.19E+05	3.18E+03	2.78E+03
	8	1.16E+05	3.15E+03	2.76E+03
	9	1.14E+05	3.12E+03	2.75E+03
	10	1.11E+05	3.09E+03	2.73E+03
	20	8.94E+04	2.82E+03	2.63E+03
	30	7.28E+04	2.60E+03	2.53E+03

Table 20. Adult Ingested ^{241}Am

^{241}Am		Umbilicus	Back Right Lung	Front Right Lung	Neck	Thigh
		CPM per 250 mSv	CPM per 250 mSv	CPM per 250 mSv	CPM per 250 mSv	CPM per 250 mSv
Days following exposure	0	1.34E+03	1.01E+02	1.07E+02	1.67E+00	3.33E-01
	1	1.54E+03	9.61E+00	9.62E+00	7.21E-01	5.26E+01
	2	4.24E+02	4.77E+00	4.11E+00	4.48E-01	3.22E+01
	3	1.34E+02	3.76E+00	2.53E+00	3.44E-01	1.42E+01
	4	4.61E+01	3.51E+00	2.02E+00	3.03E-01	5.85E+00
	5	1.71E+01	3.45E+00	1.85E+00	2.86E-01	2.48E+00
	6	7.03E+00	3.42E+00	1.78E+00	2.78E-01	1.19E+00
	7	3.39E+00	3.42E+00	1.76E+00	2.73E-01	7.06E-01
	8	2.06E+00	3.40E+00	1.74E+00	2.70E-01	5.24E-01
	9	1.56E+00	3.41E+00	1.74E+00	2.67E-01	4.55E-01
	10	1.38E+00	3.41E+00	1.73E+00	2.65E-01	4.27E-01
	20	1.21E+00	3.39E+00	1.71E+00	2.43E-01	3.80E-01
	30	1.17E+00	3.37E+00	1.69E+00	2.25E-01	3.51E-01

Table 21. Adult Ingested ^{60}Co

^{60}Co		Umbilicus	Back Right Lung	Front Right Lung	Neck	Thigh
		CPM per 250 mSv	CPM per 250 mSv	CPM per 250 mSv	CPM per 250 mSv	CPM per 250 mSv
Days following exposure	0	2.05E+05	5.06E+04	2.11E+05	1.76E+05	5.16E+04
	1	1.92E+05	8.08E+04	1.11E+05	4.90E+04	5.87E+04
	2	7.55E+04	4.18E+04	5.29E+04	2.55E+04	3.67E+04
	3	3.36E+04	2.16E+04	2.58E+04	1.37E+04	1.95E+04
	4	1.81E+04	1.29E+04	1.47E+04	8.58E+03	1.14E+04
	5	1.21E+04	9.33E+03	1.02E+04	6.43E+03	7.91E+03
	6	9.56E+03	7.74E+03	8.26E+03	5.45E+03	6.39E+03
	7	8.37E+03	6.92E+03	7.30E+03	4.93E+03	5.64E+03
	8	7.68E+03	6.41E+03	6.73E+03	4.59E+03	5.20E+03
	9	7.21E+03	6.05E+03	6.33E+03	4.33E+03	4.89E+03
	10	6.84E+03	5.75E+03	6.01E+03	4.12E+03	4.65E+03
	20	4.84E+03	4.09E+03	4.27E+03	2.93E+03	3.31E+03
	30	4.07E+03	3.45E+03	3.59E+03	2.47E+03	2.79E+03

Table 22. Adult Ingested ^{137}Cs

^{137}Cs		Umbilicus	Back Right Lung	Front Right Lung	Neck	Thigh
		CPM per 250 mSv	CPM per 250 mSv	CPM per 250 mSv	CPM per 250 mSv	CPM per 250 mSv
Days following exposure	0	7.40E+03	1.24E+03	8.58E+03	1.13E+04	2.17E+03
	1	1.93E+04	1.46E+04	1.49E+04	1.24E+04	1.68E+04
	2	1.85E+04	1.31E+04	1.37E+04	1.21E+04	1.66E+04
	3	1.80E+04	1.27E+04	1.33E+04	1.18E+04	1.62E+04
	4	1.77E+04	1.25E+04	1.30E+04	1.16E+04	1.59E+04
	5	1.74E+04	1.23E+04	1.28E+04	1.14E+04	1.57E+04
	6	1.71E+04	1.21E+04	1.27E+04	1.12E+04	1.54E+04
	7	1.69E+04	1.20E+04	1.25E+04	1.11E+04	1.53E+04
	8	1.67E+04	1.19E+04	1.24E+04	1.10E+04	1.51E+04
	9	1.66E+04	1.18E+04	1.23E+04	1.09E+04	1.50E+04
	10	1.64E+04	1.17E+04	1.22E+04	1.08E+04	1.49E+04
	20	1.53E+04	1.09E+04	1.14E+04	1.01E+04	1.39E+04
	30	1.44E+04	1.02E+04	1.07E+04	9.47E+03	1.30E+04

Table 23. Adult Ingested ^{131}I

^{131}I		Umbilicus	Back Right Lung	Front Right Lung	Neck	Thigh
		CPM per 250 mSv	CPM per 250 mSv	CPM per 250 mSv	CPM per 250 mSv	CPM per 250 mSv
Days following exposure	0	3.29E+03	5.94E+02	8.37E+02	1.76E+03	3.32E+02
	1	1.93E+03	2.05E+03	2.44E+03	6.22E+04	8.67E+02
	2	8.49E+02	2.29E+02	8.45E+02	6.02E+04	1.16E+02
	3	7.35E+02	1.31E+02	7.07E+02	5.50E+04	9.29E+01
	4	6.86E+02	1.29E+02	6.54E+02	5.00E+04	1.07E+02
	5	6.44E+02	1.31E+02	6.09E+02	4.56E+04	1.20E+02
	6	6.03E+02	1.30E+02	5.66E+02	4.15E+04	1.29E+02
	7	5.64E+02	1.29E+02	5.26E+02	3.77E+04	1.34E+02
	8	5.26E+02	1.26E+02	4.88E+02	3.44E+04	1.37E+02
	9	4.90E+02	1.22E+02	4.52E+02	3.13E+04	1.38E+02
	10	4.56E+02	1.18E+02	4.18E+02	2.85E+04	1.37E+02
	20	2.08E+02	6.57E+01	1.84E+02	1.12E+04	8.69E+01
	30	8.88E+01	3.05E+01	7.73E+01	4.41E+03	4.20E+01

Table 24. Adult Ingested ^{192}Ir

^{192}Ir		Umbilicus	Back Right Lung	Front Right Lung	Neck	Thigh
		CPM per 250 mSv	CPM per 250 mSv	CPM per 250 mSv	CPM per 250 mSv	CPM per 250 mSv
Days following exposure	0	2.14E+05	4.84E+04	3.99E+04	3.09E+04	7.28E+03
	1	6.46E+05	1.58E+04	1.99E+04	8.75E+03	6.68E+04
	2	1.44E+05	9.17E+03	1.08E+04	4.90E+03	4.12E+04
	3	3.92E+04	6.15E+03	6.60E+03	2.95E+03	1.92E+04
	4	1.37E+04	4.88E+03	4.88E+03	2.12E+03	9.13E+03
	5	6.38E+03	4.33E+03	4.17E+03	1.78E+03	5.06E+03
	6	4.02E+03	4.07E+03	3.85E+03	1.63E+03	3.48E+03
	7	3.18E+03	3.91E+03	3.68E+03	1.56E+03	2.86E+03
	8	2.84E+03	3.80E+03	3.57E+03	1.51E+03	2.59E+03
	9	2.68E+03	3.71E+03	3.48E+03	1.47E+03	2.46E+03
	10	2.58E+03	3.63E+03	3.40E+03	1.43E+03	2.38E+03
	20	2.11E+03	3.00E+03	2.81E+03	1.19E+03	1.96E+03
	30	1.80E+03	2.57E+03	2.41E+03	1.02E+03	1.68E+03

Table 25. Adipose Adult Ingested ^{241}Am

^{241}Am		Umbilicus	Back Right Lung	Neck	Thigh
		CPM per 250 mSv	CPM per 250 mSv	CPM per 250 mSv	CPM per 250 mSv
Days following exposure	0	1.06E+02	3.72E+01	2.13E+00	1.77E+00
	1	2.98E+02	5.81E+00	3.70E+00	5.76E+01
	2	1.34E+02	3.76E+00	3.87E+00	3.65E+01
	3	5.37E+01	3.10E+00	3.92E+00	1.76E+01
	4	2.07E+01	2.88E+00	3.94E+00	8.75E+00
	5	8.02E+00	2.80E+00	3.96E+00	5.21E+00
	6	3.29E+00	2.77E+00	3.96E+00	3.86E+00
	7	1.52E+00	2.76E+00	3.97E+00	3.36E+00
	8	8.64E-01	2.75E+00	3.96E+00	3.16E+00
	9	6.21E-01	2.76E+00	3.98E+00	3.10E+00
	10	5.29E-01	2.76E+00	3.98E+00	3.08E+00
	20	4.47E-01	2.75E+00	3.99E+00	3.06E+00
	30	4.21E-01	2.74E+00	3.99E+00	3.05E+00

Table 26. Adipose Adult Ingested ^{60}Co

^{60}Co		Umbilicus	Back Right Lung	Neck	Thigh
		CPM per 250 mSv	CPM per 250 mSv	CPM per 250 mSv	CPM per 250 mSv
Days following exposure	0	4.57E+04	4.50E+04	1.18E+05	3.81E+04
	1	1.26E+05	5.54E+04	3.85E+04	5.32E+04
	2	5.92E+04	2.84E+04	2.05E+04	3.29E+04
	3	2.71E+04	1.50E+04	1.15E+04	1.70E+04
	4	1.39E+04	9.33E+03	7.58E+03	9.60E+03
	5	8.55E+03	6.94E+03	5.92E+03	6.47E+03
	6	6.38E+03	5.86E+03	5.12E+03	5.12E+03
	7	5.40E+03	5.29E+03	4.67E+03	4.47E+03
	8	4.88E+03	4.92E+03	4.37E+03	4.10E+03
	9	4.55E+03	4.64E+03	4.13E+03	3.85E+03
	10	4.31E+03	4.42E+03	3.93E+03	3.65E+03
	20	3.04E+03	3.15E+03	2.81E+03	2.60E+03
	30	2.56E+03	2.65E+03	2.37E+03	2.19E+03

Table 27. Adipose Adult Ingested ^{137}Cs

^{137}Cs		Umbilicus	Back Right Lung	Neck	Thigh
		CPM per 250 mSv	CPM per 250 mSv	CPM per 250 mSv	CPM per 250 mSv
Days following exposure	0	1.68E+03	1.49E+03	8.06E+03	1.96E+03
	1	1.48E+04	1.67E+04	1.36E+04	1.54E+04
	2	1.44E+04	1.52E+04	1.32E+04	1.51E+04
	3	1.41E+04	1.48E+04	1.28E+04	1.47E+04
	4	1.38E+04	1.45E+04	1.26E+04	1.44E+04
	5	1.35E+04	1.42E+04	1.24E+04	1.42E+04
	6	1.33E+04	1.41E+04	1.22E+04	1.40E+04
	7	1.32E+04	1.39E+04	1.21E+04	1.39E+04
	8	1.30E+04	1.38E+04	1.20E+04	1.37E+04
	9	1.29E+04	1.36E+04	1.19E+04	1.36E+04
	10	1.28E+04	1.35E+04	1.18E+04	1.35E+04
	20	1.20E+04	1.26E+04	1.10E+04	1.26E+04
	30	1.12E+04	1.19E+04	1.03E+04	1.18E+04

Table 28. Adipose Adult Ingested ^{131}I

^{131}I		Umbilicus	Back Right Lung	Neck	Thigh
		CPM per 250 mSv	CPM per 250 mSv	CPM per 250 mSv	CPM per 250 mSv
Days following exposure	0	9.27E+02	2.49E+02	9.63E+02	1.62E+02
	1	1.47E+03	1.77E+03	6.21E+04	6.87E+02
	2	3.87E+02	2.75E+02	6.01E+04	8.60E+01
	3	3.04E+02	1.91E+02	5.49E+04	6.41E+01
	4	2.88E+02	1.86E+02	5.00E+04	7.35E+01
	5	2.80E+02	1.83E+02	4.55E+04	8.22E+01
	6	2.71E+02	1.79E+02	4.14E+04	8.84E+01
	7	2.62E+02	1.73E+02	3.77E+04	9.23E+01
	8	2.51E+02	1.67E+02	3.43E+04	9.43E+01
	9	2.40E+02	1.60E+02	3.12E+04	9.48E+01
	10	2.28E+02	1.53E+02	2.84E+04	9.40E+01
	20	1.19E+02	8.04E+01	1.12E+04	5.99E+01
	30	5.37E+01	3.65E+01	4.40E+03	2.90E+01

Table 29. Adipose Adult Ingested ^{192}Ir

^{192}Ir		Umbilicus	Back Right Lung	Neck	Thigh
		CPM per 250 mSv	CPM per 250 mSv	CPM per 250 mSv	CPM per 250 mSv
Days following exposure	0	7.22E+04	2.37E+04	1.86E+04	4.63E+03
	1	4.05E+05	9.26E+03	6.18E+03	6.59E+04
	2	1.81E+05	4.94E+03	3.54E+03	4.08E+04
	3	7.29E+04	3.09E+03	2.18E+03	1.88E+04
	4	2.90E+04	2.32E+03	1.60E+03	8.55E+03
	5	1.23E+04	2.02E+03	1.36E+03	4.42E+03
	6	6.02E+03	1.88E+03	1.26E+03	2.82E+03
	7	3.68E+03	1.82E+03	1.22E+03	2.21E+03
	8	2.79E+03	1.78E+03	1.19E+03	1.96E+03
	9	2.43E+03	1.75E+03	1.17E+03	1.86E+03
	10	2.27E+03	1.73E+03	1.15E+03	1.81E+03
	20	1.82E+03	1.57E+03	1.05E+03	1.63E+03
	30	1.55E+03	1.48E+03	9.87E+02	1.53E+03

Table 30. Pediatric Ingested ^{241}Am

^{241}Am		Umbilicus	Back Right Lung	Neck	Thigh
		CPM per 250 mSv	CPM per 250 mSv	CPM per 250 mSv	CPM per 250 mSv
Days following exposure	0	4.87E+03	1.75E+02	6.21E+00	1.29E+00
	1	6.79E+03	2.01E+01	6.84E+00	1.59E+02
	2	3.72E+03	1.39E+01	6.65E+00	9.40E+01
	3	1.58E+03	1.02E+01	6.52E+00	4.31E+01
	4	6.15E+02	8.59E+00	6.47E+00	1.98E+01
	5	2.34E+02	7.98E+00	6.47E+00	1.05E+01
	6	8.91E+01	7.74E+00	6.46E+00	7.00E+00
	7	3.50E+01	7.65E+00	6.46E+00	5.68E+00
	8	1.50E+01	7.60E+00	6.44E+00	5.18E+00
	9	7.56E+00	7.62E+00	6.46E+00	5.01E+00
	10	4.82E+00	7.62E+00	6.47E+00	4.95E+00
	20	3.11E+00	7.60E+00	6.45E+00	4.88E+00
	30	3.04E+00	7.59E+00	6.44E+00	4.85E+00

Table 31. Pediatric Ingested ^{60}Co

^{60}Co		Umbilicus	Back Right Lung	Neck	Thigh
		CPM per 250 mSv	CPM per 250 mSv	CPM per 250 mSv	CPM per 250 mSv
Days following exposure	0	1.40E+05	1.86E+04	8.03E+04	4.02E+04
	1	1.08E+05	3.18E+04	3.00E+04	2.84E+04
	2	4.03E+04	1.53E+04	1.43E+04	1.63E+04
	3	1.72E+04	7.96E+03	7.50E+03	8.72E+03
	4	8.81E+03	4.98E+03	4.74E+03	5.31E+03
	5	5.64E+03	3.75E+03	3.59E+03	3.86E+03
	6	4.35E+03	3.18E+03	3.06E+03	3.20E+03
	7	3.76E+03	2.88E+03	2.77E+03	2.87E+03
	8	3.43E+03	2.68E+03	2.59E+03	2.66E+03
	9	3.21E+03	2.53E+03	2.44E+03	2.51E+03
	10	3.04E+03	2.41E+03	2.32E+03	2.38E+03
	20	2.15E+03	1.72E+03	1.66E+03	1.70E+03
	30	1.81E+03	1.45E+03	1.40E+03	1.43E+03

Table 32. Pediatric Ingested ^{137}Cs

^{137}Cs		Umbilicus	Back Right Lung	Neck	Thigh
		CPM per 250 mSv	CPM per 250 mSv	CPM per 250 mSv	CPM per 250 mSv
Days following exposure	0	6.19E+04	0.00E+00	2.62E+04	0.00E+00
	1	4.07E+04	3.79E+04	2.78E+04	5.22E+04
	2	3.89E+04	3.47E+04	2.70E+04	5.12E+04
	3	3.78E+04	3.38E+04	2.63E+04	5.01E+04
	4	3.70E+04	3.31E+04	2.58E+04	4.91E+04
	5	3.63E+04	3.26E+04	2.54E+04	4.83E+04
	6	3.58E+04	3.21E+04	2.50E+04	4.77E+04
	7	3.53E+04	3.18E+04	2.48E+04	4.72E+04
	8	3.50E+04	3.15E+04	2.45E+04	4.67E+04
	9	3.46E+04	3.12E+04	2.43E+04	4.63E+04
	10	3.43E+04	3.09E+04	2.41E+04	4.59E+04
	20	3.20E+04	2.89E+04	2.25E+04	4.29E+04
	30	3.01E+04	2.71E+04	2.11E+04	4.03E+04

Table 33. Pediatric Ingested ^{131}I

^{131}I		Umbilicus	Back Right Lung	Neck	Thigh
		CPM per 250 mSv	CPM per 250 mSv	CPM per 250 mSv	CPM per 250 mSv
Days following exposure	0	2.25E+04	3.41E+02	1.04E+03	2.97E+02
	1	1.39E+03	1.79E+03	1.71E+04	7.84E+02
	2	3.85E+02	3.56E+02	1.62E+04	1.13E+02
	3	3.01E+02	2.67E+02	1.48E+04	8.95E+01
	4	2.83E+02	2.54E+02	1.34E+04	9.97E+01
	5	2.72E+02	2.45E+02	1.22E+04	1.08E+02
	6	2.60E+02	2.34E+02	1.12E+04	1.14E+02
	7	2.49E+02	2.23E+02	1.02E+04	1.18E+02
	8	2.37E+02	2.12E+02	9.26E+03	1.19E+02
	9	2.25E+02	2.01E+02	8.43E+03	1.18E+02
	10	2.13E+02	1.89E+02	7.68E+03	1.16E+02
	20	1.07E+02	9.37E+01	3.03E+03	7.18E+01
	30	4.77E+01	4.15E+01	1.20E+03	3.44E+01

Table 34.Pediatric Ingested ^{192}Ir

^{192}Ir		Umbilicus	Back Right Lung	Neck	Thigh
		CPM per 250 mSv	CPM per 250 mSv	CPM per 250 mSv	CPM per 250 mSv
Days following exposure	0	9.49E+05	3.46E+04	2.17E+04	9.67E+03
	1	8.46E+05	1.01E+04	9.70E+03	3.81E+04
	2	2.53E+05	4.90E+03	5.22E+03	2.34E+04
	3	8.53E+04	3.11E+03	3.28E+03	1.16E+04
	4	3.19E+04	2.43E+03	2.50E+03	6.10E+03
	5	1.36E+04	2.16E+03	2.18E+03	3.89E+03
	6	7.11E+03	2.04E+03	2.05E+03	3.02E+03
	7	4.72E+03	1.97E+02	1.98E+03	2.68E+03
	8	3.80E+03	1.93E+02	1.94E+03	2.53E+03
	9	3.42E+03	1.90E+02	1.91E+03	2.45E+03
	10	3.23E+03	1.88E+03	1.88E+03	2.41E+03
	20	2.60E+03	1.71E+03	1.71E+03	2.18E+03
	30	2.22E+03	1.60E+02	1.61E+03	2.05E+03

7. Conclusions

The Captus 3000 Thyroid Uptake Collimator was able to detect a committed effective dose of 250 mSv with a one minute or less counting time for ^{60}Co, ^{137}Cs, ^{131}I and ^{192}Ir. Count rate tables for each of these isotopes for each of the phantoms used are provided in Appendices A and B. The exact distribution in the body may be subject to numerical error at time zero. No further comment can be made due to lack of familiarity with numerical procedure used in DCAL

The optimal position for the thyroid uptake collimator depends on the isotope and the internal contamination pathway. For the inhalation of ^{131}I the neck yielded the highest count rate and for this reason the collimator should be placed on the neck position. ^{60}Co and ^{192}Ir tend to remain in the lungs for a longer period of time following inhalation, and the most efficient position for the detector is over the back right lung. ^{137}Cs distributes throughout the body and as a result the detector location yielding the highest count rate was phantom type dependent. However, for all the phantoms the count rates from the back right lung position were very similar to the maximum count rate position and thus, for simplicity, it is recommended that the back right lung be used for the inhalation of ^{137}Cs. The thigh should not be chosen as a detection position for the thyroid uptake collimator unless circumstances prevent use of the other two locations. This is one of the consequences of a high degree of collimation. The detection efficiency is reduced as a result of a

smaller angle seen by the detector, and the distance between the detector and the object of interest. Given a threshold of a committed effective dose of 250 mSv, the minimum necessary counting time is one minute. This can be used as a baseline for all isotopes on the back right lung, with the exception of I-131, in which the probe would need to be placed on the neck for this counting time.

For ingestion the umbilicus is the recommended location for detecting ^{60}Co, ^{137}Cs, and ^{192}Ir. For all three male phantom types used, the count rates from the umbilicus location were highest for ^{60}Co and ^{192}Ir. For ^{137}Cs the maximum count rate location was different for each phantom type. However, the umbilicus value was either the maximum or close to the maximum for all male phantoms types. For the ingestion of ^{131}I the neck yielded the highest count rate and for this reason the collimator should be placed on the neck position.

The thyroid uptake system cannot be used to detect internal contamination, through ingestion or inhalation, of Am-241. The calculated count rate per 250 mSv of Am-241 is too low to differentiate it from the background count rate of 1700 CPM observed in the laboratory. This is a consequence of the low energy of the gamma-ray emission of Am-241.

8. References

1. X-5 Monte Carlo Team. *MCNP - A General Monte Carlo N-Particle Tansport Code Version 5.* LA-CP-03-0245. Vol. II. Los Alamos National Laboratory, 2004.

2. Cristy, M., and K. F. Eckerman. *Specific absorbed fraction of energy at various ages from internal photon sources.* ORNL/TM-8381/VI, Oak Ridge: Oak Ridge National Laboratory, 1987.

3. Tanner, J.E. *Current DOE Studies on Effective Neutron Dose Equivalent*. Proceedings of the Eleventh DOE Workshop on Personnel Neutron Dosimetry, June 3-7, Las Vegas, Nevada, 1991.

4. Simpkins, R. W and N. E. Hertel.*Neutron Effective Dose and the Influence of Adipose Tissue*. Proceedings of the 12th Biennial ANS Radiation Protection and Shielding Division Topical Meeting, April 14-18, Santa Fe, New Mexico, 2002.

5. Simpkins, R. W. *Neutron Organ Dose and the Influence of Adipose Tissue.* Ph.D. Dissertation, Atlanta: Georgia Institute of Technology, 2003.

6. Van Riper, K. A. *BodyBuilder.* 2004. http://www.whiterockscience.com/bodybuilder/bodybuilder.html.

7. National Council on Radiation Protection and Measurements. *Management of Persons Contaminated with Radionuclides: Handbook.* NCRP Report No. 161, Bethesda: NCRP, 2008, 56-61,158-160.

8. The DOE/NRC Interagency Working Group Radiological Dispersal Devices. *Radiological Dispersal Devices: An Initial Study to Indentify Radioactive Materials of Greatest Concern and Approaches to Their Tracking, Tagging, and Disposition. Report to the Nuclear Regulatory Commission and the Secretary of Energy.* May 2003. ytthttp://www.nti.org/e_research/official_docs/doe/DOE052003.pdf (accessed April 2010).

9. Eckerman, K. F., et al. "Dose and Risk Calcuation Software." Ver. 8.4. Oak Ridge, Tennessee: Oak Ridge National Laboratory, 2006.

10. National Institute of Standards and Technology. *Compositions of Materials used in STAR Databases.* http://physics.nist.gov/cgi-bin/Star/compos.pl (accessed February 2009).

11. Eckerman, K. F., and A.L Sjoreen. "Radiological Toolbox." Ver. 2.0.0. Oak Ridge, Tennessee: Oak Ridge National Laboratory, 2006.

12. Schwarz, R. "MCNP Visual Editor Version 16d." *Visual Editor Consultants.* August 2004. http://www.mcnpvised.com/ (accessed November 2008).

13. International Commission on Radiological Protection. "ICRP Publication 89: Basic anatomical and physiological data for use in radiological protection: reference values." *Annals of the ICRP*, 2002.

14. International Commission on Radiological Protection. "ICRP Publication 71: Age-Dependent Dose to Members of the Public From Intake of Radionuclides: Part 4 Inhalation Dose Coefficients." *Annals of the ICRP*, 1995.

15. International Commission on Radiological Protection. "ICRP Publication 72: Age-Dependent Dose to Members of the Public From Intake of Radionuclides: Part 5 Compilation of Ingestion and Inhalation Dose Coefficients." *Annals of the ICRP*, 1996.

APPENDIX A: TABLULATED DATA FOR INHALATION

- Data are presented in graphical and tabular format for each phantom-isotope pairing for inhalation.
- Graphical data and tabular data are the count rate (counts per minute) per 250 mSv for each detection location that was simulated.

Reference Male ^{241}Am Inhalation
Reference Male ^{60}Co Inhalation
Reference Male ^{137}Cs Inhalation
Reference Male ^{131}I Inhalation
Reference Male ^{192}Ir Inhalation

Reference Female ^{241}Am Inhalation
Reference Female ^{60}Co Inhalation
Reference Female ^{137}Cs Inhalation
Reference Female ^{131}I Inhalation
Reference Female ^{192}Ir Inhalation

Adipose Male ^{241}Am Inhalation
Adipose Male ^{60}Co Inhalation
Adipose Male ^{137}Cs Inhalation
Adipose Male ^{131}I Inhalation
Adipose Male ^{192}Ir Inhalation

Adipose Female ^{241}Am Inhalation
Adipose Female ^{60}Co Inhalation
Adipose Female ^{137}Cs Inhalation
Adipose Female ^{131}I Inhalation
Adipose Female ^{192}Ir Inhalation

Post Menopausal Adipose Female ^{241}Am Inhalation
Post Menopausal Adipose Female ^{60}Co Inhalation
Post Menopausal Adipose Female ^{137}Cs Inhalation
Post Menopausal Adipose Female ^{131}I Inhalation
Post Menopausal Adipose Female ^{192}Ir Inhalation

10-year-old Child ^{241}Am Inhalation
10-year-old Child ^{60}Co Inhalation
10-year-old Child ^{137}Cs Inhalation
10-year-old Child ^{131}I Inhalation
10-year-old Child ^{192}Ir Inhalation

Reference Male ^{241}Am Inhalation

^{241}Am		Back Right Lung	Front Right Lung	Neck	Thigh
		CPM per 250 mSv	CPM per 250 mSv	CPM per 250 mSv	CPM per 250 mSv
Days following exposure	0	6.28E+00	5.99E+00	4.16E-02	0.00E+00
	1	5.21E+00	4.96E+00	4.84E-02	7.09E-02
	2	5.10E+00	4.85E+00	4.30E-02	4.67E-02
	3	5.03E+00	4.79E+00	4.07E-02	2.74E-02
	4	4.96E+00	4.73E+00	3.97E-02	1.84E-02
	5	4.90E+00	4.67E+00	3.91E-02	1.48E-02
	6	4.84E+00	4.61E+00	3.86E-02	1.35E-02
	7	4.79E+00	4.55E+00	3.82E-02	1.31E-02
	8	4.73E+00	4.50E+00	3.79E-02	1.30E-02
	9	4.67E+00	4.45E+00	3.76E-02	1.30E-02
	10	4.62E+00	4.39E+00	3.73E-02	1.31E-02
	20	4.14E+00	3.93E+00	3.44E-02	1.39E-02
	30	3.75E+00	3.56E+00	3.21E-02	1.46E-02

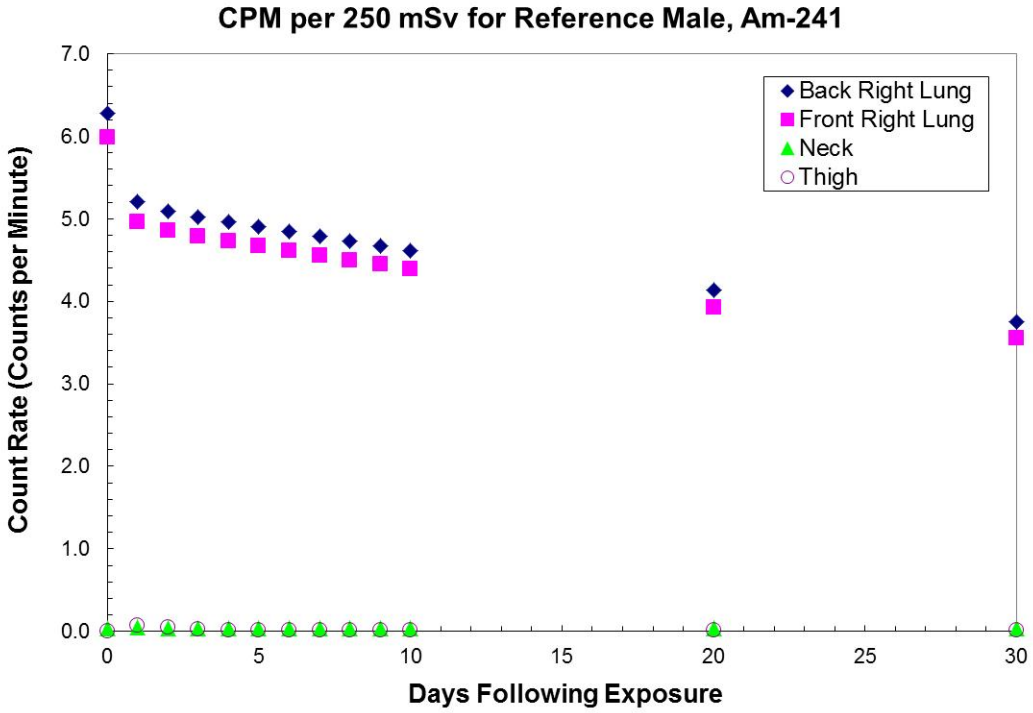

Reference Male ^{60}Co Inhalation

^{60}Co		Back Right Lung	Front Right Lung	Neck	Thigh
		CPM per 250 mSv	CPM per 250 mSv	CPM per 250 mSv	CPM per 250 mSv
Days following exposure	0	4.39E+04	4.21E+04	1.02E+04	1.04E+03
	1	4.18E+04	4.25E+04	1.22E+04	5.45E+03
	2	3.81E+04	3.75E+04	1.03E+04	4.00E+03
	3	3.60E+04	3.50E+04	9.33E+03	2.79E+03
	4	3.49E+04	3.38E+04	8.83E+03	2.20E+03
	5	3.42E+04	3.30E+04	8.56E+03	1.93E+03
	6	3.36E+04	3.24E+04	8.37E+03	1.79E+03
	7	3.30E+04	3.18E+04	8.21E+03	1.72E+03
	8	3.26E+04	3.14E+04	8.08E+03	1.66E+03
	9	3.21E+04	3.09E+04	7.95E+03	1.62E+03
	10	3.16E+04	3.05E+04	7.83E+03	1.58E+03
	20	2.77E+04	2.67E+04	6.84E+03	1.36E+03
	30	2.46E+04	2.37E+04	6.10E+03	1.24E+03

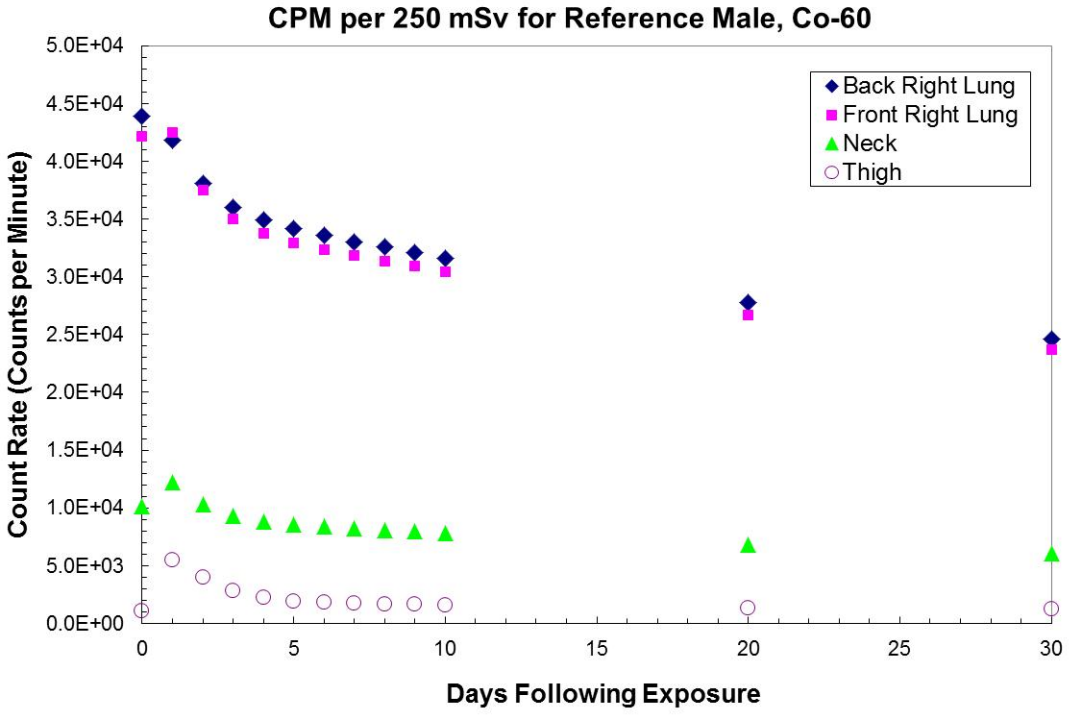

Reference Male ^{137}Cs Inhalation

^{137}Cs		Back Right Lung	Front Right Lung	Neck	Thigh
		CPM per 250 mSv	CPM per 250 mSv	CPM per 250 mSv	CPM per 250 mSv
Days following exposure	0	6.48E+04	6.21E+04	5.28E+03	4.58E+02
	1	1.73E+04	1.77E+04	1.48E+04	2.01E+04
	2	1.57E+04	1.64E+04	1.44E+04	1.98E+04
	3	1.52E+04	1.59E+04	1.41E+04	1.94E+04
	4	1.49E+04	1.56E+04	1.38E+04	1.90E+04
	5	1.47E+04	1.53E+04	1.36E+04	1.87E+04
	6	1.45E+04	1.51E+04	1.34E+04	1.85E+04
	7	1.43E+04	1.50E+04	1.33E+04	1.83E+04
	8	1.42E+04	1.48E+04	1.31E+04	1.81E+04
	9	1.41E+04	1.47E+04	1.30E+04	1.79E+04
	10	1.40E+04	1.46E+04	1.29E+04	1.78E+04
	20	1.30E+04	1.36E+04	1.21E+04	1.66E+04
	30	1.22E+04	1.28E+04	1.13E+04	1.56E+04

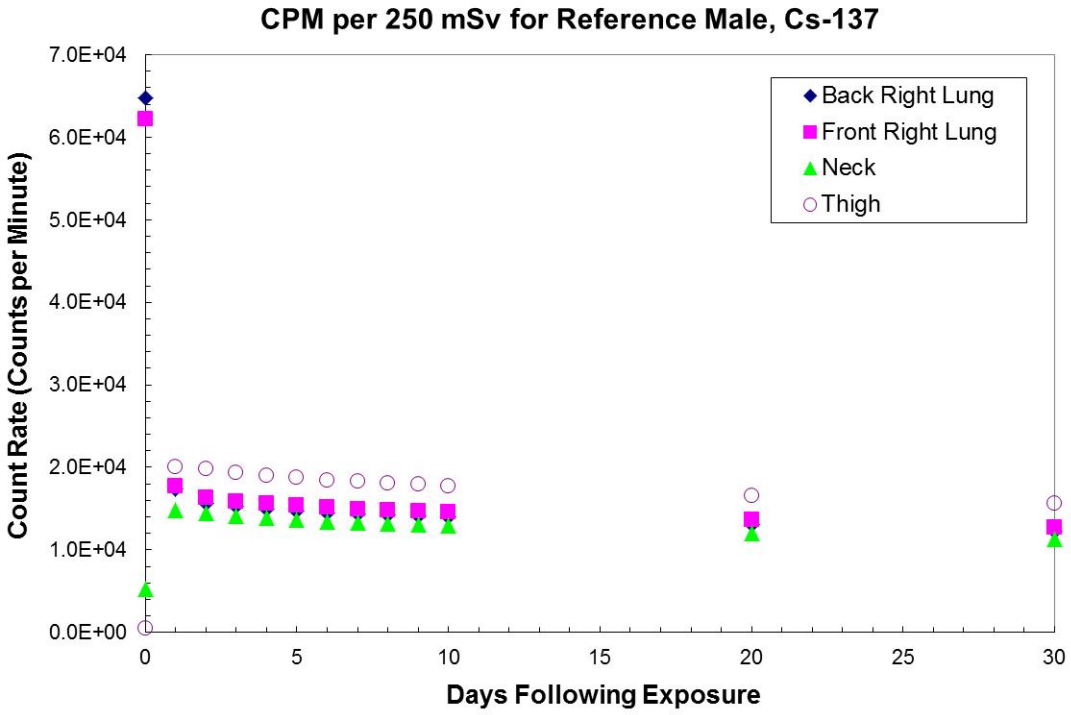

Reference Male ^{131}I Inhalation

^{131}I		Back Right Lung	Front Right Lung	Neck	Thigh
		CPM per 250 mSv	CPM per 250 mSv	CPM per 250 mSv	CPM per 250 mSv
Days following exposure	0	6.57E+04	6.31E+04	5.55E+02	4.35E+01
	1	1.93E+03	2.34E+03	6.30E+04	8.09E+02
	2	2.23E+02	8.45E+02	6.07E+04	1.10E+02
	3	1.32E+02	7.13E+02	5.55E+04	9.23E+01
	4	1.30E+02	6.60E+02	5.05E+04	1.08E+02
	5	1.32E+02	6.15E+02	4.59E+04	1.21E+02
	6	1.32E+02	5.72E+02	4.18E+04	1.30E+02
	7	1.30E+02	5.31E+02	3.81E+04	1.36E+02
	8	1.27E+02	4.92E+02	3.47E+04	1.39E+02
	9	1.23E+02	4.56E+02	3.15E+04	1.39E+02
	10	1.19E+02	4.22E+02	2.87E+04	1.38E+02
	20	6.63E+01	1.86E+02	1.13E+04	8.77E+01
	30	3.07E+01	7.80E+01	4.45E+03	4.24E+01

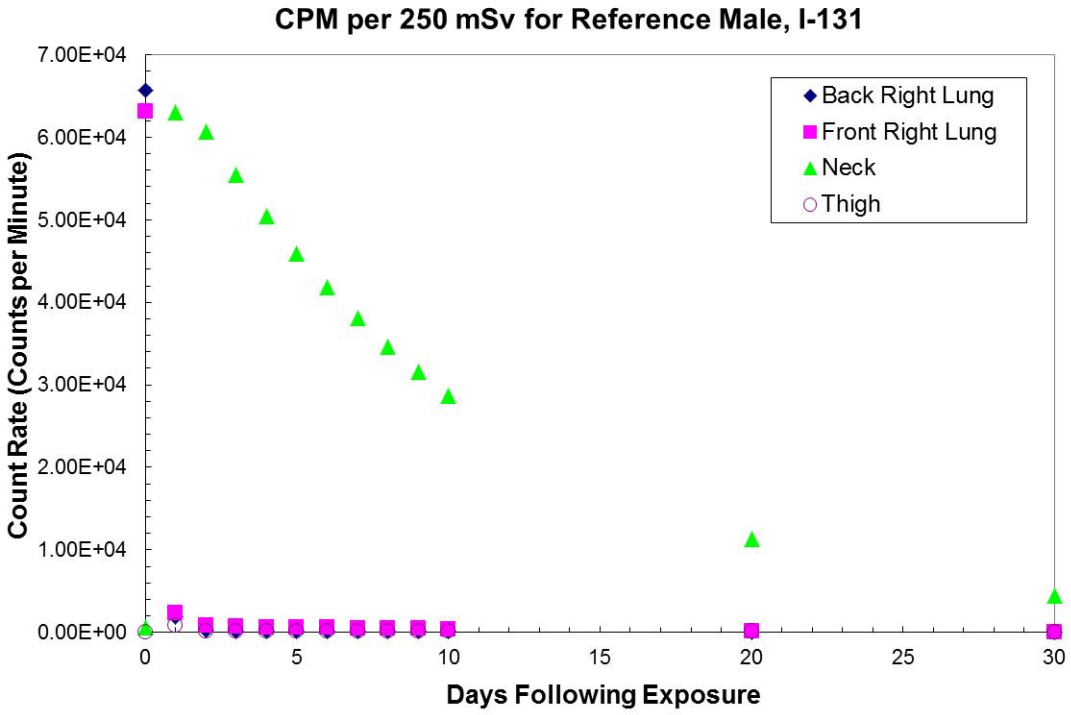

Reference Male ^{192}Ir Inhalation

^{192}Ir		Back Right Lung	Front Right Lung	Neck	Thigh
		CPM per 250 mSv	CPM per 250 mSv	CPM per 250 mSv	CPM per 250 mSv
Days following exposure	0	1.88E+05	1.80E+05	1.67E+03	9.41E+01
	1	1.53E+05	1.47E+05	3.00E+03	5.55E+03
	2	1.48E+05	1.42E+05	2.74E+03	4.30E+03
	3	1.44E+05	1.38E+05	2.60E+03	3.12E+03
	4	1.41E+05	1.35E+05	2.52E+03	2.56E+03
	5	1.37E+05	1.32E+05	2.47E+03	2.33E+03
	6	1.34E+05	1.29E+05	2.43E+03	2.23E+03
	7	1.31E+05	1.26E+05	2.40E+03	2.19E+03
	8	1.28E+05	1.23E+05	2.36E+03	2.17E+03
	9	1.26E+05	1.20E+05	2.33E+03	2.15E+03
	10	1.23E+05	1.18E+05	2.31E+03	2.14E+03
	20	9.91E+04	9.49E+04	2.06E+03	2.06E+03
	30	8.08E+04	7.74E+04	1.86E+03	1.99E+03

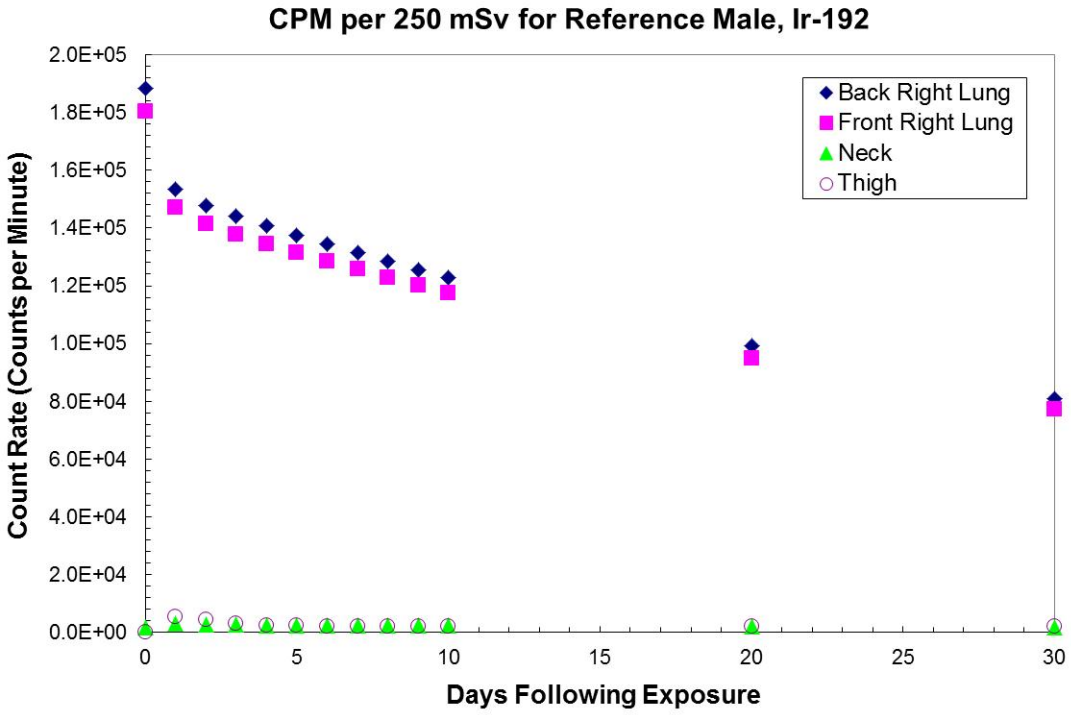

Reference Female ^{241}Am Inhalation

^{241}Am		Back Right Lung	Neck	Thigh
		CPM per 250 mSv	CPM per 250 mSv	CPM per 250 mSv
Days following exposure	0	5.81E+00	5.05E-02	0.00E+00
	1	4.72E+00	5.67E-02	8.73E-02
	2	4.60E+00	5.07E-02	5.75E-02
	3	4.53E+00	4.82E-02	3.30E-02
	4	4.47E+00	4.70E-02	2.16E-02
	5	4.41E+00	4.63E-02	1.70E-02
	6	4.35E+00	4.58E-02	1.54E-02
	7	4.30E+00	4.53E-02	1.48E-02
	8	4.24E+00	4.49E-02	1.47E-02
	9	4.19E+00	4.45E-02	1.47E-02
	10	4.13E+00	4.41E-02	1.47E-02
	20	3.67E+00	4.06E-02	1.56E-02
	30	3.29E+00	3.77E-02	1.63E-02

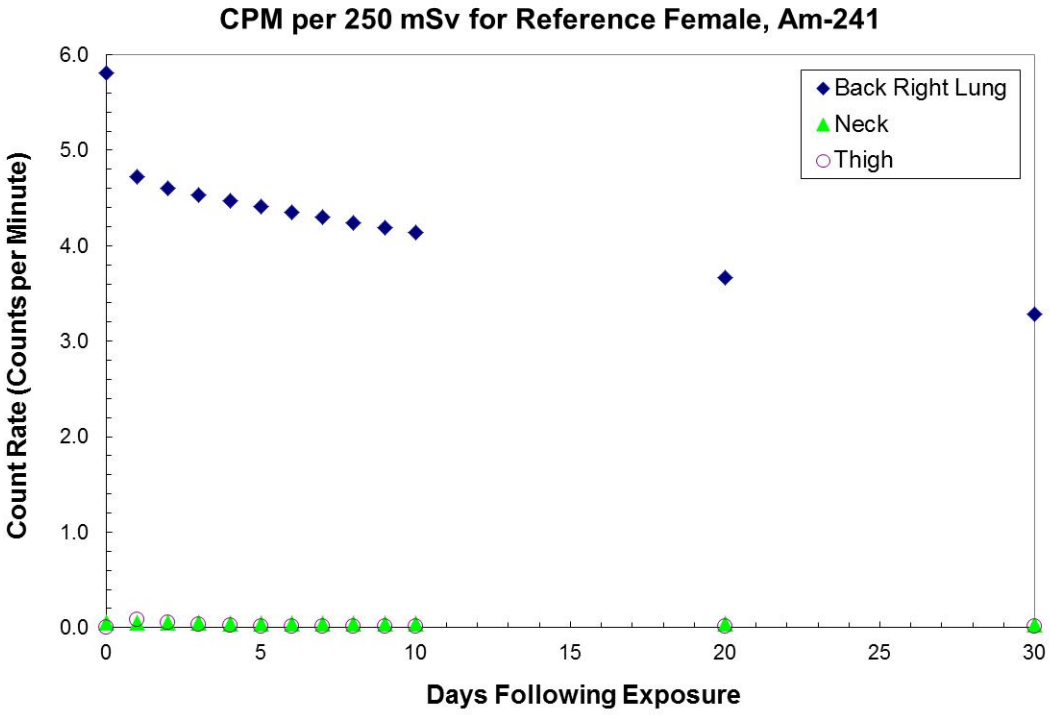

Reference Female ^{60}Co Inhalation

^{60}Co		Back Right Lung	Neck	Thigh
		CPM per 250 mSv	CPM per 250 mSv	CPM per 250 mSv
Days following exposure	0	4.39E+04	1.07E+04	1.28E+03
	1	4.15E+04	1.32E+04	6.10E+03
	2	3.79E+04	1.11E+04	4.49E+03
	3	3.59E+04	9.99E+03	3.17E+03
	4	3.48E+04	9.44E+03	2.52E+03
	5	3.41E+04	9.13E+03	2.22E+03
	6	3.35E+04	8.93E+03	2.08E+03
	7	3.30E+04	8.76E+03	1.99E+03
	8	3.25E+04	8.61E+03	1.93E+03
	9	3.21E+04	8.48E+03	1.88E+03
	10	3.16E+04	8.35E+03	1.84E+03
	20	2.77E+04	7.29E+03	1.58E+03
	30	2.46E+04	6.51E+03	1.44E+03

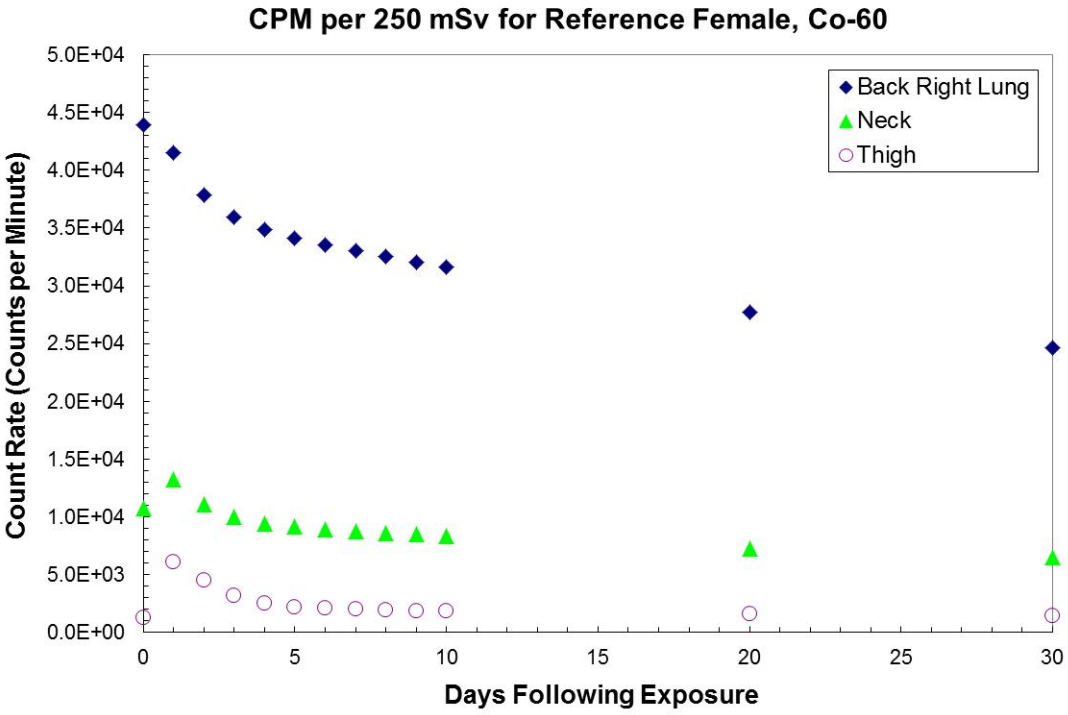

Reference Female ^{137}Cs Inhalation

^{137}Cs		Back Right Lung	Neck	Thigh
		CPM per 250 mSv	CPM per 250 mSv	CPM per 250 mSv
Days following exposure	0	6.34E+04	5.48E+03	5.83E+02
	1	2.08E+04	1.66E+04	2.28E+04
	2	1.93E+04	1.62E+04	2.25E+04
	3	1.87E+04	1.58E+04	2.20E+04
	4	1.84E+04	1.55E+04	2.15E+04
	5	1.81E+04	1.53E+04	2.12E+04
	6	1.79E+04	1.51E+04	2.09E+04
	7	1.77E+04	1.49E+04	2.07E+04
	8	1.75E+04	1.48E+04	2.05E+04
	9	1.73E+04	1.46E+04	2.03E+04
	10	1.72E+04	1.45E+04	2.02E+04
	20	1.61E+04	1.36E+04	1.88E+04
	30	1.51E+04	1.27E+04	1.77E+04

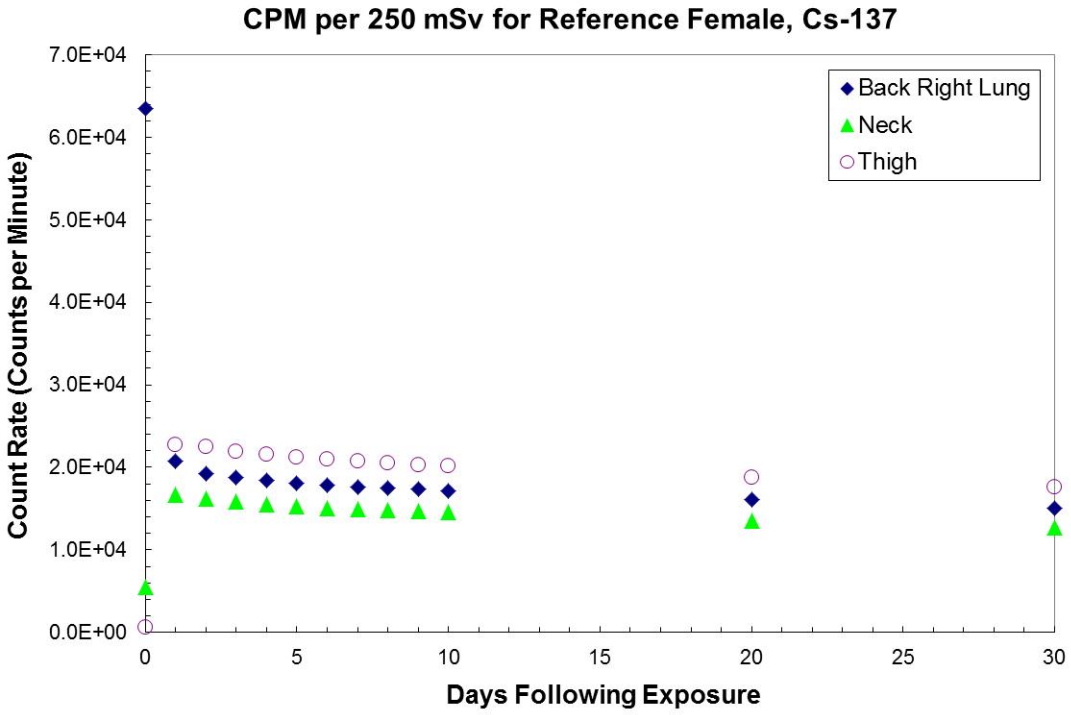

Reference Female ^{131}I Inhalation

^{131}I		Back Right Lung	Neck	Thigh
		CPM per 250 mSv	CPM per 250 mSv	CPM per 250 mSv
Days following exposure	0	6.39E+04	5.72E+02	6.04E+01
	1	2.07E+03	5.46E+04	9.28E+02
	2	3.52E+02	5.25E+04	1.26E+02
	3	2.55E+02	4.80E+04	1.05E+02
	4	2.49E+02	4.37E+04	1.24E+02
	5	2.45E+02	3.97E+04	1.39E+02
	6	2.40E+02	3.62E+04	1.50E+02
	7	2.32E+02	3.29E+04	1.56E+02
	8	2.24E+02	3.00E+04	1.59E+02
	9	2.14E+02	2.73E+04	1.60E+02
	10	2.04E+02	2.49E+04	1.58E+02
	20	1.08E+02	9.76E+03	1.01E+02
	30	4.88E+01	3.85E+03	4.87E+01

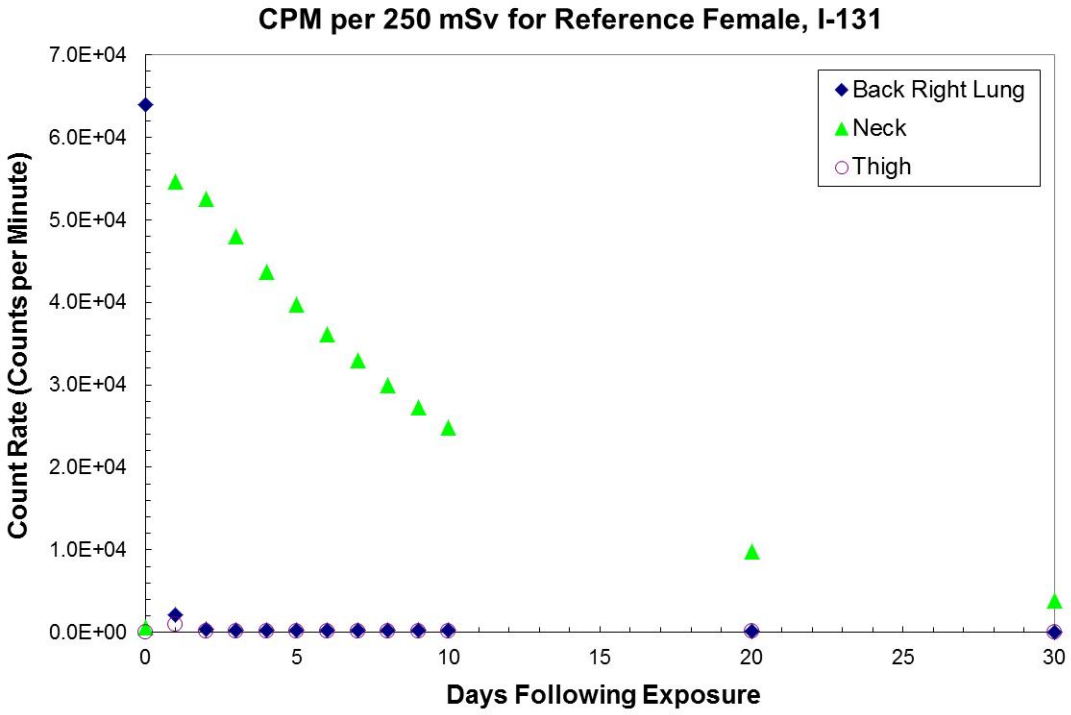

Reference Female ^{192}Ir Inhalation

^{192}Ir		Back Right Lung	Neck	Thigh
		CPM per 250 mSv	CPM per 250 mSv	CPM per 250 mSv
Days following exposure	0	1.83E+05	1.79E+03	1.24E+02
	1	1.47E+05	3.23E+03	6.01E+03
	2	1.42E+05	2.95E+03	4.70E+03
	3	1.38E+05	2.80E+03	3.48E+03
	4	1.35E+05	2.72E+03	2.90E+03
	5	1.32E+05	2.66E+03	2.66E+03
	6	1.29E+05	2.62E+03	2.56E+03
	7	1.26E+05	2.58E+03	2.51E+03
	8	1.23E+05	2.55E+03	2.49E+03
	9	1.20E+05	2.52E+03	2.47E+03
	10	1.18E+05	2.49E+03	2.46E+03
	20	9.48E+04	2.23E+03	2.37E+03
	30	7.71E+04	2.01E+03	2.28E+03

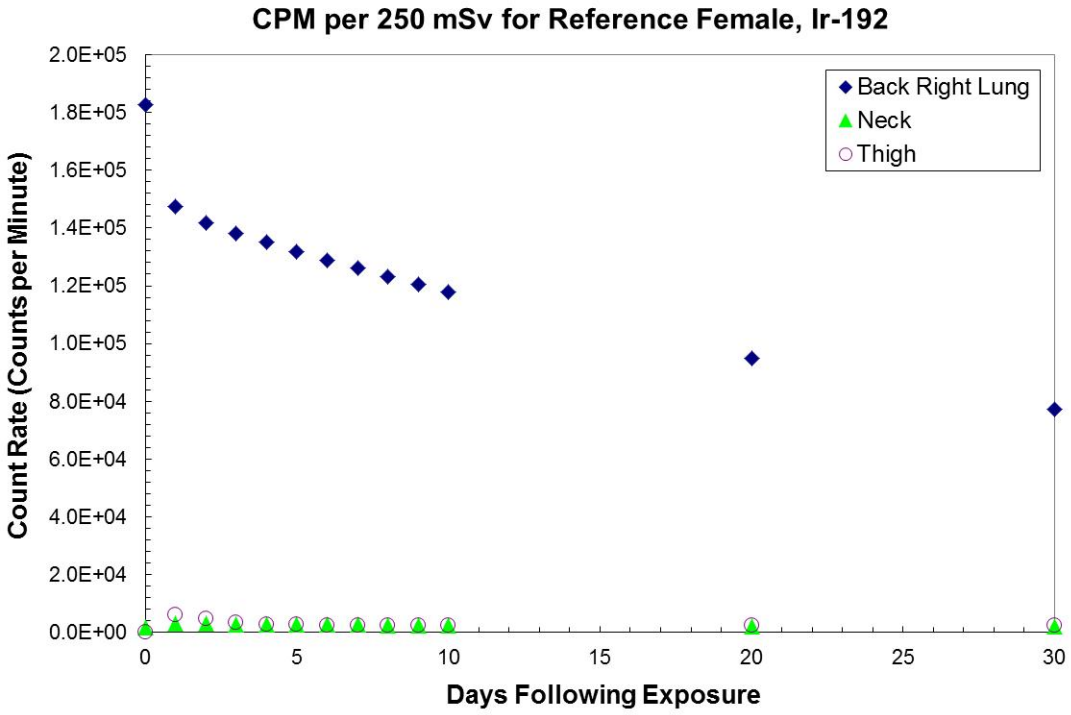

Adipose Male ^{241}Am Inhalation

^{241}Am		Back Right Lung	Neck	Thigh
		CPM per 250 mSv	CPM per 250 mSv	CPM per 250 mSv
Days following exposure	0	3.86E+00	4.21E-02	0.00E+00
	1	3.15E+00	4.46E-02	5.92E-02
	2	3.07E+00	4.04E-02	3.87E-02
	3	3.02E+00	3.87E-02	2.18E-02
	4	2.98E+00	3.78E-02	1.39E-02
	5	2.94E+00	3.72E-02	1.07E-02
	6	2.90E+00	3.67E-02	9.50E-03
	7	2.87E+00	3.64E-02	9.10E-03
	8	2.83E+00	3.60E-02	8.99E-03
	9	2.79E+00	3.56E-02	8.99E-03
	10	2.76E+00	3.53E-02	9.03E-03
	20	2.45E+00	3.23E-02	9.56E-03
	30	2.20E+00	2.98E-02	9.96E-03

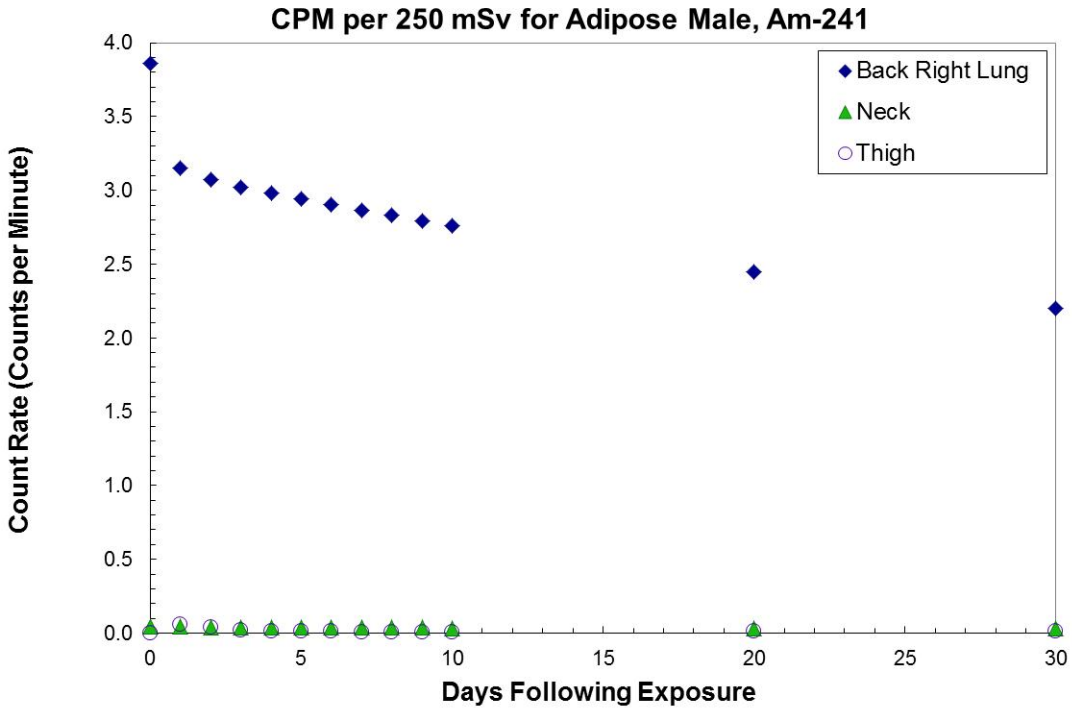

Adipose Male ^{60}Co Inhalation

^{60}Co		Back Right Lung	Neck	Thigh
		CPM per 250 mSv	CPM per 250 mSv	CPM per 250 mSv
Days following exposure	0	3.48E+04	8.60E+03	7.24E+02
	1	3.25E+04	1.02E+04	4.64E+03
	2	2.98E+04	8.70E+03	3.34E+03
	3	2.84E+04	7.94E+03	2.25E+03
	4	2.76E+04	7.55E+03	1.71E+03
	5	2.70E+04	7.33E+03	1.47E+03
	6	2.66E+04	7.17E+03	1.35E+03
	7	2.62E+04	7.04E+03	1.29E+03
	8	2.58E+04	6.92E+03	1.25E+03
	9	2.54E+04	6.81E+03	1.21E+03
	10	2.50E+04	6.71E+03	1.18E+03
	20	2.20E+04	5.86E+03	1.01E+03
	30	1.95E+04	5.23E+03	9.25E+02

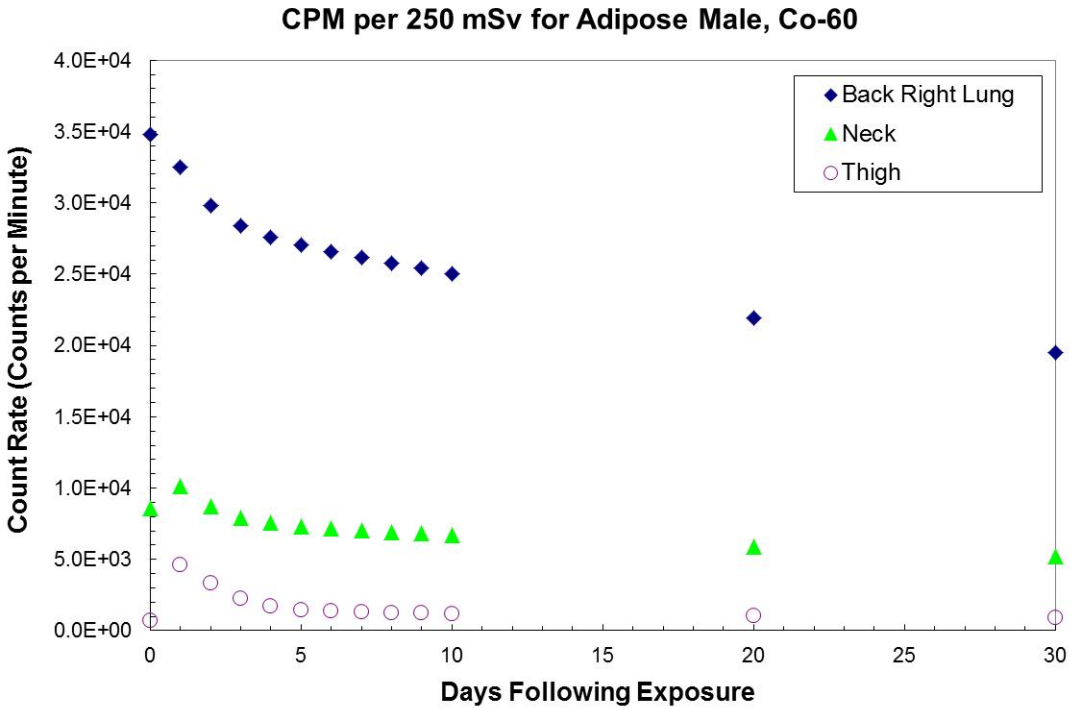

Adipose Male ^{137}Cs Inhalation

^{137}Cs		Back Right Lung	Neck	Thigh
		CPM per 250mSv	CPM per 250 mSv	CPM per 250 mSv
Days following exposure	0	4.92E+04	4.14E+03	2.58E+02
	1	1.58E+04	1.29E+04	1.46E+04
	2	1.45E+04	1.26E+04	1.44E+04
	3	1.42E+04	1.23E+04	1.41E+04
	4	1.39E+04	1.21E+04	1.38E+04
	5	1.37E+04	1.19E+04	1.36E+04
	6	1.35E+04	1.17E+04	1.35E+04
	7	1.33E+04	1.16E+04	1.33E+04
	8	1.32E+04	1.15E+04	1.32E+04
	9	1.31E+04	1.14E+04	1.31E+04
	10	1.30E+04	1.13E+04	1.29E+04
	20	1.21E+04	1.05E+04	1.21E+04
	30	1.14E+04	9.89E+03	1.13E+04

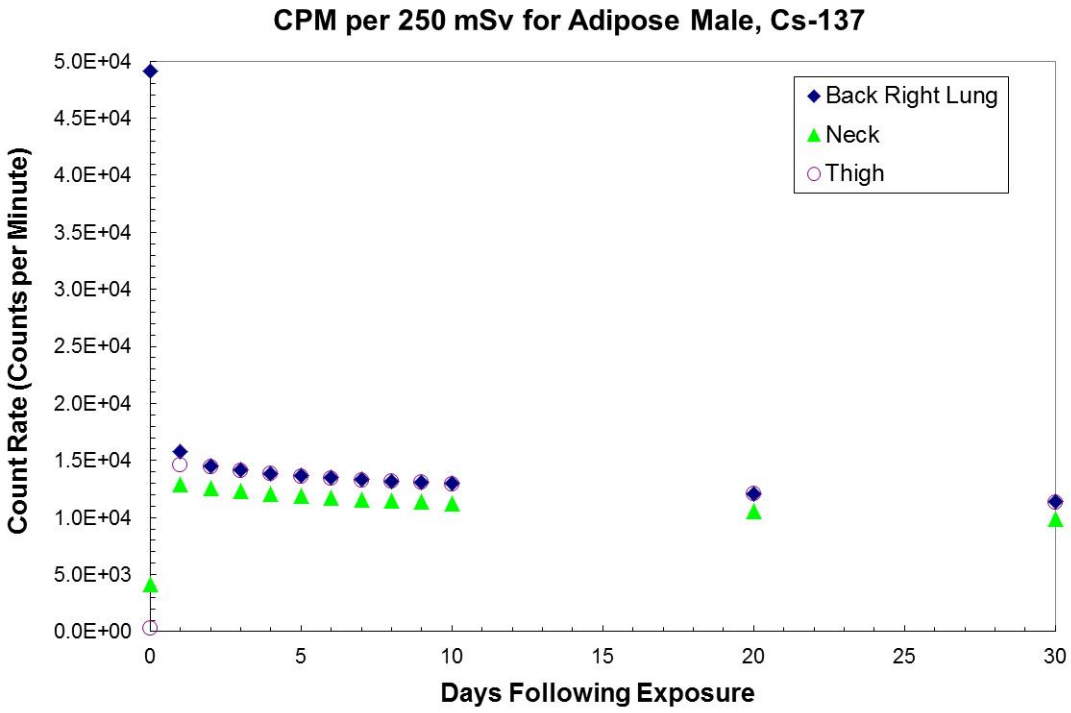

Adipose Male ^{131}I Inhalation

^{131}I		Back Right Lung	Neck	Thigh
		CPM per 250 mSv	CPM per 250 mSv	CPM per 250 mSv
Days following exposure	0	4.80E+04	4.65E+02	2.81E+01
	1	1.61E+03	6.28E+04	5.64E+02
	2	2.68E+02	6.07E+04	7.57E+01
	3	1.93E+02	5.54E+04	6.29E+01
	4	1.88E+02	5.04E+04	7.38E+01
	5	1.85E+02	4.59E+04	8.29E+01
	6	1.81E+02	4.18E+04	8.93E+01
	7	1.75E+02	3.80E+04	9.32E+01
	8	1.69E+02	3.46E+04	9.52E+01
	9	1.61E+02	3.15E+04	9.57E+01
	10	1.54E+02	2.87E+04	9.48E+01
	20	8.10E+01	1.13E+04	6.04E+01
	30	3.68E+01	4.44E+03	2.92E+01

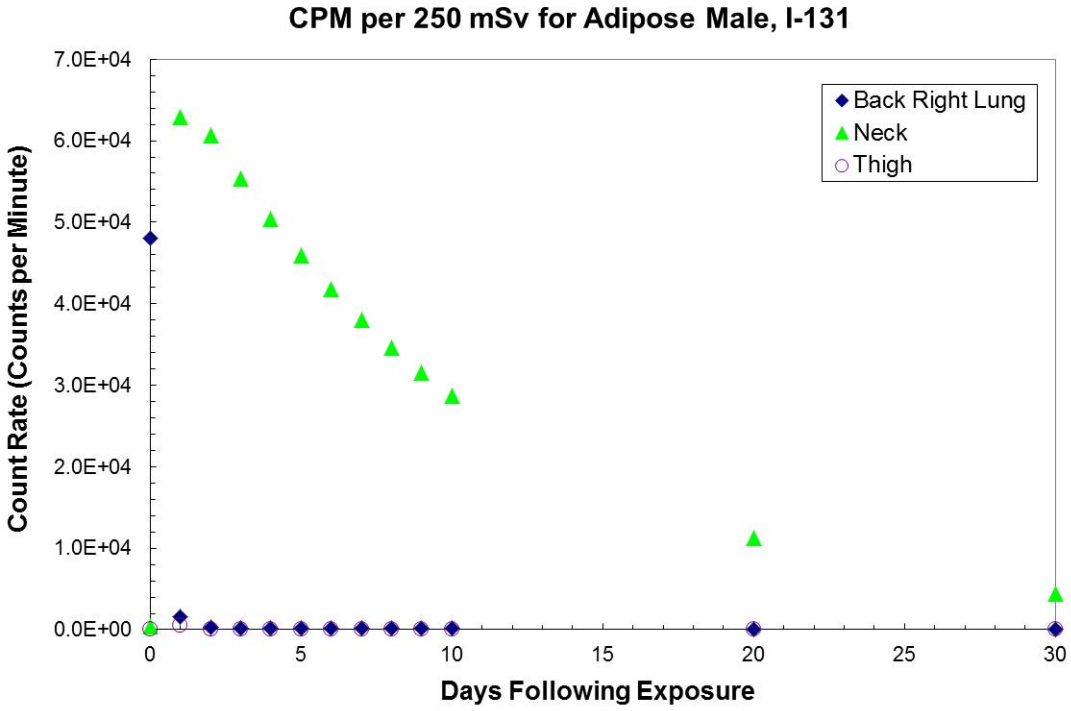

Adipose Male ^{192}Ir Inhalation

^{192}Ir		Back Right Lung	Neck	Thigh
		CPM per 250 mSv	CPM per 250 mSv	CPM per 250 mSv
Days following exposure	0	1.37E+05	1.48E+03	4.47E+01
	1	1.10E+05	2.38E+03	4.71E+03
	2	1.06E+05	2.19E+03	3.57E+03
	3	1.04E+05	2.09E+03	2.41E+03
	4	1.01E+05	2.03E+03	1.86E+03
	5	9.89E+04	1.99E+03	1.63E+03
	6	9.67E+04	1.96E+03	1.54E+03
	7	9.45E+04	1.93E+03	1.50E+03
	8	9.24E+04	1.90E+03	1.48E+03
	9	9.03E+04	1.88E+03	1.47E+03
	10	8.83E+04	1.85E+03	1.46E+03
	20	7.11E+04	1.64E+03	1.41E+03
	30	5.79E+04	1.47E+03	1.36E+03

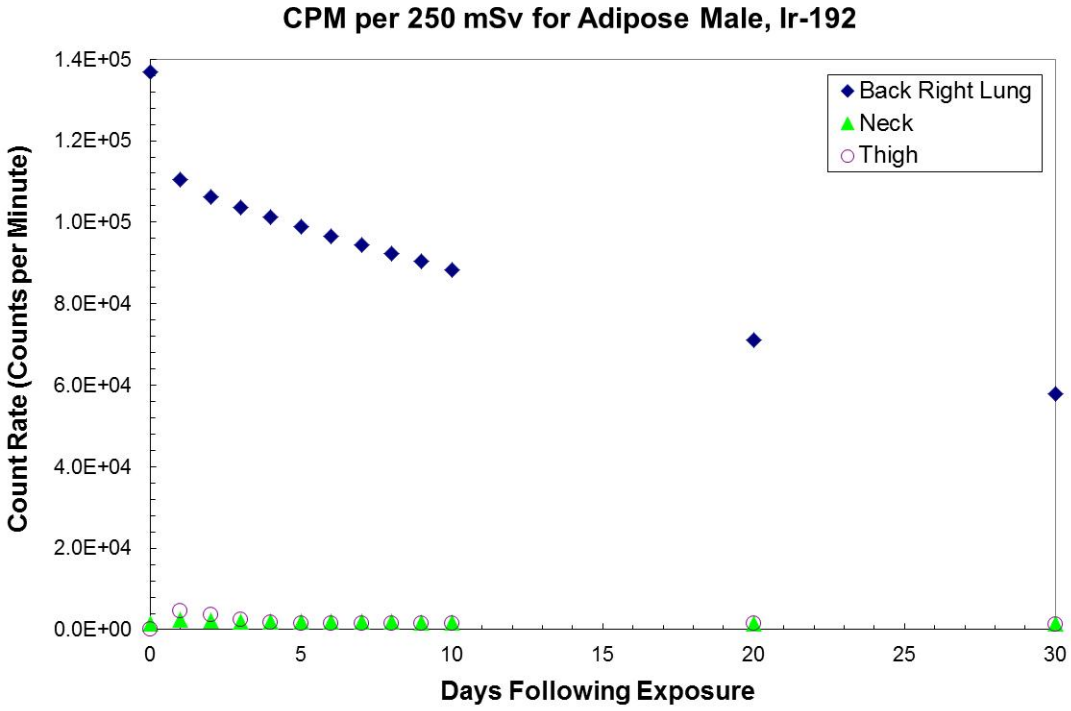

Adipose Female ^{241}Am Inhalation

^{241}Am		Back Right Lung	Neck	Thigh
		CPM per 250 mSv	CPM per 250 mSv	CPM per 250 mSv
Days following exposure	0	4.97E+00	5.08E-02	1.29E-04
	1	4.04E+00	5.27E-02	6.90E-02
	2	3.94E+00	4.81E-02	4.55E-02
	3	3.88E+00	4.61E-02	2.63E-02
	4	3.82E+00	4.51E-02	1.74E-02
	5	3.77E+00	4.44E-02	1.39E-02
	6	3.72E+00	4.39E-02	1.26E-02
	7	3.68E+00	4.34E-02	1.21E-02
	8	3.63E+00	4.29E-02	1.20E-02
	9	3.58E+00	4.25E-02	1.21E-02
	10	3.54E+00	4.21E-02	1.21E-02
	20	3.14E+00	3.84E-02	1.29E-02
	30	2.81E+00	3.54E-02	1.34E-02

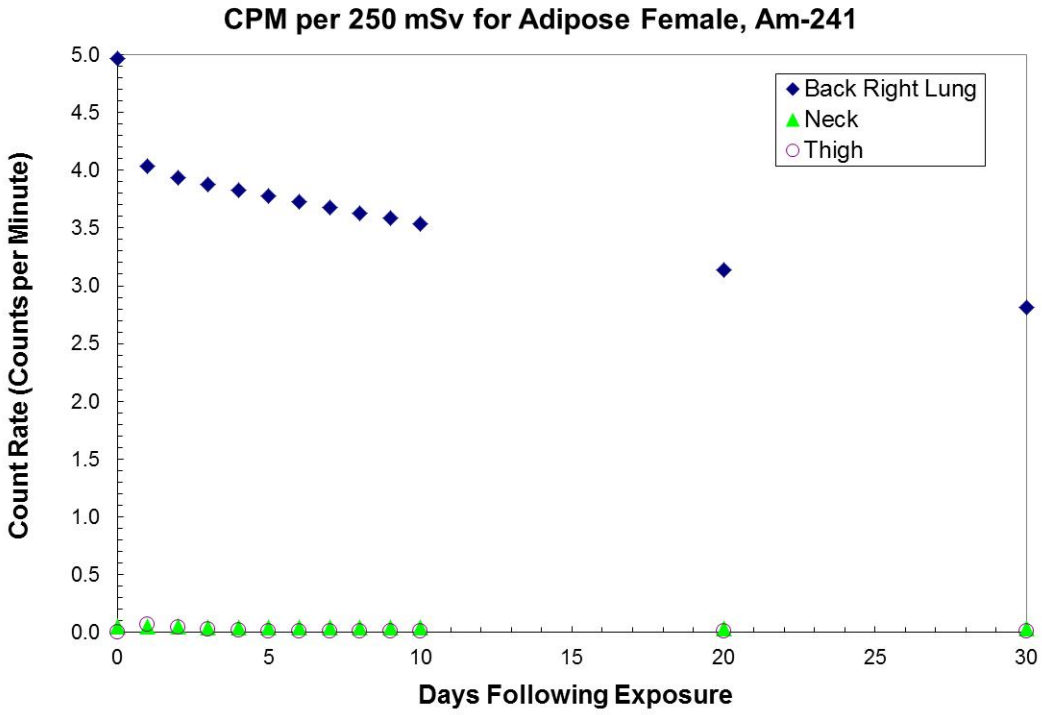

Adipose Female ^{60}Co Inhalation

^{60}Co		Back Right Lung	Neck	Thigh
		CPM per 250 mSv	CPM per 250 mSv	CPM per 250 mSv
Days following exposure	0	3.90E+04	1.00E+04	1.01E+03
	1	3.70E+04	1.18E+04	4.85E+03
	2	3.37E+04	1.01E+04	3.59E+03
	3	3.19E+04	9.17E+03	2.55E+03
	4	3.09E+04	8.72E+03	2.04E+03
	5	3.03E+04	8.45E+03	1.81E+03
	6	2.98E+04	8.27E+03	1.69E+03
	7	2.93E+04	8.12E+03	1.62E+03
	8	2.89E+04	7.99E+03	1.57E+03
	9	2.84E+04	7.86E+03	1.53E+03
	10	2.80E+04	7.74E+03	1.50E+03
	20	2.46E+04	6.77E+03	1.28E+03
	30	2.18E+04	6.04E+03	1.17E+03

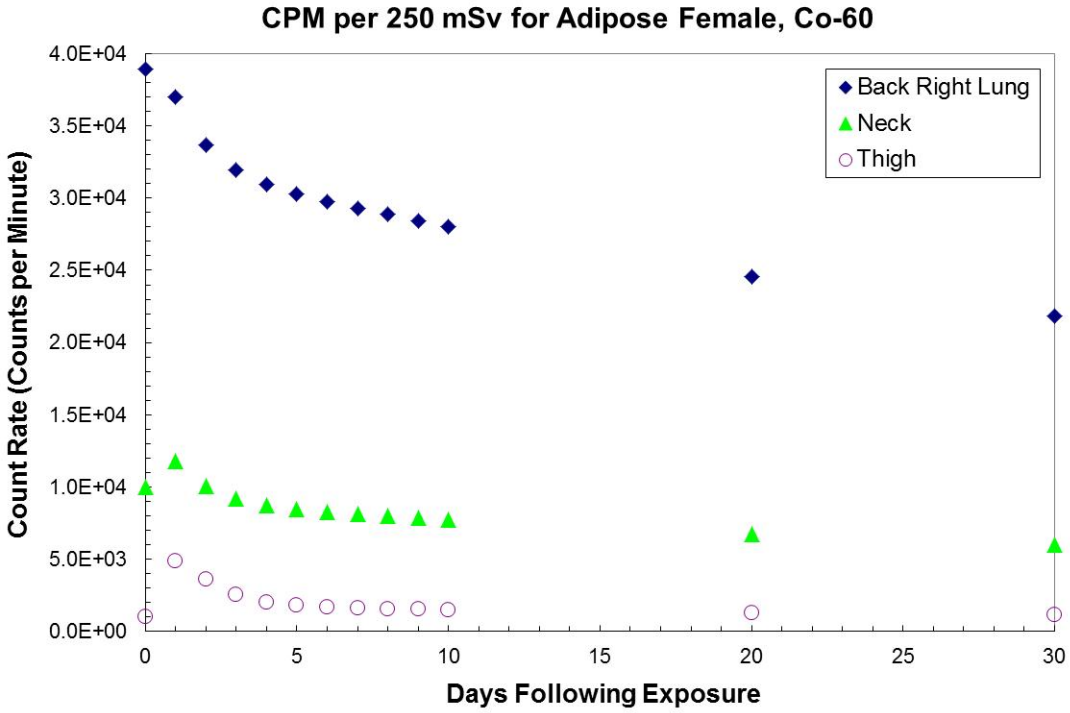

Adipose Female ^{137}Cs Inhalation

^{137}Cs		Back Right Lung	Neck	Thigh
		CPM per 250 mSv	CPM per 250 mSv	CPM per 250 mSv
Days following exposure	0	5.64E+04	5.00E+03	4.13E+02
	1	1.86E+04	1.40E+04	1.83E+04
	2	1.71E+04	1.37E+04	1.80E+04
	3	1.67E+04	1.33E+04	1.76E+04
	4	1.63E+04	1.31E+04	1.73E+04
	5	1.61E+04	1.29E+04	1.70E+04
	6	1.59E+04	1.27E+04	1.68E+04
	7	1.57E+04	1.26E+04	1.66E+04
	8	1.55E+04	1.24E+04	1.65E+04
	9	1.54E+04	1.23E+04	1.63E+04
	10	1.53E+04	1.22E+04	1.62E+04
	20	1.43E+04	1.14E+04	1.51E+04
	30	1.34E+04	1.07E+04	1.42E+04

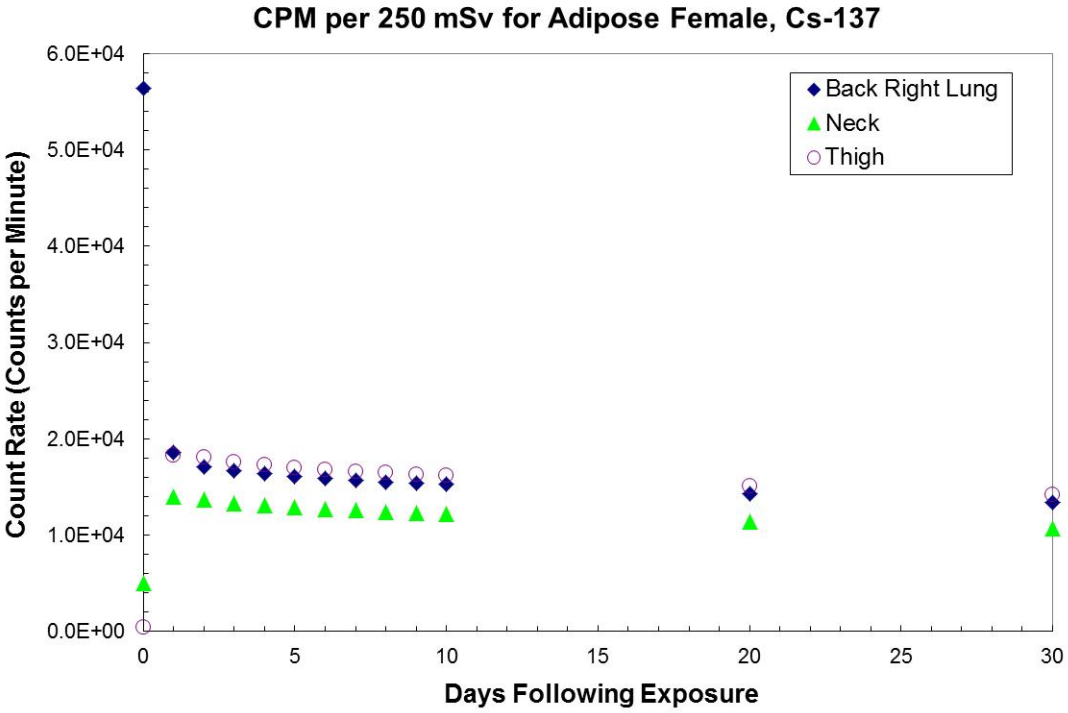

Adipose Female ^{131}I Inhalation

^{131}I		Back Right Lung	Neck	Thigh
		CPM per 250 mSv	CPM per 250 mSv	CPM per 250 mSv
Days following exposure	0	5.67E+04	5.27E+02	4.99E+01
	1	2.00E+03	5.45E+04	7.24E+02
	2	3.69E+02	5.25E+04	1.01E+02
	3	2.73E+02	4.79E+04	8.50E+01
	4	2.63E+02	4.36E+04	9.90E+01
	5	2.56E+02	3.97E+04	1.11E+02
	6	2.48E+02	3.61E+04	1.18E+02
	7	2.38E+02	3.29E+04	1.23E+02
	8	2.28E+02	3.00E+04	1.26E+02
	9	2.17E+02	2.73E+04	1.26E+02
	10	2.05E+02	2.48E+04	1.25E+02
	20	1.05E+02	9.75E+03	7.89E+01
	30	4.71E+01	3.84E+03	3.81E+01

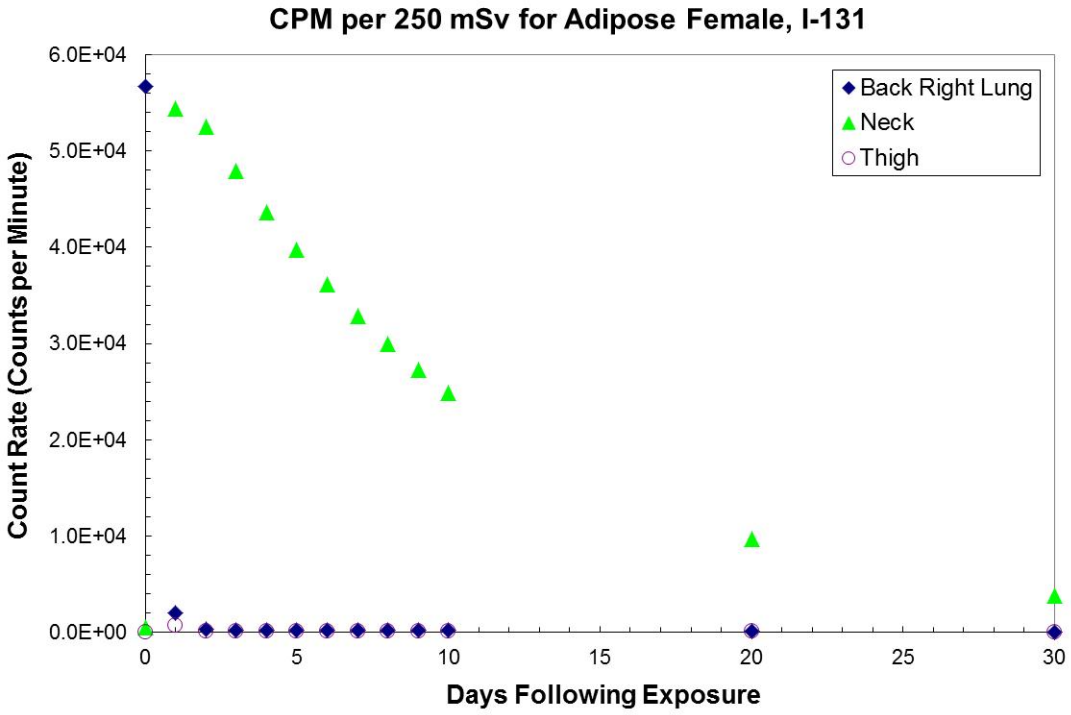

Adipose Female ^{192}Ir Inhalation

^{192}Ir		Back Right Lung	Neck	Thigh
		CPM per 250 mSv	CPM per 250 mSv	CPM per 250 mSv
Days following exposure	0	1.61E+05	1.56E+03	1.11E+02
	1	1.30E+05	2.63E+03	4.67E+03
	2	1.26E+05	2.39E+03	3.65E+03
	3	1.22E+05	2.26E+03	2.72E+03
	4	1.19E+05	2.18E+03	2.27E+03
	5	1.17E+05	2.14E+03	2.09E+03
	6	1.14E+05	2.10E+03	2.01E+03
	7	1.11E+05	2.07E+03	1.97E+03
	8	1.09E+05	2.04E+03	1.96E+03
	9	1.07E+05	2.02E+03	1.94E+03
	10	1.04E+05	1.99E+03	1.93E+03
	20	8.39E+04	1.77E+03	1.86E+03
	30	6.83E+04	1.59E+03	1.79E+03

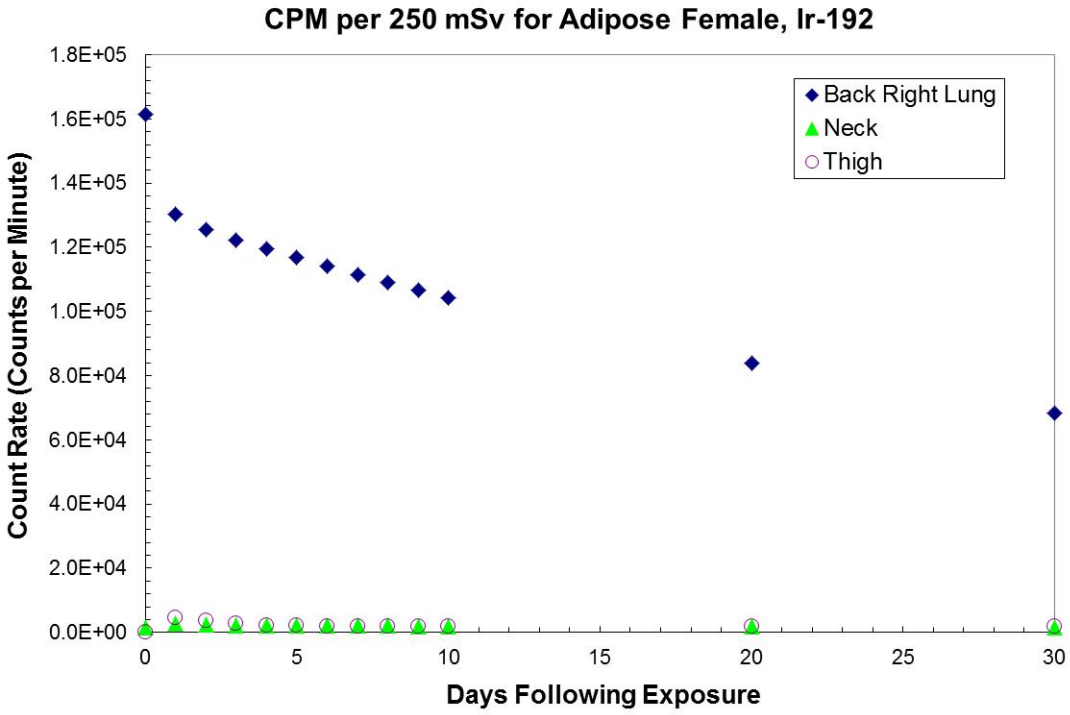

Post Menopausal Adipose Female ^{241}Am Inhalation

^{241}Am		Back Right Lung	Neck	Thigh
		CPM per 250 mSv	CPM per 250 mSv	CPM per 250 mSv
Days following exposure	0	4.10E+00	5.23E-02	0.00E+00
	1	3.33E+00	5.60E-02	6.63E-02
	2	3.25E+00	5.07E-02	4.35E-02
	3	3.20E+00	4.85E-02	2.45E-02
	4	3.16E+00	4.73E-02	1.55E-02
	5	3.12E+00	4.66E-02	1.20E-02
	6	3.08E+00	4.61E-02	1.06E-02
	7	3.04E+00	4.56E-02	1.02E-02
	8	3.00E+00	4.51E-02	1.01E-02
	9	2.96E+00	4.47E-02	1.01E-02
	10	2.92E+00	4.43E-02	1.01E-02
	20	2.60E+00	4.06E-02	1.07E-02
	30	2.33E+00	3.75E-02	1.11E-02

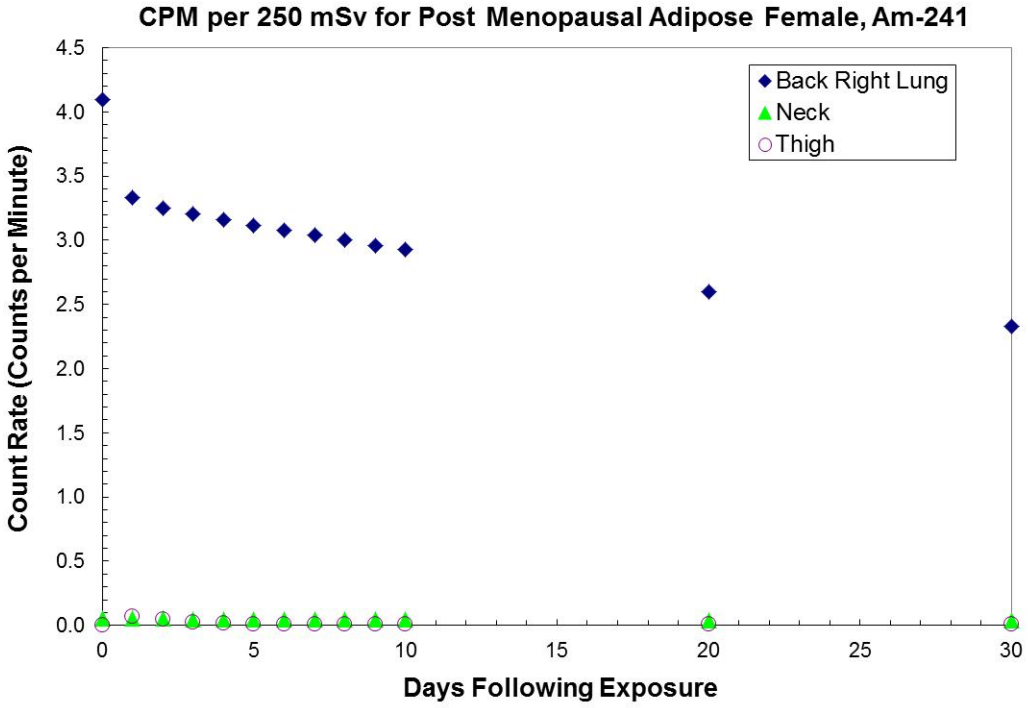

Post Menopausal Adipose Female ^{60}Co Inhalation

^{60}Co		Back Right Lung	Neck	Thigh
		CPM per 250 mSv	CPM per 250 mSv	CPM per 250 mSv
Days following exposure	0	3.53E+04	9.27E+03	8.60E+02
	1	3.34E+04	1.08E+04	4.54E+03
	2	3.05E+04	9.26E+03	3.33E+03
	3	2.89E+04	8.46E+03	2.33E+03
	4	2.80E+04	8.06E+03	1.84E+03
	5	2.74E+04	7.82E+03	1.61E+03
	6	2.70E+04	7.65E+03	1.50E+03
	7	2.65E+04	7.52E+03	1.43E+03
	8	2.61E+04	7.39E+03	1.39E+03
	9	2.58E+04	7.28E+03	1.35E+03
	10	2.54E+04	7.17E+03	1.32E+03
	20	2.23E+04	6.26E+03	1.13E+03
	30	1.98E+04	5.59E+03	1.04E+03

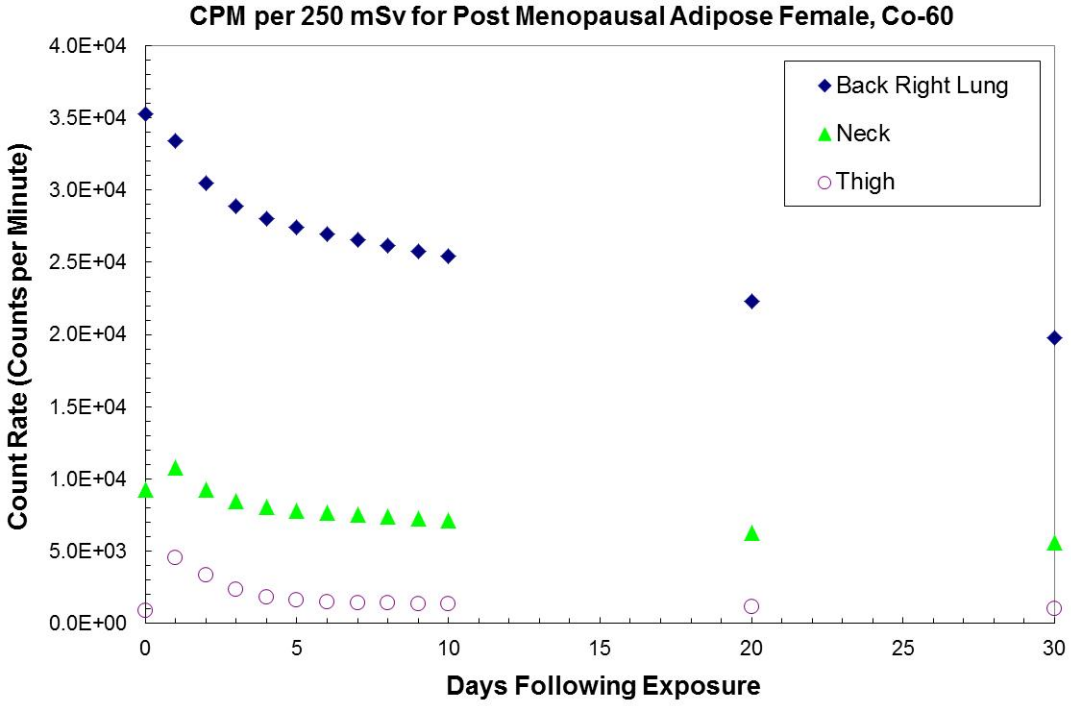

Post Menopausal Adipose Female ^{137}Cs Inhalation

^{137}Cs		Back Right Lung	Neck	Thigh
		CPM per 250 mSv	CPM per 250 mSv	CPM per 250 mSv
Days following exposure	0	8.09E+03	2.93E+03	3.25E+02
	1	5.16E+03	4.13E+03	4.57E+03
	2	4.89E+03	3.98E+03	4.51E+03
	3	4.77E+03	3.88E+03	4.41E+03
	4	4.67E+03	3.80E+03	4.32E+03
	5	4.60E+03	3.74E+03	4.25E+03
	6	4.53E+03	3.69E+03	4.19E+03
	7	4.48E+03	3.65E+03	4.14E+03
	8	4.44E+03	3.61E+03	4.10E+03
	9	4.40E+03	3.58E+03	4.07E+03
	10	4.36E+03	3.55E+03	4.03E+03
	20	4.07E+03	3.32E+03	3.77E+03
	30	3.82E+03	3.11E+03	3.53E+03

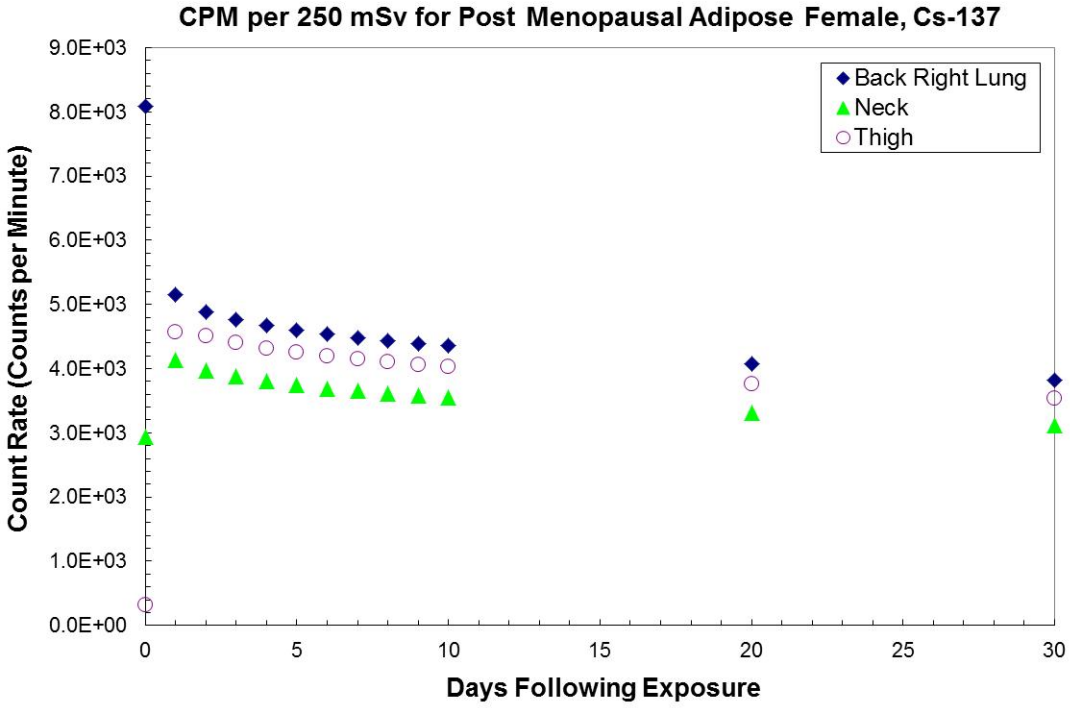

Post Menopausal Adipose Female ^{131}I Inhalation

^{131}I		Back Right Lung	Neck	Thigh
		CPM per 250 mSv	CPM per 250 mSv	CPM per 250 mSv
Days following exposure	0	4.97E+04	5.07E+02	4.11E+01
	1	1.80E+03	5.44E+04	6.43E+02
	2	3.58E+02	5.25E+04	9.11E+01
	3	2.72E+02	4.79E+04	7.63E+01
	4	2.60E+02	4.36E+04	8.83E+01
	5	2.52E+02	3.97E+04	9.82E+01
	6	2.42E+02	3.61E+04	1.05E+02
	7	2.32E+02	3.29E+04	1.09E+02
	8	2.21E+02	2.99E+04	1.11E+02
	9	2.10E+02	2.73E+04	1.11E+02
	10	1.98E+02	2.48E+04	1.10E+02
	20	9.97E+01	9.74E+03	6.95E+01
	30	4.44E+01	3.84E+03	3.35E+01

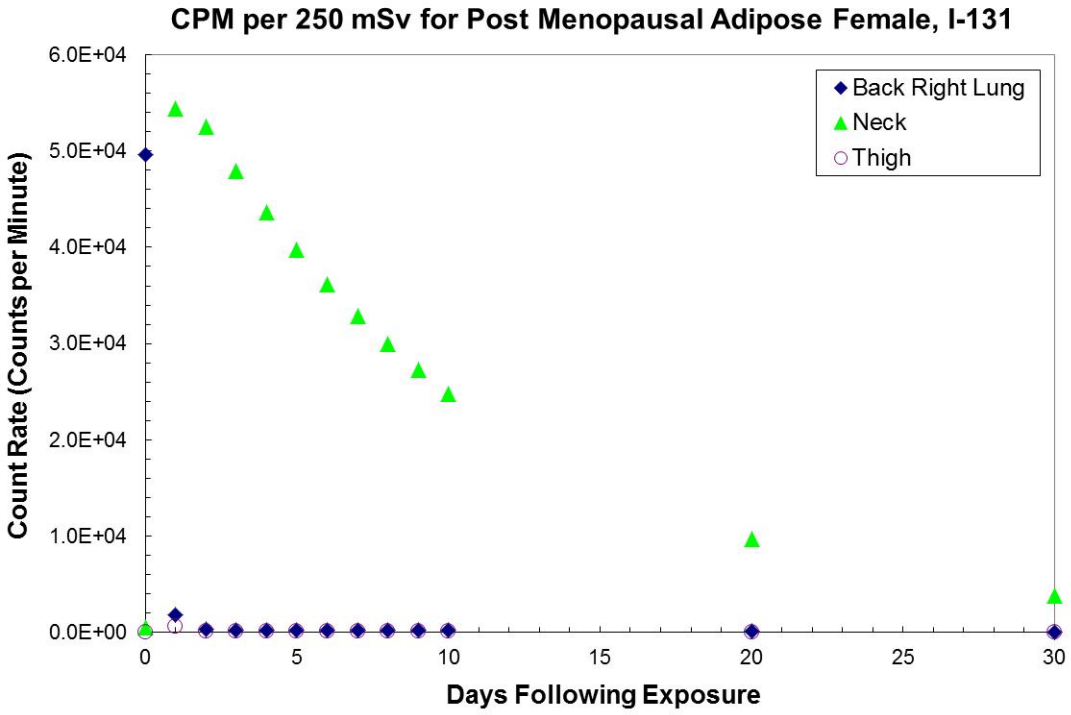

Post Menopausal Adipose Female ^{192}Ir Inhalation

^{192}Ir		Back Right Lung	Neck	Thigh
		CPM per 250 mSv	CPM per 250 mSv	CPM per 250 mSv
Days following exposure	0	1.42E+05	1.57E+03	4.53E+01
	1	1.15E+05	2.40E+03	5.09E+03
	2	1.10E+05	2.21E+03	3.82E+03
	3	1.08E+05	2.10E+03	2.64E+03
	4	1.05E+05	2.04E+03	2.07E+03
	5	1.03E+05	1.99E+03	1.84E+03
	6	1.00E+05	1.96E+03	1.75E+03
	7	9.80E+04	1.93E+03	1.71E+03
	8	9.58E+04	1.90E+03	1.69E+03
	9	9.37E+04	1.88E+03	1.67E+03
	10	9.16E+04	1.85E+03	1.67E+03
	20	7.38E+04	1.63E+03	1.61E+03
	30	6.00E+04	1.45E+03	1.55E+03

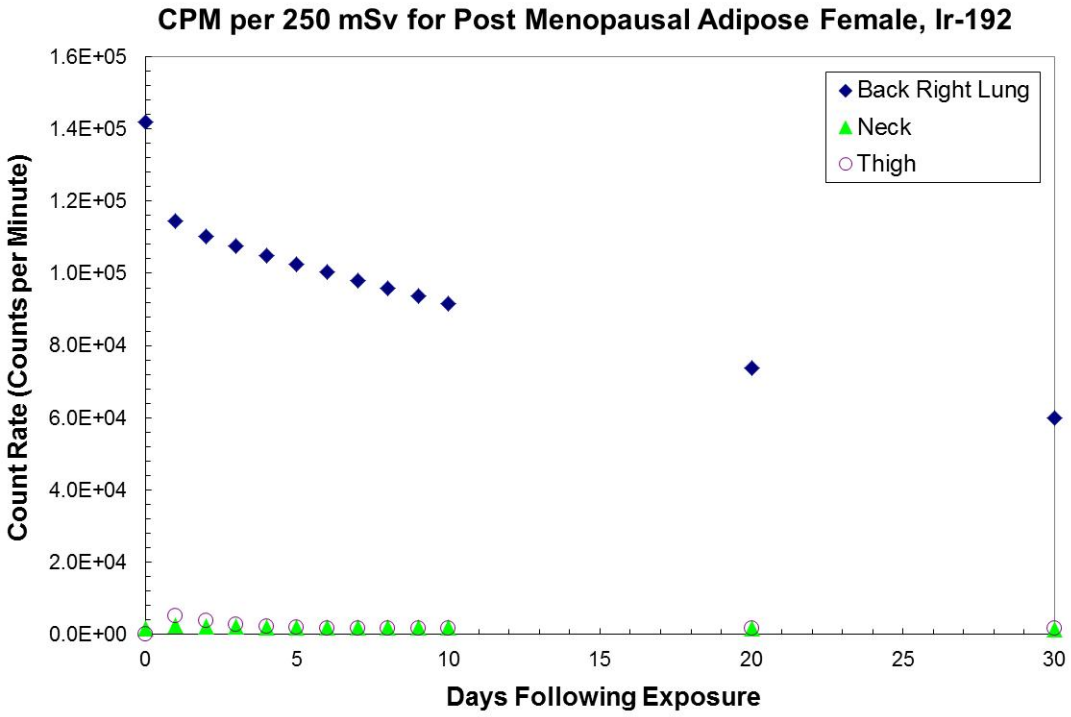

10-year-old Child ^{241}Am Inhalation

^{241}Am		Back Right Lung	Neck	Thigh
		CPM per 250 mSv	CPM per 250 mSv	CPM per 250 mSv
Days following exposure	0	8.70E+00	1.47E-01	0.00E+00
	1	7.12E+00	2.15E-01	2.53E-01
	2	6.95E+00	2.08E-01	1.79E-01
	3	6.84E+00	2.05E-01	1.21E-01
	4	6.75E+00	2.04E-01	9.52E-02
	5	6.66E+00	2.04E-01	8.55E-02
	6	6.57E+00	2.05E-01	8.27E-02
	7	6.49E+00	2.05E-01	8.24E-02
	8	6.41E+00	2.05E-01	8.32E-02
	9	6.33E+00	2.06E-01	8.43E-02
	10	6.25E+00	2.06E-01	8.55E-02
	20	5.56E+00	2.11E-01	9.76E-02
	30	4.99E+00	2.15E-01	1.08E-01

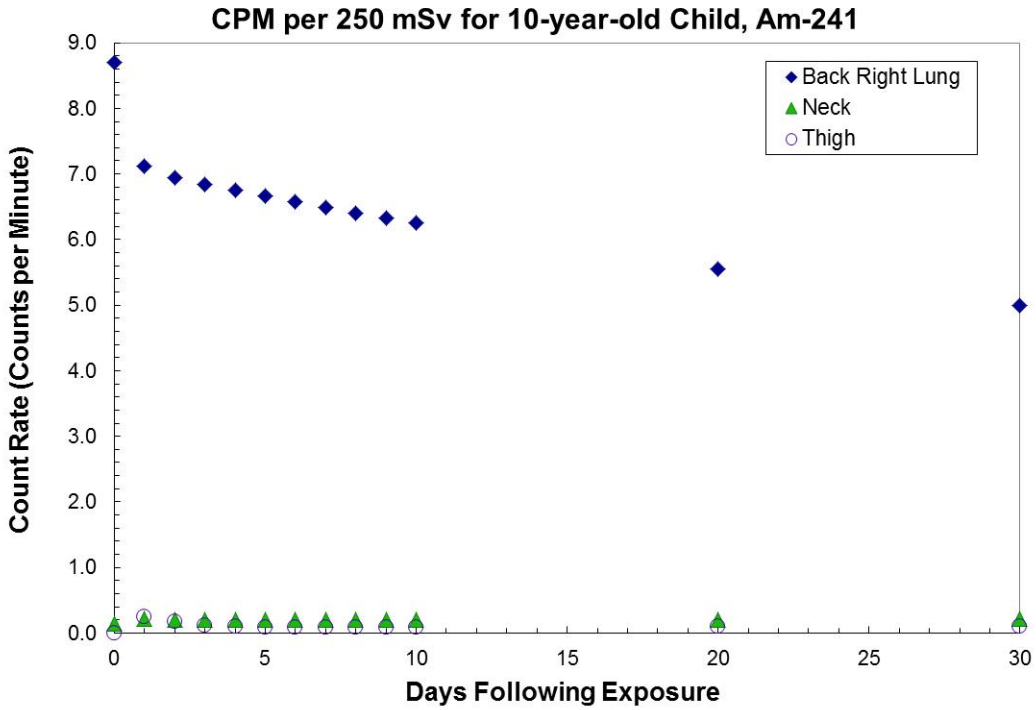

10-year-old Child ^{60}Co Inhalation

^{60}Co		Back Right Lung	Neck	Thigh
		CPM per 250 mSv	CPM per 250 mSv	CPM per 250 mSv
Days following exposure	0	3.73E+04	7.40E+03	2.13E+03
	1	3.56E+04	1.12E+04	6.56E+03
	2	3.22E+04	8.66E+03	4.81E+03
	3	3.06E+04	7.52E+03	3.65E+03
	4	2.97E+04	6.99E+03	3.09E+03
	5	2.90E+04	6.72E+03	2.83E+03
	6	2.86E+04	6.54E+03	2.69E+03
	7	2.81E+04	6.41E+03	2.60E+03
	8	2.77E+04	6.29E+03	2.53E+03
	9	2.73E+04	6.19E+03	2.48E+03
	10	2.69E+04	6.09E+03	2.43E+03
	20	2.36E+04	5.31E+03	2.09E+03
	30	2.10E+04	4.75E+03	1.90E+03

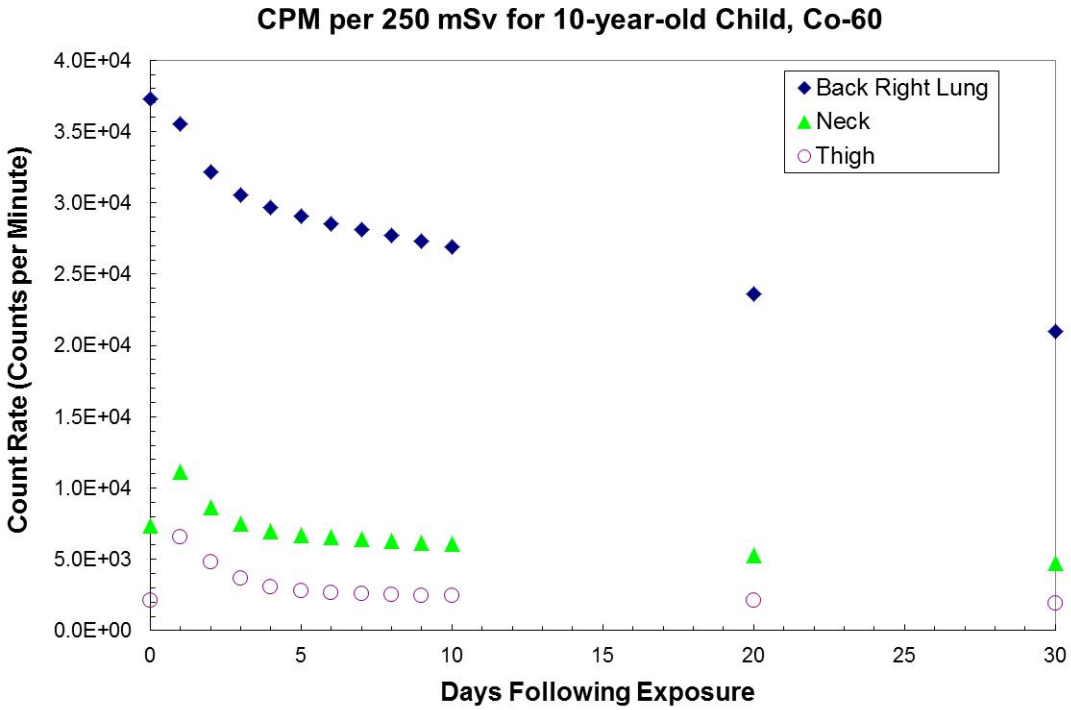

10-year-old Child ^{137}Cs Inhalation

^{137}Cs		Back Right Lung	Neck	Thigh
		CPM per 250 mSv	CPM per 250 mSv	CPM per 250 mSv
Days following exposure	0	1.04E+05	8.67E+03	0.00E+00
	1	4.28E+04	3.15E+04	5.92E+04
	2	3.96E+04	3.08E+04	5.85E+04
	3	3.85E+04	3.00E+04	5.72E+04
	4	3.78E+04	2.95E+04	5.61E+04
	5	3.72E+04	2.90E+04	5.52E+04
	6	3.67E+04	2.86E+04	5.45E+04
	7	3.63E+04	2.83E+04	5.39E+04
	8	3.59E+04	2.80E+04	5.34E+04
	9	3.56E+04	2.78E+04	5.29E+04
	10	3.53E+04	2.75E+04	5.25E+04
	20	3.30E+04	2.57E+04	4.90E+04
	30	3.10E+04	2.41E+04	4.60E+04

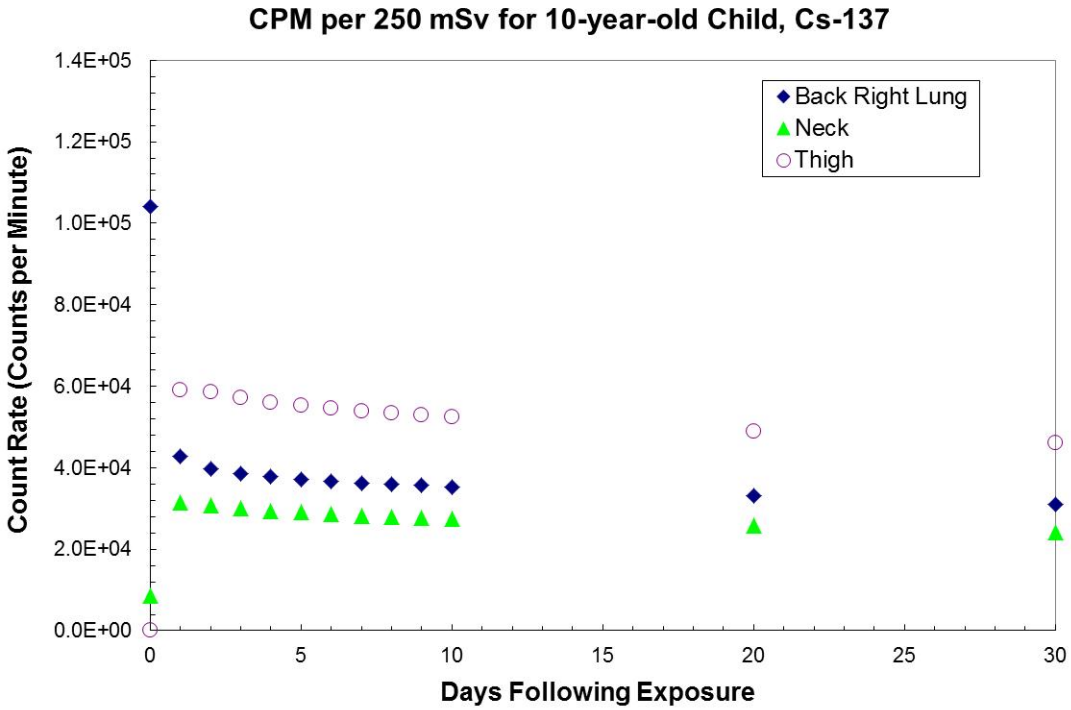

10-year-old Child ^{131}I Inhalation

^{131}I		Back Right Lung	Neck	Thigh
		CPM per 250 mSv	CPM per 250 mSv	CPM per 250 mSv
Days following exposure	0	3.42E+04	2.08E+02	7.52E+01
	1	1.51E+03	1.59E+04	6.00E+02
	2	3.21E+02	1.50E+04	9.64E+01
	3	2.48E+02	1.37E+04	8.25E+01
	4	2.36E+02	1.25E+04	9.27E+01
	5	2.27E+02	1.14E+04	1.01E+02
	6	2.18E+02	1.04E+04	1.06E+02
	7	2.07E+02	9.43E+03	1.09E+02
	8	1.97E+02	8.59E+03	1.10E+02
	9	1.86E+02	7.83E+03	1.10E+02
	10	1.76E+02	7.13E+03	1.08E+02
	20	8.70E+01	2.82E+03	6.66E+01
	30	3.85E+01	1.11E+03	3.19E+01

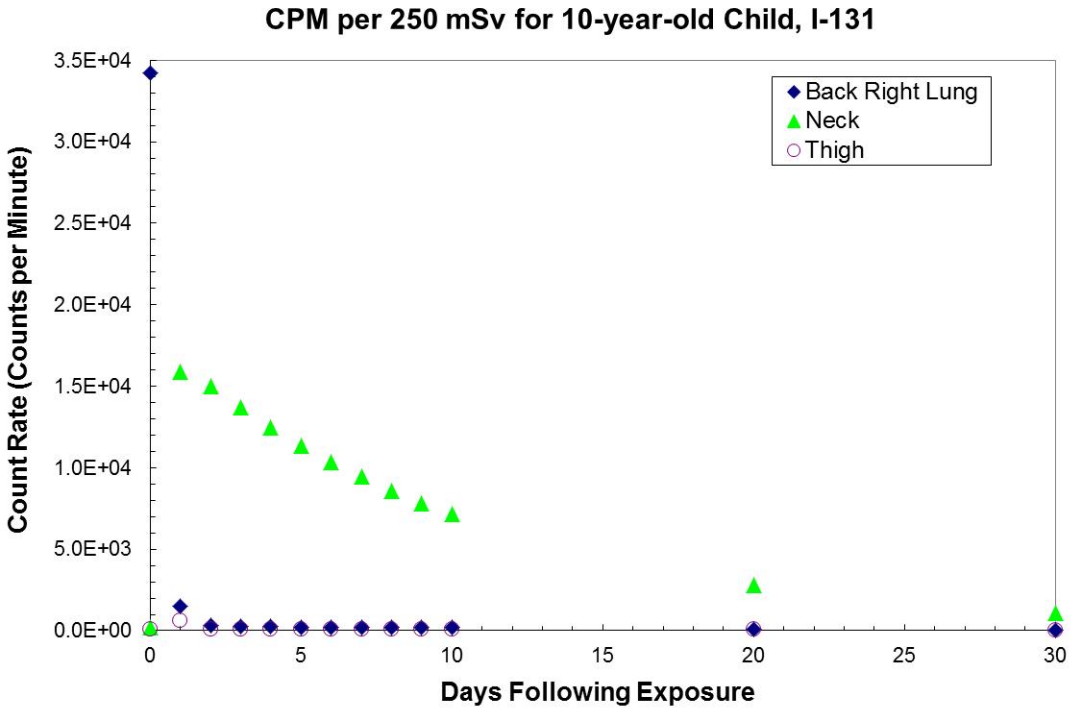

10-year-old Child ^{192}Ir Inhalation

^{192}Ir		Back Right Lung	Neck	Thigh
		CPM per 250 mSv	CPM per 250 mSv	CPM per 250 mSv
Days following exposure	0	1.71E+05	1.67E+03	2.24E+02
	1	1.39E+05	3.85E+03	5.19E+03
	2	1.34E+05	3.59E+03	4.34E+03
	3	1.30E+05	3.42E+03	3.49E+03
	4	1.27E+05	3.32E+03	3.07E+03
	5	1.24E+05	3.26E+03	2.90E+03
	6	1.21E+05	3.22E+03	2.82E+03
	7	1.19E+05	3.18E+03	2.78E+03
	8	1.16E+05	3.15E+03	2.76E+03
	9	1.14E+05	3.12E+03	2.75E+03
	10	1.11E+05	3.09E+03	2.73E+03
	20	8.94E+04	2.82E+03	2.63E+03
	30	7.28E+04	2.60E+03	2.53E+03

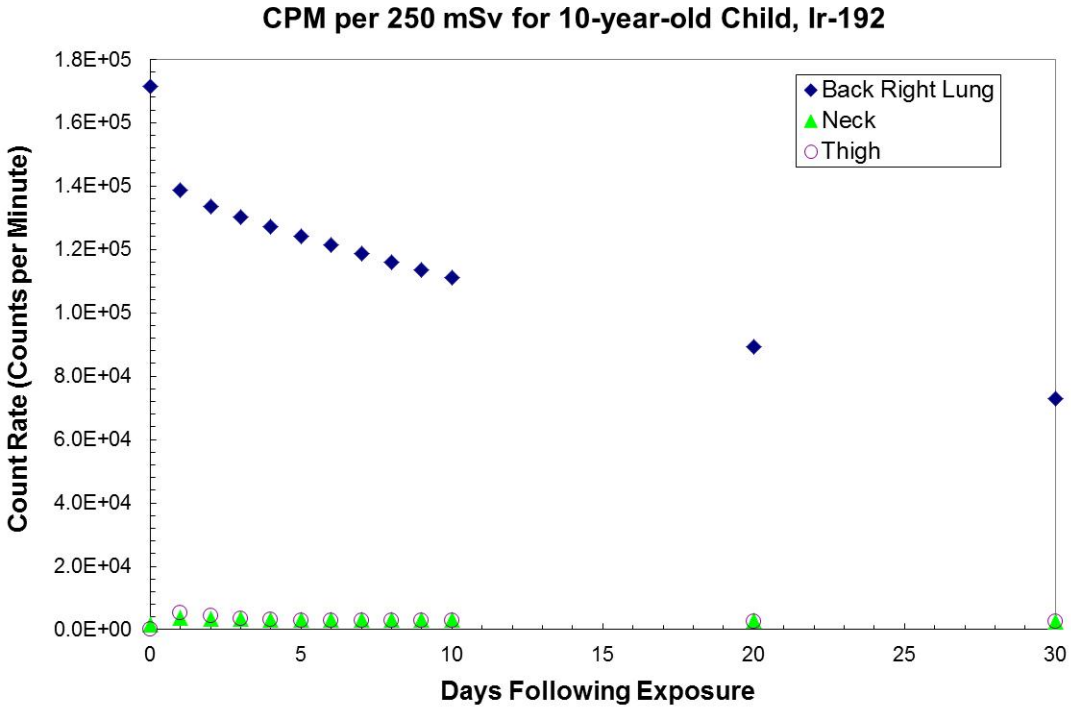
CPM per 250 mSv for 10-year-old Child, Ir-192
Count Rate (Counts per Minute)
1.8E+05
1.6E+05
1.4E+05
1.2E+05
1.0E+05
8.0E+04
6.0E+04
4.0E+04
2.0E+04
0.0E+00
0
5
10
15
20
25
30
Days Following Exposure
Back Right Lung
Neck
Thigh

APPENDIX B: TABLULATED DATA FOR INGESTION

- Data are presented in graphical and tabular format for the Adult, Adipose Adult and Child phantom-isotope pairings for ingestion.
- Graphical data and tabular data are the count rate (counts per minute) per 250 mSv for each detection location that was simulated.

Reference Male ^{241}Am Ingestion
Reference Male ^{60}Co Ingestion
Reference Male ^{137}Cs Ingestion
Reference Male ^{131}I Ingestion
Reference Male ^{192}Ir Ingestion

Adipose Male ^{241}Am Ingestion
Adipose Male ^{60}CoIngestion
Adipose Male ^{137}Cs Ingestion
Adipose Male ^{131}IIngestion
Adipose Male ^{192}IrIngestion

10-year-old Child ^{241}Am Ingestion
10-year-old Child ^{60}CoIngestion
10-year-old Child ^{137}CsIngestion
10-year-old Child ^{131}IIngestion
10-year-old Child ^{192}Ir Ingestion

Reference Male ^{241}Am Ingestion

^{241}Am		Umbilicus	Back Right Lung	Front Right Lung	Neck	Thigh
		CPM per 250 mSv	CPM per 250 mSv	CPM per 250 mSv	CPM per 250 mSv	CPM per 250 mSv
Days following exposure	0	1.34E+03	1.01E+02	1.07E+02	1.67E+00	3.33E-01
	1	1.54E+03	9.61E+00	9.62E+00	7.21E-01	5.26E+01
	2	4.24E+02	4.77E+00	4.11E+00	4.48E-01	3.22E+01
	3	1.34E+02	3.76E+00	2.53E+00	3.44E-01	1.42E+01
	4	4.61E+01	3.51E+00	2.02E+00	3.03E-01	5.85E+00
	5	1.71E+01	3.45E+00	1.85E+00	2.86E-01	2.48E+00
	6	7.03E+00	3.42E+00	1.78E+00	2.78E-01	1.19E+00
	7	3.39E+00	3.42E+00	1.76E+00	2.73E-01	7.06E-01
	8	2.06E+00	3.40E+00	1.74E+00	2.70E-01	5.24E-01
	9	1.56E+00	3.41E+00	1.74E+00	2.67E-01	4.55E-01
	10	1.38E+00	3.41E+00	1.73E+00	2.65E-01	4.27E-01
	20	1.21E+00	3.39E+00	1.71E+00	2.43E-01	3.80E-01
	30	1.17E+00	3.37E+00	1.69E+00	2.25E-01	3.51E-01

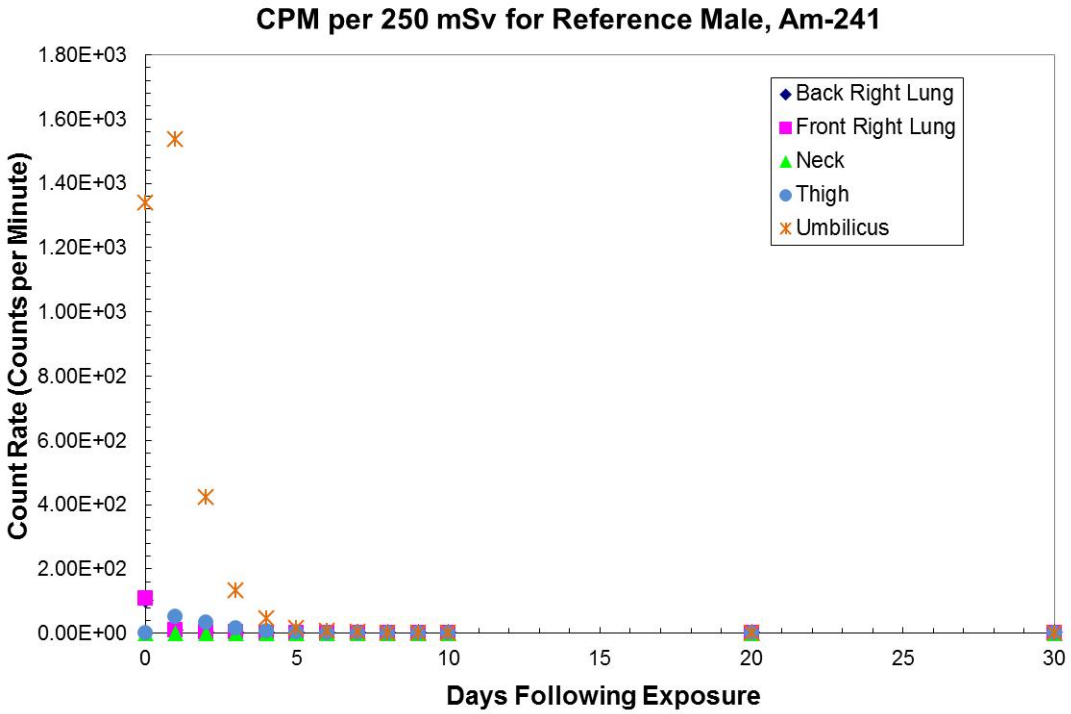

Reference Male ^{60}Co Ingestion

^{60}Co		Umbilicus	Back Right Lung	Front Right Lung	Neck	Thigh
		CPM per 250 mSv	CPM per 250 mSv	CPM per 250 mSv	CPM per 250 mSv	CPM per 250 mSv
Days following exposure	0	2.05E+05	5.06E+04	2.11E+05	1.76E+05	5.16E+04
	1	1.92E+05	8.08E+04	1.11E+05	4.90E+04	5.87E+04
	2	7.55E+04	4.18E+04	5.29E+04	2.55E+04	3.67E+04
	3	3.36E+04	2.16E+04	2.58E+04	1.37E+04	1.95E+04
	4	1.81E+04	1.29E+04	1.47E+04	8.58E+03	1.14E+04
	5	1.21E+04	9.33E+03	1.02E+04	6.43E+03	7.91E+03
	6	9.56E+03	7.74E+03	8.26E+03	5.45E+03	6.39E+03
	7	8.37E+03	6.92E+03	7.30E+03	4.93E+03	5.64E+03
	8	7.68E+03	6.41E+03	6.73E+03	4.59E+03	5.20E+03
	9	7.21E+03	6.05E+03	6.33E+03	4.33E+03	4.89E+03
	10	6.84E+03	5.75E+03	6.01E+03	4.12E+03	4.65E+03
	20	4.84E+03	4.09E+03	4.27E+03	2.93E+03	3.31E+03
	30	4.07E+03	3.45E+03	3.59E+03	2.47E+03	2.79E+03

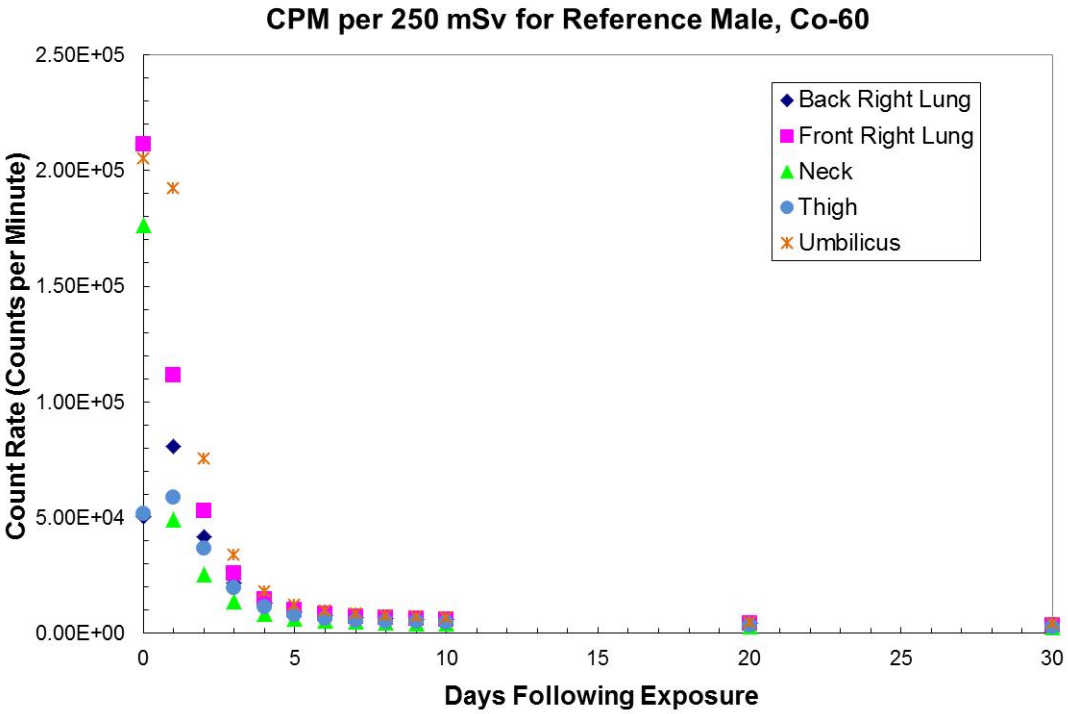

Reference Male ^{137}Cs Ingestion

^{137}Cs		Umbilicus	Back Right Lung	Front Right Lung	Neck	Thigh
		CPM per 250 mSv	CPM per 250 mSv	CPM per 250 mSv	CPM per 250 mSv	CPM per 250 mSv
Days following exposure	0	7.40E+03	1.24E+03	8.58E+03	1.13E+04	2.17E+03
	1	1.93E+04	1.46E+04	1.49E+04	1.24E+04	1.68E+04
	2	1.85E+04	1.31E+04	1.37E+04	1.21E+04	1.66E+04
	3	1.80E+04	1.27E+04	1.33E+04	1.18E+04	1.62E+04
	4	1.77E+04	1.25E+04	1.30E+04	1.16E+04	1.59E+04
	5	1.74E+04	1.23E+04	1.28E+04	1.14E+04	1.57E+04
	6	1.71E+04	1.21E+04	1.27E+04	1.12E+04	1.54E+04
	7	1.69E+04	1.20E+04	1.25E+04	1.11E+04	1.53E+04
	8	1.67E+04	1.19E+04	1.24E+04	1.10E+04	1.51E+04
	9	1.66E+04	1.18E+04	1.23E+04	1.09E+04	1.50E+04
	10	1.64E+04	1.17E+04	1.22E+04	1.08E+04	1.49E+04
	20	1.53E+04	1.09E+04	1.14E+04	1.01E+04	1.39E+04
	30	1.44E+04	1.02E+04	1.07E+04	9.47E+03	1.30E+04

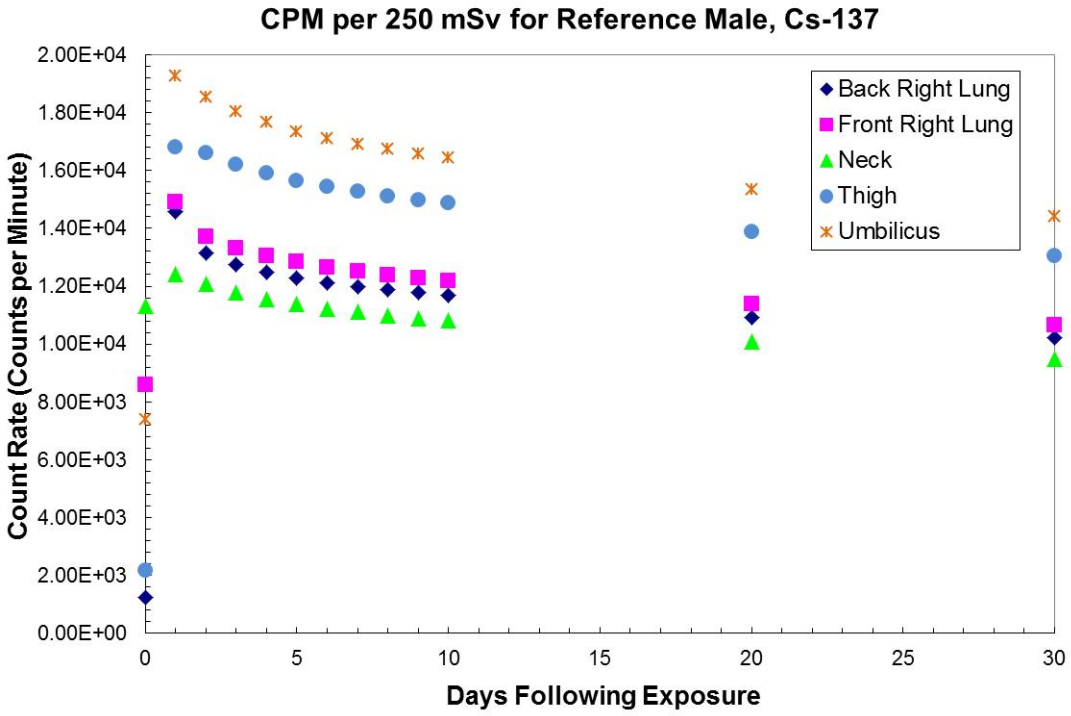

Reference Male ^{131}I Ingestion

^{131}I		Umbilicus	Back Right Lung	Front Right Lung	Neck	Thigh
		CPM per 250 mSv	CPM per 250 mSv	CPM per 250 mSv	CPM per 250 mSv	CPM per 250 mSv
Days following exposure	0	3.29E+03	5.94E+02	8.37E+02	1.76E+03	3.32E+02
	1	1.93E+03	2.05E+03	2.44E+03	6.22E+04	8.67E+02
	2	8.49E+02	2.29E+02	8.45E+02	6.02E+04	1.16E+02
	3	7.35E+02	1.31E+02	7.07E+02	5.50E+04	9.29E+01
	4	6.86E+02	1.29E+02	6.54E+02	5.00E+04	1.07E+02
	5	6.44E+02	1.31E+02	6.09E+02	4.56E+04	1.20E+02
	6	6.03E+02	1.30E+02	5.66E+02	4.15E+04	1.29E+02
	7	5.64E+02	1.29E+02	5.26E+02	3.77E+04	1.34E+02
	8	5.26E+02	1.26E+02	4.88E+02	3.44E+04	1.37E+02
	9	4.90E+02	1.22E+02	4.52E+02	3.13E+04	1.38E+02
	10	4.56E+02	1.18E+02	4.18E+02	2.85E+04	1.37E+02
	20	2.08E+02	6.57E+01	1.84E+02	1.12E+04	8.69E+01
	30	8.88E+01	3.05E+01	7.73E+01	4.41E+03	4.20E+01

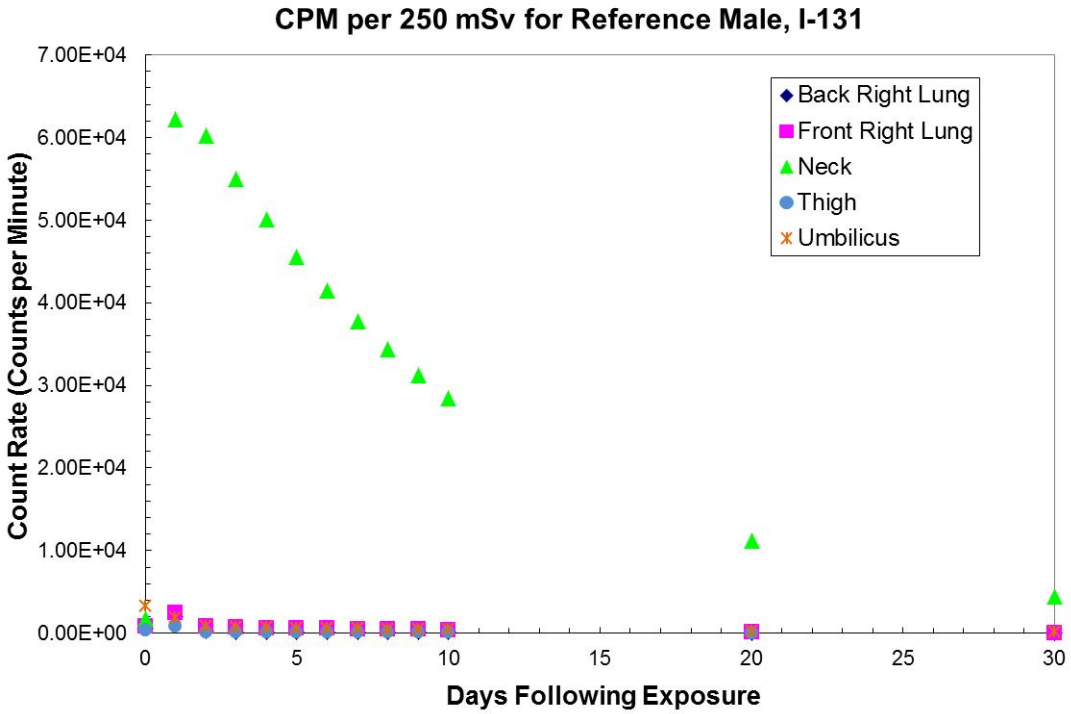

Reference Male ^{192}Ir Ingestion

^{192}Ir		Umbilicus	Back Right Lung	Front Right Lung	Neck	Thigh
		CPM per 250 mSv	CPM per 250 mSv	CPM per 250 mSv	CPM per 250 mSv	CPM per 250 mSv
Days following exposure	0	2.14E+05	4.84E+04	3.99E+04	3.09E+04	7.28E+03
	1	6.46E+05	1.58E+04	1.99E+04	8.75E+03	6.68E+04
	2	1.44E+05	9.17E+03	1.08E+04	4.90E+03	4.12E+04
	3	3.92E+04	6.15E+03	6.60E+03	2.95E+03	1.92E+04
	4	1.37E+04	4.88E+03	4.88E+03	2.12E+03	9.13E+03
	5	6.38E+03	4.33E+03	4.17E+03	1.78E+03	5.06E+03
	6	4.02E+03	4.07E+03	3.85E+03	1.63E+03	3.48E+03
	7	3.18E+03	3.91E+03	3.68E+03	1.56E+03	2.86E+03
	8	2.84E+03	3.80E+03	3.57E+03	1.51E+03	2.59E+03
	9	2.68E+03	3.71E+03	3.48E+03	1.47E+03	2.46E+03
	10	2.58E+03	3.63E+03	3.40E+03	1.43E+03	2.38E+03
	20	2.11E+03	3.00E+03	2.81E+03	1.19E+03	1.96E+03
	30	1.80E+03	2.57E+03	2.41E+03	1.02E+03	1.68E+03

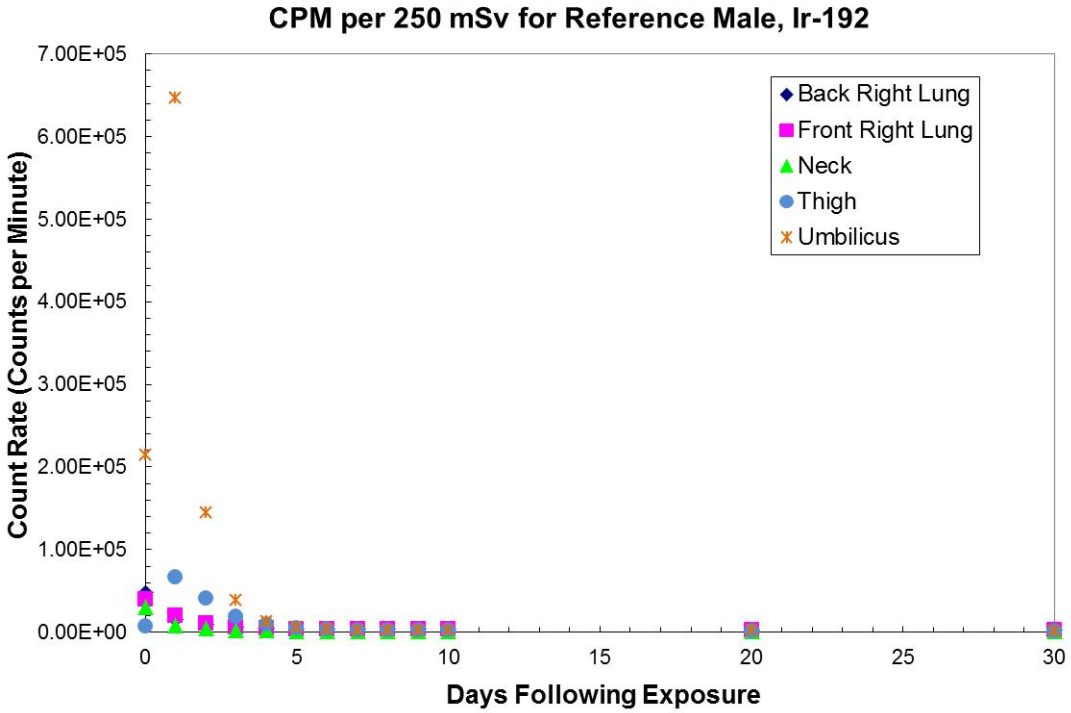

Adipose Male ^{241}Am Ingestion

^{241}Am		Umbilicus	Back Right Lung	Neck	Thigh
		CPM per 250 mSv	CPM per 250 mSv	CPM per 250 mSv	CPM per 250 mSv
Days following exposure	0	1.06E+02	3.72E+01	2.13E+00	1.77E+00
	1	2.98E+02	5.81E+00	3.70E+00	5.76E+01
	2	1.34E+02	3.76E+00	3.87E+00	3.65E+01
	3	5.37E+01	3.10E+00	3.92E+00	1.76E+01
	4	2.07E+01	2.88E+00	3.94E+00	8.75E+00
	5	8.02E+00	2.80E+00	3.96E+00	5.21E+00
	6	3.29E+00	2.77E+00	3.96E+00	3.86E+00
	7	1.52E+00	2.76E+00	3.97E+00	3.36E+00
	8	8.64E-01	2.75E+00	3.96E+00	3.16E+00
	9	6.21E-01	2.76E+00	3.98E+00	3.10E+00
	10	5.29E-01	2.76E+00	3.98E+00	3.08E+00
	20	4.47E-01	2.75E+00	3.99E+00	3.06E+00
	30	4.21E-01	2.74E+00	3.99E+00	3.05E+00

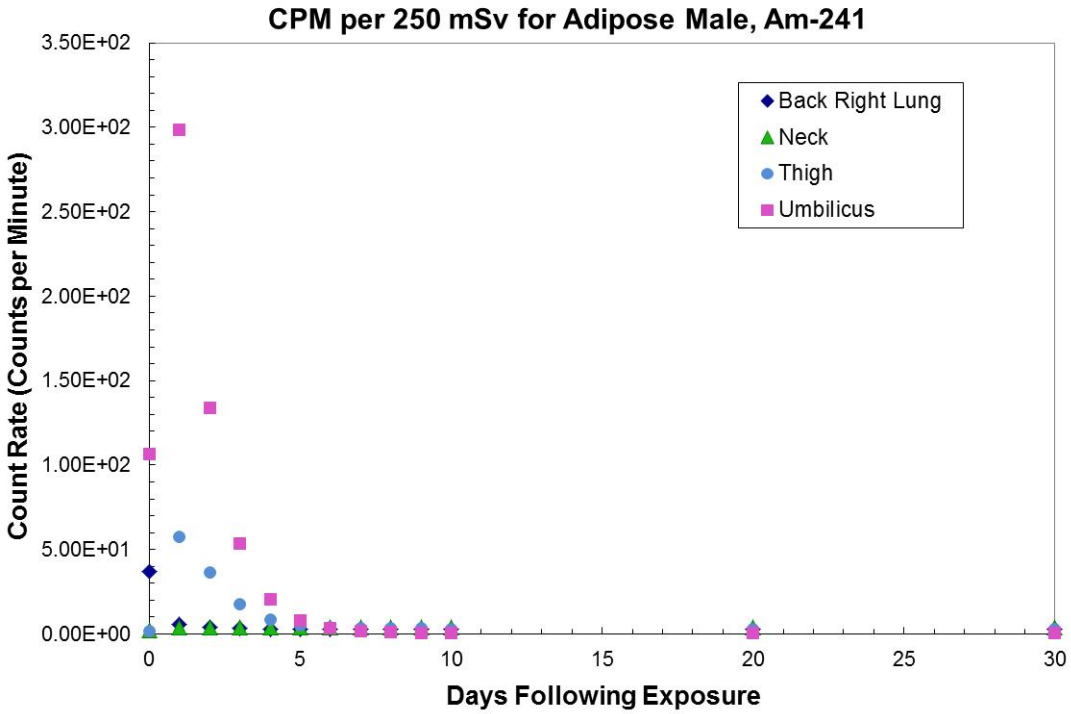

Adipose Male ^{60}Co Ingestion

^{60}Co		Umbilicus	Back Right Lung	Neck	Thigh
		CPM per 250 mSv	CPM per 250 mSv	CPM per 250 mSv	CPM per 250 mSv
Days following exposure	0	4.57E+04	4.50E+04	1.18E+05	3.81E+04
	1	1.26E+05	5.54E+04	3.85E+04	5.32E+04
	2	5.92E+04	2.84E+04	2.05E+04	3.29E+04
	3	2.71E+04	1.50E+04	1.15E+04	1.70E+04
	4	1.39E+04	9.33E+03	7.58E+03	9.60E+03
	5	8.55E+03	6.94E+03	5.92E+03	6.47E+03
	6	6.38E+03	5.86E+03	5.12E+03	5.12E+03
	7	5.40E+03	5.29E+03	4.67E+03	4.47E+03
	8	4.88E+03	4.92E+03	4.37E+03	4.10E+03
	9	4.55E+03	4.64E+03	4.13E+03	3.85E+03
	10	4.31E+03	4.42E+03	3.93E+03	3.65E+03
	20	3.04E+03	3.15E+03	2.81E+03	2.60E+03
	30	2.56E+03	2.65E+03	2.37E+03	2.19E+03

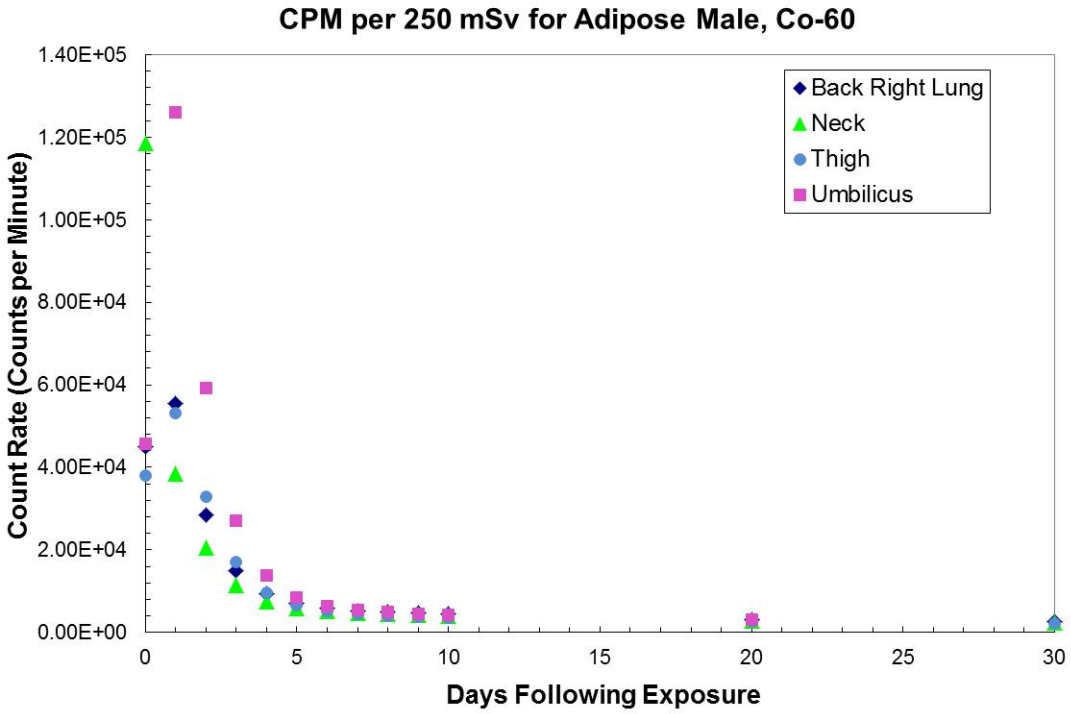

Adipose Male ^{137}Cs Ingestion

^{137}Cs		Umbilicus	Back Right Lung	Neck	Thigh
		CPM per 250 mSv	CPM per 250 mSv	CPM per 250 mSv	CPM per 250 mSv
Days following exposure	0	1.68E+03	1.49E+03	8.06E+03	1.96E+03
	1	1.48E+04	1.67E+04	1.36E+04	1.54E+04
	2	1.44E+04	1.52E+04	1.32E+04	1.51E+04
	3	1.41E+04	1.48E+04	1.28E+04	1.47E+04
	4	1.38E+04	1.45E+04	1.26E+04	1.44E+04
	5	1.35E+04	1.42E+04	1.24E+04	1.42E+04
	6	1.33E+04	1.41E+04	1.22E+04	1.40E+04
	7	1.32E+04	1.39E+04	1.21E+04	1.39E+04
	8	1.30E+04	1.38E+04	1.20E+04	1.37E+04
	9	1.29E+04	1.36E+04	1.19E+04	1.36E+04
	10	1.28E+04	1.35E+04	1.18E+04	1.35E+04
	20	1.20E+04	1.26E+04	1.10E+04	1.26E+04
	30	1.12E+04	1.19E+04	1.03E+04	1.18E+04

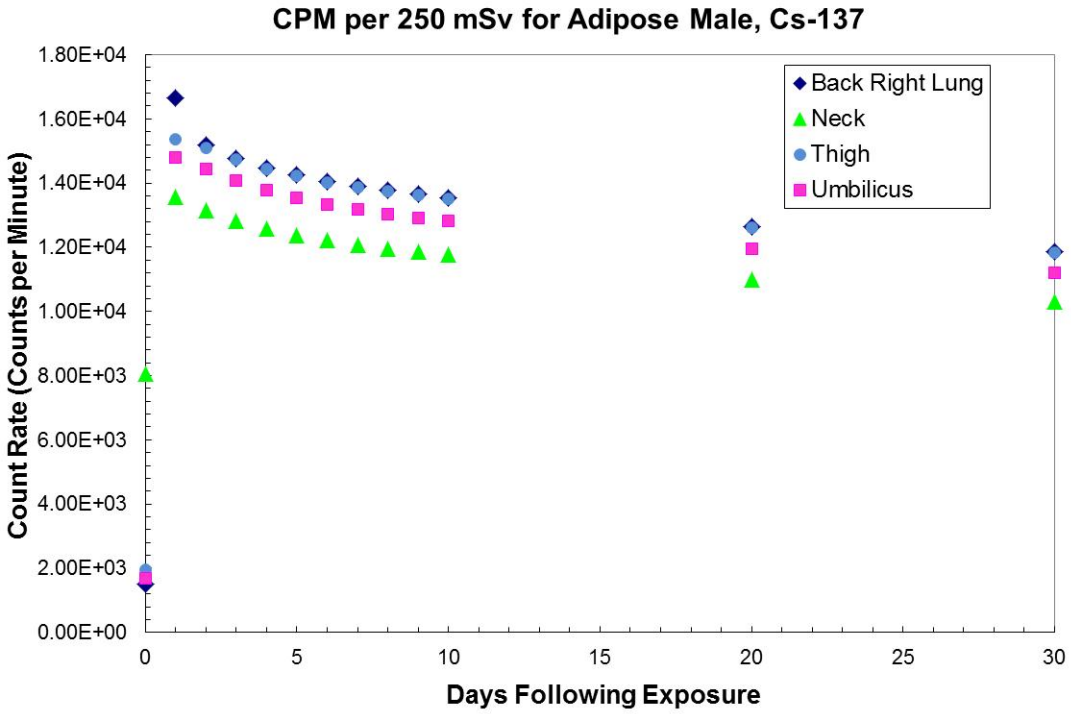

Adipose Male ^{131}I Ingestion

^{131}I		Umbilicus	Back Right Lung	Neck	Thigh
		CPM per 250 mSv	CPM per 250 mSv	CPM per 250 mSv	CPM per 250 mSv
Days following exposure	0	9.27E+02	2.49E+02	9.63E+02	1.62E+02
	1	1.47E+03	1.77E+03	6.21E+04	6.87E+02
	2	3.87E+02	2.75E+02	6.01E+04	8.60E+01
	3	3.04E+02	1.91E+02	5.49E+04	6.41E+01
	4	2.88E+02	1.86E+02	5.00E+04	7.35E+01
	5	2.80E+02	1.83E+02	4.55E+04	8.22E+01
	6	2.71E+02	1.79E+02	4.14E+04	8.84E+01
	7	2.62E+02	1.73E+02	3.77E+04	9.23E+01
	8	2.51E+02	1.67E+02	3.43E+04	9.43E+01
	9	2.40E+02	1.60E+02	3.12E+04	9.48E+01
	10	2.28E+02	1.53E+02	2.84E+04	9.40E+01
	20	1.19E+02	8.04E+01	1.12E+04	5.99E+01
	30	5.37E+01	3.65E+01	4.40E+03	2.90E+01

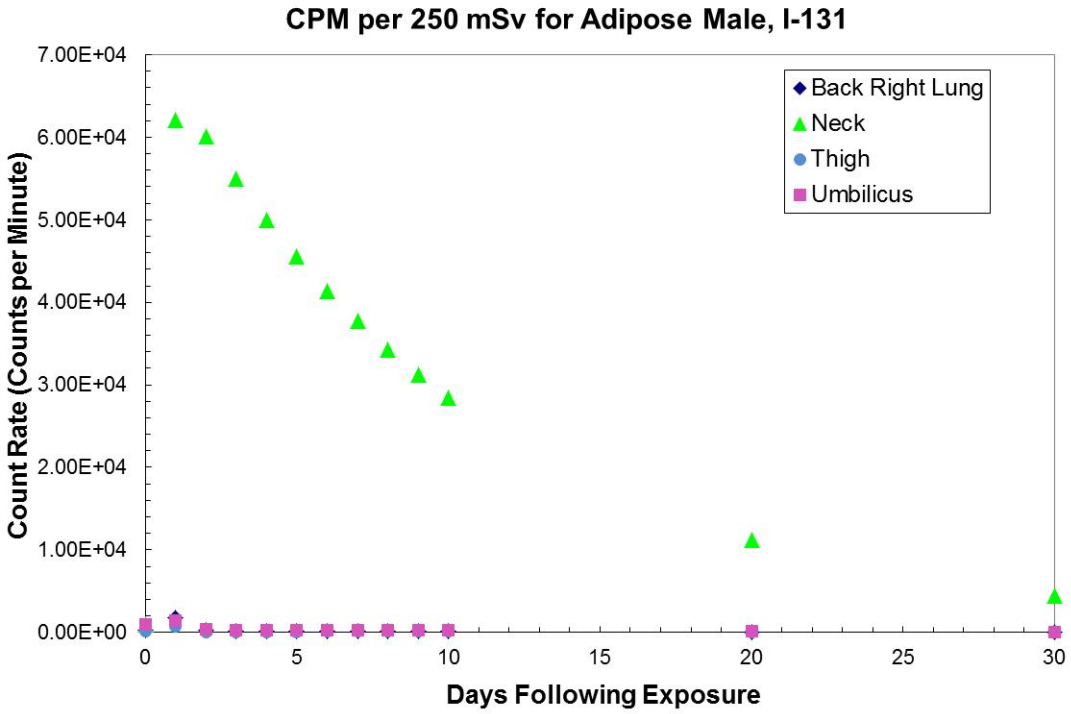

Adipose Male ^{192}Ir Ingestion

^{192}Ir		Umbilicus	Back Right Lung	Neck	Thigh
		CPM per 250 mSv	CPM per 250 mSv	CPM per 250 mSv	CPM per 250 mSv
Days following exposure	0	7.22E+04	2.37E+04	1.86E+04	4.63E+03
	1	4.05E+05	9.26E+03	6.18E+03	6.59E+04
	2	1.81E+05	4.94E+03	3.54E+03	4.08E+04
	3	7.29E+04	3.09E+03	2.18E+03	1.88E+04
	4	2.90E+04	2.32E+03	1.60E+03	8.55E+03
	5	1.23E+04	2.02E+03	1.36E+03	4.42E+03
	6	6.02E+03	1.88E+03	1.26E+03	2.82E+03
	7	3.68E+03	1.82E+03	1.22E+03	2.21E+03
	8	2.79E+03	1.78E+03	1.19E+03	1.96E+03
	9	2.43E+03	1.75E+03	1.17E+03	1.86E+03
	10	2.27E+03	1.73E+03	1.15E+03	1.81E+03
	20	1.82E+03	1.57E+03	1.05E+03	1.63E+03
	30	1.55E+03	1.48E+03	9.87E+02	1.53E+03

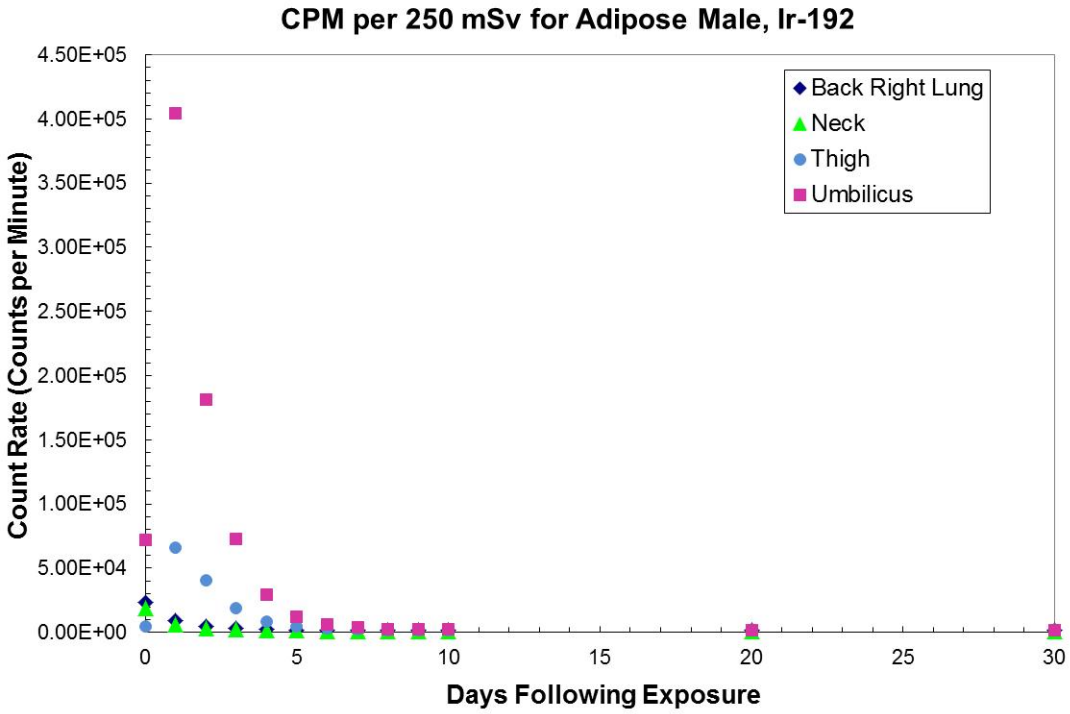

10-year-old Child ^{241}Am Ingestion

^{241}Am		Umbilicus	Back Right Lung	Neck	Thigh
		CPM per 250 mSv	CPM per 250 mSv	CPM per 250 mSv	CPM per 250 mSv
Days following exposure	0	4.87E+03	1.75E+02	6.21E+00	1.29E+00
	1	6.79E+03	2.01E+01	6.84E+00	1.59E+02
	2	3.72E+03	1.39E+01	6.65E+00	9.40E+01
	3	1.58E+03	1.02E+01	6.52E+00	4.31E+01
	4	6.15E+02	8.59E+00	6.47E+00	1.98E+01
	5	2.34E+02	7.98E+00	6.47E+00	1.05E+01
	6	8.91E+01	7.74E+00	6.46E+00	7.00E+00
	7	3.50E+01	7.65E+00	6.46E+00	5.68E+00
	8	1.50E+01	7.60E+00	6.44E+00	5.18E+00
	9	7.56E+00	7.62E+00	6.46E+00	5.01E+00
	10	4.82E+00	7.62E+00	6.47E+00	4.95E+00
	20	3.11E+00	7.60E+00	6.45E+00	4.88E+00
	30	3.04E+00	7.59E+00	6.44E+00	4.85E+00

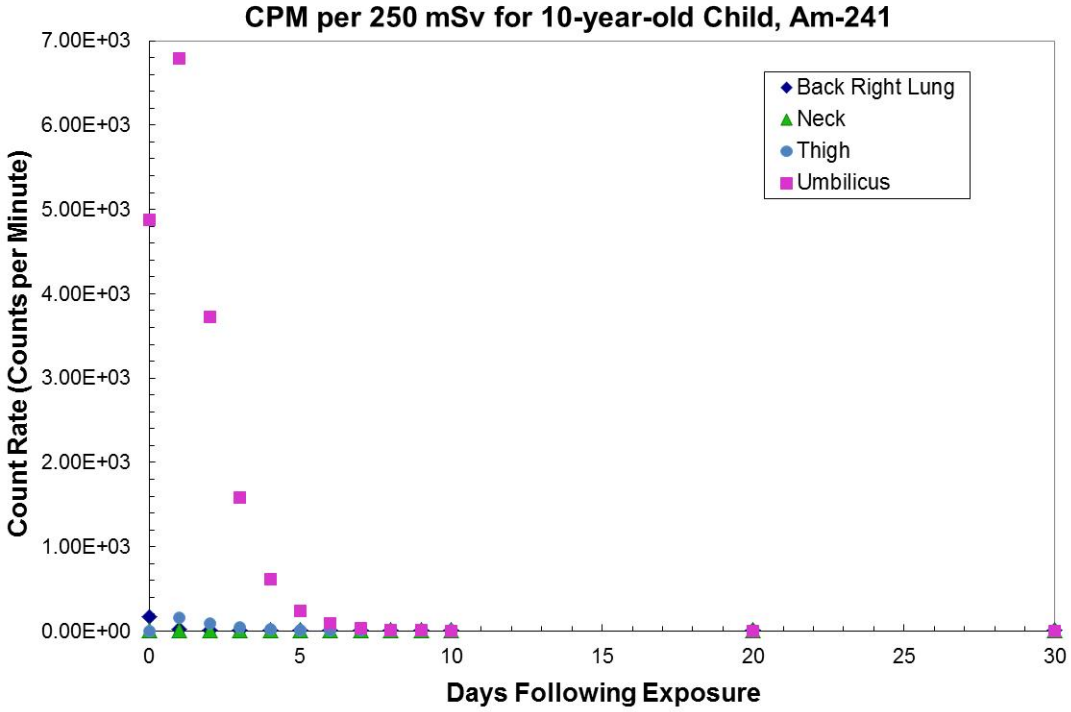

10-year-old Child ^{60}Co Ingestion

^{60}Co		Umbilicus	Back Right Lung	Neck	Thigh
		CPM per 250 mSv	CPM per 250 mSv	CPM per 250 mSv	CPM per 250 mSv
Days following exposure	0	1.40E+05	1.86E+04	8.03E+04	4.02E+04
	1	1.08E+05	3.18E+04	3.00E+04	2.84E+04
	2	4.03E+04	1.53E+04	1.43E+04	1.63E+04
	3	1.72E+04	7.96E+03	7.50E+03	8.72E+03
	4	8.81E+03	4.98E+03	4.74E+03	5.31E+03
	5	5.64E+03	3.75E+03	3.59E+03	3.86E+03
	6	4.35E+03	3.18E+03	3.06E+03	3.20E+03
	7	3.76E+03	2.88E+03	2.77E+03	2.87E+03
	8	3.43E+03	2.68E+03	2.59E+03	2.66E+03
	9	3.21E+03	2.53E+03	2.44E+03	2.51E+03
	10	3.04E+03	2.41E+03	2.32E+03	2.38E+03
	20	2.15E+03	1.72E+03	1.66E+03	1.70E+03
	30	1.81E+03	1.45E+03	1.40E+03	1.43E+03

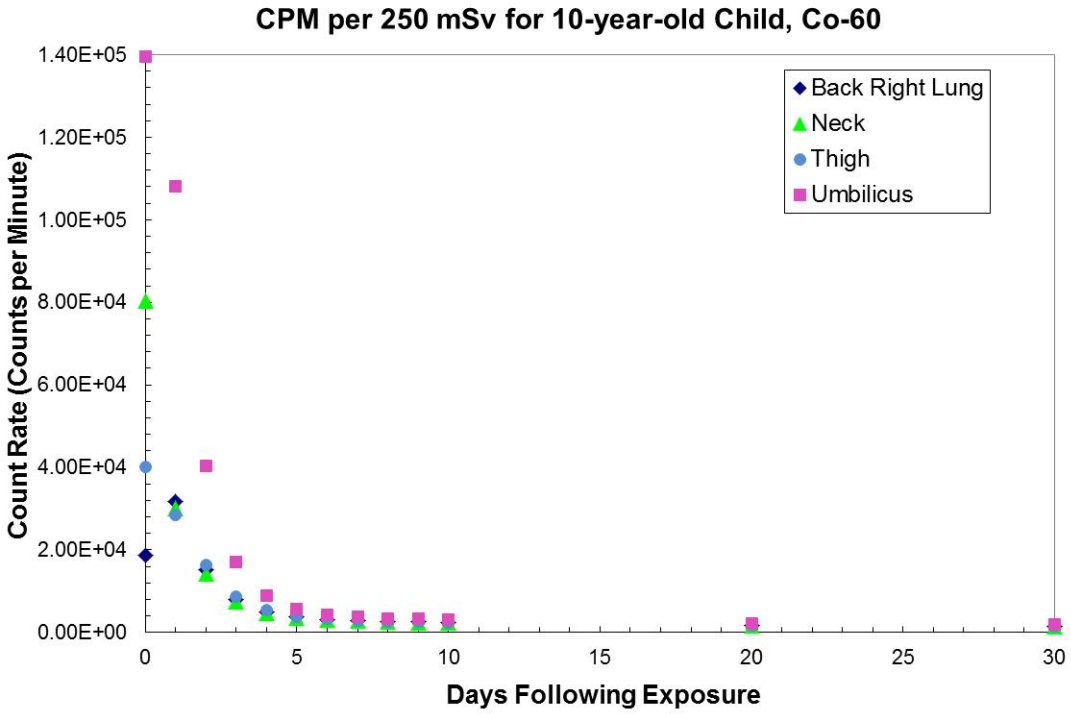

10-year-old Child ^{137}Cs Ingestion

^{137}Cs		Umbilicus	Back Right Lung	Neck	Thigh
		CPM per 250 mSv	CPM per 250 mSv	CPM per 250 mSv	CPM per 250 mSv
Days following exposure	0	6.19E+04	0.00E+00	2.62E+04	0.00E+00
	1	4.07E+04	3.79E+04	2.78E+04	5.22E+04
	2	3.89E+04	3.47E+04	2.70E+04	5.12E+04
	3	3.78E+04	3.38E+04	2.63E+04	5.01E+04
	4	3.70E+04	3.31E+04	2.58E+04	4.91E+04
	5	3.63E+04	3.26E+04	2.54E+04	4.83E+04
	6	3.58E+04	3.21E+04	2.50E+04	4.77E+04
	7	3.53E+04	3.18E+04	2.48E+04	4.72E+04
	8	3.50E+04	3.15E+04	2.45E+04	4.67E+04
	9	3.46E+04	3.12E+04	2.43E+04	4.63E+04
	10	3.43E+04	3.09E+04	2.41E+04	4.59E+04
	20	3.20E+04	2.89E+04	2.25E+04	4.29E+04
	30	3.01E+04	2.71E+04	2.11E+04	4.03E+04

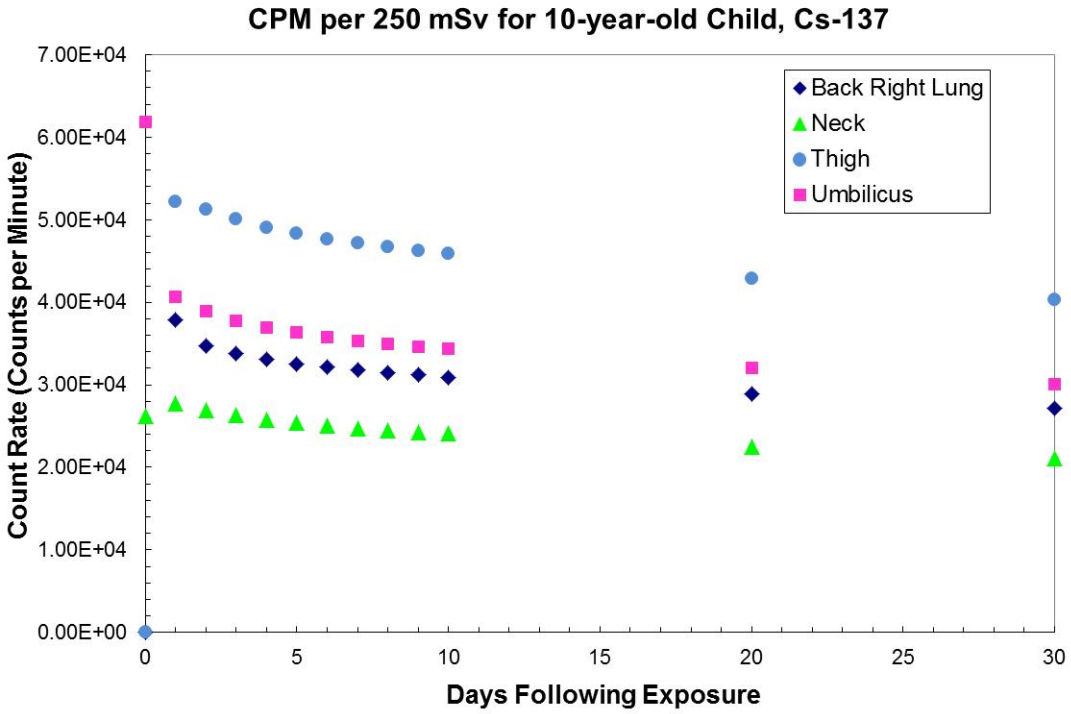

10-year-old Child ^{131}I Ingestion

^{131}I		Umbilicus	Back Right Lung	Neck	Thigh
		CPM per 250 mSv	CPM per 250 mSv	CPM per 250 mSv	CPM per 250 mSv
Days following exposure	0	2.25E+04	3.41E+02	1.04E+03	2.97E+02
	1	1.39E+03	1.79E+03	1.71E+04	7.84E+02
	2	3.85E+02	3.56E+02	1.62E+04	1.13E+02
	3	3.01E+02	2.67E+02	1.48E+04	8.95E+01
	4	2.83E+02	2.54E+02	1.34E+04	9.97E+01
	5	2.72E+02	2.45E+02	1.22E+04	1.08E+02
	6	2.60E+02	2.34E+02	1.12E+04	1.14E+02
	7	2.49E+02	2.23E+02	1.02E+04	1.18E+02
	8	2.37E+02	2.12E+02	9.26E+03	1.19E+02
	9	2.25E+02	2.01E+02	8.43E+03	1.18E+02
	10	2.13E+02	1.89E+02	7.68E+03	1.16E+02
	20	1.07E+02	9.37E+01	3.03E+03	7.18E+01
	30	4.77E+01	4.15E+01	1.20E+03	3.44E+01

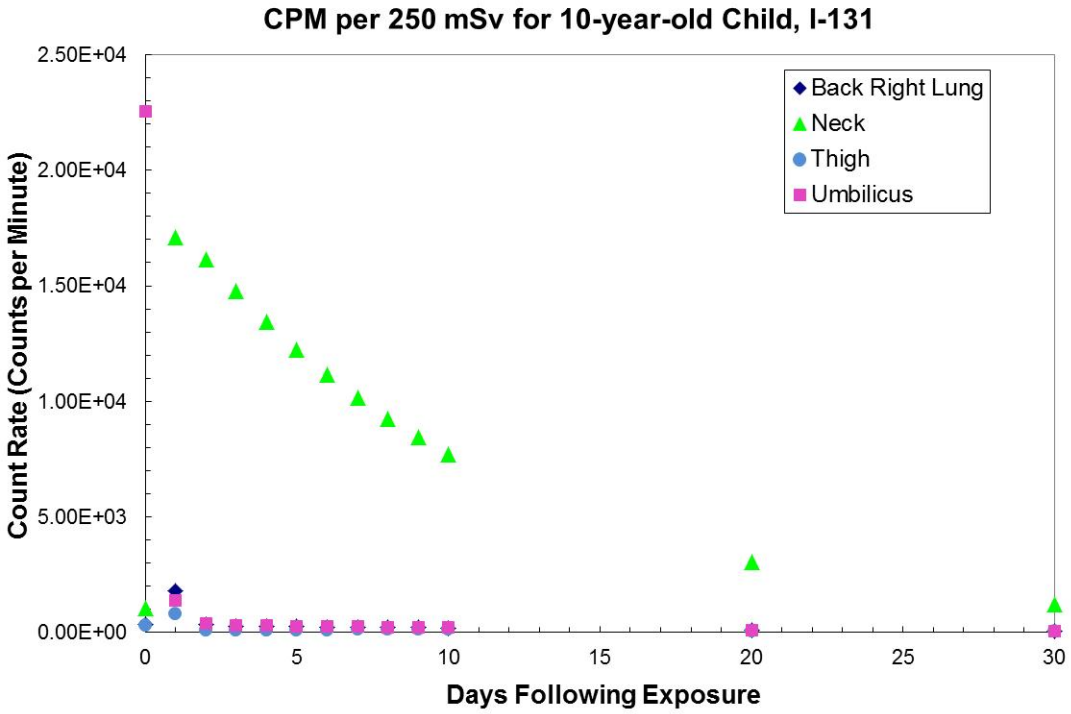

10-year-old Child ^{192}Ir Ingestion

^{192}Ir		Umbilicus	Back Right Lung	Neck	Thigh
		CPM per 250 mSv	CPM per 250 mSv	CPM per 250 mSv	CPM per 250 mSv
Days following exposure	0	9.49E+05	3.46E+04	2.17E+04	9.67E+03
	1	8.46E+05	1.01E+04	9.70E+03	3.81E+04
	2	2.53E+05	4.90E+03	5.22E+03	2.34E+04
	3	8.53E+04	3.11E+03	3.28E+03	1.16E+04
	4	3.19E+04	2.43E+03	2.50E+03	6.10E+03
	5	1.36E+04	2.16E+03	2.18E+03	3.89E+03
	6	7.11E+03	2.04E+03	2.05E+03	3.02E+03
	7	4.72E+03	1.97E+02	1.98E+03	2.68E+03
	8	3.80E+03	1.93E+02	1.94E+03	2.53E+03
	9	3.42E+03	1.90E+02	1.91E+03	2.45E+03
	10	3.23E+03	1.88E+03	1.88E+03	2.41E+03
	20	2.60E+03	1.71E+03	1.71E+03	2.18E+03
	30	2.22E+03	1.60E+02	1.61E+03	2.05E+03

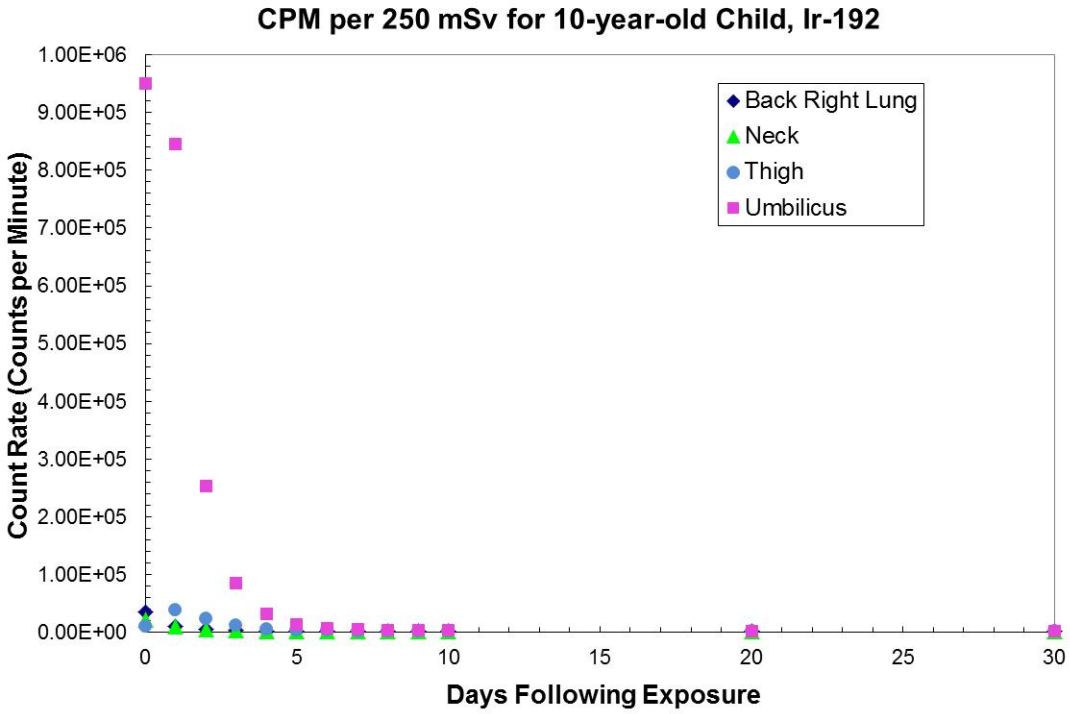
CPM per 250 mSv for 10-year-old Child, Ir-192
Count Rate (Counts per Minute)
1.00E+06
9.00E+05
8.00E+05
7.00E+05
6.00E+05
5.00E+05
4.00E+05
3.00E+05
2.00E+05
1.00E+05
0.00E+00
0
5
10
15
20
25
30
Days Following Exposure
Back Right Lung
Neck
Thigh
Umbilicus

APPENDIX C: SAMPLE MCNP INPUT MCNP INPUT FILES

This is the MCNP5 input file for the slab phantom at a thickness of 24mm with a Co-60 source. The other input files for the slab phantoms only differed in isotope type and the thickness of the PMMA (Lucite).

```
Thyroid Uptake System Co-60 24mm
c Cell Cards
1    1   -0.0012    1 2 3 17 19 20 -99        imp:p=1 $ Outside Air
2    2   -3.67     -5                         imp:p=1 $ NaI crystal
3    4   -1.19     -1:-2 3 4                  imp:p=1 $ PMMA
4    3   -7.82      (-17 10):(-19 18): -20    imp:p=1 $ Steel
5    5   -1.03     -3 2                       imp:p=1 $ Virtual Water
6    6   -2.7       5 14 -6                   imp:p=1 $ Aluminum
7    7   -1        -4                         imp:p=1 $ Source
8    0             -9 5                       imp:p=1 $ Vacuum
9    1   -0.0012   -7                         imp:p=1 $ Air in coll
10   3   -7.82      (7 -11)                   imp:p=1 $ Inner Steel Liner
11   8   -11.4     (-10 11):(-18 11 12 16 21)  imp:p=1 $ Pb innards
12   1   -.0012     -18 16 -21                imp:p=1 $ air in back
13   9   -8.4      (-14 15):(-12 13)          imp:p=1 $ Brass Ring
14   1   -0.0012    6 11 -15                  imp:p=1 $ Air ret ring
15   1   -0.0012   -13 6 9 14 15              imp:p=1 $ Air in brass tube
16   10  -11.4     -16 12                     imp:p=1 $ Pure Led sheet
99   0             99                         imp:p=0 $ Universe

c Surface Cards
1       rpp  0 2.4 -30 30 -30 30                $ PMMA slab
2       rpp  2.4 3.0 -30 30 -30 30              $ Source Holder
3       rpp  3.0001 13.0 -30 30 -30 30          $ Virtual Water
4       rcc  2.7001 -1.15 0 0 2.3 0 .2          $ Source
5       rcc -21.5051 0 0 5.08 0 0 2.54          $ NaI Crystal
6       rcc -21.5051 0 0 5.1308 0 0 2.824       $ Al Housing
9       rcc -34.7893 0 0 13.2842 0 0 2.921      $ PMT Tubes space
10      trc -11.5824 0 0 11.5824 0 0 4.445 5.3975   $ Outer Detector Housing ID
17      trc -11.5824 0 0 11.5824 0 0 4.7625 5.715   $ Outer Detector Housing OD
11      trc -15.7393 0 0 15.7393 0 0 2.7344 4.8018  $ Inner Steel Liner
7       trc -15.7393 0 0 15.7393 0 0 2.5344 4.6018  $ Air in collimator
12      rcc -40.8223 0 0 25.083 0 0 3.505       $ Inner Tube OD around PMT
13      rcc -40.8223 0 0 25.083 0 0 3.175       $ Inner Tube ID
14      rcc -16.3743 0 0 0.635 0 0 3.175        $ Retaining Ring OD
15      rcc -16.3743 0 0 0.635 0 0 2.565        $ Retaining Ring ID (air)
16      rcc -40.8223 0 0 14.9225 0 0 3.823      $ Detector Side Shield (Pb)
18      rcc -40.8223 0 0 29.2399 0 0 4.445      $ Cyl Detector Housing ID
```

```
19      rcc -40.8223 0 0 29.2399 0 0 4.7625        $ Cyl Detector Housing OD
20      rcc -41.8223 0 0 1.0 0 0 4.7625            $ Back end cap
21      px -25.8998                          $ air plane!
99      rpp -50 50 -50 50 -50 50                   $ Universe

c Data Cards
c Material Card for Air (NIST DRY AIR)
m1    8016.          -0.232
      7014.          -0.755
      6012           -1.20E-4
      18000.42c      -1.28E-2
c Material Card for Sodium Iodide
m2    11000.04p        0.5
      53000.04p        0.5
c Material Card for grain controlled mild steel AISI 1000 from Matls.com
m3    26054          -0.05821
      26056          -0.9137
      26057          -0.0211
      26058          -0.00281
       6012          -0.0006
      25055          -0.0035
      15031          -0.00004
      16000          -0.00005
c Material Card for PMMA
m4    6000.          0.3333
      8016.          0.1333
      1001.          0.5333
c Material Card for Virtual Water
m5    1001.          0.0802
      6000.          0.6703
      7015.          0.0214
      8016.          0.1991
      17000.         0.0014
      20000.         0.0231
c Material Card for Aluminum
m6    13027.  1
c Material Card for polyester (sources)
m7    6000.          0.333
      1001.          0.533
      8016.          0.133
c Material Card for Antimonial Lead
m8    82000   0.96
      51000   0.04
c Material Card for High Brass
```

```
m9    29000    0.65
      30000    0.35
c Material Card for Pure Lead
m10    82000   1
mode  p
phys:p 4j 1
sdef par=2 rad=d1 ext=d2 pos=2.7 0 0 axs=0 1 0 vec=0 0 1 erg=d3
si1 0 0.2
sp1 -21 1
si2 -1.15 1.15
sp2 -21 0
si3 l 1.17 1.33
sp3   .999 .999824
c Two Tallys
f8:p 2  $ volume of crystal
f18:p 2  $ same volume
c energy bins
e0 0 1e-8 0.005 1024i 2.046
c Gaussian Energy Broadening
ft8 GEB -0.00298579 0.0925102 -0.4
print
nps 1E8
```

This is the MCNP5 input file for the Reference Male anthropomorphic phantom with a I-131 source. The other input files differ by phantom type and source isotopes.

```
Male With I-131
1    1 -.001293    -1 (607:-37:606) (-606:601:35) (600:-35) &
                   (-615:37:-43:44:4:-616) (37:-608:609) &
                   (37:-608:610) 900 901 902 903
2    2 -0.2958     ((-2 -4 3):(-2 4)) 5                    $ left lung
3    3 -0.9869     -7 51 -6 (-8:32) 84 101 #2 #24 #28 #58 #59
                   (113:115) (114:115) #62 #700            $ torso insd ribs/lvrtop-shldr
4    3 -0.9869     -7 8 -32 117 113 114 #15 #16 #17 #18 #19 #20 #700
                   (-4:-9:116:118:-119) (-4:-9:116:120:-121)  $torso
5    3 -0.9869     -7 8 -117 51 113 114 #9 #13 #14 #700      $ torso
6    3 -0.9869     -7 50 -51 56 84 96 105 106 113 114 #10 #11 #12
                   #27 #32 #43 #44 #47 #700                $ torso
7    3 -0.9869     -7 97 -50 (83:-86:87:-88) 113 114 #30 #33 #38 #39
                   #63 #64 #65 #700                        $ torso abdoman
8    3 -0.9869     -7 37 -97 95 113 114 #31 #33 #38 #65 #66 #700   $ torso abdoman
9    4 -1.4862     8 -9 5 -10                              $ rib
10   4 -1.4862     8 -9 11 -12                             $ rib
11   4 -1.4862     8 -9 13 -14                             $ rib
12   4 -1.4862     8 -9 15 -16                             $ rib
13   4 -1.4862     8 -9 17 -18                             $ rib
14   4 -1.4862     8 -9 19 -20                             $ rib
15   4 -1.4862     8 -9 21 -22                             $ rib
16   4 -1.4862     8 -9 23 -24                             $ rib
17   4 -1.4862     8 -9 25 -26                             $ rib
18   4 -1.4862     8 -9 27 -28                             $ rib
19   4 -1.4862     8 -9 29 -30                             $ rib
20   4 -1.4862     8 -9 31 -32                             $ rib
21   3 -0.9869     ((35 -34):(-33 6 -35)) 102 (84:85)
                   #37 #60 #61 #62 #700                    $ head
22   3 -0.9869     -37 38 -39 103 #700                     $ left leg
23   3 -0.9869     -37 38 -40 104 #22 #700                 $ right leg
24   2 -0.2958     ((-41 -4 42):(-41 4)) 5                 $ right lung
25   3 -0.9869     715 -37 43 -44 -4 716 39 40 72 73 #700 #600   $ genitalia
26   3 -0.9869     -47                                     $ brain
27   3 -0.9869     50 -51 -48 -49 #10 #11 #12              $ liver
28   3 -0.9869     (-52 54):(-53 -54 55)                   $ heart
29   3 -0.9869     -56                                     $ stomach
30   3 -0.9869     138 -57 58 -59                          $ Ascending Colon Wall
31   3 -0.9869     (-63 141 65 -61):(-64 142 37 -65)       $ Sigmoid Colon Wall
32   3 -0.9869     -62 139 66 -67 59                       $ Transverse Colon Wall
33   3 -0.9869     -60 140 61 -59 -83                      $ Descending Colon Wall
```

```
35   3 -0.9869    -72                                   $ testicle
36   3 -0.9869    -73                                   $ testicle
37   3 -0.9869    -74 75 -76 6 -77                          $ thyroid
38   4 -1.4862    -82 83 37 -78 80 (79:-81)                 $ pelvis
39   4 -1.4862    -84 78 -85 102                        $ spine
40   3 -0.9869    -83 86 -50 88 -87 #30 #32 #33 #63 #64 #65      $ small int.
41   1 -0.001293   -107 606 -4                          $ air
42   1 -0.001293   -108 606 -4                          $ air
43   3 -0.9869    -92 65                                $ kidney
44   3 -0.9869    -93 -94                               $ kidney
45   3 -0.9869    -95                                   $ bladder
46   3 -0.9869    -96                                   $ spleen
47   3 -0.9869    -98 99 (-65:100)                          $ pancreas
48   3 -0.9869    -101                                  $ thymus
49   4 -1.4862    47 -102 #60 #61                           $ skull
50   4 -1.4862    -103 38 -37                           $ leg bone
51   4 -1.4862    -104 38 -37                           $ leg bone
52   3 -0.9869    -105 92                               $ adrenal
53   3 -0.9869    -106 93                               $ adrenal
54   4 -1.4862    37 -115 -113                          $ arm bone
55   4 -1.4862    37 -115 -114                          $ arm bone
56   4 -1.4862    4 9 -32 -116 117 -118 119                 $ scapulae
57   4 -1.4862    4 9 -32 -116 117 -120 121                 $ scapulae
58   4 -1.4862    -4 -122 -123 124                      $ clavicle
59   4 -1.4862    -4 -122 -125 126                      $ clavicle
60   3 -0.9869    -33 128 129 -130 133 -134 -4 #700          $ eye lense
61   3 -0.9869    -33 128 -131 132 133 -134 -4 #700          $ eye lense
62   3 -0.9869    -77 -137 51                           $ oesophagus
63   3 -0.9869    -138 58 -59                           $ Ascending Colon Interior
64   3 -0.9869    -139 66 -67                           $ Transvers Colon Interior
65   3 -0.9869    -140 61 -59 -83                       $ Decending Colon Interior
66   3 -0.9869    (-141 65 -61) : (-142 37 -65)             $ Sigmoid Colon Interior
600  0          -600 35 34 902 : -601 33 -35 606 902 : &          $ Head & Neck
                -606 6 33 -607 902: -607 7 -6 37 900 901 902 : &   $ Shoulders & Torso
 (((-46 616) (43 -44) (615 -37)):((615 -45)(610 609)(46 -4)(43 -44))): & $ Genitalia
                -610 40 -37 38 : -609 39 -37 38 903: &         $ Legs
                -708 608 -609 : -708 608 -610 : &             $ Feet
                -38 708 -610 40 : -38 708 -609 39
700  5 -1.04      700 35 102 -34 : 701 -33 -35 6 : &            $ Head & Neck
                706 -6 701 -707 : 707 -7 -6 37 114 113 : &     $ Shoulders & Torso
 (((46 -716)(43 -44)(609 610)(715 -37)):((-715 45)(610 609)(46 -4)(43 -44))): & $ Genitalia
                -40 710 -37 38 : -39 709 -37 38 : &            $ Legs
                -38 708 -39 : -38 708 -40                  $ Feet
900  1 -.001293   -900 7 515 514 505 504
```

```
901   1 -.001293    -901 7 535 534 525 524
902   1 -.001293    -902 6 33 34 555 554 545 544
903   1 -.001293    -903 39 575 574 565 564
c Detector in box 900
502   502   -3.67     -501                        $ NaI crystal
503   503   -7.82      (-505 504):(-514 513): -515       $ Steel
504   506   -2.7       501 510 -502                $ Aluminum
505   501   -0.00012  -503                         $ Vacuum
506   501   -0.0012   -507                        $ Air in coll
507   503   -7.82     (507 -506)                   $ Inner St Liner
508   508   -11.4     (-504 506):(-513 506 508 512 516)  $ Pb innards
509   501  -.0012    -513 512 -516                 $ air in back
510   509   -8.4      (-510 511):(-508 509)        $ Brass Ring
511   501   -0.0012   502 506 -511                 $ Air ret ring
512   501   -0.0012  -509 502 503 510 511          $ Air in brs tube
513   510  -11.4     -512 508                     $ Pure Led sheet
c Detector in box 901
522   502   -3.67     -521                        $ NaI crystal
523   503   -7.82      (-525 524):(-534 533): -535       $ Steel
524   506   -2.7       521 530 -522                $ Aluminum
525   501   -0.00012  -523                         $ Vacuum
526   501   -0.0012   -527                        $ Air in coll
527   503   -7.82     (527 -526)                   $ Inner St Liner
528   508   -11.4     (-524 526):(-533 526 528 532 536)  $ Pb innards
529   501  -.0012    -533 532 -536                 $ air in back
530   509   -8.4      (-530 531):(-528 529)        $ Brass Ring
531   501   -0.0012   522 526 -531                 $ Air ret ring
532   501   -0.0012  -529 522 523 530 531          $ Air in brs tube
533   510  -11.4     -532 528                     $ Pure Led sheet
c Detector in box 902
542   502   -3.67     -541                        $ NaI crystal
543   503   -7.82      (-545 544):(-554 553): -555       $ Steel
544   506   -2.7       541 550 -542                $ Aluminum
545   501   -0.00012  -543                         $ Vacuum
546   501   -0.0012   -547                        $ Air in coll
547   503   -7.82     (547 -546)                   $ Inner St Liner
548   508   -11.4     (-544 546):(-553 546 548 552 556)  $ Pb innards
549   501  -.0012    -553 552 -556                 $ air in back
550   509   -8.4      (-550 551):(-548 549)        $ Brass Ring
551   501   -0.0012   542 546 -551                 $ Air ret ring
552   501   -0.0012  -549 542 543 550 551          $ Air in brs tube
553   510  -11.4     -552 548                     $ Pure Led sheet
c Detector in box 903
562   502   -3.67     -561                        $ NaI crystal
```

```
563   503   -7.82      (-565 564):(-574 573): -575       $ Steel
564   506   -2.7       561 570 -562                      $ Aluminum
565   501   -0.00012   -563                              $ Vacuum
566   501   -0.0012    -567                              $ Air in coll
567   503   -7.82      (567 -566)                        $ Inner St Liner
568   508   -11.4      (-564 566):(-573 566 568 572 576)  $ Pb innards
569   501   -.0012     -573 572 -576                     $ air in back
570   509   -8.4       (-570 571):(-568 569)             $ Brass Ring
571   501   -0.0012    562 566 -571                      $ Air ret ring
572   501   -0.0012    -569 562 563 570 571              $ Air in brs tube
573   510   -11.4      -572 568                          $ Pure Led sheet
67    0           1

1     SO  200
2     SQ  23.04 10.24 1 0 0 0 -576 8.5 0 43.5
3     SQ  23.04 10.24 1 0 0 0 -576 2.5 0 43.5
4     PY  0.0
5     PZ  43.5
6     PZ  70
706   PZ  69.8
606   PZ  70.2
7     SQ  1 4.0 0 0 0 0 -400.0 0 0 0
707   SQ  0.002551 0.010412 0 0 0 0 -1 0 0 0
607   SQ  0.002451 0.00961  0 0 0 0 -1 0 0 0
8     SQ  1 3.15 0 0 0 0 -272.25 0 0 0
9     SQ  1 3.01 0 0 0 0 -289.0 0 0 0
10    PZ  44.9
11    PZ  35.1
12    PZ  36.5
13    PZ  37.9
14    PZ  39.3
15    PZ  40.7
16    PZ  42.1
17    PZ  46.3
18    PZ  47.7
19    PZ  49.1
20    PZ  50.5
21    PZ  51.9
22    PZ  53.3
23    PZ  54.7
24    PZ  56.1
25    PZ  57.5
26    PZ  58.9
27    PZ  60.3
```

```
28    PZ  61.7
29    PZ  63.1
30    PZ  64.5
31    PZ  65.9
32    PZ  67.3
33    SQ  100 49 0 0 0 0 -4900 0 0 0
701   SQ  0.021626 0.010412 0 0 0 0 -1 0 0 0
601   SQ  0.01929 0.009612 0 0 0 0 -1 0 0 0
34    SQ  7225 3540.25 4900 0 0 0 -354025 0 0 85.5
700   SQ  0.021626 0.010412 0.014516 0 0 0 -1 0 0 85.5
600   SQ  0.01929 0.009612 0.013212 0 0 0 -1 0 0 85.5
35    PZ  85.5
36    PZ  94
37    PZ  0
38    PZ  -80
708   PZ  -80.215
608   PZ  -80.415
39  601  GQ  5.025 5 0 0 0 -1 -100 0 0 0
709 603  GQ  5.05 5 0 0 0 -1 -100 0 0 0
609 605  GQ  4.963 5 0 0 0 -1 -100 0 0 0
40  600  GQ  5.025 5 0 0 0 1 100 0 0 0
710 602  GQ  5.089 5 0 0 0 1 100 0 0 0
610 604  GQ  4.963 5 0 0 0 1 100 0 0 0
41    SQ  23.04 10.24 1 0 0 0 -576 -8.5 0 43.5
42    SQ  23.04 10.24 1 0 0 0 -576 -2.5 0 43.5
43    P   10 0 1 -100
44    P   10 0 -1 100
45    PZ  -4.8
715   PZ  -4.6
615   PZ  -5.0
46    P   0 10 1 -100
716   P   0 10.2 1 -100
616   P   0 9.8 1 -100
47    SQ  2.25 1 1.91716 0 0 0 -81 0 0 86.5
48    SQ  64 272.25 0 0 0 0 -17424 0 0 0
49    P   9 7 -7.3256 -315
50    PZ  27
51    PZ  43
52    GQ  45.2 59.9 47.9 17.5 -16.2 34.8 -1632.1 1204.8 -4898.2 124295.2
53    SQ  1 1 1 0 0 0 -25 -1 -3 51
54    P   .6943 -.3237 -.6428 -32.506
55    P   5.2193 -2.4336 -0.916 -59.6345
56    SQ  4 7.11 1 0 0 0 -64 8 -4 35
57    SQ  1 1 0 0 0 0 -6.25 -8.5 -2.36 0
```

```
58   PZ  14.45
59   PZ  24
60   GQ  4.54 3.53 .096 0 1.16 -0.166 -77.68 -10.08 -.223 323.52
61   PZ  8.72
62   SQ  0 2.25 6.25 0 0 0 -14.0625 0 -2.36 25.5
63   TY  3 0 8.72 5.72 1.57 1.57
64   TY  3 0 0 3 1.57 1.57
65   PX  3
66   PX  -10.5
67   PX  10.5
68   PX  -20
69   PX  20
70   PY  -30
71   PY  -29
72   SQ  11.9025 8.9401 3.8025 0 0 0 -20.115225 1.3 -8 -2.3
73   SQ  11.9025 8.9401 3.8025 0 0 0 -20.115225 -1.3 -8 -2.3
74   C/Z 0 -6 2.2
75   C/Z 0 -6 1
76   PY  -6
77   PZ  75
78   PZ  22
79   PZ  14
80   PY  -3
81   PY  5
82   C/Z 0 -3 12
83   C/Z 0 -3.8 11.3
84   SQ  6.25 4 0 0 0 0 -25 0 5.5 0
85   PZ  78.5
86   PZ  17
87   PY  2.2
88   PY  -4.86
89   C/Z 0 -11. 0.6350
90   C/Z 0 -11. 0.8636
91   PZ  56.335
92   SQ  1.49 13.44 1 0 0 0 -30.25 6 6 32.5
93   SQ  1.49 13.44 1 0 0 0 -30.25 -6 6 32.5
94   PX  -3
95   SQ  1 2.0557 2.0557 0 0 0 -24.5818 0 -4.5 8
96   SQ  2.94 9 1 0 0 0 -36 11 3 37
97   PZ  12
98   SQ  1 225 25 0 0 0 -225 0 0 37
99   PX  0
100  PZ  37
101  SQ  1.78 64 1 0 0 0 -16 -2 -6 60.5
```

```
102   SQ  2.08 1 1.39 0 0 0 -96.04 0 0 85.5
103   GQ  1 1 .0091 0 0 -.2005 -20 0 1.7857 87.75
104   GQ  1 1 .0091 0 0 .2005 20 0 1.7857 87.75
105   SQ  100 900 9 0 0 0 -225 4.5 6.5 38
106   SQ  100 900 9 0 0 0 -225 -4.5 6.5 38
107   SQ  1.39 .5 2 0 0 0 -70 -6.5 -3 50
108   SQ  1.39 .5 2 0 0 0 -70 6.5 -3 50
109   PX  17
110   PX  6
111   PX  -6
112   PX  -17
113   GQ  503.01 135.24 0 0 0 10.206 -19215 0 -202.0788 183257
114   GQ  503.01 135.24 0 0 0 -10.206 19215 0 -202.0788 183257
115   PZ  69
116   SQ  1 3.7589 0 0 0 0 -361 0 0 0
117   PZ  50.9
118   P   0.25 -1 0 0
119   P   0.8 -1 0 0
120   P   -0.25 -1 0 0
121   P   -0.8 -1 0 0
122   TZ  0 11.1 68.25 20 0.7883 0.7883
123   P   0.89415 1 0 11.1
124   P   7.0342 1 0 11.1
125   P   -0.89415 1 0 11.1
126   P   -7.0342 1 0 11.1
C     2 concentric elliptical cylinders and planes to define eye lenses
127   SQ  100 64 0 0 0 0 -6400 0 0 0
128   SQ  88.36 40.96 0 0 0 0 -3619.2256 0 0 0
129   PX  2
130   PX  4
131   PX  -2
132   PX  -4
133   PZ  82.5
134   PZ  84.5
C     segmenting planes for RBM regions in leg and arm bones
135   PZ  -22.8
136   PZ  52.6
C     Oesophagus
137   SQ 0.16 1.0 0 0 0 0 -0.16 0.5 2.5 0                    $ Oesophagus Exterior
C     Colon Wall
138   SQ 1 1 0 0 0 0 -3.209 -8.5 -2.36 0                     $ Ascending Colon Interior
139   SQ 0 0.9467 3.8927 0 0 0 -3.6854 0 -2.36 25.5
140   GQ 1.796 2.496 0.0674 0 0.818 -0.066 -30.75 -7.12 -0.602 132.2
141   TY 3 0 8.72 5.72 0.91 0.91                             $ Upper Sigmoid Interior
```

```
142   TY 3 0 0 3 0.91 0.91                          $ Lower Sigmoid Interior
C Boxes for Detectors
900 900 BOX 0.39 10.9607 38.36   -17.78 0 0 &
      0 50.8 0      0 0 17.78
901 901 BOX 0.39 -10.9609 38.35  -17.78 0 0 &
      0 -50.8 0     0 0 17.80
902 BOX -8.89 -10 70.01  17.78 0 0  0 -50.8 0   0 0 17.78
903 903 BOX 19.98 -8.89 0  50.8 0 0  0 17.78 0  0 0 -17.78
c
c c
c Detector in Box 900
501 501   rcc -21.5051 0 0 5.08 0 0 2.54          $ NaI Crystal
502 501   rcc -21.5051 0 0 5.1308 0 0 2.824        $ Al Housing
503 501   rcc -34.7893 0 0 13.2842 0 0 2.921       $ PMT Tubes space
504 501   trc -11.5824 0 0 11.5824 0 0 4.445 5.3975   $ Outer Detector Housing ID
505 501   trc -11.5824 0 0 11.5824 0 0 4.7625 5.715   $ Outer Detector Housing OD
506 501   trc -15.7393 0 0 15.7393 0 0 2.7344 4.8018  $ Inner Steel Liner
507 501   trc -15.7393 0 0 15.7393 0 0 2.5344 4.6018  $ Air in collimator
508 501   rcc -40.8223 0 0 25.083 0 0 3.505        $ Inner Tube OD around PMT
509 501   rcc -40.8223 0 0 25.083 0 0 3.175        $ Inner Tube ID
510 501   rcc -16.3743 0 0 0.635 0 0 3.175         $ Retaining Ring OD
511 501   rcc -16.3743 0 0 0.635 0 0 2.565         $ Retaining Ring ID (air)
512 501   rcc -40.8223 0 0 14.9225 0 0 3.823       $ Detector Side Shield (Pb)
513 501   rcc -40.8223 0 0 29.2399 0 0 4.445       $ Cyl Detector Housing ID
514 501   rcc -40.8223 0 0 29.2399 0 0 4.7625      $ Cyl Detector Housing OD
515 501   rcc -41.8223 0 0 1.0 0 0 4.7625          $ Back end cap
516 501   px -25.8998                      $ air plane!
c Detector in Box 901
521 502   rcc -21.5051 0 0 5.08 0 0 2.54          $ NaI Crystal
522 502   rcc -21.5051 0 0 5.1308 0 0 2.824        $ Al Housing
523 502   rcc -34.7893 0 0 13.2842 0 0 2.921       $ PMT Tubes space
524 502   trc -11.5824 0 0 11.5824 0 0 4.445 5.3975   $ Outer Detector Housing ID
525 502   trc -11.5824 0 0 11.5824 0 0 4.7625 5.715   $ Outer Detector Housing OD
526 502   trc -15.7393 0 0 15.7393 0 0 2.7344 4.8018  $ Inner Steel Liner
527 502   trc -15.7393 0 0 15.7393 0 0 2.5344 4.6018  $ Air in collimator
528 502   rcc -40.8223 0 0 25.083 0 0 3.505        $ Inner Tube OD around PMT
529 502   rcc -40.8223 0 0 25.083 0 0 3.175        $ Inner Tube ID
530 502   rcc -16.3743 0 0 0.635 0 0 3.175         $ Retaining Ring OD
531 502   rcc -16.3743 0 0 0.635 0 0 2.565         $ Retaining Ring ID (air)
532 502   rcc -40.8223 0 0 14.9225 0 0 3.823       $ Detector Side Shield (Pb)
533 502   rcc -40.8223 0 0 29.2399 0 0 4.445       $ Cyl Detector Housing ID
534 502   rcc -40.8223 0 0 29.2399 0 0 4.7625      $ Cyl Detector Housing OD
535 502   rcc -41.8223 0 0 1.0 0 0 4.7625          $ Back end cap
536 502   px -25.8998                      $ air plane!
```

```
c Detector in Box 902
541 503   rcc -21.5051 0 0 5.08 0 0 2.54            $ NaI Crystal
542 503   rcc -21.5051 0 0 5.1308 0 0 2.824          $ Al Housing
543 503   rcc -34.7893 0 0 13.2842 0 0 2.921         $ PMT Tubes space
544 503   trc -11.5824 0 0 11.5824 0 0 4.445 5.3975   $ Outer Detector Housing ID
545 503   trc -11.5824 0 0 11.5824 0 0 4.7625 5.715   $ Outer Detector Housing OD
546 503   trc -15.7393 0 0 15.7393 0 0 2.7344 4.8018  $ Inner Steel Liner
547 503   trc -15.7393 0 0 15.7393 0 0 2.5344 4.6018  $ Air in collimator
548 503   rcc -40.8223 0 0 25.083 0 0 3.505          $ Inner Tube OD around PMT
549 503   rcc -40.8223 0 0 25.083 0 0 3.175          $ Inner Tube ID
550 503   rcc -16.3743 0 0 0.635 0 0 3.175           $ Retaining Ring OD
551 503   rcc -16.3743 0 0 0.635 0 0 2.565           $ Retaining Ring ID (air)
552 503   rcc -40.8223 0 0 14.9225 0 0 3.823         $ Detector Side Shield (Pb)
553 503   rcc -40.8223 0 0 29.2399 0 0 4.445         $ Cyl Detector Housing ID
554 503   rcc -40.8223 0 0 29.2399 0 0 4.7625        $ Cyl Detector Housing OD
555 503   rcc -41.8223 0 0 1.0 0 0 4.7625            $ Back end cap
556 503   px -25.8998                                $ air plane!
c Detector in Box 903
561 504   rcc -21.5051 0 0 5.08 0 0 2.54            $ NaI Crystal
562 504   rcc -21.5051 0 0 5.1308 0 0 2.824          $ Al Housing
563 504   rcc -34.7893 0 0 13.2842 0 0 2.921         $ PMT Tubes space
564 504   trc -11.5824 0 0 11.5824 0 0 4.445 5.3975   $ Outer Detector Housing ID
565 504   trc -11.5824 0 0 11.5824 0 0 4.7625 5.715   $ Outer Detector Housing OD
566 504   trc -15.7393 0 0 15.7393 0 0 2.7344 4.8018  $ Inner Steel Liner
567 504   trc -15.7393 0 0 15.7393 0 0 2.5344 4.6018  $ Air in collimator
568 504   rcc -40.8223 0 0 25.083 0 0 3.505          $ Inner Tube OD around PMT
569 504   rcc -40.8223 0 0 25.083 0 0 3.175          $ Inner Tube ID
570 504   rcc -16.3743 0 0 0.635 0 0 3.175           $ Retaining Ring OD
571 504   rcc -16.3743 0 0 0.635 0 0 2.565           $ Retaining Ring ID (air)
572 504   rcc -40.8223 0 0 14.9225 0 0 3.823         $ Detector Side Shield (Pb)
573 504   rcc -40.8223 0 0 29.2399 0 0 4.445         $ Cyl Detector Housing ID
574 504   rcc -40.8223 0 0 29.2399 0 0 4.7625        $ Cyl Detector Housing OD
575 504   rcc -41.8223 0 0 1.0 0 0 4.7625            $ Back end cap
576 504   px  -25.8998                               $ air plane!

C Data Cards
tr600 -0.1
tr601 0.1
tr602 -0.15
tr603 0.15
tr604 -0.051
tr605 0.051
tr900 0 -0.2 0 0.973527 0.228573 0 -0.228573 0.973527 0 0 0 1
tr901 0 0.2 0 0.973527 -0.228573 0 0.228573 0.973527 0 0 0 1
```

```
tr903 -0.35 0 0 0.979903 0 -0.199474 0 1 0 0.199474 0 0.979903
tr501 -10.5 8.75 47.5 0.229 -0.973 0 -0.973 -0.229 0 0 0 1
tr502 -10.5 -8.75 47.5 0.229 0.973 0 0.973 -0.229 0 0 0 1
tr503 0 -10.03 78.88 0 1 0 1 0 0 0 0 1
tr504 17.55 0 -12.5 -0.979903 0 -0.199474 0 1 0 0.199474 0 0.979903
c VOL   0 9.89817E3 5.12539E4 7.01171E3 4.12839E3 3.75367E4 4.1204E4 &
c     3.96266E4 3.42787E2 3.43057E2 3.41728E2 3.41505E2 3.3914E2 &
c     3.38905E2 3.37704E2 3.38854E2 3.36585E2 3.35548E2 3.34261E2 &
c     3.3525E2 1.09049E4 5.26806E4 5.19336E4 9.87788E3 8.35231E2 &
c     8.24983E3 1.08532E4 3.48665E3 2.39203E3 5.46974E2 4.19631E2 &
c     7.21861E2 5.2306E2 1.1077E2 1.11655E2 1.72154E2 3.63227E3 &
c     5.17342E3 6.31233E3 0 0 8.49751E2 8.55366E2 1.48895E3 1.04544E3 &
c     3.58882E2 1.45325E2 4.77509E3 8.25008E3 8.23095E3 5.80561E1 &
c     5.70516E1 2.81453E3 2.80523E3 5.80932E2 5.89508E2 1.56404E2 &
c     1.56141E2 1.09588E1 1.10836E1 2.31698E2 5.781E2 7.58053E2 &
c     6.152E2 2.15848E2 1.23531E4 1.09131E4 1.6059E4 1.6059E4&
c     1.6059E4 1.6059E4 23.9241 9.2379 53.9171 10.2532 28.10780 &
c     23.9241 9.2379 53.9171 10.2532 28.1078 23.9241 9.2379 53.9171 &
c     10.2532 28.1078 23.9241 9.2379 53.9171 10.2532 28.1078 0
IMP:P 1 118R 0
C
C Sources
SDEF  PAR=2  ERG=D1  CEL=D2  RAD=fcel=D3  &
POS=fcel=D4  EXT=fcel=D5  AXS=fcel=D6
SI1 L 0.029458 0.722893 0.0297792 0.080183 0.284298 0.636973 0.36448
SP1 0.013568 0.01752 0.025171 0.025448 0.058825 0.07057 0.788898
C Left Lung, Right Lung, Stomach, Small Int., Heart, Ascending Colon,
C Sigmoid Colon, Transvers Colon, Descending Colon, Bladder,
C Body Tissue (3, 4, 5, 6, 7, 8, 21, 22, 23, 25), Thyroid
SI2 L 2 24 29 40 28 30 31 32 33 45 3 4 5 6 7 8 21 22 23 25 37
SP2 D 1 1 1 1 1 1 1 1 1 1 1 1 1 1 1 1 1 1 1 1 1
DS3 S 7 8 9 10 11 12 13 14 15 16 17 18 19 20 21 22 23 24 25 26 27
DS4 L 8.5 0 43.4   -8.5 0 43.4   8 -4 35   0 -3.8 11.3   -1 -3 51   &
    -8.5 -2.36 14.35   5 0 -0.1   -10.6 -2.36 25.5   8.72 0 8.52  &
    0 -4.5 8   0 0 42.9   0 0 50.8   0 0 42.9   0 0 26.9         &
    0 0 11.9   0 0 -0.1   0 0 69.9   10.5 0 -80.1   -10.5 0 -80.1 &
    0 -8 -4.9   0 -6 69.9
DS5 S 30 31 0 32 0 33 34 35 36 0 37 38 39 40 41 42 43 44 45 46 47
DS6 L 0 0 1   0 0 1   0 0 0   0 0 1   0 0 0   0 0 1   0 0 1 &
    1 0 0   0 0 1   0 0 0   0 0 1   0 0 1   0 0 1   0 0 1 &
    0 0 1   0 0 1   0 0 1   0 0 1   0 0 1   0 0 1   0 0 1
SI7  0 7.6
SP7  -21 1
SI8  0 7.6
```

SP8 -21 1
SI9 0 8.2
SP9 -21 2
SI10 0 11.4
SP10 -21 1
SI11 0 8.2
SP11 -21 2
SI12 0 2.6
SP12 -21 1
SI13 0 7.1
SP13 -21 1
SI14 0 3.85
SP14 -21 1
SI15 0 4
SP15 -21 1
SI16 0 5.2
SP16 -21 2
SI17 0 20.2
SP17 -21 1
SI18 0 20.3
SP18 -21 1
SI19 0 20.3
SP19 -21 1
SI20 0 20.3
SP20 -21 1
SI21 0 20.3
SP21 -21 1
SI22 0 20.3
SP22 -21 1
SI23 0 10.1
SP23 -21 1
SI24 0 11
SP24 -21 1
SI25 0 11
SP25 -21 1
SI26 0 8.1
SP26 -21 1
SI27 0 2.2
SP27 -21 1
SI30 0 24.6
SP30 -21 0
SI31 0 24.6
SP31 -21 0
SI32 0 10.2

SP32 -21 0
SI33 0 9.75
SP33 -21 0
SI34 0 8.92
SP34 -21 0
SI35 0 21.2
SP35 -21 0
SI36 0 16
SP36 -21 0
SI37 0 27.2
SP37 -21 0
SI38 0 16.6
SP38 -21 0
SI39 0 8.1
SP39 -21 0
SI40 0 16.2
SP40 -21 0
SI41 0 15.2
SP41 -21 0
SI42 0 12.2
SP42 -21 0
SI43 0 24.2
SP43 -21 0
SI44 0 80.2
SP44 -21 0
SI45 0 80.2
SP45 -21 0
SI46 0 5
SP46 -21 0
SI47 0 5.2
SP47 -21 0
C
C
C Tally Cards
c Back Right Lung
F8:P 502
E8 0 1e-8 0.005 1024i 2.046
FT8 SCX 2 GEB -0.00298579 0.0925102 -0.4
c Front Right Lung
F18:P 522
E18 0 1e-8 0.005 1024i 2.046
FT18 SCX 2 GEB -0.00298579 0.0925102 -0.4
c Front Neck Under Chin
F28:P 542

```
E28 0 1e-8 0.005 1024i 2.046
FT28 SCX 2 GEB -0.00298579 0.0925102 -0.4
c Outer Left Leg
F38:P 562
E38 0 1e-8 0.005 1024i 2.046
FT38 SCX 2 GEB -0.00298579 0.0925102 -0.4
C
C Material Cards
C       THIS IS THE COMPOSITION FOR AIR
M1    7014 -.7558 8016 -.2314 18000 -.0128
C      THIS IS THE COMPOSITION FOR LUNG TISSUE
M2    1001 -.1021
      6012 -.1001
      7014 -.0280
      8016 -.7596
     11023 -.0019
     15031 -.0008
     16032 -.0023
     17000 -.0027
     19000 -.0020
     20000 -.0001
     26000 -.0004
C       THE COMPOSITION FOR TOTAL BODY MINUS SKELETON AND LUNGS
M3    1001 -.1047
      6012 -.2302
      7014 -.0234
      8016 -.6321
     11023 -.0013
     12000 -.0002
     15031 -.0024
     16032 -.0022
     17000 -.0014
     19000 -.0021
C      THE COMPOSITION FOR SKELETAL TISSUE
M4    1001 -.0704
      6012 -.2279
      8016 -.4856
      7014 -.0387
     11023 -.0032
     12000 -.0011
     15031 -.0694
     16032 -.0017
     17000 -.0014
     19000 -.0015
```

```
     20000 -.0991
c      Adult Tissues (Density = 1.04 g/cc)
M5       1001  -0.10454
         6012  -0.22663
         7014  -0.02490
         8016  -0.63525
        11023  -0.00112
        12000  -0.00013
        14000  -0.00030
        15031  -0.00134
        16032  -0.00204
        17000  -0.00133
        19000  -0.00208
        20000  -0.00024
        26000  -0.00005
        30000  -0.00003
        37085  -0.000007217
        37087  -0.000002783
        40000  -0.00001
c Detectors Materials
c Material Card for Air (NIST DRY AIR)
m501  8016.           -0.232
      7014.           -0.755
      6012            -1.20E-4
      18000.42c       -1.28E-2
c Material Card for Sodium Iodide
m502  11000.04p         0.5
      53000.04p         0.5
c Material Card for grain controlled mild steel AISI 1000 from Matls.com
m503  26054           -0.05821
      26056           -0.9137
      26057           -0.0211
      26058           -0.00281
       6012           -0.0006
      25055           -0.0035
      15031           -0.00004
      16000           -0.00005
c Material Card for Aluminum
m506  13027.  1
c Material Card for Antimonial Lead
m508  82000   0.96
      51000   0.04
c Material Card for High Brass
m509  29000    0.65
```

```
     30000    0.35
c Material Card for Pure Lead
m510  82000   1
lost 50
c STOP NPS 1E8 F38 0.01
NPS 4E9
RANDGEN=2 SEED=1561615651
PHYS:P 4J 1
PRINT
MODE P
```

APPENDIX D: ROI SHIFT ANALYSIS

This brief study was performed in analyze the effect of the apparent gain shift in the greater energies on the results. This work was reviewed by Dr. Nolan Hertel, Georgia Tech, and Dr. Jon Links, Johns Hopkins.

Evaluation of ROI Placement

Sarah Scarboro, Georgia Institute of Technology
June 1, 2008

Background

A recent work was completed using the Captus 3000 Thyroid Uptake System to determine internal contamination following a Radiological Dispersal Device (RDD). [1] This work included a series of benchmark measurements using the Captus 3000 device and Monte Carlo simulations using various human phantoms.

The benchmark measurements were completed in order to validate a Monte Carlo model of the Captus 3000 detector and collimator system. Actual data collected using the device was compared to the calculated detector response using the model for the same laboratory setup and gamma-emitting isotope. This process ensured that the model of the device was capable of reproducing the laboratory results in a consistent manner, and that the model was valid at various amounts of tissue attenuation. To complete the benchmark measurements, six gamma-ray emitting isotopes were used in conjunction with a slab phantom composed of PMMA. Details concerning the PMMA slab phantom and the procedure for the benchmark measurements are not the primary focus of this brief study and can be found in Reference 1 or 2.

The purpose of this "ROI Shift Test" is to examine the effect of using the default Capintec ROI values rather than centering the ROI symmetrically over the Monte Carlo calculated photopeak. A comparison of spectral data from the MCA module of the Captus 3000 and MCNP simulated data showed that for some of the higher energy isotopes, the MCNP spectra appear to be shifted to a higher energy than the measured spectra. This effect can be seen in the following comparison of Co-60 at a PMMA thickness of 60mm. The measured spectrum is noticeably lower in energy than the MCNP calculated spectrum.

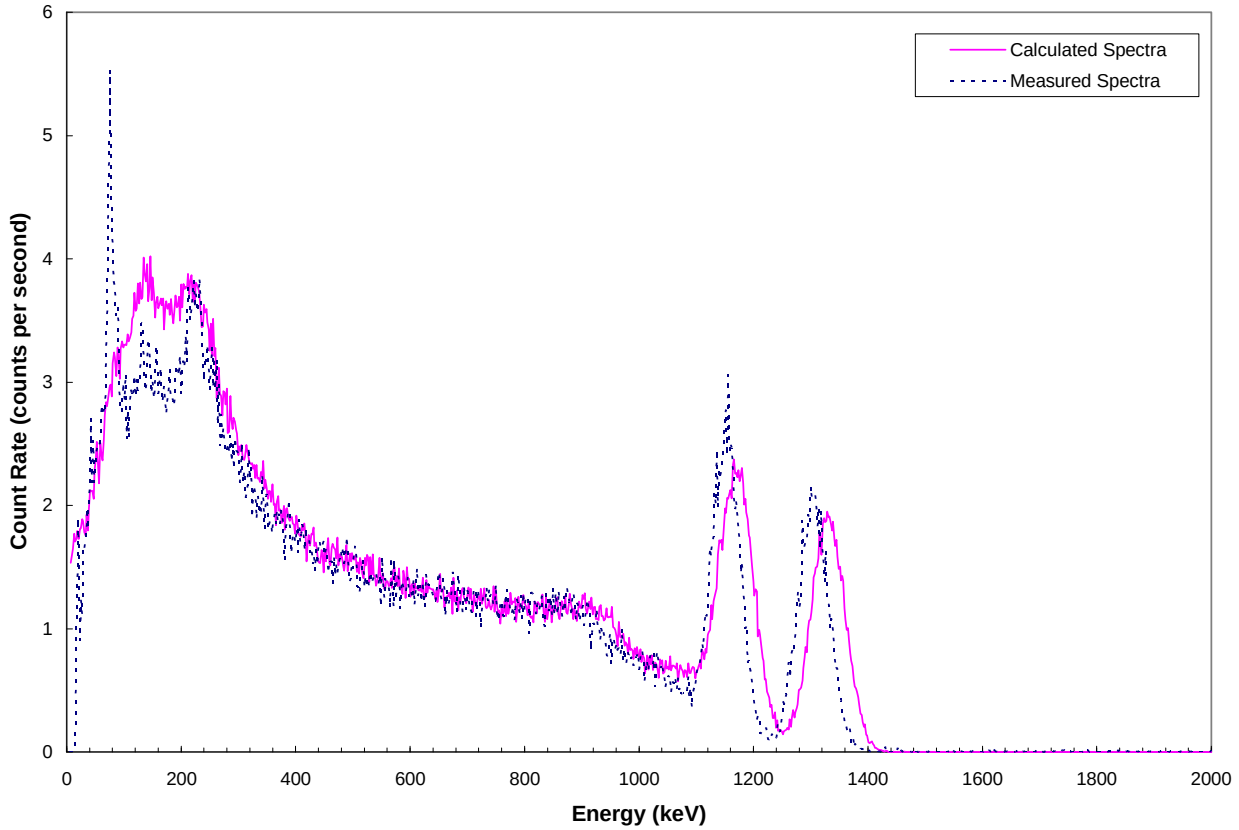

As shown in the following table (Table 6.1.1, [1]) the regions of interest (ROI) around the photopeaks were defined using the default values for the upper and lower discriminators in the Capintec software. These values are provided in units of keV and were selected by Capintec based on an energy calibration using Eu-152.

Isotope	Default ROI (keV)
Am-241	49-70
Ba-133	70-100, 334-384
Cs-137	627-697
Co-60	1126-1382
Mn-54	792-878
Na-22	480-546, 1220-1328

The ROI values shown were used consistently for both the measured and MCNP calculated data in the Captus 3000 work. By doing this, a scaling factor was developed to account for differences in the coverage of the photopeak between the spectra, thus converting between the measured and calculated data. The Scaling Factor is the ratio between the MCNP calculated count rate in the Capintec ROI and the measured count rate in the Capintec ROI for each isotope.

$$\text{Scaling Factor} = \frac{\text{MCNP Calculated Count Rate in Capintec ROI}}{\text{Measured Count Rate in Capintec ROI}}$$

The Scaling Factor was used for the primary purpose of converting the MCNP result to an equivalent result that would be seen in the Capintec MCA system. The scaling factor was used on the phantom simulated data, in order to convert it back to an equivalent value in the Capintec system, as shown in the following equation.

$$\text{MCNP Phantom Data} * \text{Scaling Factor}^{-1} = \text{Equivalent Count Rate in Capintec ROI}$$

Scaling factors were determined using this methodology for the three isotopes that were to be used in both the model validation and the actual phantom simulations (Am-241, Cs-137, and Co-60). For the purpose of this work, each of the six isotopes used in the benchmark measurements was examined to determine the effects of the ROI placement.

Methodology

The following simple methodology was used to determine the percent difference in count rate as a result of shifting the ROI to symmetrically surround the MCNP calculated photopeak.

1. Determine the median value of the Capintec ROI in keV. This value is the current center of the ROI used for each scenario. It must be noted that this point may **not** be the center of the measured photopeak. For all measured data, the Captus 3000 device was calibrated using the built-in auto calibration method which is used in the field. Each time, the calibration was successful according to the Capintec parameters.

2. Find the peak count rate in the MCNP calculated photopeak. This is done by visual inspection to find the highest value count rate in the calculated photopeak.

3. If the center of the Capintec ROI and the peak MCNP count rate are not equal, then shift the Capintec ROI (preserving the width in channels) such that it is symmetrically situated around the MCNP calculated photopeak. The width of the Capintec ROI is preserved, and the center of the ROI will be moved to coincide with the center of the calculated spectra. If the center of the Capintec ROI and the peak MCNP count rate are equal, then it is not necessary to shift the ROI. In this case, it is assumed that the ROI is optimally placed.

4. For the isotopes where the ROI must be shifted, determine the percent difference in count rate (counts per second). This will be performed on the 60mm PMMA slab thickness for each isotope. 60 mm was chosen as an average thickness for the purpose of this study. The percent difference was calculated using the following equation:

$$\text{Percent Difference}(\%) = \frac{\text{Count Rate in Shifted ROI} - \text{Count Rate in Capintec ROI}}{\text{Count Rate in Shifted ROI}} \times 100$$

For isotopes with more than one photopeak (Na-22, Ba-133) each photopeak was treated separately.

Co-60 was a special case because although the Capintec software specifies two ROIs (one for each photopeak), they have since moved to only one ROI to encompass both photopeaks. As a result the

process of finding the center of the calculated peak is not applicable. To deal with this isotope, the initial two ROIs were used, one for the 1.17 MeV peak and one for the 1.33 MeV peak.

Results

The following table summarizes the results of shifting the ROI to be centered around the MCNP calculated photopeak. For the "Shift in ROI" a negative number indicates a shift to lower energy, and a positive number indicates a shift to higher energy.

Isotope	CapintecROICenter (keV)	MCNPPeak Count Rate (keV)	Shift in ROI (Number of Channels)	% Difference in Count Rate
Am-241 (59.5 keV)	59.5	58.7	-3	25.27%
Ba-133 (81 keV)	85	76.7	-8	29.03%
Ba-133 (356 keV)	359	349.5	-9	14.94%
Cs-137 (662 keV)	662	662	-2	1.26%
Co-60 (1.17 MeV)	1173	1166	-4	6.26%
Co-60 (1.33 MeV)	1332.5	1331	+1	-2.92%
Mn-54 (835 keV)	835	829.4	-4	0.74%
Na-22 (511 keV)	513	508.8	-5	4.30%
Na-22 (1.275 MeV)	1274	1277	+2	-0.29%

In general, larger percent differences in the count rate as a result of shifting the ROI occurred in the lower energies (Am-241, Ba-133, and Na-22). The median energies (Cs-137, Mn-54) showed very little change, and the higher energies showed a slightly larger change.

For Am-241 and Ba-133, shifting the ROI resulted in large changes in the count rate under the photopeak. Errors in the simulation of these two isotopes have been identified in the associated work. [1] These errors are primarily associated with the depiction of the energy resolution using a Gaussian smoothing function and are most likely a cause for the large percent difference due to the ROI shift.

In the case of Cs-137, the center of the Capintec ROI and the peak number of counts in the calculated spectra are the same. 662 keV on the simulated energy scale corresponds to 659 keV on the Capintec energy axis. Due to this, the MCNP ROI was shifted 2 channels down in energy in order to symmetrically center it on the calculated photopeak. This shift caused a difference of 1.26% in the count rate at a PMMA thickness of 60mm.

With the exception of Am-241 and Ba-133, the isotope showing the largest percent difference in count rate is Co-60. Further examination of this isotope shows that the initial suggestion that the MCNP

spectrum is shifted to higher energies is incorrect. In fact, it appears that the measured spectrum is shifted to a lower energy. The following graph shows the same comparison as above, this time with the Capintec ROIs placed over the spectra. Also, the center points of the Capintec ROIs are illustrated by a straight vertical line through the ROI. While the majority of the photopeaks are encompassed in the ROIs, the ROIs seem to better fit the simulated photopeaks.

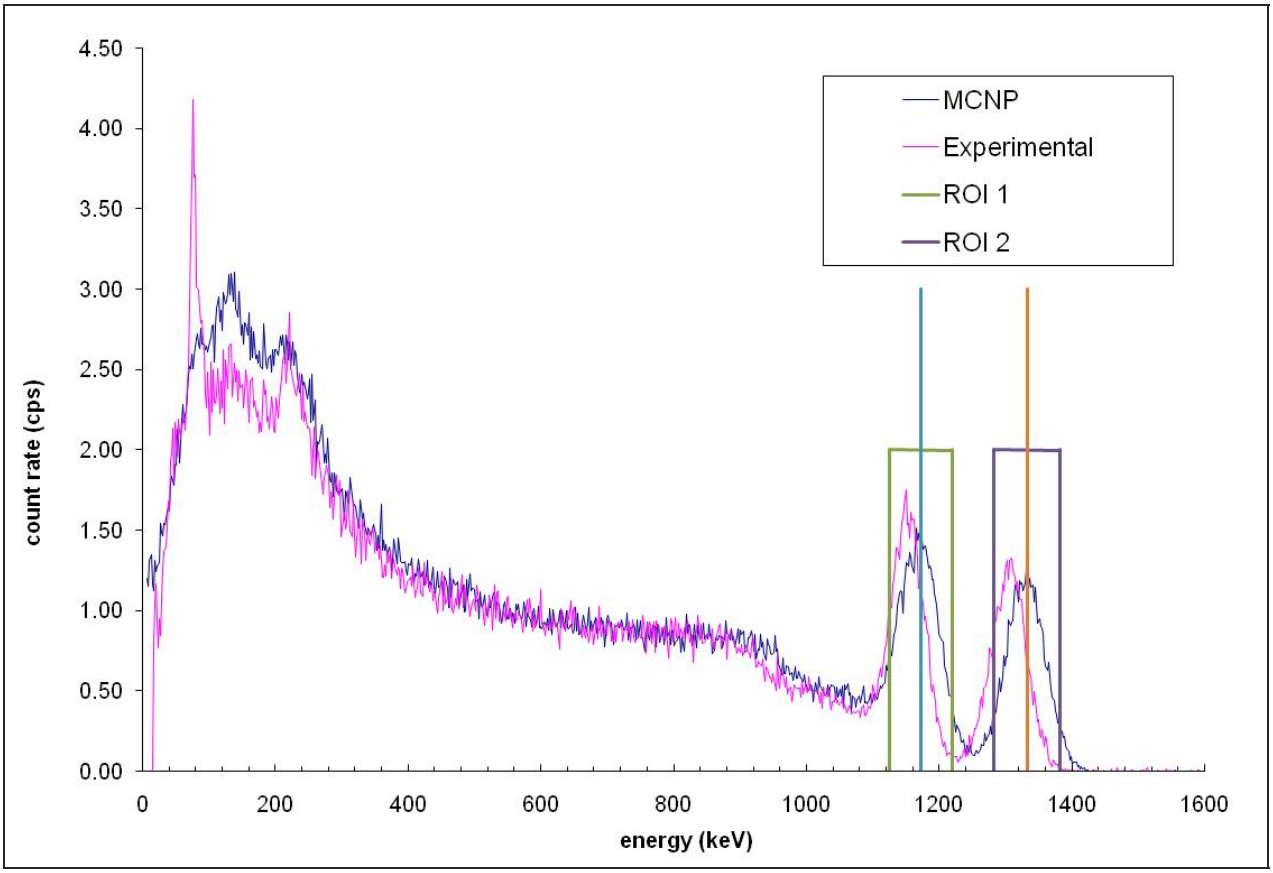

Ba-133, Na-22, and Mn-54 were not used in the subsequent phantom simulation work. These three isotopes were only used as a validation tool for the MCNP model of the Captus 3000 device.

Conclusions

Based on this brief study of the placement of the ROI, there is an appreciable difference in the count rate under the photopeak in low-energy gamma emitting isotopes when the ROI is shifted between the centered MCNP and the Capintec ROI. This difference is decreased for the higher energies, and does not effect the determination or use of the scaling factor used in the associated work. This study was done purely for academic interest, and therefore bears no effect on the other publications related to this work.

The primary reason for the difference in the measured spectra and Monte Carlo calculated spectra is a result of the MCNP parameters regarding the energy distribution. The energy binning for the MCNP simulations was a linear distribution between 5 keV and 2.046 MeV between 1024 channels, resulting in

approximately 2 keV per channel. The Capintec energy distribution is more sophisticated, using a point-to-point method and a Eu-152 source.

The phantom results were adjusted using the scaling factor for three isotopes: Am-241, Cs-137, and Co-60. The remaining two isotopes that were used in the phantom simulations (I-131 and Ir-192) did not have scaling factors applied to the results. These isotopes were not used in the benchmark study, and therefore no experimental data was collected for these isotopes.

References

1. Scarboro, S., Hertel, N. The Use of A Thyroid Uptake System for Assaying Internal Contamination Following a Radioactive Dispersal Event. (May 2008) Georgia Institute of Technology: A Thesis Presented to the Faculty

2. Sarah Scarboro, Nolan Hertel, Eric Burgett, Rebecca Howell, and Armin Ansari, **Validation of Monte Carlo Simulation of a Thyroid Uptake System using Various Sources and a Slab Phantom**, Nuclear Technology, 168, 169-172, 2009.

Deleted: Ansari, Val Thyroid Up Slab Phanto Conference RPSD-14) Technology

EVALUATION OF INTERNAL CONTAMINATION LEVELS AFTER A RADIOLOGICAL DISPERSAL DEVICE INCIDENT USING PORTAL MONITORS

R. C. Palmer[1], N. E. Hertel[1,*], A. Ansari[2], R. P. Manger[1,+], E. J. Freibert[1]
Georgia Institute of Technology, Nuclear and Radiological Engineering Department, Atlanta, GA, 30332, USA
Radiation Studies Branch, Centers for Disease Control and Prevention, Atlanta, GA, USA

+ Currently at Oak Ridge National Laboratory, PO Box 2008 MS6153, Oak Ridge, TN, 37831, USA

*Corresponding author: nolan.hertel@me.gatech.edu
404-894-3601
Fax: 404-894-3733
Postal Address: 770 State Street, Atlanta, GA, 30332-0745

INTERNAL CONTAMINATION USING PORTAL MONITORS

EVALUATION OF INTERNAL CONTAMINATION LEVELS AFTER A RADIOLOGICAL DISPERSAL DEVICE INCIDENT USING PORTAL MONITORS

Randahl Christelle Palmer, Nolan E. Hertel, Armin Ansari, Eric A. Burgett, Ryan P.Manger, Emily J. Freibert

(Needs to be Under 150 Words)

Following a radioactive dispersal device (RDD) incident, it may be necessary to evaluate the internal contamination levels of a large number of potentially affected individuals to determine if immediate medical follow-up is necessary. Since the current laboratory capacity to screen for internal contamination is limited, rapid field screening methods can be useful in prioritizing individuals. This study evaluated the suitability of a radiation portal monitor for such screening. A model of the portal monitor was created for use with models of six anthropomorphic phantoms in Monte Carlo N-Particle Transport Code Version 5 (MCNP) [1]. The count rates of the portal monitor were simulated for inhalation and ingestion of likely radionuclides from an RDD for each of the phantoms. The time-dependant organ concentrations of the radionuclides were determined using Dose and Risk Calculation Software (DCAL) [2]. Portal monitor count rates corresponding to a committed effective dose (CED) of 10 milisieverts (mSv) are reported.

INTRODUCTION

Many countries in the world are developing programs to respond to terrorist attacks utilizing radiological and nuclear materials. One device of concern is a radioactive dispersal device (RDD), which is any method of dispersing radioactive material through active or passive means. An active method would be through an explosive device, referred to as a dirty bomb; while examples of passive methods include an aerial release of a radionuclide, contamination of a water supply, or release into the ventilation system of a building [3]. In addition to potentially causing physical harm and destruction, an RDD could create widespread panic or anxiety [4].

For individuals in the immediate vicinity of an RDD, external and internal contamination could potentially occur. These individuals will need to be evaluated for radioactive contamination. The majority of external contamination can be eliminated by removing clothing and washing the body with soap and water [3]. Once the external contamination is removed, screening for internal contamination should occur. In this work, two possible pathways leading to internal contamination are considered: inhalation and ingestion.

In the event of an RDD, the triaging of a large population will likely be necessary. In the triage decision process it is necessary to distinguish individuals who are internally contaminated from those who are clean or whose contamination level is below a screening threshold. The goal of ongoing research at the Georgia Institute of Technology is to see if readily available radiation detectors can be utilized as initial screening and

prioritization tools. The purpose of this initial screening is to identify individuals in the public who have potentially received a committed effective dose exceeding a predefined level. These individuals will be prioritized for further testing and possibly decorporation treatment.

Conventional methods to determine internal contamination include *in-vitro* monitoring through bioassay and *in-vivo* monitoring through non-portable whole body counters. Bioassays of urine, feces, nose blow, or blood can be performed to "determine quantity, location and retention of radionuclides in the body" [6]. However, all bioassay samples, other than the nasal swab for the nose blow bioassay, must be taken by organizations that specialize in handling blood and excreta samples [6]. In addition, whole body counters are principally located at nuclear facilities that are remote from most urban centers and are much more sensitive than required for initial triage. Using whole body counters at such facilities would also require the transport of the potentially contaminated individuals. Since a large population could possibly be affected by an RDD, rapid methods are needed to prioritize individuals for further testing via more conventional and sensitive methods.

Using criteria such as radiological toxicity, quantity and accessibility, half-life, and dispersibility, the U.S. Department of Energy (DOE) and Nuclear Regulatory Commission (NRC) have identified particular radioisotopes as being of greatest concern for use in an RDD [7]. Previously, several hand-held gamma radiation detectors have been investigated for rapid screening of RDD isotopes [8, 9]. The present study focused on determining the validity of using portal monitors as an initial screening and prioritization tool for possible internal contamination of the following gamma emitting radionuclides: ^{60}Co, ^{137}Cs, ^{131}I, and ^{192}Ir. This study was performed with an end goal of developing count-rate data that can be used by emergency response personnel to prioritize people for further screening, laboratory analysis, and possible treatment.

Portal monitors have several features that make them useful when a large population is potentially affected by an RDD. These features include their transportability, ease of assembly and operation, and wide availability. Because of the long linear extent of the detectors in the vertical legs of the device, portal monitors, in essence, act as whole body counters. As a result of detector size, portal monitors are highly sensitive to radionuclides with gamma energies above the detection threshold of the plastic scintillators. The ability to collect a whole body count with a single measurement helps to increase the throughput, which is a very important attribute for an initial field screening tool. This study focuses on the TPM-903B Portal Monitor by Thermo Scientific; however, a similar approach can be used to investigate other manufacturers' portal monitors.

METHODOLOGY AND MATERIALS

The goal of this study was to determine the count rates which would be registered by the TPM-903B Portal Monitor for potential RDD radionuclides distributed in the body at various times following ingestion or inhalation of each radionuclide. This was accomplished by computer simulations of the human body and the detector.

Prior to developing a model of the TPM-903B, a series of point source attenuation (benchmark) measurements were taken with the TPM-903B Portal Monitor. These

measurements were performed for ^{133}Ba, ^{60}Co, ^{137}Cs, and ^{22}Na point sources surrounded by various thicknesses of polymethyl methacrylate (PMMA). A model of the TPM-903B Portal Monitor was generated for use in Monte Carlo N-Particle Transport Code, Version 5 (MCNP) [1]. The MCNP detector model was validated by simulating the point source attenuation measurements and comparing them to the portal monitor readings.

Scaling factors between the simulated and measured values for the point source measurements were calculated by dividing the MCNP counts by the measured counts to compensate for inadequacies in the detector model. Once the detector model was validated, MCNP models of Medical Internal Radiation Dose (MIRD)-type phantoms and the portal monitor were combined with organ concentrations from the activity calculation (ACTACAL) module of Dose and Risk Calculation Software (DCAL) to determine the count rate corresponding to a reference committed effective dose (CED) value [2]. Dose coefficients from International Commission on Radiological Protections (ICRP) Publication 72 were used to relate intakes in becquerel (Bq) to CED in milisieverts (mSv) [10].

The National Council on Radiation Protection and Measurements (NCRP) Report No. 161 recommends that 250 mSv be used as the target committed effective dose value for further testing and possible treatment[5]. Based on this NCRP recommendation, this study originally chose 250 mSv as the reference committed effective dose screening value. However, due to the sensitivity of portal monitors, this study reports count rates corresponding to a CED of 10 mSv.

TPM-903B Portal Monitor

Thermo Scientific's TPM-903B Transportable Radiation Portal Monitor consists of two BC408 plastic scintillators, with a total volume of 10.4 liters, surrounded on the three sides by 1.6 mm of lead shielding and with the detector and lead encased in polyvinyl chloride (PVC) piping [11, 12]. According to the manufacturer, the TPM 903B Portal Monitor detects gamma rays in the energy range of 60 keV to 2 MeV. Further specifications of the detector can be found on the manufacturer's website [12].

PMMA Benchmark Measurements

Benchmark measurements were performed using a box composed of 6 mm thick PMMA sheets. Measurements were taken for 13 different PMMA thicknesses ranging from 6 mm to 115 mm on both sides of the source holder (including the source box thickness). In the benchmark measurements, PMMA was used because its attenuation of photons is similar to that of tissue and the multiple thicknesses of PMMA served to represent the attenuation effect of varying tissue thicknesses between the source and the detector. The 13 different PMMA thickness measurements were performed for the ^{133}Ba, ^{60}Co, ^{137}Cs, and ^{22}Na sources. These four isotopes were chosen because they represent a wide range of photon energies, 30 keV to 1.33 MeV, with adequate photon emissions that lie within the TPM-903B's nominal detectable energy range of 60 keV to 2 MeV.

In addition, the benchmark measurements were taken with the source box located in five different positions. For three of the positions, the source box was centered in the portal monitor at three different heights. In the first location, position 1, the source was at a height of 140 cm from the floor, while the height of position 2 was 133 cm and position

3 was 116 cm. For the other two benchmark measurement positions, the source box was at a height of 133 cm and was positioned 50 cm outside the center of the portal monitor on either side. All five source positions are illustrated in Figure 1. The lower limit of detection was calculated for the background observed during measurements to determine if the observed count rates were distinguishable from the background [13].

The detector was operated in background mode, instead of fast count mode, since this was deemed to be the best mode of operation for the application. In this mode, the counts recorded in the most recent 5-second interval were combined with the counts recorded for the previous three 5-second intervals to yield the counts per second. Individuals being monitored would be required to remain in the portal monitor for at least 20 seconds to ensure that the actual "background" counts are not included in the individual's screening count rate. The count rates for the benchmark measurements were recorded after the PMMA slab had been in the portal monitor for 60 seconds.

TPM-903B MCNP Model Validation

A detailed MCNP model of the TPM-903B was constructed for use in photon transport simulations [1, 14]. The dimensions of the TPM-903B were measured on the physical device. The source, PMMA box, and PMMA attenuation slabs were added to the MCNP model to simulate the benchmark measurements. Models were created for all sources, source positions, and attenuation thicknesses. VisED representations of the MCNP models of the benchmark measurements and detector are shown in Figure 2 [15].

To simulate the detector response for each MCNP input file, a pulse height tally was performed in the BC408 plastic scintillation volume, yielding the pulse-height spectra for each isotope, PMMA thickness, and position. Since MCNP5 normalizes pulse-height tallies to unit photon emissions, the count rates from the MCNP simulations were multiplied by the activity of the source and the photons per decay. The pulse-height tally was then summed above various energy thresholds and compared to the measured count rate readings obtained during the benchmark measurements after background subtraction. The ratio of MCNP count rates to the measured count rate were computed and analyzed for positions 1-3, all four isotopes, and all 13 PMMA thicknesses. The comparison of the MCNP count rates to the measured count rates allows for validation of MCNP model of the detector as well as the selection of a detection threshold (energy cutoff). The energy cutoff was determined by summing the MCNP pulse height tally above various low energy cutoffs and finding the ratio that was most constant over all PMMA thicknesses for all isotopes and positions. The resulting energy cutoff was then applied to all simulation results by summing the MCNP pulse height tally for energies above the cutoff energy.

The mean value of the ratio for a given isotope over all thicknesses and different height locations was used to obtain the scaling factor for that isotope. This scaling factor was used to adjust the simulated count rate of the detector when used with the phantoms. Benchmark measurements were not taken with ^{131}I and ^{192}Ir; their scaling factors were calculated by performing a mean energy, linear interpolation of the scaling factors from the isotopes used in the benchmark measurements. The scaling factors were then used to convert the count rates from the MCNP simulation of the TPM-903B and phantoms to the detector count rates.

MIRD Phantoms

Using the validated MCNP5 detector model in conjunction with MCNP models of stylized phantoms based on the MIRD male and female anthropomorphic phantoms, the response of the portal monitor was simulated for the inhalation and ingestion of radionuclides considered radioisotopes of concern in the event of an RDD [7]. The four radioisotopes considered in this study were ^{60}Co, ^{137}Cs, ^{131}I, and ^{192}Ir. Along with these four isotopes, six MIRD-based phantoms were considered: a Reference Male, a Reference Female, an Adipose Male, an Adipose Female, a Post-Menopausal Adipose Female, and a 10-Year-Old Child. These varying body-type phantoms were used to provide the distribution of the count rates over a wide range of body shapes. In the MCNP simulation, the phantom was placed such that the anterior and posterior sides of the phantom faced the portal monitor's legs containing the detectors. This orientation was chosen to achieve the highest count rate and is the authors' recommended orientation of potentially contaminated individuals.

The Reference Male and Reference Female phantoms were developed at Oak Ridge National Laboratory, and the basic MCNP inputs used in this work for the reference phantoms were generated at Pacific Northwest National Laboratory [16, 17]. The three adipose phantoms were developed at the Georgia Institute of Technology, by adding adipose tissue to the Reference Male and Reference Female [8, 18-19]. The model of the 10 year old androgynous child was constructed using Body Builder [8, 20].

The distributions of ^{60}Co, ^{137}Cs, ^{131}I and ^{192}Ir within the human body vary with radioisotope, contamination pathway, and time. The organs and tissues in the body where each radioisotope concentrates were ascertained using biokinetic modeling. The organs and tissues where concentration occurs are source organs, or tissue, of interest; examples include the lungs, stomach and blood. For each radionuclide-phantom-pathway combination, a unit source was placed in each source organ of interest, and a pulse height tally was performed over the detector volume to obtain the counts from a unit source in each organ. Since plastic scintillating detectors were investigated, the simulated pulse-height for each MIRD organ or tissue of interest was summed above the energy threshold determined from the slab measurements and simulation comparisons. The sum was then multiplied by the number of photons per decay converting the MCNP output of counts per source particle to counts per second (CPS) per Bq. For each radionuclide, the number of photons per decay was determined using the data provided by Radiological Toolbox, which was taken from ICRP Publication 38 and the Japan Atomic Energy Research Institute (JAERI) [21]. These steps were repeated for all radionuclide-phantom-pathway combinations.

Biokinetics and Committed Effective Dose Value

The activity calculation module, ACTACAL, of DCAL was used to determine the distribution of the radionuclides in the body for inhalation and ingestion pathways [2]. Developed at Oak Ridge National Laboratory, DCAL provides the fraction of radioactivity distributed in each organ or tissues of interest in the body as a function of time [2].

The resulting count rate per Bq for each organ of interest from the simulations for each phantom was multiplied by the corresponding organ activities. In the ACTACAL module, the method of uptake for both inhalation and ingestion was set to

"environmental" and was assumed to be an acute intake [2]. For inhalation the aerosol particle size was set to an activity median aerodynamic diameter (AMAD) of 1μm, which is DCAL's default setting for particle size for environmental exposures [2].

For both modes of uptake, the DCAL blood activity was distributed among the body organs based on the blood distributions fractions listed in ICRP 89 [22]. The remaining fraction of blood that was not distributed to individual organs was uniformly distributed in the body tissue, excluding skin. For the child simulations, the biokinetic models were used because this resulted in a lower count rate, thus providing more conservative screening criteria for the child.

The values for the simulated count rate per Bq of intake were divided by the scaling factor to predict the portal monitor count rates. The resulting count rates per Bq were then multiplied by the dose coefficients from Radiological Toolbox for public ingestion and inhalation to obtain count rates per 10 mSv [21].

The dose coefficients listed in Radiological Toolbox are the ICRP Publication 72 values for ^{60}Co, ^{137}Cs, ^{131}I, and ^{192}Ir [21, 10]. Based on ICRP Publication 72 recommendations, the inhalation class was set to fast for ^{137}Cs and ^{131}I and moderate for ^{60}Co [10]. Since a recommended inhalation class for ^{192}Ir was not specified in ICRP Publication 72, its inhalation class was assumed to be moderate, reducing the likelihood of overestimating or underestimating the dose coefficient [23].

Detector Linearity

Since the portal monitor uses plastic scintillators, the upper count rate for detector linearity is isotope dependent. However, homeland security performance standards for portal monitors are based on ^{137}Cs sources [12]. For this reason, measurements were taken for various ^{137}Cs activities in order to estimate the upper limit of detector count rate linearity for ^{137}Cs. Two sets of measurements were taken by placing ^{137}Cs sources on one detector leg near the location used for calibration. The first set of measurements were taken with Detector A turned on and Detector B turned off; various activities were placed on the leg containing Detector A, and the count rates were recorded. For the second set of measurements Detector A was turned off and Detector B was on with the sources placed on the leg containing Detector B.

Assumptions

In order to characterize the detectors for use in the event of an RDD, several assumptions had to be made in this work. The first assumption made was that all external contamination will be removed by showering and changing clothing before the individual enters the portal monitors for internal contamination screening [24]. It is also assumed that only one isotope is used in the RDD, and that the isotope has been identified prior to triage. If there are multiple isotopes, the use of the sum-of-the-fractions rule could be used to determine the mixed isotope count rates for screening. Finally, it was assumed that the initial screening of the individuals will occur between six hours and 30 days after the time of contamination and that the initial time of inhalation or ingestion known.

RESULTS AND DISCUSSION

The benchmark measurements taken with the TPM-903B portal monitor are shown in Figures 3-6. For each of the radioisotopes the variation in count rate with change in attenuation thickness and source position can be seen in the corresponding figure. For ^{133}Ba, ^{60}Co, ^{137}Cs, and ^{22}Na, the count rates from the MCNP simulations were compared to the benchmark measurement in order to validate the detector model. An example of the pulse-height spectrum computed for the ^{137}Cs source after attenuation by 0.559 cm of PMMA on both sides is illustrated in Figure 7. As expected, the pulse-height spectrum was dominated by the Compton scattering interactions. For pulse-heights above the Compton edge, a multiple scatter component was observed followed by a very small photopeak. This spectrum was consistent with the expected response of a plastic scintillator. No attempt was made to add detector resolution to the computed spectrum.

The ratios between the MCNP and measured count rates of ^{137}Cs for different energy cutoffs are shown in Figure 8 as a function of PMMA thickness. Based on these ratios, an energy cutoff of 60 keV was selected as it yielded a constant ratio. This threshold value agrees with the manufacturer's stated threshold [12]. The energy detection threshold of 60 keV was further supported by similar comparisons for the other three isotopes used in the benchmark measurements. Since the resolution of the actual detector was not included in the simulations, the ratios are not exactly unity. After selection of the pulse-height threshold, the scaling factors for the three positions inside the detector (Figure 1) were determined. The scaling factors for positions 1, 2, and 3 are shown in Figure 9. Constant ratios of calculated to measured counts for all attenuator thicknesses were observed for all three positions and all four radioisotopes used in the benchmark measurements, resulting in the validation of the MCNP model of the detector. Since all three locations are of importance, as they represent individuals of differing heights, the scaling factors at the three heights were averaged to obtain the value applied in the anthropomorphic phantom modeling. The scaling factors of the isotopes considered in the phantom models, both averaged and interpolated, are listed in Table 1.

With the validation of the MCNP model complete, the TPM's count rates corresponding to a committed effective dose of 10 mSv were determined for the inhalation and ingestion of ^{60}Co, ^{137}Cs, ^{131}I and ^{192}Ir. Two representative phantoms were chosen; the Adult (Adipose Male) and the Pediatric (Child) phantoms. The Adipose Male was chosen because it yielded the lowest adult count rate per CED of 10 mSv for both inhalation and ingestion for all isotopes and thus represented a conservative model for an adult. Comparison of the count rate per CED of 10 mSv for each phantom type can be seen in Figures 10- 17.

The count rates corresponding to the various ^{137}Cs activities, used to estimate the upper limit of detector linearity, are shown in Figure 18. From Figure 18 it can be seen that the detector's response remained relatively linear up to 50,000 CPS for each detector leg. Above 50,000 CPS, a slight drop off in linearity was observed. Higher count rates were not obtained due to the activities of the available Cs-137 sources. Based on these observations, a combined count rate of approximately 100,000 CPS, for both detector legs turned on, was estimated to be the upper limit of detector linearity for the TPM-903B Portal Monitor, for ^{137}Cs.

The count rates in this work were initially calculated for a CED of 250 mSv. However, the count rates corresponding to a CED of 250 mSv far exceeded the estimated

upper count rate for which no pileup/dead time effects become important. For this reason, count rates corresponding to a CED of 10 mSv were reported herein. The count rates, corresponding to the trigger levels for initial screening, for the four isotopes of concern and the two representative phantom types are shown in Tables 2-5. Trigger levels that are less than or equal to the lower limit of detection, calculated for the background measured during the benchmark measurements, are shaded in light gray.

CONCLUSIONS

The TPM-903B Portal Monitor is a viable initial screening tool for use in assaying internal contamination following an RDD if the radionuclide of concern is a gamma emitter. The sensitivity of the TPM-903B detector exceeded expectations, resulting in the ability to detect contamination levels that are significantly lower than the originally investigated CED of 250 mSv. The TPM-903B has sufficient sensitivity to identify individuals in the public who have received an approximate CED of 10 mSv through inhalation or ingestion of ^{60}Co, ^{137}Cs, ^{192}Ir, or ^{131}I for up to 30 days following exposure. The only exception was ^{131}I, whose shorter effective half-life did not allow detection with this method 30 days after exposure. The trigger levels for both phantom types and both internal contamination pathways are below the upper count rate of the detectors linearity. The Adipose Male anthropomorphic phantom consistently gave the most conservative count rates of all the adult phantoms for each of the isotopes investigated. Thus, to provide more conservative triage criteria and for simplicity, trigger levels were listed only for the Adipose Male anthropomorphic phantom. In conclusion the TPM-903B portal monitor is a useful tool in the initial screening of a large population after a radiological dispersal device.

FUNDING

This work was funded by the Centers for Disease Control and Prevention, Radiation Studies Branch through TKCIS.

ACKNOWLEDGEMENTS

The authors would like to thank Dr. Eric Burgett for his technical support and Atlanta East Metro Health District for supplying the TPM-903 Portal Monitor.

REFERENCES

1. X-5 Monte Carlo Team. MCNP - A General Monte Carlo N-Particle Tansport Code Version 5. LA-CP-03-0245. Vol. II. (Los Alamos National Laboratory) (2004).

2. Eckerman, K. F., Leggett, R. W., Cristy, M., Nelson, C. B., Ryman, J. C., Sjoreen, A. L. and Ward, R. C. Dose and Risk Calcuation Software Ver. 8.4. ORNL/TM-2001/190. (Oak Ridge National Laboratory) (2006).

3. Radiaiton Studies Branch of Centers for Disease Control and Prevention. Population Monitoring in Radiation Emergencies: A Guide for State and Local Public Health Planners. (2007). http://www.bt.cdc.gov/radiation/pdf/population-monitoring-guide.pdf (Accessed April 2010).

4. Ansari, A. Radiation Threats and Your Safety: A Guide to Preparation and Response for Professionals and Community. (Boca Raton, Florida: Chapman & Hall/CRC) (2010) ISBN 978-1-4200-8361-3.

5. National Council on Radiation Protection and Measurements. Management of Persons Contaminated with Radionuclides: Handbook. NCRP Report 161. 56-61,158-160 (2008).

6. Jerstad, A. TMT Handbook: Triage, Monitoring and Treatment of People Exposed to Ionising Radiation Following a Malevolent Act. (2009). http://www.tmthandbook.org/ (Accessed April 2010).

7. The DOE/NRC Interagency Working Group Radiological Dispersal Devices. Radiological Dispersal Devices: An Initial Study to Identify Radioactive Materials of Greatest Concern and Approaches to Their Tracking, Tagging, and Disposition. Report to the Nuclear Regulatory Commission and the Secretary of Energy. (2003). http://www.nti.org/e_research/official_docs/doe/DOE052003.pdf (Accessed April 2010).

8. Manger, R. P. , Hertel, N. E., Burgett, E. A., Ansari. A. Using Handheld Plastic Scintillator Detectors to Triage Individuals Exposed to a Radiological Dispersal Device. Radiat. Prot. Dosim. (Submitted for publication).

9. Bolch, W. E., Hurtado, J. L., Choonsik, L., Manger, R. P., Hertel, N. E., Dickerson, W. Guidance on the Use of Hand-Held Survey Meters for Radiological Triage: Time-Dependent Detector Count Rates Corresponding to 50, 250, and 500 mSv Effective Dose for Adult Males and Adult Females. Health Phys. (Submitted for publication).

10. International Commission on Radiological Protection. ICRP Publication 72: Age-Dependent Dose to Members of the Public From Intake of Radionuclides: Part 5 Compilation of Ingestion and Inhalation Dose Coefficients. Annals of the ICRP (1996).

11. Saint-Gobain Crystals. Premium Plastic Scintillators Product Data Sheet. (2005). http://prod.detectors.saintgobain.com/uploadedFiles/SGdetectors/Documents/Product_Data_Sheets/BC400-404-408-412-416-Data-Sheet.pdf (Accessed April 2011).

12. Thermo Fisher Scientific. "Thermo Scientific TPM-903B Transportable Radiation Portal Monitor." (2008). http://www.thermoscientific.com (Accessed May 2009).

13. Knoll, G. F. Radiation Detection and Measurements. 3rd Edition. (Hoboken, New Jersey: John Wiley & Sons, Inc.) (2000) ISBN 0-471-07338-5.

14. National Institute of Standards and Technology. Compositions of Materials used in STAR Databases. http://physics.nist.gov/cgi-bin/Star/compos.pl (Accessed February 2009).

15. Schwarz, R. MCNP Visual Editor Version 16d. Visual Editor Consultants. (2004). http://www.mcnpvised.com/ (Accessed November 2008).

16. Cristy, M., and Eckerman, K. F. *Specific absorbed fraction of energy at various ages from internal photon sources.* ORNL/TM-8381/VI. (Oak Ridge National Laboratory) (1987).

17. Tanner, J.E. Current DOE Studies on Effective Neutron Dose Equivalent. Proceedings of the Eleventh Department of Energy Workshop on Personnel Neutron Dosimetry (Las Vegas, Nevada) (1991).

18. Simpkins, R. W and Hertel. N. E. Neutron Organ Dose and the Influence of Adipose Tissue. Proceedings of the 12th Biennial Topical Meeting of the Radiation Protection and Shielding Division of ANS (Santa Fe, New Mexico) (2002).

19. Simpkins, R. W. Neutron Organ Dose and the Influence of Adipose Tissue. Ph.D. Dissertation (Atlanta: Georgia Institute of Technology) (2003).

20. Van Riper, K. A. BodyBuilder. 2004. http://www.whiterockscience.com/bodybuilder/bodybuilder.html.

21. Eckerman, K. F., and A.L Sjoreen. Radiological Toolbox Ver. 2.0.0. ORNL/TM-2004/27. (Oak Ridge National Laboratory) (2006).

22. International Commission on Radiological Protection. ICRP Publication 89: Basic anatomical and physiological data for use in radiological protection: reference values. Annals of the ICRP (2002).

23. International Commission on Radiological Protection. ICRP Publication 71. Age-Dependent Dose to Members of the Public From Intake of Radionuclides: Part 4 Inhalation Dose Coefficients. Annals of the ICRP (1995).

24. Centers for Disease Control and Prevention. Dirty Bombs. (2005). http://www.bt.cdc.gov/radiation/pdf/dirtybombs.pdf (Accessed April 2010).

Table 1. Scaling factors

Isotope	Scaling Factor
Ba-133	0.96
Co-60	0.98
Cs-137	1.02
I-131	1.00
Ir-192	0.99
Na-22	1.02

Table 2. Adult trigger levels for inhalation with values below the lower limit of detection, as evaluated for laboratory conditions, shaded in gray.

Adult	Trigger Levels if Inhaled (CPS per 10 mSv)			
Time (days)	Co-60	Cs-137	I-131	Ir-192
0.25	5633	5157	2320	8003
0.50	5404	5142	1650	7757
1.00	4699	5079	1086	6901
2.00	3476	4940	852	5274
3.00	2838	4821	772	4390
4.00	2547	4724	706	3976
5.00	2408	4646	647	3770
6.00	2331	4582	592	3647
7.00	2278	4529	543	3557
8.00	2235	4482	497	3480
9.00	2198	4441	455	3410
10.00	2163	4404	416	3343
20.00	1885	4113	169	2772
30.00	1683	3859	68	2330

Table 3. Adult trigger levels for ingestion with values below the lower limit of detection, as evaluated for laboratory conditions, shaded in gray

Adult	Trigger Levels if Ingested (CPS per 10 mSv)			
Time (days)	Co-60	Cs-137	I-131	Ir-192
0.25	46618	5409	2264	73423
0.50	43612	5393	1603	69610
1.00	33649	5321	1036	54253
2.00	16449	5164	801	25229
3.00	7842	5034	723	10485
4.00	4232	4930	661	4416
5.00	2769	4848	605	2081
6.00	2152	4780	554	1201
7.00	1866	4724	507	867
8.00	1704	4675	464	735
9.00	1597	4633	425	677
10.00	1513	4594	389	648
20.00	1072	4290	158	528
30.00	904	4025	64	451

Table 4. Child trigger levels for inhalation with values below the lower limit of detection, as evaluated for laboratory conditions, shaded in gray

Child	Trigger Levels if Inhaled (CPS per 10 mSv)			
Time (days)	Co-60	Cs-137	I-131	Ir-192
0.25	4324	7190	1049	7754
0.50	4136	7124	739	7471
1.00	3574	7004	476	6534
2.00	2613	6802	369	4833
3.00	2115	6637	334	3932
4.00	1889	6503	306	3518
5.00	1782	6394	280	3317
6.00	1723	6305	257	3202
7.00	1684	6230	235	3120
8.00	1652	6165	215	3051
9.00	1625	6109	197	2989
10.00	1599	6058	180	2929
20.00	1394	5656	73	2425
30.00	1244	5306	30	2034

Table 5. Child trigger levels for ingestion with values below the lower limit of detection, as evaluated for laboratory conditions, shaded in gray

Child	Trigger Levels if Ingested (CPS per 10 mSv)			
Time (days)	Co-60	Cs-137	I-131	Ir-192
0.25	17112	7907	1181	24967
0.50	15923	7828	829	23691
1.00	12202	7683	525	27519
2.00	5901	7442	401	16831
3.00	2770	7251	361	7508
4.00	1462	7100	330	3196
5.00	935	6979	302	1469
6.00	715	6881	276	808
7.00	614	6798	253	557
8.00	559	6728	232	459
9.00	523	6666	212	418
10.00	495	6610	194	397
20.00	350	6172	79	323
30.00	295	5790	32	276

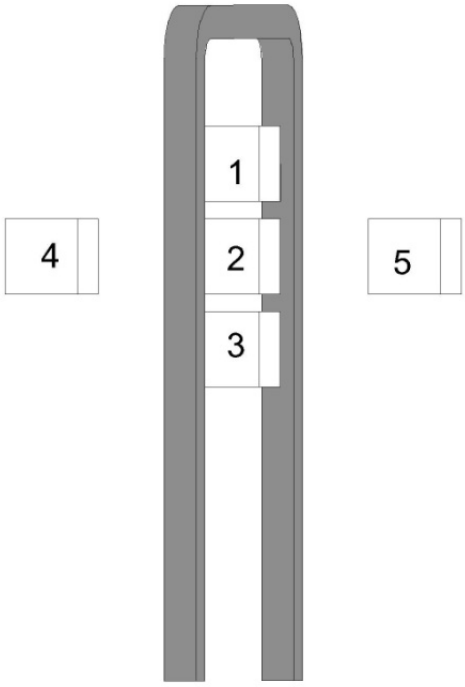

Figure 1. Source and PMMA positions with respect to the portal monitor.

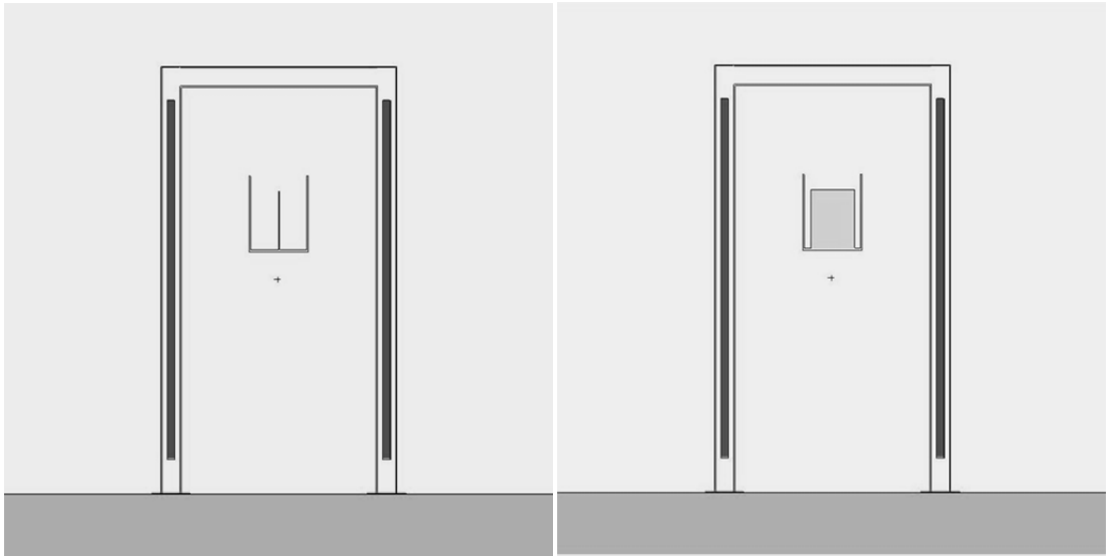

Figure 2. MCNP model of the benchmark measurements for position 2 as displayed in VisEd. In the figures the PVC casing, plastic scintillation material, PMMA source holder, and PMMA source box are shown with A) minimum attenuation B) maximum attenuation.

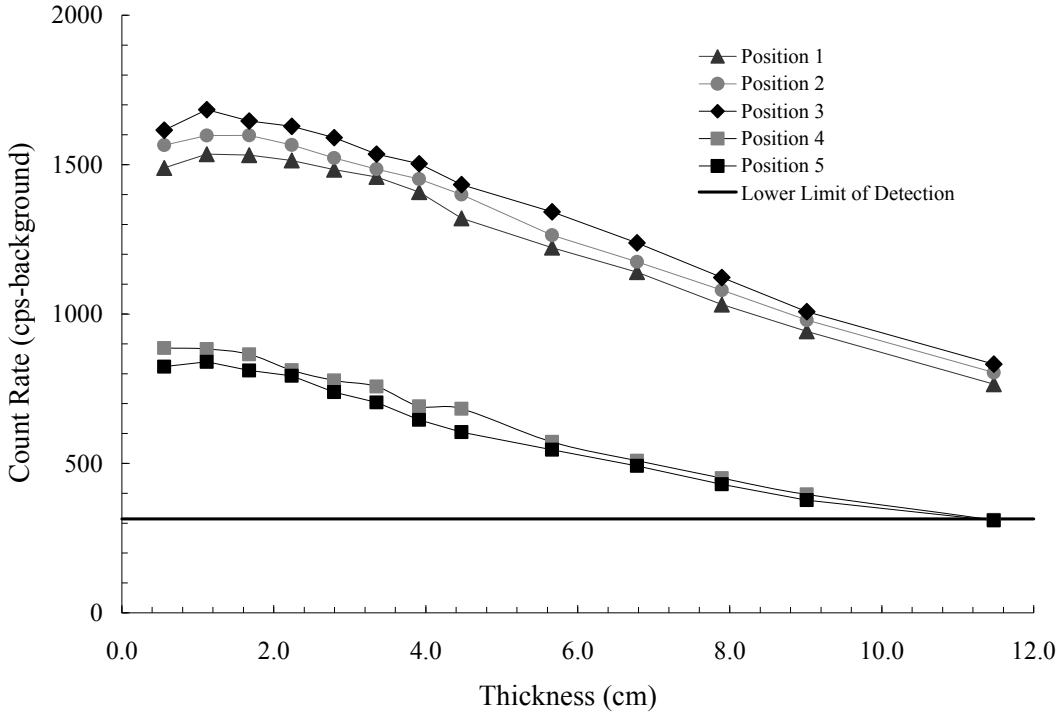

Figure 3. TPM-903B benchmark measurements for ^{133}Ba (0.14 MBq) minus background. Lower limit of detection was based on background values measured in the Georgia Tech laboratory.

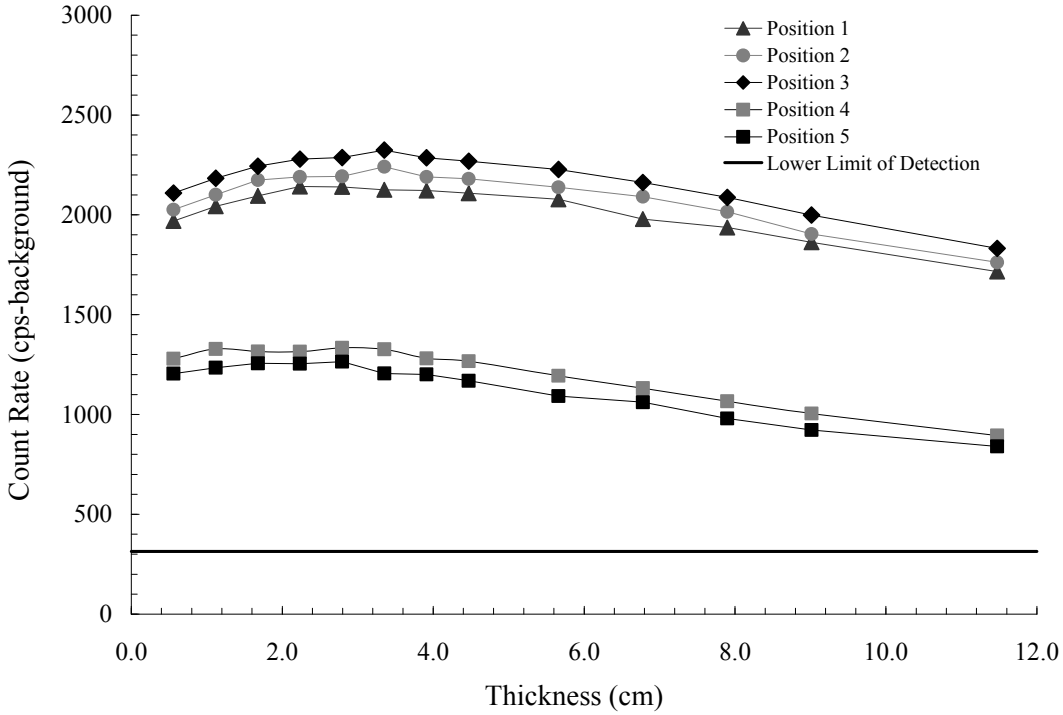

Figure 4. TPM-903B benchmark measurements for ^{60}Co (0.10 MBq) minus background. Lower limit of detection was based on background values measured in the Georgia Tech laboratory.

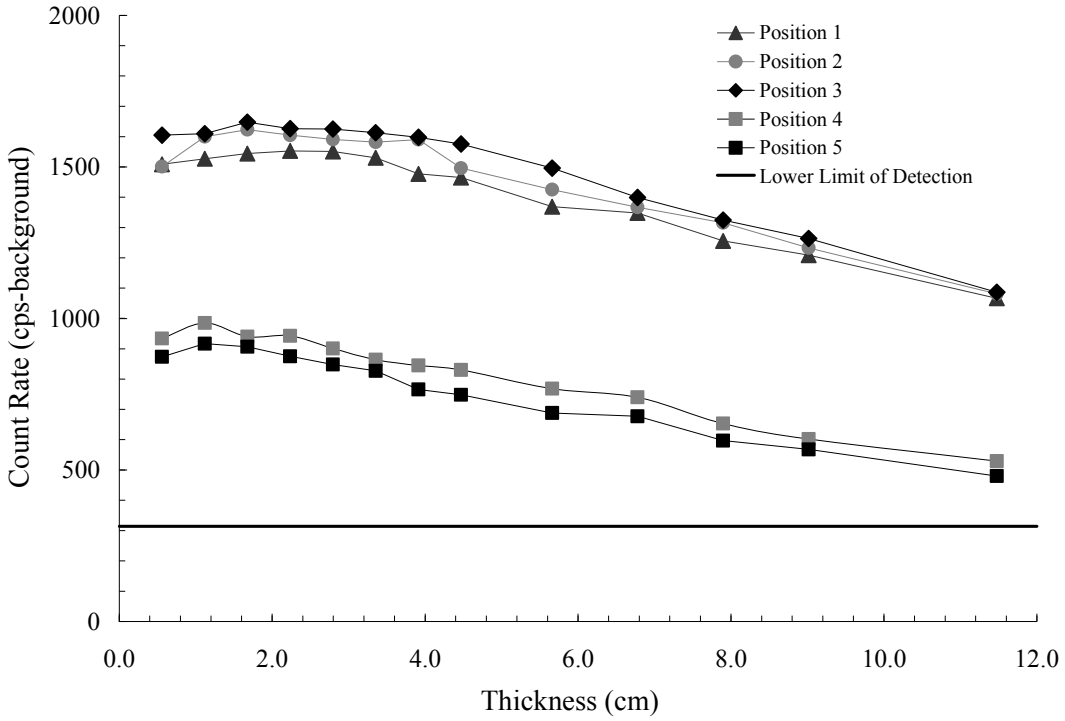

Figure 5. TPM-903B benchmark measurements for ^{137}Cs (0.16 MBq) minus background. Lower limit of detection was based on background values measured in the Georgia Tech laboratory.

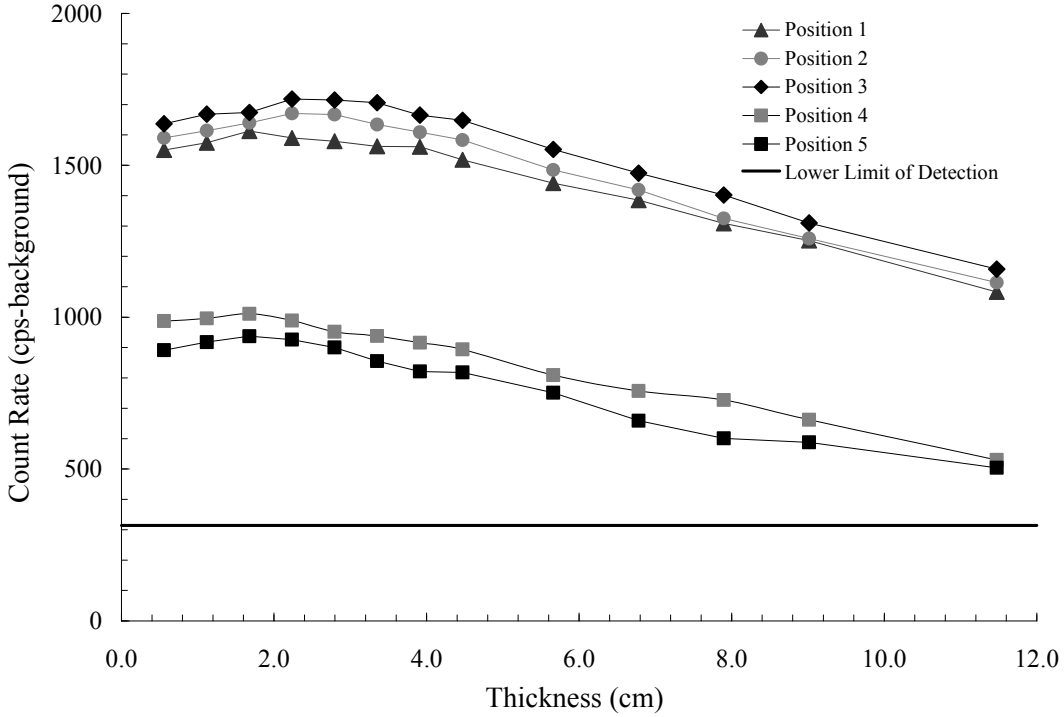

Figure 6. TPM-903B benchmark measurements for ^{22}Na (55 kBq) minus background. Lower limit of detection was based on background values measured in the Georgia Tech laboratory.

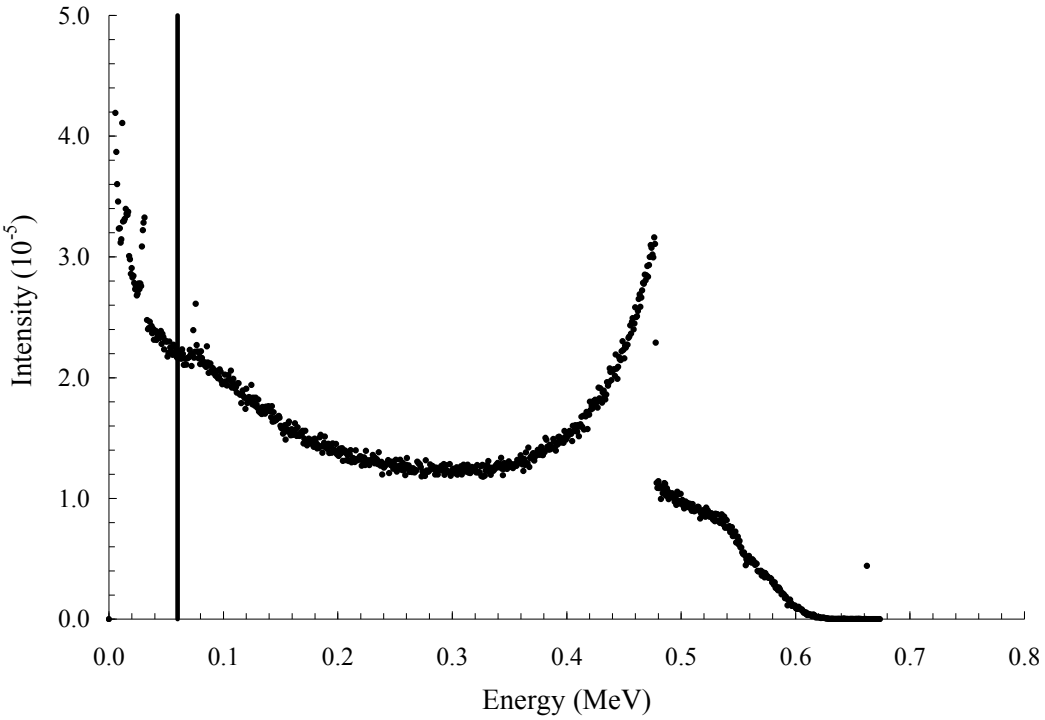

Figure 7. MCNP output for ^{137}Cs per gamma emitted, position 3 with 0.559 cm of PMMA attenuation on each side. No resolution broadening was performed. The vertical line represents the energy threshold of 60 keV, above which the MCNP pulse height tally was summed for all simulations.

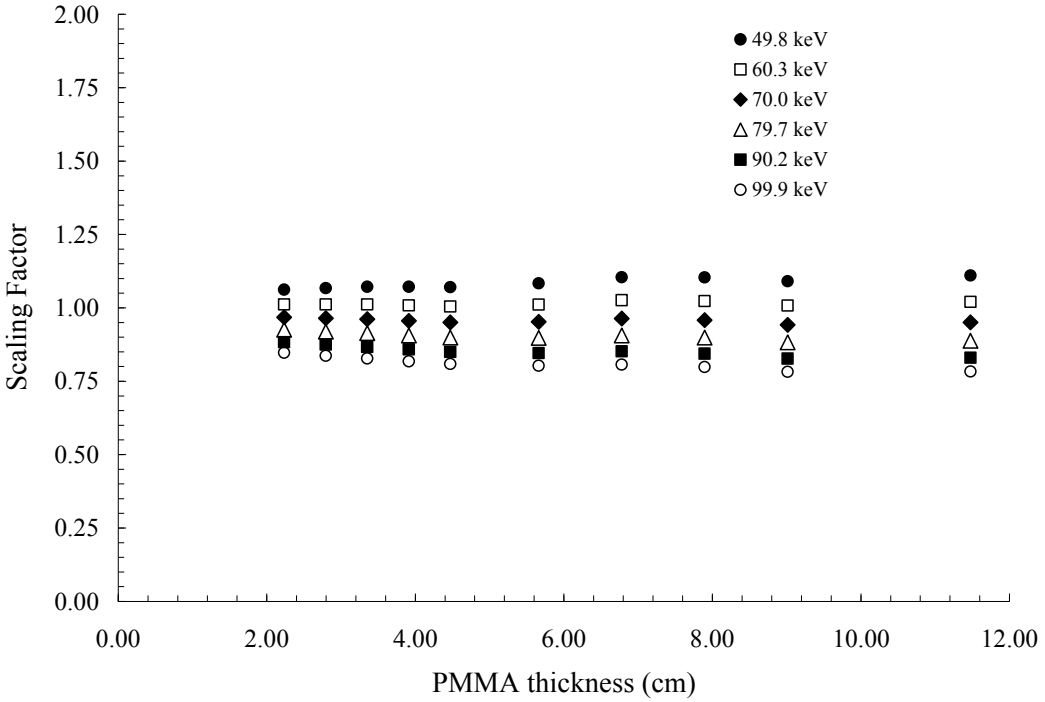

Figure 8. Scaling factors for Cs-137, position 3, for various energy thresholds and all PMMA attenuation thicknesses. An energy cutoff of 60 keV was selected as it yielded relatively constant ratios for all isotopes at positions 1-3.

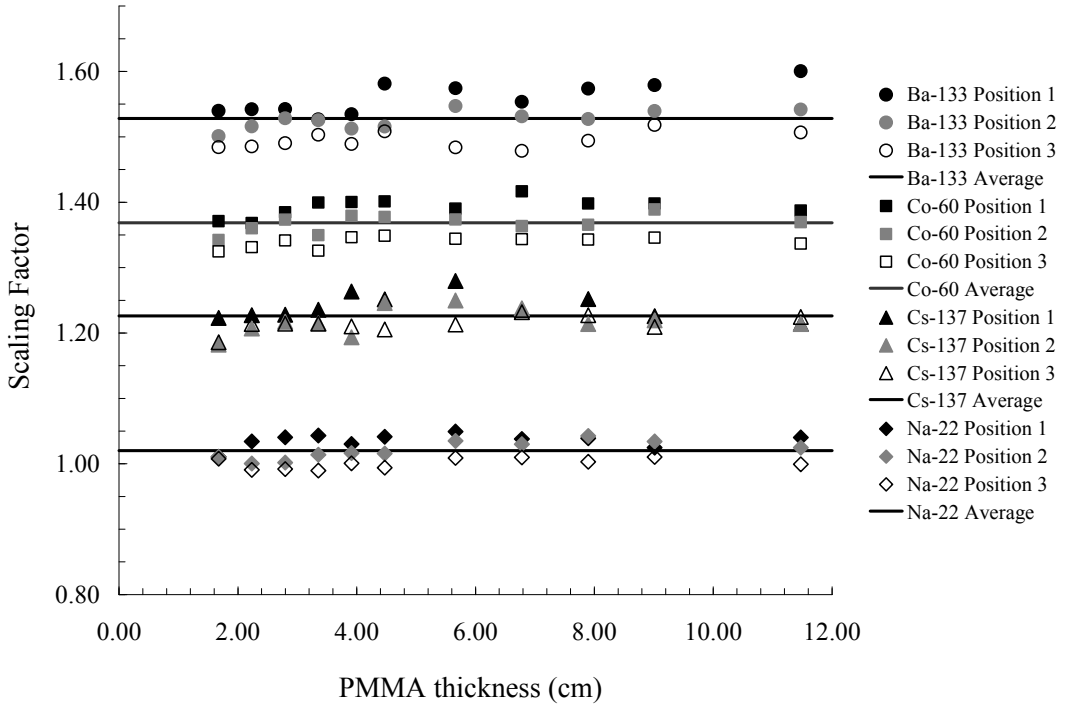

Figure 9. Scaling factors: MCNP simulated count rates divided by benchmark measurements for ^{133}Ba (multiplied by 1.6), ^{60}Co (multiplied by 1.4), ^{137}Cs (multiplied by 1.2), and ^{22}Na (multiplied by 1.0).

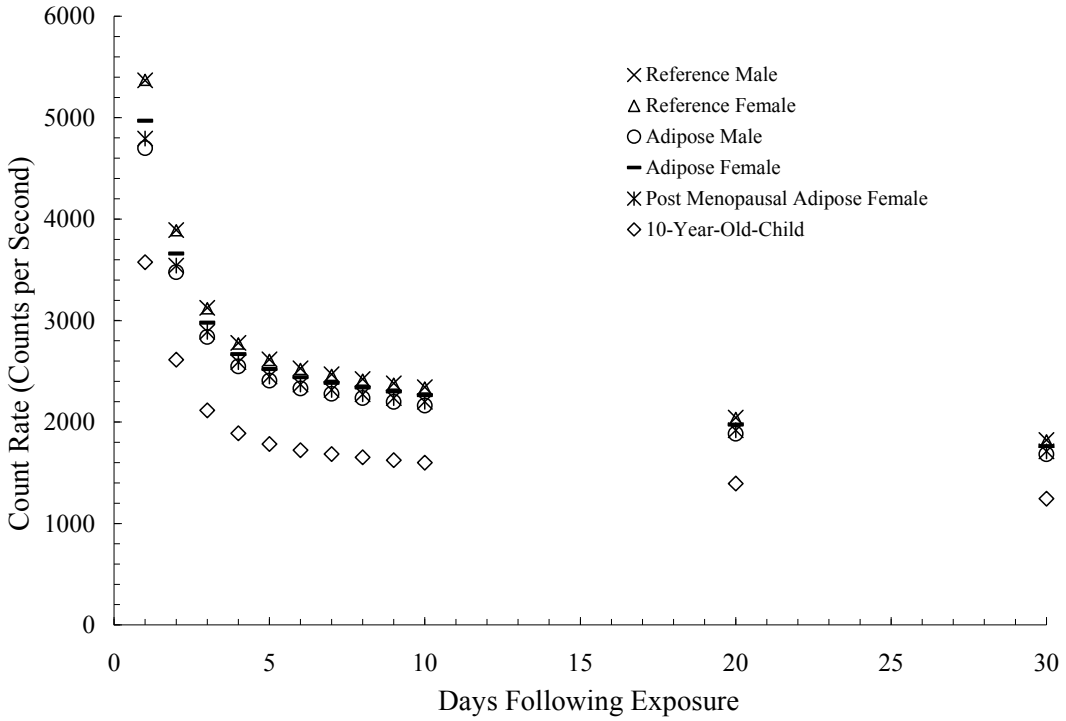

Figure 10. TPM-903B Portal Monitor CPS per 10 mSv for Anthropomorphic Phantoms for inhaled ^{60}Co.

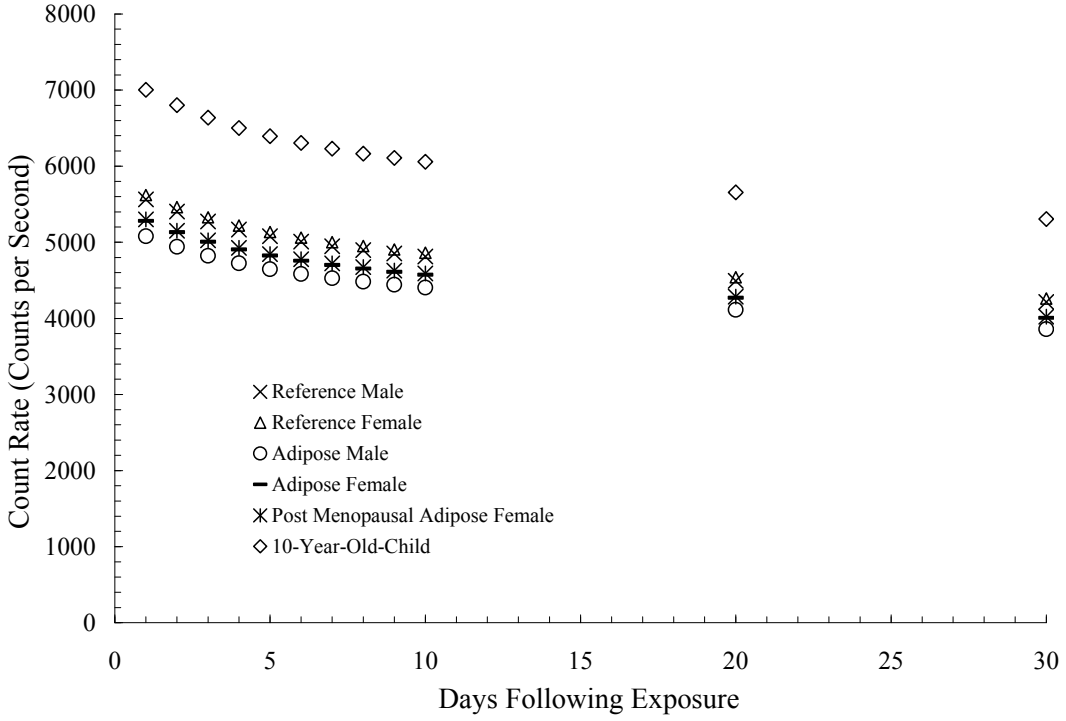

Figure 11. TPM-903B Portal Monitor CPS per 10 mSv for Anthropomorphic Phantoms for inhaled ^{137}Cs.

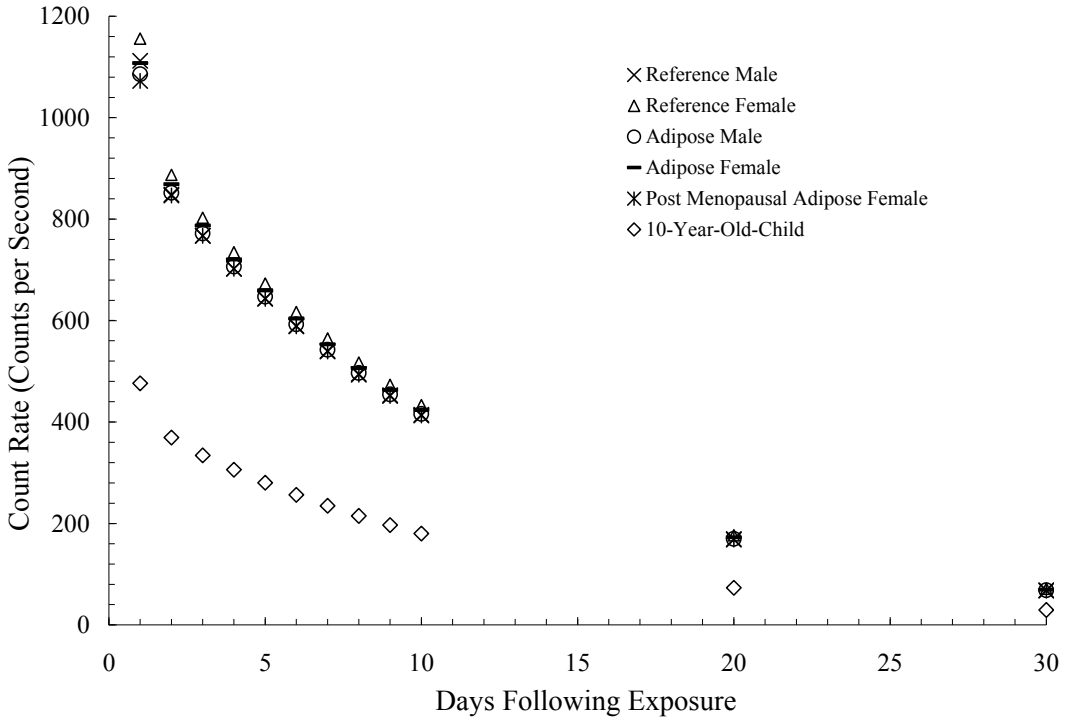

Figure 12. TPM-903B Portal Monitor CPS per 10 mSv for Anthropomorphic Phantoms for inhaled ^{131}I.

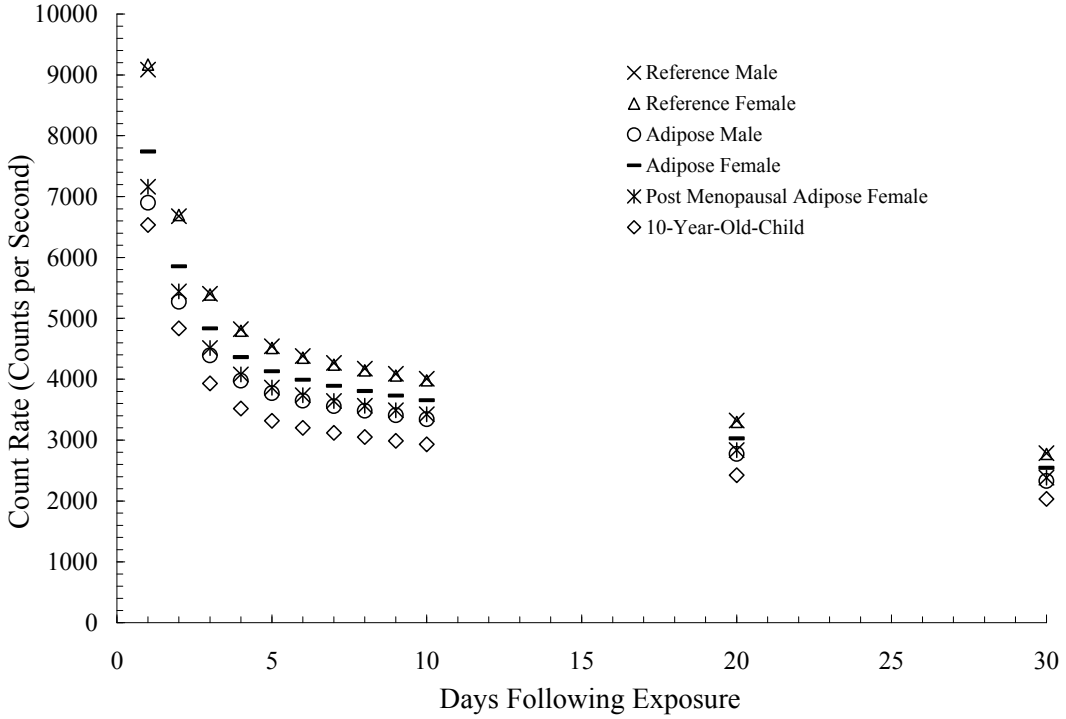

Figure 13. TPM-903B Portal Monitor CPS per 10 mSv for Anthropomorphic Phantoms for inhaled ^{192}Ir.

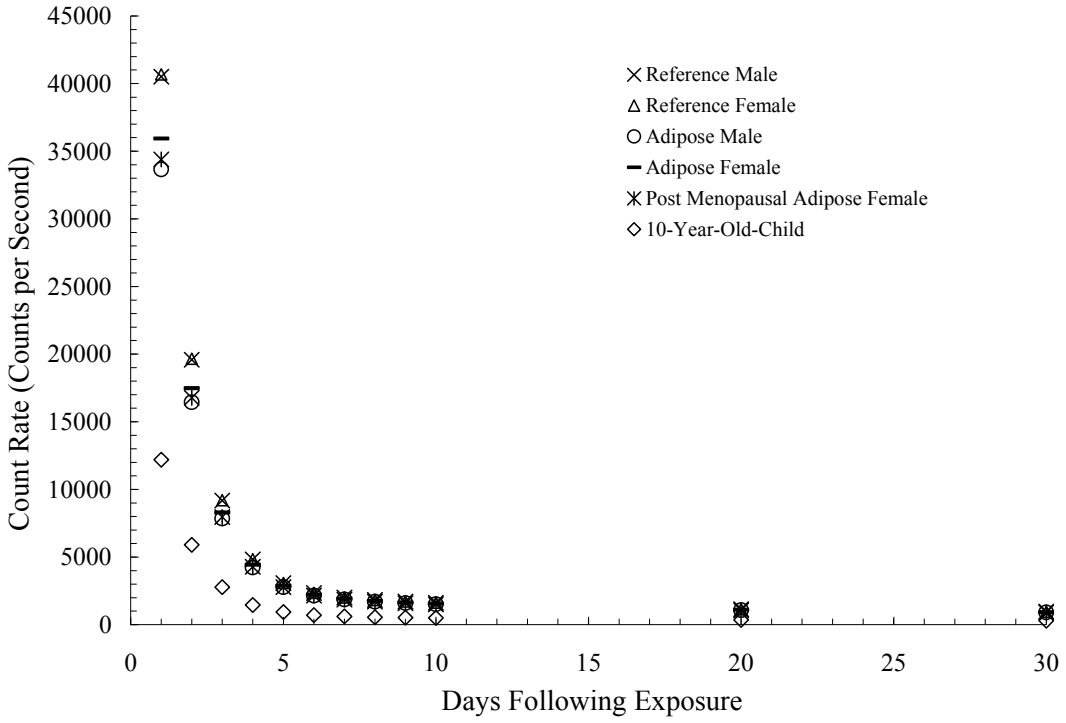

Figure 14. TPM-903B Portal Monitor CPS per 10 mSv for Anthropomorphic Phantoms for ingested ^{60}Co.

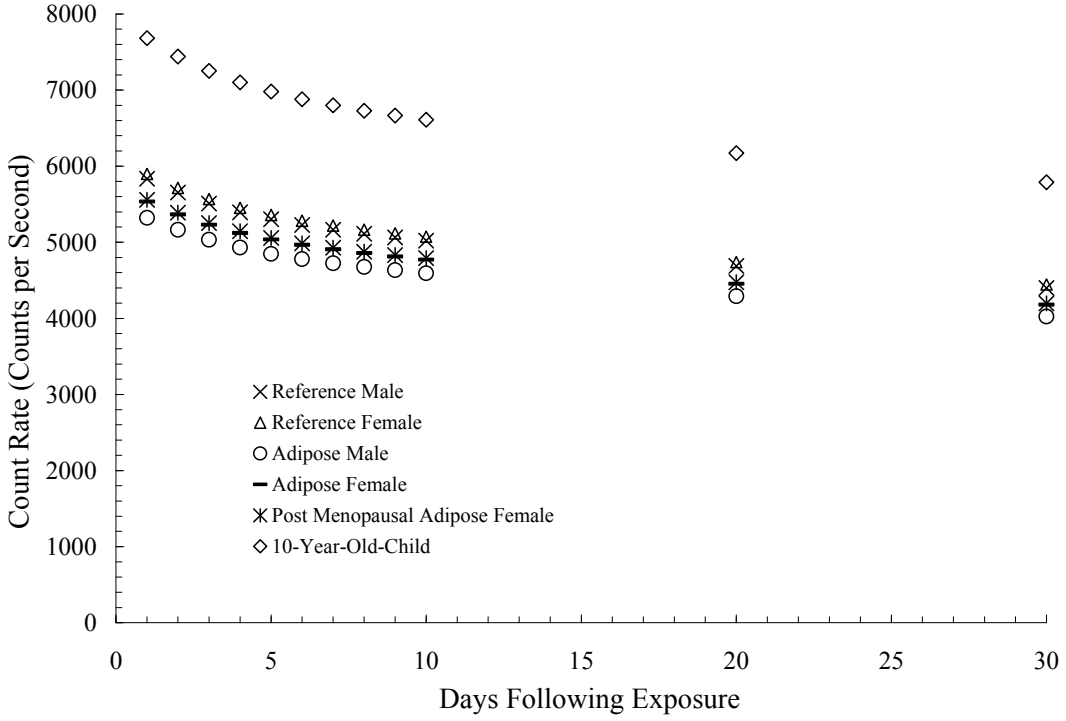

Figure 15. TPM-903B Portal Monitor CPS per 10 mSv for Anthropomorphic Phantoms for ingested ^{137}Cs.

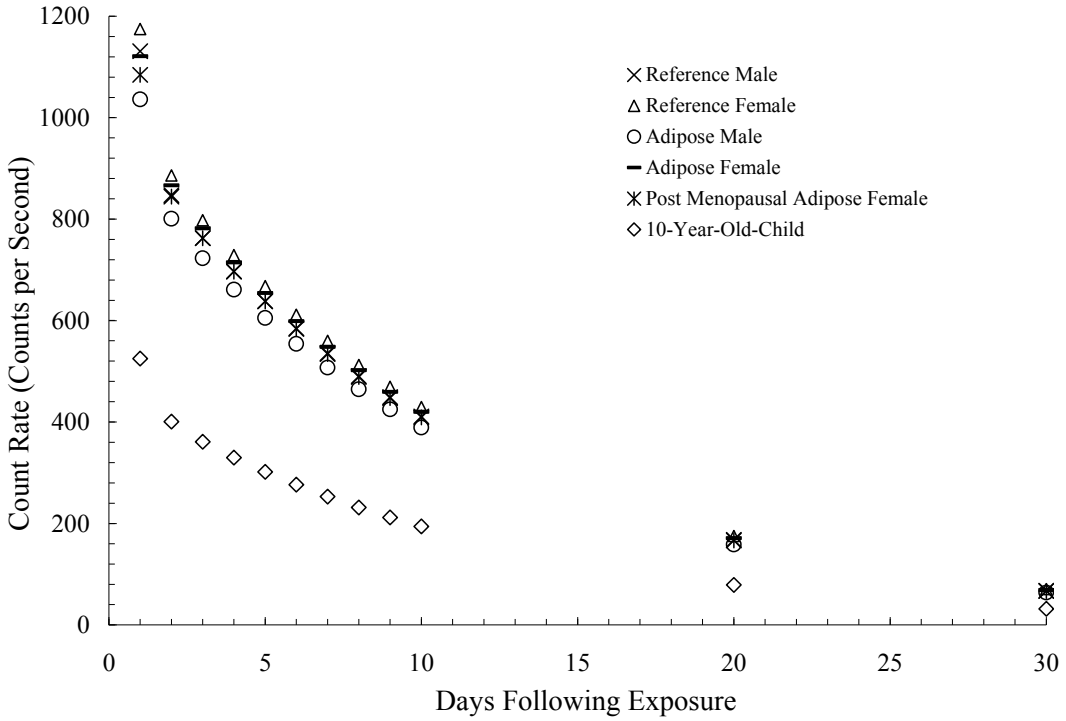

Figure 16. TPM-903B Portal Monitor CPS per 10 mSv for Anthropomorphic Phantoms for ingested ^{131}I.

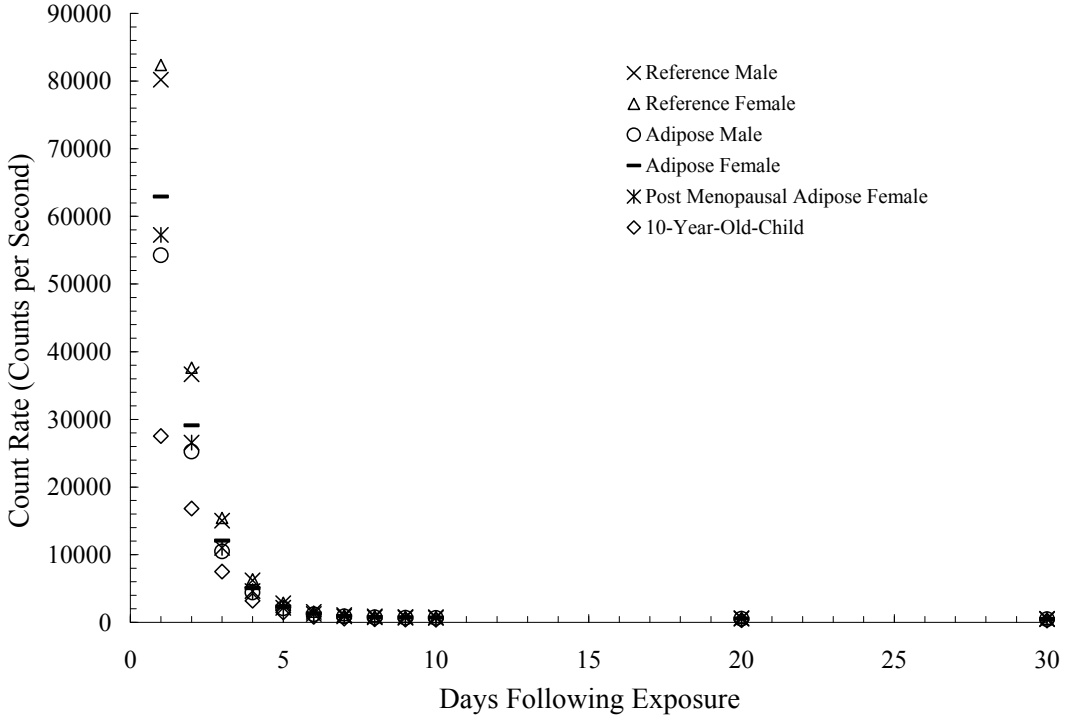

Figure 17. TPM-903B Portal Monitor CPS per 10 mSv for Anthropomorphic Phantoms for ingested ^{192}Ir.

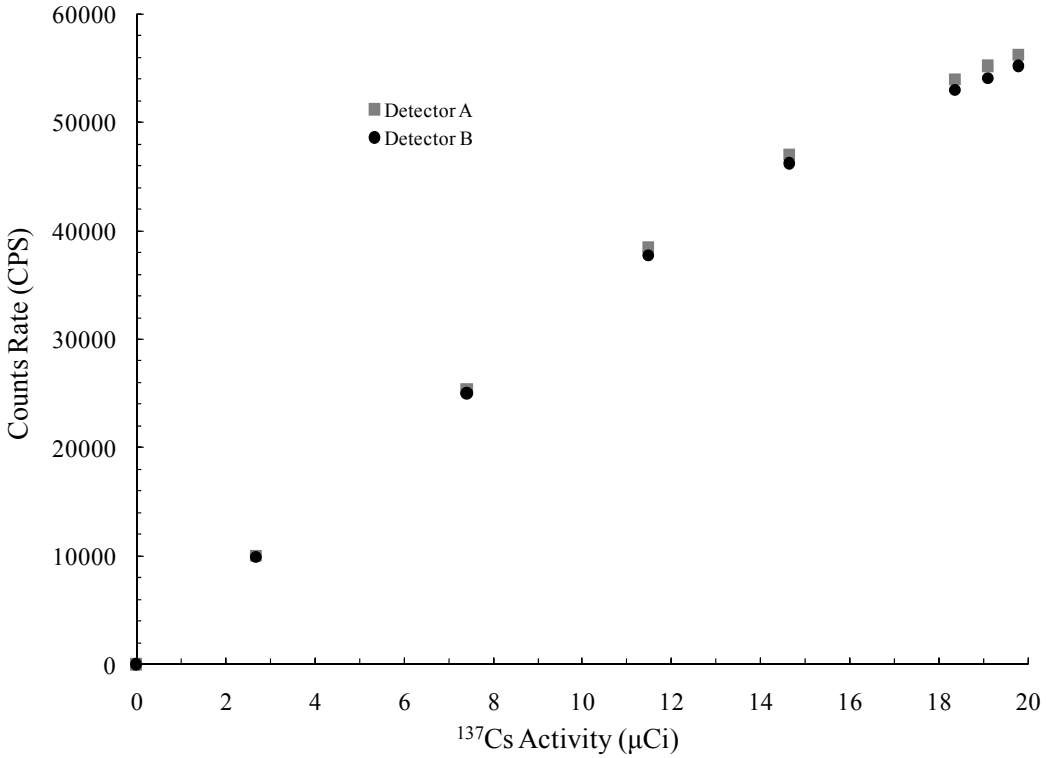

Figure 18. Detector linearity: detector response to various ^{137}Cs activities minus background. Data labeled 'Detector A' was taken with the sources placed on the leg containing Detector A with only Detector A turned on and data labeled 'Detectors B' was taken with only Detector B turned on and the sources placed on the leg corresponding to Detector B.

FISSION PRODUCT INTERNAL CONTAMINATION TITLE

Emily Freibert[1], Dr. Armin Ansari[2], Dr. Nolan Hertel[3], Randahl Palmer[4]
[1]770 State Street, NRE/MP Department, Atlanta, GA 30332 *emily.freibert@gmail.com*
[2]Centers for Disease Control and Prevention, 1600 Clifton Rd, Atlanta, GA 30333 a*sa4@cdc.gov*
[3]770 State Street, NRE/MP Department, Atlanta, GA 30332 *nolan.hertel@nre.gatech.edu*
[4]770 State Street NRE/MP Department, Atlanta, GA 30332 *palmer.rc@gmail.com*

SHORT TITLE GOES HERE

FISSION PRODUCT TITLE

Emily Freibert[1], Dr. Armin Ansari[2], Dr. Nolan Hertel[3], Randahl Palmer[4]
[1]770 State Street, NRE/MP Department, Atlanta, GA 30332. *emily.freibert@gmail.com*
[2]Centers for Disease Control and Prevention, 1600 Clifton Rd, Atlanta, GA 30333. a*sa4@cdc.gov*
[3]770 State Street, NRE/MP Department, Atlanta, GA 30332. *nolan.hertel@nre.gatech.edu*
[4]770 State Street NRE/MP Department, Atlanta, GA 30332. *palmer.rc@gmail.com*

ABSTRACT

Write abstract text here…

FISSION PRODUCT TITLE

Emily Freibert[1], Dr. Armin Ansari[2], Dr. Nolan Hertel[3], Randahl Palmer[4]
[1]770 State Street, NRE/MP Department, Atlanta, GA 30332. *emily.freibert@gmail.com*
[2]Centers for Disease Control and Prevention, 1600 Clifton Rd, Atlanta, GA 30333. a*a4@cdc.gov*
[3]770 State Street, NRE/MP Department, Atlanta, GA 30332. *nolan.hertel@nre.gatech.edu*
[4]770 State Street NRE/MP Department, Atlanta, GA 30332. *palmer.rc@gmail.com*

Received month date year, amended month date year, accepted month date year

Abstract info goes here.

INTRODUCTION

This research focuses on assessing the ability of the TPM 903B portal monitor to detect internal contamination from an inhalation of fission products released from a nuclear reactor. The purpose of this research is to facilitate the use of this portal monitor in the triage of members of the public in areas surrounding a nuclear reactor accident. The aim was to determine the count rate registered by the TPM903B corresponding to a specific dose threshold. The dose threshold was chosen to be a committed effective dose of 250 mSv, as recommended in NCRP 161 [1]. Using MCNP modeling and biokinetic data, count rates above background were computed for an inhalation of the mixture of fission products corresponding to the dose threshold.

MATERIALS AND METHODS

Fission Product Selection

A severe core melt ex-vessel release was chosen as the accident scenario for investigation in this research. Release fractions for this accident scenario were extracted from NUREG report 1465 for a Pressurized Water Reactor [2]. To explore the core inventories of the elements released, the ORIGEN-ARP [3] code provided in the SCALE 6.0 software package was utilized. Using reactor characteristics defined in Table 1, the isotopic inventories of each released element were determined for a release occurring at the end of the fuel lifetime. Selection criteria were established to shorten the extensive list of released fission products. Fission products with half-lives of less than 20 minutes were eliminated from the list. A toxicity index, defined in Equation 1, was used to focus the list of fission products to those that would contribute the most to the dose of contaminated individuals.

$$TI = RF \times A \times DC \qquad (1)$$

A toxicity index threshold was established, and fission products with toxicity indexes smaller than this threshold were eliminated from the analysis. The remaining fission products were examined to determine the existence of decay products not already present in the fission product list. These daughter products were added to the list if they decayed by gamma emission. The final list of fission products was separated into two groups based on decay modes. Fission products that emit gamma rays were placed in Group 1, while the remaining fission products were placed in Group 2.

Monte Carlo N- Particle Model

A Monte Carlo N- Particle code Version 5.0 [4] model was constructed to characterize the detector response to internal contamination of each fission product in Group 1. The MCNP model consisted of the previously constructed and validated model of the TPM 903B portal monitor [5] and an anthropomorphic MIRD phantom model. The adipose male phantom was selected as the representative phantom type because it has consistently resulted in the most conservative results [5]. The visual editor representation of the MCNP model is shown in Figure 1. A separate model was created for each fission product individually. Each model established a separate detector reading for a unit volume source placed in each source organ inside the adipose male phantom. Source organs were defined as organs in which significant quantities of the fission product would concentrate in if inhaled. The detector response for each source organ was separated into energy bins. A summation of the output over all energy bins above the detector energy cut off of 60 keV [5] was performed. Using the branching ratio for each fission product, the detector reading was converted into the count rate per bequerel of the fission product present in each source organ. Biokinetic data was used to determine the time-dependent activity distribution of the fission product when inhaled.

Biokinetic data

Dose and Risk Calculation Software (DCAL) [6] was used to compute biokinetic data for each fission product in Group 1. DCAL incorporates user-specified data to determine the activity distribution throughout the source organs as a function of time post inhalation. For a given fission product, DCAL was used to compute the time-dependent activity of any radioactive daughter products as their activity builds from decay of the fission product. Time-dependent activity distributions were computed for each fission product in Group 1.

Combining MCNP and biokinetic data

To determine the detector response to the distribution of the fission product as a function of time post-inhalation, the MCNP output and biokinetic data were combined. The detector response for each source organ was multiplied by the corresponding time-dependent activity distribution for the specified organ. The activity of the fission product within the blood was distributed throughout the source organs according to ICRP 89 [7]. A summation was performed over all source organs for each time post-inhalation. The average scaling factor [5] was applied to

the summation to determine the count rate registered by the TPM903B per bequerel of fission product inhaled.

The next steps were completed for existing daughter products of fission products in Group 1. The DCAL output accounting for the build-up of the daughter product internally from the decay of the parent fission product was combined with the detector response for the daughter product. This result was multiplied by the yield of the daughter product and then summed with the results from the parent product. The count rate per bequerel of each fission product accounts for any additional count rates acquired from the gamma emission of the daughter product as it builds up internally.

Count rates for fission product mixture

In order to combine the individual fission product count rates into a count rate for the fission product mixture, the following steps were taken. The computation of the count rate for the mixture of fission products in Group 1 is shown in Equation 2.

$$C_{mix} = \frac{\sum_F A_F \times RF_F \times C_F}{\sum_F A_F \times RF_F} \quad (2)$$

where A_F represents the activity of the fission product, RF_F represents the release fraction of the fission product and C_F is the count rate in CPS, per 1 bequerel of the fission product. The calculation of the effective dose coefficient for the mixture of the fission products is shown in Equation 3.

$$DC_{eff} = \frac{\sum_F A_F \times RF_F \times DC_F}{\sum_F A_F \times RF_F} \quad (3)$$

where the dose coefficient, DC_F, is in units of mSv/Bq. Multiplication of the count rate for the mixture and the effective dose coefficient for the mixture resulted in the count rate per mSv for the mixture of fission products. This is shown in Equation 4.

$$\frac{C_{Mix}}{mSv} = \frac{C_{mix}}{DC_{eff}} = \frac{\left[\frac{\sum_F A_F \times RF_F \times C_F}{\sum_F A_F \times RF_F}\right]}{\left[\frac{\sum_F A_F \times RF_F \times DC_F}{\sum_F A_F \times RF_F}\right]} = \frac{\sum_F A_F \times RF_F \times C_F}{\sum_F A_F \times RF_F \times DC_F} \quad (4)$$

To scale the count rate to the committed effective dose threshold of 250 mSv, the result was multiplied by 250 as shown in Equation 5.

$$\frac{C_{mix}}{250mSv} = \left[\frac{\sum_F A_F \times RF_F \times C_F}{\sum_F A_F \times RF_F \times DC_F}\right] \times 250 \quad (5)$$

Accounting for Group 2 Fission Products

To account for the dose from Group 2 fission products, a weighted ratio of the dose coefficients from both groups was used. The equation for this ratio is shown below.

$$Ratio = \frac{\sum DC_F^1 \times RF_F^1 \times A_F^1}{\sum DC_F^1 \times RF_F^1 \times A_F^1 + \sum DC_F^2 \times RF_F^2 \times A_F^2} \quad (6)$$

where DC_F represents the dose coefficients, RF_F represents the corresponding normalized release fraction, and A_F represents the normalized activity of the fission product, with the superscripts denoting the fission product group. This number was then multiplied by the count rates for Group 1 fission products to scale down the count rate to account for the dose from Group 2 fission products.

RESULTS AND DISCUSSION

The toxicity index cut off was determined to be 1.0E-17. Fission products with toxicity indexes below this cut off were eliminated. Group 1 fission products are displayed in Table 2. Group 2 fission products are displayed in Table 3.

The count rates above backgrounds per 250 mSv of committed effective dose from Group 1 fission products only are shown in Table 4 for times post-inhalation of the mixture of fission products.

The dose coefficient ratio was computed to be 0.953 from Equation 6. This ratio was applied to the count rates for Group 1 fission products. The count rates above background corresponding to a committed effective dose of 250 mSv for all fission products of concern are shown in Table 5.

The lower limit of detection above background was determined to be 314 cps for the TPM 903B when computed based on the observed background in Georgia Tech's Lab [5]. The computed count rates are far above the lower limit of detection for all reported times post fission product inhalation.

Recent data suggests that the linearity of the detector response begins to degrade at count rates approaching 50,000 cps [5]. If this is accurate, the detector response can only be considered accurate for times greater than 20 days post fission product inhalation. This suggests that the detector is more sensitive than previously anticipated and can actually be used to screen at a much smaller dose threshold. The reported count rates can be scaled for doses other than 250 mSv.

CONCLUSIONS

The TPM 903B is a useful tool in screening for internal contamination after a nuclear reactor accident resulting in a fission product release. While these results are based on the most conservative phantom type, other phantom types could be used. Future work could include expanding the scope of this work to include additional MIRD phantom types or incorporating voxel phantoms.

This work focused on a specific accident scenario; however, the methodology can be applied to other accident scenarios involving other reactor types. Changes in the accident scenario or the reactor type will result in a different mixture of fission products of concern, and thus different results.

FUNDING

This work was supported in part by the Centers for Disease Control and Prevention.

ACKNOWLEDGEMENTS

REFERENCES

1. National Council on Radiation Protection and Measurements. “Management of Persons Contaminated with Radionuclides: Handbook.” NCRP Report No. 161, Bethesda: NCRP, 2008.
2. Soffer, L., et al. Accident Source Terms for Light-Water Nuclear Power Plants. Final Report. Washington: U.S. Nuclear Regulatory Commission, 1995.
3. SCALE Version 6.0 Oak Ridge National Laboratory, 2009.
4. X-5 Monte Carlo Team. MCNP - A General Monte Carlo N-Particle Transport Code Version 5. LA-CP-03-0245. Vol. II. Los Alamos National Laboratory, (2004).
5. Palmer et al. Evaluation of internal contamination levels after a radiological dispersal device using portal monitors. Submitted for publication, (2011).
6. Eckerman, K. F., Cristy, M., Leggett, R. W., Ryman, J. C., Sjoreen, A. L., & Ward, R. C. (2006). Dose and Risk Calculation System. Version 8.4. Computer Software. U.S. Environmental Protection Agency, 2006. Available from http://www.epa.gov/rpdweb00/assessment/dcal.html
7. International Commission on Radiological Protection. "ICRP Publication 89: Basic anatomical and physiological data for use in radiological protection: reference values." Annals of the ICRP, 2002.
8. Schwarz, R. "MCNP Visual Editor Version 16d." Visual Editor Consultants. August 2004. http://www.mcnpvised.com/ (accessed November 2008).

Table 1. Reactor characteristics used in ORIGEN-ARP [3] to determine fission product inventories at the end of the fuel life-time

ORIGEN-ARP Reactor Characteristics	
Uranium (g)	27,271,000
Enrichment (%)	3.3
Burn-up (MWd)	33,000
Cycles	1
Libraries (#/cycle)	1
Cooling time	30 minutes
Power History	100%
Average Power (MW/MTU)	95.5

Table 2. Group 1 fission products with daughter products

Group 2 Fission Products	
Ba-139	Ru-103
Ba-140/La-140	Pm-151
Br-82	Pr-142
Br-83	Rb-86
Br-84	Rh-105
Ce-141	Ru-105/Rh-105
Ce-143	Ru-106/Rh-106
Ce-144/Pr-144m/Pr-144	Sb-122
Cs-134	Sb-124
Cs-134m/Cs-134	Sb-125
Cs-135m	Sb-126
Cs-136	Sb-127/Te-127m/Te-127
Cs-137/Ba-137m	Sb-129/Te-129m/Te-129
Cs-138	Sb-130
Eu-154	Sb-131/Te-131m/Te-131/I-131
Eu-156	Se-83/Br-83
I-130	Sm-153
I-131	Sr-91/Y-91m
I-132	Sr-92/Y-92
I-133/Xe-133m/Xe-133	Te-127
I-134	Te-127m/Te-127
I-135/Xe-135m/Xe-135	Te-129
La-140	Te-129m/Te-129
La-141/Ce-141	Te-131/I-131
La-142	Te-131m/Te-131/I-131
Mo-99/Tc-99m	Te-132/I-132
Nb-95	Te-133/Xe-133m/Xe-133/I-133
	Te-133m/Te-133/Xe-133m/Xe-133/I-133
Nb-97	
Nd-149/Pm-149	Te-134/I-134
Pd-109	Y-92
Pm-148	Y-93
Pm-148m/Pm-148	Zr-95/Nb-95
Pm-149	Zr-97/Nb-97m/Nb-97

Table 3. Group 2 fission products

Group 2 Fission Products	
Pm-147	Sr-90
Pr-143	Te-125m
Pr-145	Y-90

Table 4. Group 1 count rates in cps above background for times post fission product inhalation

Time post ingestion (days)	Count Rate above BKG (cps)
0.25	3.69E+05
0.5	3.27E+05
1	2.94E+05
2	2.52E+05
3	2.19E+05
4	1.90E+05
5	1.66E+05
6	1.47E+05
7	1.31E+05
8	1.18E+05
9	1.07E+05
10	9.78E+04
20	5.03E+04
30	2.99E+04

Table 5. Count rates above background for all fission products of concern for times after inhalation of the mixture of fission products

Time post ingestion (days)	Count Rate above BKG (cps)
0.25	3.52E+05
0.5	3.12E+05
1	2.80E+05
2	2.40E+05
3	2.08E+05
4	1.81E+05
5	1.58E+05
6	1.40E+05
7	1.25E+05
8	1.12E+05
9	1.02E+05
10	9.32E+04
20	4.79E+04
30	2.85E+04

Figure 1. Visual Editor representation of the MCNP model with adipose male phantom [8]. The TPM903B model and phantom were combined in MCNP so that the front of the phantom is facing one of the detector legs and centered between the two detector pillars.